

Johannes Zschocke
K. Michael Gibson
Garry Brown
Eva Morava
Verena Peters *Editors*

JIMD Reports

Volume 12

SSIEM

 Springer

JIMD Reports
Volume 12

Johannes Zschocke · K. Michael Gibson
Editors-in-Chief

Garry Brown · Eva Morava
Editors

Verena Peters
Managing Editor

JIMD Reports Volume 12

 Springer

SSIEM

Editor-in-Chief

Johannes Zschocke
Medizinische Universität Innsbruck
Sektionen für Humangenetik und Klinische
Innsbruck
Austria

Editor-in-Chief

K. Michael Gibson
WSU Division of Health Sciences
Clinical Pharmacology Unit
Spokane
USA

Editor

Garry Brown
University of Oxford
Department of Biochemistry
Genetics Unit
Oxford
United Kingdom

Editor

Eva Morava
Radboud University Nijmegen
Medical Center
Department of Pediatrics
IGMD
Nijmegen
Netherlands

Managing Editor

Verena Peters
Center for Child and Adolescent
Medicine
Heidelberg University Hospital
Heidelberg
Germany

ISSN 2192-8304 ISSN 2192-8312 (electronic)
ISBN 978-3-319-03460-7 ISBN 978-3-319-03461-4 (eBook)
DOI 10.1007/978-3-319-03461-4
Springer Cham Heidelberg New York Dordrecht London

© SSIEM and Springer International Publishing Switzerland 2014

This work is subject to copyright. All rights are reserved by the Publisher, whether the whole or part of the material is concerned, specifically the rights of translation, reprinting, reuse of illustrations, recitation, broadcasting, reproduction on microfilms or in any other physical way, and transmission or information storage and retrieval, electronic adaptation, computer software, or by similar or dissimilar methodology now known or hereafter developed. Exempted from this legal reservation are brief excerpts in connection with reviews or scholarly analysis or material supplied specifically for the purpose of being entered and executed on a computer system, for exclusive use by the purchaser of the work. Duplication of this publication or parts thereof is permitted only under the provisions of the Copyright Law of the Publisher's location, in its current version, and permission for use must always be obtained from Springer. Permissions for use may be obtained through RightsLink at the Copyright Clearance Center. Violations are liable to prosecution under the respective Copyright Law.

The use of general descriptive names, registered names, trademarks, service marks, etc. in this publication does not imply, even in the absence of a specific statement, that such names are exempt from the relevant protective laws and regulations and therefore free for general use.

While the advice and information in this book are believed to be true and accurate at the date of publication, neither the authors nor the editors nor the publisher can accept any legal responsibility for any errors or omissions that may be made. The publisher makes no warranty, express or implied, with respect to the material contained herein.

Printed on acid-free paper

Springer is part of Springer Science+Business Media (www.springer.com)

Contents

Propionic Acidemia and Optic Neuropathy: A Report of Two Cases.	1
Carolina Arias, Erna Raimann, Pilar Peredo, Juan Francisco Cabello, Gabriela Castro, Alf Valiente, Alicia de la Parra, Paulina Bravo, Cecilia Okuma, and Verónica Cornejo	
Chronic Kidney Disease in an Adult with Propionic Acidemia.	5
H.J. Vernon, S. Bagnasco, A. Hamosh, and C.J. Sperati	
Transient Massive Trimethylaminuria Associated with Food Protein–Induced Enterocolitis Syndrome	11
Natalie B. Miller, Avraham Beigelman, Elizabeth Utterson, and Marwan Shinawi	
Increased Prevalence of Hypertension in Young Adults with High Heteroplasmy Levels of the MELAS m.3243A>G Mutation	17
Fady Hannah-Shmouni, Sandra Sirrs, Michelle M. Mezei, Paula J. Waters, and Andre Mattman	
Niemann-Pick Disease Type C: New Aspects in a Long Published Family – Partial Manifestations in Heterozygotes	25
Klaus Harzer, Stefanie Beck-Wödl, and Peter Bauer	
Chiari 1 Malformation and Holocord Syringomyelia in Hunter Syndrome.	31
Renzo Manara, Daniela Concolino, Angelica Rampazzo, Alessandra Zanetti, Rossella Tomanin, Roberto Faggin, and Maurizio Scarpa	
A Patient with Complex I Deficiency Caused by a Novel ACAD9 Mutation Not Responding to Riboflavin Treatment.	37
Jessica Nouws, Flemming Wibrand, Mariël van den Brand, Hanka Venselaar, Morten Duno, Allan M. Lund, Simon Trautner, Leo Nijtmans, and Elsebet Østergard	
Pulmonary Manifestations in a Patient with Transaldolase Deficiency	47
Nada Jassim, Mohammed AlGhaihab, Suhail AI Saleh, Majid Alfadhel, Mirjam M.C. Wamelink, and Wafaa Eyaid	
Burden of Lysosomal Storage Disorders in India: Experience of 387 Affected Children from a Single Diagnostic Facility	51
Jayesh Sheth, Mehul Mistri, Frenny Sheth, Raju Shah, Ashish Bavdekar, Koumudi Godbole, Nidhish Nanavaty, Chaitanya Datar, Mahesh Kamate, Nrupesh Oza, Chitra Ankleshwaria, Sanjeev Mehta, and Marie Jackson	
A Japanese Adult Case of Guanidinoacetate Methyltransferase Deficiency.	65
Tomoyuki Akiyama, Hitoshi Osaka, Hiroko Shimbo, Tomoshi Nakajiri, Katsuhiko Kobayashi, Makio Oka, Fumika Endoh, and Harumi Yoshinaga	

Accumulation of Ordered Ceramide-Cholesterol Domains in Farber Disease Fibroblasts	71
Natalia Santos Ferreira, Michal Goldschmidt-Arzi, Helena Sabanay, Judith Storch, Thierry Levade, Maria Gil Ribeiro, Lia Addadi, and Anthony H. Futerman	
Infantile Sialic Acid Storage Disease: Two Unrelated Inuit Cases Homozygous for a Common Novel <i>SLC17A5</i> Mutation	79
Matthew A. Lines, C. Anthony Rugar, Jack W. Rip, Berivan Baskin, Peter N. Ray, Robert A. Hegele, David Grynspan, Jean Michaud, and Michael T. Geraghty	
Motor Development Skills of 1- to 4-Year-Old Iranian Children with Early Treated Phenylketonuria	85
Sepideh Nazi, Farzaneh Rohani, Firoozeh Sajedi, Akbar Biglarian, and Arya Setoodeh	
A Novel Large Deletion Encompassing the Whole of the Galactose-1-Phosphate Uridyltransferase (<i>GALT</i>) Gene and Extending into the Adjacent Interleukin 11 Receptor Alpha (<i>IL11RA</i>) Gene Causes Classic Galactosemia Associated with Additional Phenotypic Abnormalities	91
Rena Papachristoforou, Petros P. Petrou, Hilary Sawyer, Maggie Williams, and Anthi Drousiotou	
Successful Desensitisation in a Patient with CRIM-Positive Infantile-Onset Pompe Disease	99
J. Baruteau, A. Broomfield, V. Crook, N. Finnegan, K. Harvey, D. Burke, M. Burch, G. Shepherd, and A. Vellodi	
Heterozygous Mutations in the <i>ADCK3</i> Gene in Siblings with Cerebellar Atrophy and Extreme Phenotypic Variability	103
Lubov Blumkin, Esther Leshinsky-Silver, Ayelet Zerem, Keren Yosovich, Tally Lerman-Sagie, and Dorit Lev	
Clinical Presentation and Positive Outcome of Two Siblings with Holocarboxylase Synthetase Deficiency Caused by a Homozygous L216R Mutation	109
T.P. Slavin, S.J. Zaidi, C. Neal, B. Nishikawa, and L.H. Seaver	
No Mutation in the <i>SLC2A3</i> Gene in Cohorts of GLUT1 Deficiency Syndrome–Like Patients Negative for <i>SLC2A1</i> and in Patients with AHC Negative for <i>ATPIA3</i>	115
C. Le Bizec, S. Nicole, E. Panagiotakaki, N. Seta, and S. Vuillaumier-Barrot	
Novel Association of Early Onset Hepatocellular Carcinoma with Transaldolase Deficiency	121
Charles A. LeDuc, Elizabeth E. Crouch, Ashley Wilson, Jay Lefkowitz, Mirjam M.C. Wamelink, Cornelis Jakobs, Gajja S. Salomons, Xiaoyun Sun, Yufeng Shen, and Wendy K. Chung	
Lathosterolosis: A Disorder of Cholesterol Biosynthesis Resembling Smith-Lemli-Opitz Syndrome	129
A.C.C. Ho, C.W. Fung, T.S. Siu, O.C.K. Ma, C.W. Lam, S. Tam, and V.C.N. Wong	

Propionic Acidemia and Optic Neuropathy: A Report of Two Cases

Carolina Arias · Erna Raimann · Pilar Peredo ·
Juan Francisco Cabello · Gabriela Castro ·
Alf Valiente · Alicia de la Parra · Paulina Bravo ·
Cecilia Okuma · Verónica Cornejo

Received: 26 February 2013 / Revised: 13 April 2013 / Accepted: 17 April 2013 / Published online: 2 July 2013
© SSIEM and Springer-Verlag Berlin Heidelberg 2013

Abstract *Introduction:* Propionic acidemia is a metabolic disease produced by a deficiency of the enzyme propionyl-CoA carboxylase. It can lead to coma, with severe neurologic encephalopathy or present later in life with vomiting, hypotonia, and seizures. An early diagnosis with adequate treatment helps to prevent the sequelae. Among the described complications is optic neuropathy, although not commonly reported, it is very disabling. *Objectives:* To describe two patients with propionic acidemia and optic neuropathy. *Patients and Methods:* Patient 1: 16 years old, male, parents without consanguinity. He was diagnosed at 5 months of age because of hypotonia and seizures. Until the age of 9 years, he evolved satisfactorily; therefore, he stopped treatment. At 13 years, he presented bilateral optic neuropathy. Patient 2: 20 years, female, parents without consanguinity. She was diagnosed with PA at 11 months of age because of hypotonia and seizures. She evolved satisfactorily until the age of 9 years when she presented a metabolic decompensation followed by a bad metabolic control. At 18 years, she presented bilateral progressive optic neuropathy. *Results:* Both patients have psychometric scores with borderline IQ 84–75 (WISC-R) beside optic neuropathy. They were evaluated by an ophthalmologist

and also by neuroimaging (MRI of optic pathway). *Conclusions:* Pathophysiology of optic neuropathy is not completely understood. There is evidence that the damage is due to an accumulation of neurotoxic compounds secondary to the metabolic block increasing the oxidative stress. We suggest an annual ophthalmologic evaluation in the long-term follow-up of organic acidurias with visual loss, in order to detect this disabling sequela at an earlier stage.

Introduction

Propionic acidemia (PA) (OMIM 606054) is an organic aciduria (OA) due to propionyl CoA carboxylase enzyme deficit, composed by two subunits: α (PCCA, OMIM 232000), chromosome 13q32 and β (PCCB, OMIM 232050), chromosome 6p21. The incidence is 1:100.000 newborns.

There are two clinical presentations: an acute neonatal form, characterized by severe metabolic decompensation and a late chronic progressive form with hypotonia, failure to thrive, and developmental delay. The diagnosis is confirmed by enzyme or molecular analysis (Cornejo and Raimann 2010; Ogier de Baulny and Saudubray 2002).

The accumulation of organic acids, either transported through the blood-brain barrier (BBB) or synthesized in the central nervous system, leads to secondary metabolic alterations due to their toxicity (Schreiber et al. 2012). This causes brain damage and inhibition of mitochondrial metabolism explaining acidosis, hypoglycemia, and hyperammonemia. It has been suggested that there is an imbalance of amino acids transport through the BBB leading to a low protein synthesis and secondary carnitine deficit, which can generate less energy (Wajner and Goodman 2011). Recently, oxidative stress has been

Communicated by: Daniela Karall

Competing interests: None declared

C. Arias (✉) · E. Raimann · P. Peredo · J.F. Cabello · G. Castro ·
A. Valiente · A. de la Parra · P. Bravo · V. Cornejo
Laboratory of Genetics and Metabolic Diseases, Institute of Nutrition
and Food Technology, (INTA) University of Chile, El Líbano 5524,
Santiago 7830490, Chile
e-mail: carias@inta.uchile.cl

C. Okuma
Division of Neuroradiology, Institute of Neurosurgery (INCA)
Dr. Alfonso Asenjo, Santiago, Chile

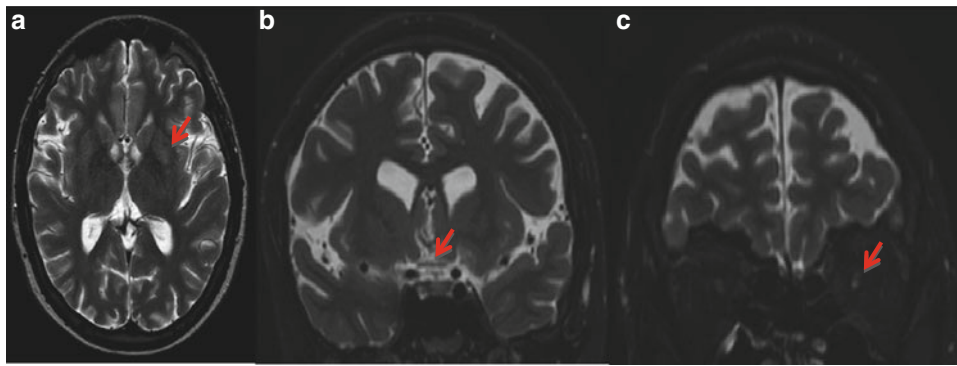


Fig. 1 MRI brain and orbits: Case 1 at 15 years old. **(a)** T2-weighted axial image, *red arrow* shows discrete hyperintense signal in putamen nucleus, there is also signs of brain atrophy. **(b)** T2-weighted coronal image, *red arrow* shows decreased volume and

increased signal of optic chiasm (chiasmal atrophy). **(c)** Coronal T2-weighted STIR, *red arrow* shows decreased volume and increased signal in intraorbital portions of both optic nerves (severe bilateral optic atrophy)

reported in OA due to decreased antioxidant capacity (Ianchulev et al. 2003; Wajner and Goodman 2011). These pathophysiological effects explain the multisystemic complications in OA, most frequently neurologic (symmetrical necrosis of globus pallidus), renal, dermatologic, pancreatic, and cardiac. Optic nerve atrophy has been reported in organic acidemias, mainly, propionic acidemia and methylmalonic acidemia (Ianchulev et al. 2003; Williams et al. 2009; Patton et al. 2000; Gerth et al. 2008; Grünert et al. 2013); however, it is very disabling.

Case Reports

The first case: Male, 16 years old, parents without consanguinity. His brother died at 27 weeks of gestational age (GA) of undetermined cause. He was born at 34 weeks GA, birth weight 2,160 g, length 46 cm, Apgar 9–9.

Diagnosis was suspected at 5 months of age by developmental delay, hypotonic syndrome and focal seizures. Increased glycine and propionylcarnitine were found. Nutritional treatment was started with natural protein restriction (1.2 g/kg/day), L-carnitine (100 mg/kg/day), and biotin (10 mg) for improving seizure control and psychomotor development. From age 9, he showed poor adherence to nutritional therapy with elevated levels of propionylcarnitine (C3) and ammonia and decreased levels of free carnitine (C0). Plasma levels of amino acids involved in the metabolic pathway were below the recommended range, with the exception of methionine and threonine. Total IQ assessed by WISC-R was 78 at 12 years of age (borderline).

He presented a bilateral visual loss at age 13. The ophthalmologic evaluation detected visual field contraction of all isopters in both eyes (remaining at 10 °). Visual acuity was 0.05 to 1 meter in both eyes. The fundus revealed pale papillae and dystrophic retina speckled with pigment migration, consistent with bilateral progressive

optic neuropathy. Magnetic resonance imaging (MRI) of the brain and optic pathway was performed, demonstrating severe bilateral optic neuropathy (Fig. 1).

The second case: Female, 20 years old, parents without consanguinity, and a family history of three brothers who died in the neonatal period of undetermined cause. She presented at 11 months of age with focal seizures and hypotonia leading to the diagnosis of PA. After nutritional treatment was started with natural protein restriction (0.7 g/kg/day), L-carnitine (100 mg/kg/day), and biotin (10 mg/day) she progressively improved her psychomotor development. At age 9, she had a severe metabolic decompensation, subsequently metabolic control was irregular with elevation of C3, high ammonia and decreased free carnitine. The amino acids supplementation was poor. In the cognitive evaluation (WISC-R) at age 12, total IQ was 81 (low normal range).

At age 18, she presented progressive visual loss. Ophthalmologic evaluation found a decreased visual acuity in both eyes at 20 cm 20/800, color vision 0/10, visual field and ocular motility was preserved. The fundus showed a pale papillae whit small central excavation and an unaltered retina and macula, consistent with bilateral optic nerve atrophy. Brain and optic path MRI revealed bilateral optic neuropathy (Fig. 2).

Discussion

The pathophysiology of optic nerve atrophy in OA is still unknown, but the accumulation of neurotoxic substrates due to the metabolic block can produce the damage (Williams et al. 2009). This compromise can usually affect several organs as liver, bone marrow, kidney, pancreas, heart, and brain. The central nervous system and optic nerve are particularly susceptible to damage because of the high concentration of polyunsaturated fatty acids in mitochondrial membranes (Schreiber et al. 2012).

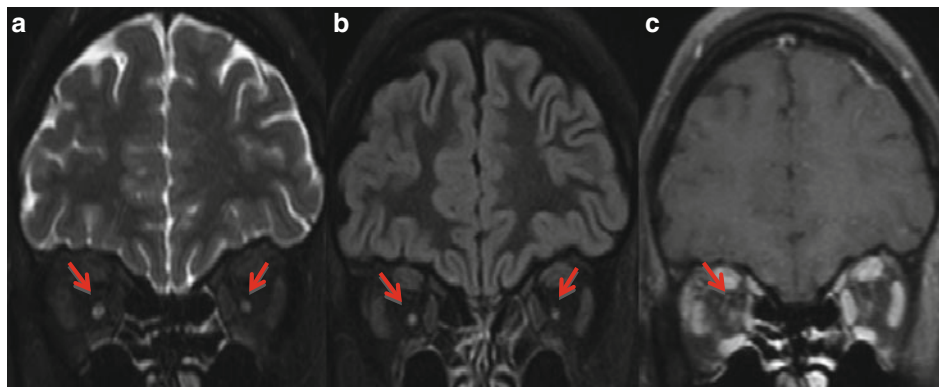


Fig. 2 MRI brain and orbits: Case 2 at 17 years old. Coronal images (a) T2-weighted STIR and (b) STIR-FLAIR, red arrows demonstrate hyperintense signal in intraorbital portions of both optic nerves.

(c) T1FS-weighted contrast, red arrow shows discrete impregnation of optic nerves, left more evident

Moreover, the accumulation of propionyl-CoA in mitochondria induces ultrastructural changes, producing inhibition of pyruvate dehydrogenase, alpha-ketoglutarate dehydrogenase, complexes of the respiratory chain and glutathione synthetase. This favors the hypothesis of mitochondrial dysfunction induced by the accumulation of enzymatic block-derived compounds (Schwab et al. 2006). The oxidative phosphorylation is reduced generating cytotoxic free radicals which can induce apoptosis (Gallego-Villar et al. 2012). In addition, there are decreased cellular antioxidant reserves (alpha-tocopherol and glutathione) (Wajner and Goodman 2011; Mc Guire et al. 2009).

In this report, both patients had poor metabolic control for years, developing progressive optic neuropathy. In the literature, there is no consensus about the lack of adherence to treatment as the cause of this complication (Sutton et al. 2012). However, being a late complication, it could be influenced by an increased oxidative stress as a trigger. In addition, both patients have cognitive impairment in borderline range, which could be explained by a delayed diagnosis (de Baulny et al. 2005; Loren et al. 2012). We suggest an ophthalmologic evaluation in patients with OA and early visual loss symptoms. This could lead to early detection of this disabling complication (Sutton et al. 2012; Loren et al. 2012). There are some studies showing that cohorts of patients with OA detected with expanded newborn screening programs (NBS) have improved survival with better prognosis and quality of life (Dionisi-Vici et al. 2006; Hori et al. 2005; Schulze et al. 2003). However it is not clear that early detection by NBS can prevent long-term complications such as optic neuropathy, cognitive delay, or metabolic crises (Grünert et al. 2012). Our patients in this report show disabling complications at long-term follow-up, probably because they were already symptomatic at the time of diagnosis and had also a bad metabolic control.

Synopsis

Optic neuropathy complication organic acidemia.

References

- Cornejo V, Raimann E (2010) Errores innatos del metabolismo de los aminoácidos. In: Colombo M, Cornejo V, Raimann E (eds) Errores innatos en el metabolismo del niño. Santiago de Chile, Editorial Universitaria, pp 71–138
- de Baulny HO, Benoist JF, Rigal O, Touati G, Rabier D et al (2005) Methylmalonic and propionic acidemias: management and outcome. *J Inherit Metab Dis* 28:415–423
- Dionisi-Vici C, Deodato F, Röschinger W, Rhead W, Wilcken B (2006) Classical organic acidurias, propionic aciduria, methylmalonic aciduria and isovaleric aciduria: long-term outcome and effects of expanded newborn screening using tandem mass spectrometry. *J Inherit Metab Dis* 29:383–389
- Gallego-Villar L, Pérez Cerda C, Pérez B, Abia D, Ugarte M et al (2012) Functional characterization of novel genotypes and cellular oxidative stress studies in propionic acidemia. *J Inherit Metab Dis* ISSN 1573–2665, DOI 10.1007/s10545-012-9545-3
- Gerth C, Morel CF, Feigenbaum A, Levin AV (2008) Ocular phenotype in patients with methylmalonic aciduria and homocystinuria, cobalamin C type. *J AAPOS* 12:591–596
- Grünert SC, Müllerleile S, de Silva L, Barth M, Walter M et al (2013) Propionic acidemia: clinical course and outcome in 55 pediatric and adolescent patients. *Orphanet J Rare Dis* 10(8):6
- Grünert SC, Müllerleile S, de Silva L, Barth M, Walter M et al (2012) Propionic acidemia: neonatal versus selective metabolic screening. *J Inherit Metab Dis* 35:41–49
- Hori D, Hasewaga Y, Kimura M, Yang Y, Verma IC et al (2005) Clinical onset and prognosis of Asian children with organic acidemias, as detected by analysis of urinary organic acids using GC/MS, instead of mass screening. *Brain Dev* 27:39–45
- Ianchulev T, Kolin T, Moseley K, Sadun A (2003) Optic nerve atrophy in propionic acidemia. *Ophthalmology* 110:1850–1854
- Loren P, Jill F, Chapman K, Gropman A, Ah Mew N et al (2012) Natural history of propionic acidemia. *Mol Genet Metab* 105:5–9
- Mc Guire PJ, Parikh A, Diaz GA (2009) Profiling of oxidative stress in patients with inborn errors of Metabolism. *Mol Genet Metab* 98:173–180

- Ogier de Baulny H, Saudubray JM (2002) Branched-chain organic acidurias. *Semin Neonatol* 7:65–74
- Patton N, Beatty S, Lloyd IC, Wraith JE (2000) Optic atrophy in association with Cobalamin C (cblC) disease. *Ophthalmic Genet* 21:151–154
- Schreiber J, Chapman KA, Summar M, AhMew N, Sutton VR, Mcleod E et al (2012) Neurologic considerations in propionic acidemia. *Mol Genet Metab* 105:10–15
- Schwab MA, Sauer SW, Okun JG, Nijtmans LG, Rodenburg RJ et al (2006) Secondary mitochondrial dysfunction in propionic aciduria: a pathogenic role for endogenous mitochondrial toxins. *Biochem J* 398:107–112
- Schulze A, Linder M, Kohlmuller D, Mayatepek E et al (2003) Expanded newborn screening for inborn errors of metabolism by electrospray ionization-tandem mass spectrometry: results, outcome, and implications. *Pediatrics* 111:1399–1406
- Sutton R, Chapman K, Gropman A, Mcleod E, Stagni K et al (2012) Chronic management and health supervision of individuals with propionic acidemia. *Mol Genet Metab* 105(1):26–33
- Wajner M, Goodman S (2011) Disruption of mitochondrial homeostasis in organic acidurias: insights from animal studies. *J Bioenerg Biomembr* 43:31–38
- Williams ZR, Hurley PE, Altiparmark UE, Feldon SE, Arnold GL et al (2009) Late onset optic neuropathy in methylmalonic and propionic acidemia. *Am J Ophthalmol* 147:929–933

Chronic Kidney Disease in an Adult with Propionic Acidemia

H.J. Vernon • S. Bagnasco • A. Hamosh • C.J. Sperati

Received: 14 February 2013 / Revised: 23 April 2013 / Accepted: 29 April 2013 / Published online: 12 June 2013
© SSIEM and Springer-Verlag Berlin Heidelberg 2013

Abstract We report an adult male with classic propionic acidemia (PA) who developed chronic kidney disease in the third decade of his life. This diagnosis was recognized by an increasing serum creatinine and confirmed by reduced glomerular filtration on a ^{99m}Tc -diethylenetriamine pentaacetate (DTPA) scan. Histopathology of the kidney showed moderate glomerulo- and tubulointerstitial fibrosis with very segmental mesangial IgA deposits. This is the second reported case of kidney disease in an individual with propionic acidemia possibly indicating that chronic kidney disease may be a late-stage complication of propionic acidemia. Additionally, this is the first description of the histopathology of kidney disease in an individual with propionic acidemia. As more cases emerge, the clinical course and spectrum of renal pathology in this disorder will be better defined.

Introduction

Propionic acidemia (PA) is a chronic, life-threatening organic acidemia that presents in childhood due to deficiency of the enzyme propionyl-CoA carboxylase (PCC), which catalyzes the conversion of propionyl-CoA to methylmalonyl-CoA (Fenton et al. 2001; de Baulny et al. 2012). Biochemical findings in affected patients include an elevation of the plasma C3 acylcarnitine species and elevated urine organic acids such as 3-hydroxypropionate, methylcitrate, tiglylglycine, and propionylglycine. Plasma amino acids demonstrate elevated glycine. The diagnosis can be confirmed by showing deficient enzyme activity in leukocytes or fibroblasts, or mutations in both alleles of either *PCCA* or *PCCB*, the genes that encode the subunits of PCC (Desviat et al. 2004; Ugarte et al. 1999).

Well-recognized morbidities of PA include acute episodes of hyperammonemia and metabolic acidosis. Affected individuals are susceptible to acute basal ganglia infarctions, pancreatitis, and bone marrow suppression. Chronic issues include intellectual disability, poor growth, cardiomyopathy, prolonged QT_c, and immune defects (de Baulny et al. 2012; Lee et al. 2009; Lücke et al. 2004; Surtees et al. 1992; Grünert et al. 2012; Sutton et al. 2012; Carillo-Carrasco and Venditti 2012; Baumgartner et al. 2007). As individuals with this disorder live longer, new complications potentially related to the disorder are being recognized. Acute-onset optic neuropathy is one of the more recently identified complications of this disorder (Williams et al. 2009; Ianchulev et al. 2003).

To date, only one case report has attempted to associate PA with chronic kidney disease (CKD) (Lam et al. 2011). Herein, we report an adult male with classic

Communicated by: John H Walter, MD FRCPCH

Competing interests: None declared

H.J. Vernon (✉)
McKusick-Nathans Institute of Genetic Medicine, Johns Hopkins University, 733 North Broadway, BRB 529, Baltimore, MD 21205, USA
e-mail: hvern1@jhmi.edu

S. Bagnasco
Department of Pathology, Johns Hopkins University, Baltimore, MD, USA

A. Hamosh
McKusick-Nathans Institute of Genetic Medicine, Johns Hopkins University, 600 North Wolfe Street, Blalock Building Room 1012D, Baltimore, MD 21287, USA

C.J. Sperati
Division of Nephrology, Department of Medicine, Johns Hopkins University, Baltimore, MD, USA

propionic acidemia who developed CKD in the third decade of life. We propose that CKD is a late complication of PA.

Methods and Results

Clinical Summary

The patient, now 29 years of age, first came to medical attention at 8 days of life. He presented with dehydration, lethargy, metabolic acidosis with total CO₂ 19 mEq/L and anion gap 24 mEq/L, hyperammonemia at 114 μmol/L (nl. 0–32 μmol/L), and a plasma glycine level of 900 μmol/L (nl. 87–323 μmol/L). The diagnosis of PA was supported by increased urinary excretion of hydroxypropionic acid and methylcitrate. The diagnosis was subsequently confirmed by absence of propionyl-CoA carboxylase and normal 3-methylcrotonyl carboxylase activities in peripheral leukocytes. Due to refractory hyperammonemia at 11 days of life (peak 690 μmol/L), he received peritoneal dialysis for approximately 1 month but has not required renal replacement therapy in the ensuing years.

The patient was recognized to have developmental delay at 13 months of age, when his development was estimated to be at around 8–9 months globally. Obsessive compulsive symptoms and anxiety symptoms were noted early in the second decade of life. Currently, he is considered to have mild intellectual disability with diagnoses of autistic disorder, anxiety disorder, and obsessive compulsive disorder. He is followed regularly by psychiatry, lives with his parents, and attends a 5-day-a-week day program.

Later in the second decade, he developed debilitating bowel dysmotility and was discovered to have intestinal malrotation. He underwent a Ladd procedure at 18 years of age, but continues to have severely delayed gastric emptying with intermittent bilious vomiting. He receives gastrostomy tube feedings of PediaSure®, Polycose, valine, and carnitine to provide 33 kcal/kg/day and 0.8 g/kg/day of protein.

At 15 years of life, mild to moderate left ventricular dysfunction was noted by echocardiography with prolonged QT_c interval. At 21 years of life, his left ventricular fractional shortening had decreased from baseline 25% to 18%, and he was initiated on lisinopril 5 mg daily. Hypertension was not present, and echocardiography at 29 years of life demonstrated mild to moderate global hypokinesis of the left ventricle with an ejection fraction of 40%. Additional past medical history was notable for osteoporosis with a femur fracture at 6 years of life and hypothyroidism diagnosed at 23 years of life.

Renal Evaluation

The patient was referred to nephrology at 29 years of age due to an elevated serum creatinine which had slowly risen over the preceding 7 years from 0.8 mg/dL to 1.5 mg/dL. The estimated glomerular filtration rate (eGFR) by the 4-variable Modification of Diet in Renal Disease equation was 51 mL/min/1.73 m², consistent with stage 3 CKD. At the time of referral to nephrology, the only urinary symptom was nocturnal enuresis attributed to 20-h enteral feedings. His medication regimen had not changed in several years and consisted of lisinopril 5 mg daily, risperidone, domperidone, ondansetron, levothyroxine, cetirizine, mirtazapine, omeprazole, sodium bicarbonate, and the above-listed enteral feedings. Family history was significant for the absence of kidney disease. Physical examination was normal, with blood pressure 90/60 mmHg, weight 66.2 kg, and height 163.8 cm. Additional laboratory evaluation (Table 1) was notable only for mild anemia and normal urinary protein excretion in the setting of angiotensin-converting enzyme inhibitor use. Liver function testing was normal. Computed tomography imaging of the abdomen with intravenous and oral contrast 5 years earlier had demonstrated structurally normal kidneys, as did renal ultrasonography at the time of kidney biopsy. A ^{99m}Tc-diethylenetriamine pentaacetate (DTPA) scan calculated a GFR of 38.5 mL/min/1.73 m², confirming reduced glomerular filtration reasonably consistent with the creatinine-based eGFR.

An ultrasound-guided percutaneous kidney biopsy was performed for further evaluation. Light microscopy revealed up to 31 glomeruli per section, of which up to 9 were globally sclerosed. One subcapsular glomerulus had a focal scar, and the remaining glomeruli were unremarkable (Fig. 1a). Immunofluorescence was performed on a frozen, non-sclerosed glomerulus, demonstrating fine granular, very segmental mesangial staining for IgG 2+, IgA 3-4+, IgM 1-2+, C3 2-3+ very sparse, kappa light chain 2+, and lambda light chain 2+. Glomerular staining was negative for C1q, with nonspecific linear staining for albumin 2+ in capillary loops and tubular basement membrane and fibrinogen 1-2+ in the interstitium (Fig. 1b, c). Electron microscopy was performed on one normal appearing glomerulus. Ultrastructurally, there was mild expansion of the mesangial matrix with a segmentally wrinkled but otherwise unremarkable glomerular basement membrane. There were very sparse small electron-dense deposits at the periphery of the mesangium (Fig. 1d). Podocytes demonstrated occasional vacuolizations and mild focal effacement of the foot processes estimated to involve less than 10% of the capillary surface. With such sparse glomerular electron-dense deposits and lack of mesangial proliferation, the

Table 1 Selected laboratory values at the time of nephrology evaluation

Variable	Value	Reference
Blood urea nitrogen (mg/dL)	18	7–22
Creatinine (mg/dL)	1.7	0.6–1.3
Sodium (mEq/L)	136	135–148
Total CO ₂ (mEq/L)	24	21–31
Calcium (mg/dL)	9.2	8.4–10.5
Phosphorous (mg/dL)	4.1	2.5–4.5
Uric acid (mg/dL)	4.2	3.7–8.6
Albumin (g/dL)	3.8	3.5–5.3
Ammonia (μ/dL)	100	27–102
Hemoglobin (g/dL)	11.3	13.9–16.3
Platelets (cells/mm ³)	162,000	150,000–350,000
Urinalysis		
pH	5	4.6–8.0
Protein	negative	negative
Red blood cells (per HPF)	1	0–5
White blood cells (per HPF)	0	0–5
Urine microalbumin/creatinine (mg/g)	3.2	0.0–30.0
25-vitamin D (ng/mL)	36.7	30–100
Complement C3 (mg/dL)	130	90–180
Complement C4 (mg/dL)	26	9–36
Antinuclear antibody	Negative	Negative
Free plasma carnitine (μmol/L)	12.6	22–66
Total plasma carnitine (μmol/L)	122.8	28–84
Urine citrate* (μg/mg creatinine)	12	12–96
Urine methylcitrate* (μg/mg creatinine)	105	0

*Semi-quantitative values derived from urine organic acid analysis. methylcitrate/citrate ratio is 8.75

possibility of a secondary nature of IgA deposition could not be excluded.

The tubules showed focal injury with cell blebbing and vacuolization, focal dilatation, and flattened epithelium. Ultrastructurally, the tubular cells showed focally enlarged mitochondria with disorganized cristae (Fig. 2a and b).

The interstitium showed mild, lymphocytic inflammatory infiltrate with rare eosinophils mostly associated with areas of fibrosis. Moderate tubular atrophy and interstitial fibrosis was present, involving approximately 25–30% of the cortical parenchyma. Three arteries up to interlobular size were present and appeared unremarkable, as did the arterioles.

Summary and Discussion

We report a patient with classical PA who presented with progressive CKD in the third decade of life. The clinical history did not reveal a likely etiology for CKD, apart from a low-normal blood pressure in the context of lisinopril administration at the time of referral. The kidney biopsy

demonstrated moderate glomerular and tubulointerstitial scarring, evidence of significant chronicity although non-specific for an etiology.

While the glomerular immunofluorescence demonstrated fine mesangial IgA deposits with small electron-dense deposits on electron microscopy, the absence of both mesangial proliferative changes and clinically significant proteinuria and hematuria render a primary diagnosis of autoimmune IgA nephropathy less likely. Autoimmune IgA nephropathy is the most common glomerulonephritis worldwide, estimated to account for 10% of all glomerulonephritis in the United States (Tumlin et al. 2007). Secondary forms of IgA nephropathy have been associated with multiple disorders, including cirrhosis, celiac disease, and inflammatory bowel disease. These are commonly due to impaired IgA clearance in the setting of cirrhosis or the formation of alternative immune complexes such as gliadin/anti-gliadin IgA with celiac disease (Pouria and Barratt 2008). In autoimmune IgA nephropathy, at least mild mesangial hypercellularity is typically present, with absent glomerular changes potentially suggesting a secondary

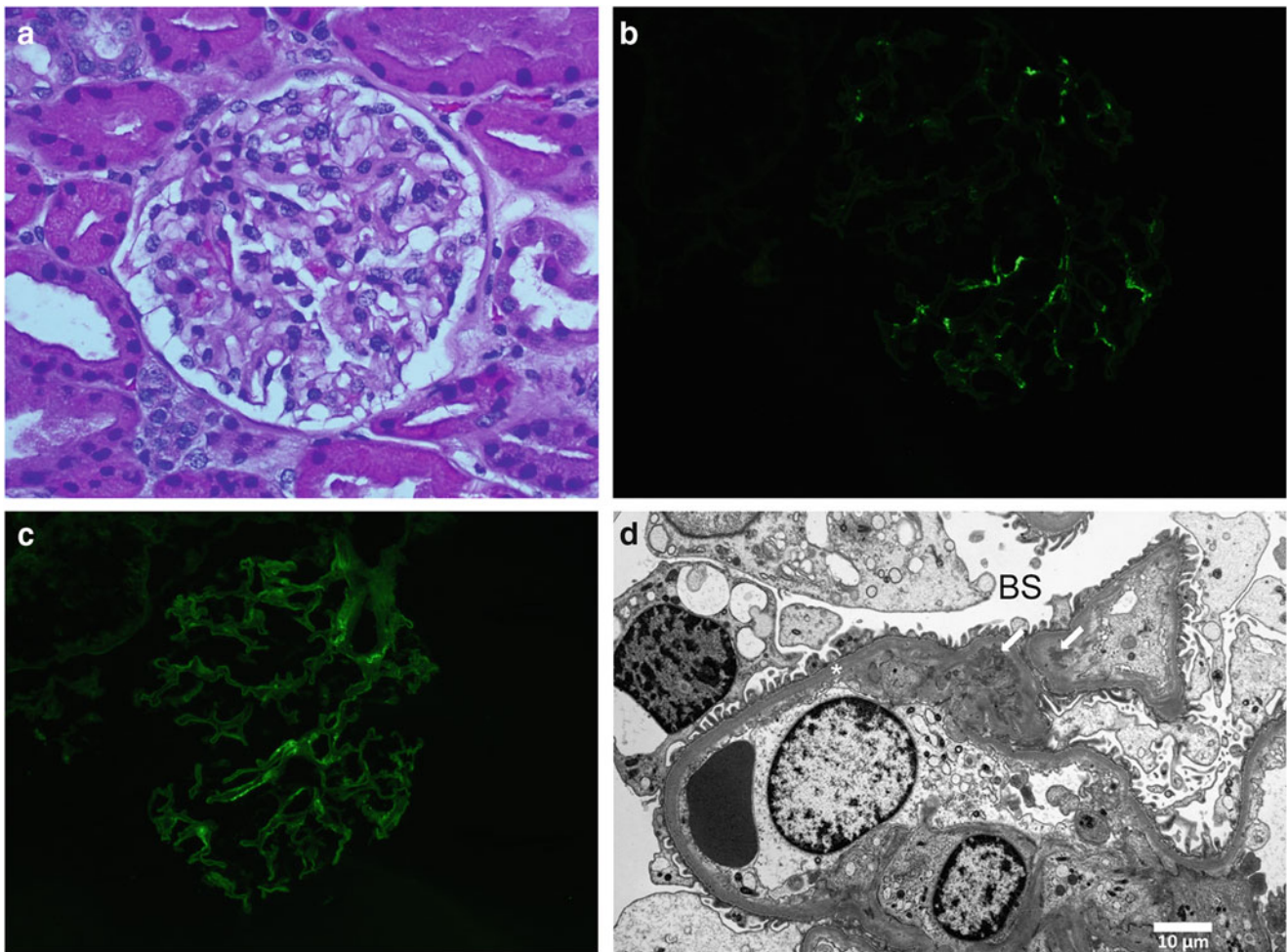


Fig. 1 (a) Histologically normal glomerulus by light microscopy (400x); (b) sparse IgA and (c) IgG mesangial deposits by immunofluorescence; (d) sparse electron-dense mesangial deposits (*arrows*) on electron microscopy. Glomerular basement membrane (*) and Bowman's space (*BS*)

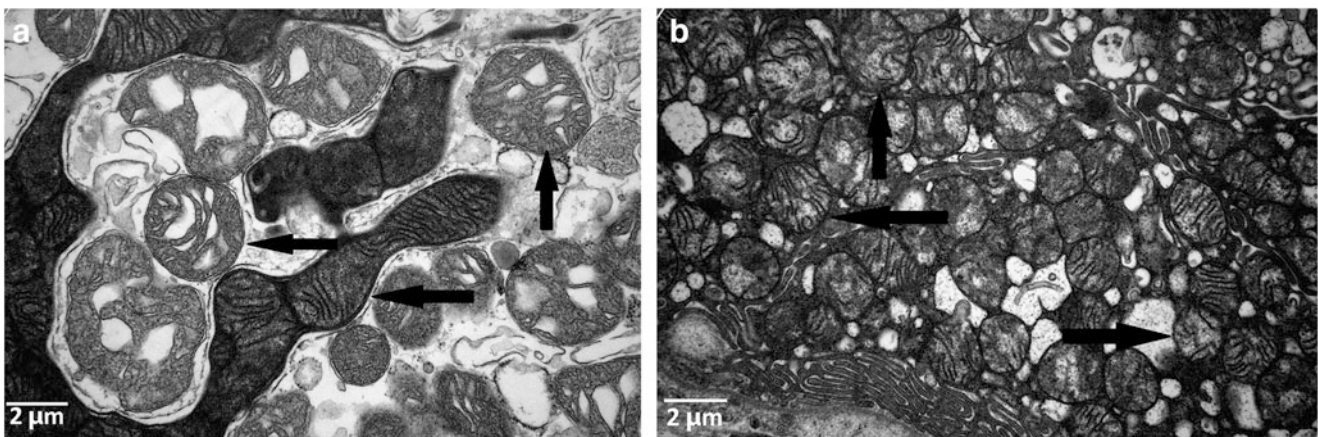


Fig. 2 (a and b) Enlarged abnormal mitochondria in tubular cells with disruption of cristae (indicated by *arrows*)

etiology (Haas 1997). Deposition of complement in the mesangium is also characteristic of autoimmune IgA nephropathy, and this patient had only sparse C3 by immunofluorescence perhaps more consistent with nonspecific immunoglobulin trapping or a secondary etiology. It is not known if IgA metabolism is altered in the setting of PA.

Renal pathology in humans affected with PA has not been previously described. In a mouse model of PA (*PCCA* knockout), all mice died within 24–36 h of birth due to dehydration and severe ketoacidosis (Miyazaki et al. 2001). Kidney histology revealed enlarged collecting ducts with protein resorption droplets. It was possible these findings stemmed from dehydration and malnutrition rather than an intrinsic renal process specific to PA. The early death of these animals precludes the observation of long-term renal sequelae of PA.

Renal pathology in the related disorder, methylmalonic acidemia (MMA), has been well described in both affected humans and in mouse models. Kidney biopsies from individuals with MMA classically show tubulointerstitial inflammation with mononuclear cell infiltrates and interstitial fibrosis with tubular atrophy (Rutledge et al. 1993; Walter et al. 1989; D'Angio et al. 1991; Molteni et al. 1991; Hörster and Hoffmann 2004). Kidneys from affected mice demonstrate dysmorphic mitochondria with abnormal cristae in the proximal tubular cells of the kidney, beginning at the end of the first week of life. Kidneys from older mice have severe and widespread tubulointerstitial changes similar to those reported in patients with MMA (Chandler et al. 2009). As noted, these tubulointerstitial changes are nonspecific but are consistent with those seen in our patient. Tubular cell mitochondria in our patient also appeared mildly dysmorphic, further suggesting a role for altered cellular metabolism in the pathology of PA-associated CKD.

We identified another published case of late-onset kidney disease in PA in the literature (Lam et al. 2011). The kidney failure in this patient was discovered in her fourth decade of life based on a rising serum creatinine. No additional laboratory characterization of the CKD was described and a kidney biopsy was not performed. Serum creatinine has often been deemed an unreliable marker of kidney function in some organic acidemias due to the low muscle mass of these patients and the restricted protein intake. Nevertheless, these two cases demonstrate the importance of monitoring eGFR in patients with PA. In our patient, creatinine-based estimation of GFR correlated acceptably well with measured GFR by ^{99m}Tc -DTPA scan. As no reversible lesion was identified on kidney biopsy, therapy has focused on surveillance for complications of CKD, avoidance of potentially nephrotoxic agents, and ongoing provision of optimal nutrition. The lisinopril dose was reduced to 2.5 mg daily and continued given the mild cardiomyopathy.

With advances in treatment and care of many inborn errors of metabolism, later-onset complications potentially related to the underlying disorder are now starting to emerge. While the etiology of this patient's CKD cannot be established with certainty, the histopathological findings do demonstrate tubulointerstitial disease for which PA must be entertained as a cause. We expect that as more cases emerge, the clinical course and spectrum of renal pathology in this disorder will be better defined.

Synopsis

This is the second reported case of kidney disease in an individual with propionic acidemia, and the first report with pathologic information, indicating that chronic kidney disease may be a late-stage complication of propionic acidemia.

References

- Baumgartner D, Scholl-Bürgi S, Sass JO et al (2007) Prolonged QTc intervals and decreased left ventricular contractility in patients with propionic acidemia. *J Pediatr* 150:192–197
- Carrillo-Carrasco N, Venditti C (2012) **Propionic Acidemia**. In: R.A. Pagon, T.D. Bird, C.R. Dolan, K. Stephens, M.P. Adam (eds) *GeneReviews™* [Internet]. University of Washington, Seattle; 1993–2012. Available from: <http://www.ncbi.nlm.nih.gov/books/NBK92946/>
- Chandler RJ, Zerfas PM, Shanske S et al (2009) Mitochondrial dysfunction in mutant methylmalonic acidemia. *FASEB J* 23:1252–1261
- D'Angio CT, Dillon MJ, Leonard JV (1991) Renal tubular dysfunction in methylmalonic acidemia. *Eur J Pediatr* 150:259–263
- de Baulny HO, Dionisi-Vici C, Wendel U (2012) Branched chain organic acidurias/acidemias. In: Saudubray JM, van den Berghe G, Walter JH (eds) *Inborn metabolic diseases- diagnosis and treatment*. Springer, New York, pp 277–296
- Desviat LR, Pérez B, Pérez-Cerdá C et al (2004) Propionic acidemia: mutation update and functional and structural effects of the variant alleles. *Mol Genet Metab* 83:28–37
- Fenton WA, Grave RA, Rosenblatt DA (2001) Disorders of propionate and methylmalonate metabolism. In: Valle D, Beaudet AL, Vogelstein B, Kinzler KW, Antonarakis SE, Ballabio A (eds) *The online metabolic & molecular bases of inherited disease* [Internet]. Available from: http://www.ommbid.com/OMMBID/a/c.html/organic_acids/disorders_propionate_methylmalonate_metabolism
- Grünert SC, Müllerleile S, de Silva L et al (2012) Propionic acidemia: neonatal versus selective metabolic screening. *J Inher Metab Dis* 35:41–49
- Haas M (1997) Histologic subclassification of IgA nephropathy: a clinicopathologic study of 244 cases. *Am J Kidney Dis* 29:829–842
- Hörster F, Hoffmann GF (2004) Pathophysiology, diagnosis, and treatment of methylmalonic aciduria-recent advances and new challenges. *Pediatr Nephrol* 19:1071–1074
- Ianchulev T, Kolin T, Moseley K et al (2003) Optic nerve atrophy in propionic acidemia. *Ophthalmology* 110:1850–1854

- Lam C, Desviat LR, Perez-Cerdá C et al (2011) 45-Year-old female with propionic acidemia, renal failure, and premature ovarian failure: late complications of propionic acidemia? *Mol Genet Metab* 103:338–340
- Lee TM, Addonizio LJ, Barshop BA et al (2009) Unusual presentation of propionic acidemia as isolated cardiomyopathy. *J Inher Metab Dis* 32:97–101
- Lücke T, Pérez-Cerdá C, Baumgartner M et al (2004) Propionic acidemia: unusual course with late onset and fatal outcome. *Metabolism* 53:809–810
- Miyazaki T, Ohura T, Kobayashi M et al (2001) Fatal propionic acidemia in mice lacking propionyl-CoA carboxylase and its rescue by postnatal, liver-specific supplementation via a transgene. *J Biol Chem* 276:35995–35999
- Molteni KH, Oberley TD, Wolff JA et al (1991) Progressive renal insufficiency in methylmalonic acidemia. *Pediatr Nephrol* 5:323–326
- Pouria S, Barratt J (2008) Secondary IgA nephropathy. *Semin Nephrol* 28:27–37
- Rutledge SL, Geraghty M, Mroczek E et al (1993) Tubulointerstitial nephritis in methylmalonic acidemia. *Pediatr Nephrol* 7:81–82
- Surtees RA, Matthews EE, Leonard JV (1992) Neurologic outcome of propionic acidemia. *Pediatr Neurol* 8:333–337
- Sutton VR, Chapman KA, Gropman AL et al (2012) Chronic management and health supervision of individuals with propionic acidemia. *Mol Genet Metab* 105:26–33
- Tumlin JA, Madaio MP, Hennigar R (2007) Idiopathic IgA nephropathy: pathogenesis, histopathology, and therapeutic options. *Clin J Am Soc Nephrol* 2:1054–1061
- Ugarte M, Pérez-Cerdá C, Rodríguez-Pombo P et al (1999) An overview of mutations in the PCCA and PCCB genes causing propionic acidemia. *Hum Mutat* 14:275–282
- Walter JH, Michalski A, Wilson WM et al (1989) Chronic renal failure in methylmalonic acidemia. *Eur J Pediatr* 148:344–348
- Williams SR, Hurley PE, Altiparmak UE et al (2009) Late onset optic neuropathy in methylmalonic and propionic acidemia. *Am J Ophthalmol* 147:929–933

Transient Massive Trimethylaminuria Associated with Food Protein–Induced Enterocolitis Syndrome

Natalie B. Miller • Avraham Beigelman •
Elizabeth Utterson • Marwan Shinawi

Received: 05 December 2012 / Revised: 03 April 2013 / Accepted: 13 May 2013 / Published online: 3 July 2013
© SSIEM and Springer-Verlag Berlin Heidelberg 2013

Abstract Trimethylaminuria (TMAU) is an autosomal recessive disease caused by excessive excretion into body fluids and breath of unoxidized trimethylamine (TMA) derived from the enterobacterial metabolism of dietary precursors. The condition is caused by deficiency of flavin-containing monooxygenase 3 (FMO3) which leads to impairment of hepatic TMA oxidation to the odorless trimethylamine *N*-oxide. Secondary TMAU is due to substrate overload in individuals with genetically determined reduced enzyme activity. Food protein–induced enterocolitis syndrome (FPIES) is characterized by recurrent episodes of emesis, diarrhea, dehydration, and lethargy after ingestion of offending foods. Its pathophysiology involves local non-IgE-mediated inflammation of the gastrointestinal tract, which leads to increased intestinal permeability. We report on an 8-month-old male who presented with typical episodes of FPIES associated with intense fish-like body odor. Further investigation in our patient revealed massive urinary TMA excretion during acute FPIES presentation and complete normalization between these episodes. The patient was found

to be heterozygous for a novel, paternally inherited nonsense p.Tyr331X mutation and for two maternally inherited common polymorphisms, E158K and E308G, in the *FMO3* gene. We propose that our patient was able to cope with the daily burden of TMA, but when challenged with substrate overload, he failed to oxidize TMA due to limited reserve enzyme capacity. We discuss the pathophysiology of TMAU and FPIES and suggest potential mechanisms for the clinical and biochemical findings. Our report illustrates the complex interplay of genetic and environmental factors in TMAU and sheds light on the pathophysiology of FPIES.

Introduction

Trimethylamine (TMA) is a volatile, fish-smelling compound that is formed via the reduction of trimethylamine-*N*-oxide (TMAO) and choline (Phillips and Shephard 2011). Choline is found in peas, beans, organ meats, and egg yolks. Different foods contain different amounts of choline: breast milk 160 mg/L of choline (approximately 120 mg/100 g food), formula 175 mg/L (approximately 130 mg/100 g food), banana 9.8 mg/100 g food, rice 2.1 mg/100 g food, oat 32 mg/100 g food (<http://www.nal.usda.gov/fnic/foodcomp/Data/Choline/Choln02.pdf>) (US Database for the Choline Content of Common Foods 2008). TMAO is found in high concentrations in marine fish. Bacteria in rotting fish reduce TMAO to TMA, producing a fish-like odor. Bacteria in the mammalian gut also reduce TMAO to TMA, which then enters the enterohepatic circulation. In the liver, the hepatic enzyme FMO3 oxidizes TMA back to TMAO, an odorless, water-soluble compound excreted in the urine. Trimethylaminuria (TMAU) is caused by excessive accumulation of the fish-smelling TMA, which is excreted in the urine, sweat, breath as well as other bodily secretions (Mackay et al. 2011).

Communicated by: Johannes Zschocke

Competing interests: None declared

N.B. Miller • A. Beigelman

Department of Pediatrics, Division of Allergy, Immunology, and Pulmonary Medicine, Washington University School of Medicine, St. Louis, MO, USA

E. Utterson

Department of Pediatrics, Division of Gastroenterology and Nutrition, Washington University School of Medicine, St. Louis, MO, USA

M. Shinawi (✉)

Department of Pediatrics, Division Genetics and Genomic Medicine, Washington University School of Medicine, One Children's Place, Northwest Tower, 9132, Campus Box 8116, St. Louis 63110, MO, USA

e-mail: Shinawi_M@kids.wustl.edu

The superfluous excretion of trimethylamine is the result of a mismatch between enzyme capacity (its ability to form the non-odorous TMAO) and the amount of the substrate (TMA) (Mitchell and Smith 2001). Factors that increase the substrate burden include (1) microbial liberation of TMA from dietary precursor chemicals (bacterial overgrowth, and renal and hepatic diseases), (2) increased TMA absorption (gastrointestinal problems), or (3) simply an enriched diet. Diagnosis is made via measurement of TMA and TMAO in the urine: a TMAO/ (TMA + TMAO) ratio (also known as FMO3 metabolic capacity) (Yamazaki et al. 2004) of <92 % and/or a urinary concentration of free TMA of 18–20 $\mu\text{mol}/\text{mmol}$ creatinine is diagnostic of TMAU (Mayatepek and Kohlmüller 1998; Mitchell and Smith 2001; Cashman et al. 2003).

“Secondary trimethylaminuria” is due to substrate overload in individuals with genetically determined reduced enzyme activity and who might not exhibit any symptoms until they challenged with excessive amounts of TMA or its precursors (Mackay et al. 2011).

Food protein–induced enterocolitis syndrome (FPIES) is a non-IgE-mediated gastrointestinal hypersensitivity to food. It typically presents before 6 months of age, and usually resolves by 3 years of age. It is characterized by repeated episodes of profound vomiting and often diarrhea, beginning 1–5 h after ingestion of the offending food, and leads to lethargy, dehydration, and occasionally to shock. The most common offending foods are milk, soy, and rice (Mehr et al. 2009; Leonard and Nowak-Węgrzyn 2011). The repetitive nature of the condition and its association with lethargy and vomiting may suggest metabolic conditions.

The pathophysiology of FPIES is not clearly elucidated. It likely involves defects in both barrier and immunologic function of the gastrointestinal tract. Ingestion of food allergens causes local inflammation, which may lead to increased intestinal permeability and fluid shifts, and may lead to vomiting and diarrhea (Leonard and Nowak-Węgrzyn 2011). Multiple studies have suggested a role of the pro-inflammatory cytokine, TNF- α (Chung et al. 2002; Caubet et al. 2011). High amounts of TNF- α have been found to be released by antigen-specific T cells in the GI tract. TNF- α works synergistically with IFN- γ to increase intestinal permeability (Heyman et al. 1994). High levels of TNF- α have also been observed in infants with FPIES and associated villous atrophy (Caubet and Nowak-Węgrzyn 2011; Chung et al. 2002). Another cytokine implicated is TGF- β 1, which suppresses T cells, protects the epithelial barrier of the gut, enhances binding between epithelial cells and the extracellular matrix, and stimulates the expression of extracellular matrix proteins. Infants less than 3 months old have decreased expression of TGF- β 1, and this expression increases with age (Chung et al. 2002). This developmental deficiency of TGF- β 1 may allow for increased intestinal permeability and less T cell suppression in young infants (Caubet and Nowak-Węgrzyn 2011).

Here, we describe an infant with repeated episodes of adverse food reactions, consistent with FPIES, associated with a “fishy” odor. He was found to have excessive excretion of TMA during FPIES episodes and to be heterozygous for the novel nonsense p.Tyr331X mutation and for two common polymorphisms, E158K and E308G, in the *FMO3* gene.

Case Presentation

The proband is a Caucasian male infant who has had recurrent episodes of adverse reactions to food since the age of 4 months. Initially, he developed repeated episodes of profound emesis and lethargy 2 h after eating rice cereal mixed with expressed breast milk. Vomiting was followed by diarrhea that occurred 6–8 h after food ingestion. His symptoms seemed to improve about 8 h after ingestion, and resolved within 24 h. During this episode, his mother noted a strong, “fishy” odor, which had never been noted previously. He had four more similar episodes, at 5 months, 7 months, and 10 months of age, after eating rice cereal, oat, and banana. During each of these episodes, the “fishy” odor was noted, but was not noted between episodes. He was evaluated in the Emergency Department for all the three episodes, and required hospitalization for intravenous hydration during the 10-month episode.

The proband was born full-term at 37 weeks gestation via spontaneous vaginal delivery. His birth weight was 3.29 kg and birth length was 53 cm. The mother was 22 years old at delivery, this was her second pregnancy and it was conceived naturally. She was treated with Procardia and prenatal vitamins. Pregnancy was complicated by premature contractions at 26 weeks gestation. The mother was treated with two injections of steroids for lung maturity at 27 weeks gestation. There were no perinatal or neonatal complications. The patient had normal newborn metabolic and hearing screens, and was discharged home 48 h after delivery. He met his developmental milestones and there has been no history of developmental regression. His past medical history is significant for ptosis status post surgical repair at 6 months of age. He was followed by cardiology for a VSD, which spontaneously closed. His mother is of white Caucasian descent (German/Scottish). She is healthy except for irritable bowel syndrome and Gilbert disease. She has a history of spontaneous abortion at 3 months gestation. His father is 26 years old and is of white Caucasian descent (German). He is healthy except for irritable bowel syndrome.

Food-specific IgE testing, using the Phadia ImmunoCAP system FEIA (Phadia, Uppsala, Sweden), to multiple foods, including rice, banana, oat, beef, chicken, and turkey, were all below level of detection (<0.34 kU/L). CBC, electrolytes, and renal and liver function were all within normal limits. Due to concerns of metabolic disorders, acylcarnitine

Table 1 Urinary excretion of TMA, TMA-N-oxide (TMAO) [($\mu\text{mol}/\text{mmol}$ creatinine)] and the percentage of total TMA excreted as TMAO in our patient, patients with trimethylaminuria, and healthy controls

Timing of the testing	TMA (normal <1)	TMAO (normal 15–125)	Percentage of total urine TMA excreted as TMAO (normal >92 %)
Before FPIES	2.3	54.2	95.9
During FPIES	551.91	4423.38	88.9
After FPIES	3.4	63.7	94.9
During acute gastroenteritis	8.8	51.9	85.5
Reported cases of fish-odor syndrome ($n = 4$) (Mayatepek & Kohlmuller 1998)	>18	<2	<10

panel, serum amino acids, urine organic acids, ammonia, lactate/pyruvate, and CK were obtained and were within normal limits. Due to mother's complaints of "fishy odor", a quantitative analysis of urine TMA and TMAO using electrospray ionization tandem mass spectrometry (ESI-MS/MS), as previously described (Johnson 2008), was ordered 3 days before an acute episode of FPIES and revealed normal results. However, during admission for acute FPIES episode, a massive urinary TMA and TMAO excretion with decreased total TMA percentage excreted as TMAO was documented (Table 1). On a follow-up visit after the hospitalization, urine TMA and TMAO levels as well as total TMA percentage excreted as TMAO normalized. During a subsequent hospitalization for gastroenteritis, which was not consistent with FPIES and was not associated with fishy odor, TMA and TMAO levels were normal, but percentage of total urine TMA excreted as TMAO was mildly decreased.

Sequencing of *FMO3*, the gene for trimethylaminuria, revealed paternally inherited nonsense, c.993_994delTA (p.Tyr331Stop) mutation. This truncating mutation has not been previously reported, but its effect on the protein is predicted to be pathogenic. The sequencing also revealed two maternally inherited common polymorphisms, E158K and E308G. Deletion studies of the *FMO3* gene were normal.

Discussion

Primary TMAU is due to an inherited deficiency of the enzyme FMO3, leading to inefficient conversion of TMA to the odorless TMAO in the liver. It is an autosomal recessive condition, and carriers are described as asymptomatic (Mackay et al. 2011). However, carriers can be

detected by using an oral challenge of TMA and measurement of TMA and TMAO concentrations in urine. One study specifically examined asymptomatic parents of six patients with TMAU. After an oral challenge with 600 mg of TMA, all obligate carriers showed significant increase in TMA excretion, while healthy volunteers did not show increased TMA excretion until challenged with at least 900 mg of TMA (Al-Waiz et al. 1989). This suggests that the FMO3 enzyme can be overwhelmed by an influx of substrate, and the threshold is lower in heterozygotes, likely due to lower enzyme availability. Functional analysis of several mutations revealed a genotype-phenotype correlation; the greater the effect of the mutation on the FMO3 enzyme activity the more severe the symptoms (Phillips and Shephard 2011). Null mutations predominantly result in more severe and persistent malodor.

Secondary TMAU has been documented, and some have associated genetic variations. Case reports in the literature describe TMAU in patients with viral hepatitis or impaired hepatocellular function, during treatment with therapeutic choline in Alzheimer's patients and even in association with the menstrual cycle (Shimizu et al. 2007; Mackay et al. 2011). There are also case reports of transient childhood TMAU (Mayatepek and Kohlmuller 1998). These children ingested normal childhood diets, some breast fed and some fed choline-containing formula. These children present with typical malodor and demonstrate increased TMA urine excretion and total TMA percentage excreted as TMAO less than 90 %. Without intervention, the malodor resolved and the TMA urinary excretion normalized (Mayatepek and Kohlmuller 1998). It was postulated that the metabolic capacity of FMO3 is overwhelmed in these cases, either because of relative developmental deficiency of FMO3 that normalized with age (Koukouritaki et al. 2002) or an overproduction of substrate (TMA) by gut flora (Mayatepek and Kohlmuller 1998). Interestingly, sequencing of the *FMO3* gene in patients with transient TMAU revealed compound heterozygosity for severe mutations on one chromosome and variant alleles, carrying two amino acid polymorphisms, c.472G > A and c.923A > G (E308G; E158K) on the other chromosome (Zschocke et al. 1999; Zschocke and Mayatepek 2000). It was shown that homozygosity for the allele E158K/E308G can be also associated with symptomatic FMO3 deficiency as in transient childhood TMAU (Zschocke and Mayatepek 2000) or transient TMAU associated with menstruation (Shimizu et al. 2007). This supports the spectrum of phenotypes observed, and the important interplay between genetic and environmental effects in TMAU.

The fish-odor in our patient was only noted during acute episodes consistent with FPIES. At first glance, FPIES and TMAU appear unrelated and, since both conditions are

rare, they are less likely to coexist in the same individual. However, further investigation in our patient revealed massive urinary TMA excretion during acute FPIES presentation and complete normalization between these episodes. Genetic analysis of the *FMO3* gene revealed that he was heterozygous for the novel nonsense p.Tyr331X mutation and for the two above-mentioned common polymorphisms, E158K and E308G.

Our patient showed remarkable increase in TMAO excretion during FPIES with approximately 12.5 % of total trimethylamine excreted as TMA, suggesting a relatively high in vivo residual oxidative activity of FMO3. He was probably able to cope with the daily burden of TMA (from dietary TMAO and choline), but when challenged with a large substrate load, his limited enzyme capacity was overwhelmed. We hypothesize that the mild decrease in FMO3 activity in our patient is linked to relative developmental deficiency of FMO3 (Koukouritaki et al. 2002) and to genetic susceptibility caused by compound heterozygosity for a severe mutation (p.Tyr331X) on one allele and two polymorphisms (E308G; E158K) on the second allele, as was previously described with transient childhood TMAU (Zschocke et al. 1999; Zschocke and Mayatepek 2000). In addition, FPIES-induced increased inflammation in the gastrointestinal tract (Caubet and Nowak-Wegrzyn 2011; Chung et al. 2002; Heyman et al. 1994) may have also played a role in the downregulation of *FMO3*, which has been observed previously in a mouse model of inflammation using *C. rodentium* infection (Zhang et al. 2009).

The patient has exhibited massive TMAU with only mildly decreased urinary TMAO/Total TMA ratio. This suggests that TMAU was caused predominantly by substrate overload rather than severe enzyme deficiency. These levels of urinary trimethylamines are rarely observed even following fish meal or choline loads (Chalmers et al. 2006). We are puzzled over the origin of the substrate as the patient did not take significant amounts of fish, choline, or lecithin. In addition, he has never received supplements such as carnitine or betaine. Other rare causes of secondary TMAU including chronic hepatic disease and renal failure were not present in this patient. Congenital intrahepatic portal-systemic shunt was associated with TMAU but with low TMAO/total TMA ratio. Abnormal overgrowth of small intestinal bacteria can greatly increase TMA production but FPIES is not typically associated with excessive bacterial proliferation. The function of enterocytes tight junctions as a significant barrier to diffusion can be severely altered in FPIES (Caubet and Nowak-Wegrzyn 2011), potentially causing enhanced transepithelial influx of different types of molecules. However, it is unclear whether the increased intestinal permeability contributed to TMAU in this patient. We speculate that the remarkable FPIES-related inflammation can cause local

gastrointestinal tissue damage, which subsequently releases significant amounts of choline and lecithin.

To our knowledge, this is the first report of episodic TMAU associated with FPIES, which should be added to the growing list of conditions linked to secondary TMAU. This report illustrates the complex interplay of genetic and environmental factors in TMAU and sheds light on the pathophysiology of TMAU and FPIES. Additional studies and cases are needed to improve our understanding of potential association between these two conditions.

Synopsis

Transient massive trimethylaminuria can be associated with food protein-induced enterocolitis syndrome in genetically susceptible individuals. The findings illustrate the pathogenicity and complex interplay of genetic and environmental factors in trimethylaminuria.

References

- Al-Waiz M, Ayesh R, Mitchell SC, Idle JR, Smith RL (1989) Trimethylaminuria: the detection of carriers using a trimethylamine load test. *J Inher Metab Dis* 12(1):80–85
- Cashman JR, Camp K, Fakharzadeh SS, Fennessey PV, Hines RN, Mamer OA et al (2003) Biochemical and clinical aspects of the human flavin-containing monooxygenase form 3 (FMO3) related to trimethylaminuria. *Curr Drug Metab* 4:151–170
- Caubet JC, Nowak-Wegrzyn A (2011) Current understanding of the immune mechanisms of food protein-induced enterocolitis syndrome. *Expert Rev Clin Immunol* 7(3):317–327
- Chalmers RA, Bain MD, Michelakakis H, Zschocke J, Iles RA (2006) Diagnosis and management of trimethylaminuria (FMO3 deficiency) in children. *J Inher Metab Dis* 29:162–72
- Chung HL, Hwang JB, Park JJ, Kim SG (2002) Expression of transforming growth factor b1, transforming growth factor type I and II receptors, and TNF-a in the mucosa of the small intestine in infants with food protein-induced enterocolitis syndrome. *J Allergy Clin Immunol* 109(1):150–154
- Heyman M, Darmon N, Dupont C, Dugas B, Hirribaren A, Blaton MA, et al. (1994) Mononuclear cells from infants allergic to cow's milk secrete tumor necrosis factor alpha, altering intestinal function. *Gastroenterology* 106(6):1514–1523
- Johnson DW (2008) A flow injection electrospray ionization tandem mass spectrometric method for the simultaneous measurement of trimethylamine and trimethylamine N-oxide in urine. *J Mass Spectrom* 43:495–499
- Koukouritaki SB, Simpson P, Yeung CK, Rettie AE, Hines RN (2002) Human hepatic flavin-containing monooxygenases 1 (FMO1) and 3 (FMO3) developmental expression. *Pediatr Res* 51:236–243
- Leonard SA, Nowak-Wegrzyn A (2011) Food protein-induced enterocolitis syndrome: an update on natural history and review of management. *Ann Allergy Asthma Immunol* 107(2): 95–101
- Mackay RJ, McEntyre CJ, Henderson C, Lever M, George PM (2011) Trimethylaminuria: causes and diagnosis of a socially distressing condition. *Clin Biochem Rev* 32(1):33–43
- Mayatepek E, Kohlmuller D (1998) Transient trimethylaminuria in childhood. *Acta Paediatr* 87(11):1205–1207

- Mehr S, Kakakios A, Frith K, Kemp AS (2009) Food protein-induced enterocolitis syndrome: 16-year experience. *Pediatrics* 123(3): e459–e464
- Mitchell SC, Smith RL (2001) Trimethylaminuria: the fish malodor syndrome. *Drug Metab Dispos* 29(4 Pt 2):517–521
- Phillips IR, Shephard EA [2007 Oct 8 (Updated 2011 Apr 19)]. Trimethylaminuria. In: Pagon RA, Bird TD, Dolan CR, et al (eds) *GeneReviews™* [Internet]. University of Washington, Seattle (WA); Seattle, 1993–. Available from: <http://www.ncbi.nlm.nih.gov/books/NBK1103/>
- Shimizu M, Cashman JR, Yamazaki H (2007) Transient trimethylaminuria related to menstruation. *BMC Med Genet* 8:2
- US Database for the Choline Content of Common Foods, 2008. <http://www.nal.usda.gov/fnic/foodcomp/Data/Choline/Choln02.pdf>. Accessed 5/11/12
- Yamazaki H, Fujieda M, Togashi M, Saito T, Preti G, Cashman JR et al (2004) Effects of the dietary supplements, activated charcoal and copper chlorophyllin, on urinary excretion of trimethylamine in Japanese trimethylaminuria patients. *Life Sci* 74(22): 2739–2747
- Zhang J, Chaluvadi MR, Reddy R, Motika MS, Richardson TA, Cashman JR et al (2009) Hepatic flavin-containing monooxygenase gene regulation in different mouse inflammation models. *Drug Metab Dispos* 37(3):462–468
- Zschocke J, Mayatepek E (2000) Biochemical and molecular studies in mild flavin monooxygenase 3 deficiency. *J Inherit Metab Dis* 23(4):378–382
- Zschocke J, Kohlmüller D, Quak E, Meissner T, Hoffmann GF, Mayatepek E (1999) Mild Trimethylaminuria by common variants in FMO3 gene. *Lancet* 354(9181):834–835

Increased Prevalence of Hypertension in Young Adults with High Heteroplasmy Levels of the MELAS m.3243A>G Mutation

Fady Hannah-Shmouni • Sandra Sirrs •
Michelle M. Mezei • Paula J. Waters • Andre Mattman

Received: 12 December 2012 / Revised: 06 May 2013 / Accepted: 13 May 2013 / Published online: 12 July 2013
© SSIEM and Springer-Verlag Berlin Heidelberg 2013

Abstract Background: The pathophysiology of hypertension in patients with mitochondrial diseases is different from that of the general population. Growing evidence exists linking mtDNA, its mutations, and mitochondrial dysfunction to the pathogenesis of hypertension. No reports on the prevalence of hypertension in late-onset mtDNA diseases have been described.

Methods: We performed a retrospective chart review of adult patients with late-onset mtDNA diseases between January 1999 and January 2012 at our center. We grouped them into age categories to allow comparison with previously reported Canadian Health Measures Survey (CHMS) prevalence data.

Communicated by: Garry Brown

Competing interests: None declared

F. Hannah-Shmouni (✉)
Internal Medicine Resident, Yale-New Haven Hospital,
Yale University School of Medicine, New Haven, CT, USA
e-mail: fady.hannah-shmouni@yale.edu

S. Sirrs
Medical Director, Adult Metabolic Diseases Clinic, Division of
Endocrinology & Metabolism, Vancouver General Hospital, UBC,
Vancouver, BC, Canada

M.M. Mezei
Adult Metabolic Diseases Clinic, Division of Endocrinology &
Metabolism, and Division of Neurology, Vancouver General Hospital,
UBC, Vancouver, BC, Canada

P.J. Waters
Medical Genetics Service, Centre Hospitalier Universitaire de
Sherbrooke, Fleurimont, QC, Canada

A. Mattman
Adult Metabolic Diseases Clinic, Division of Endocrinology &
Metabolism, Vancouver General Hospital, UBC, Vancouver, BC,
Canada

Results: Twenty-three subjects with hypertension were identified for a crude prevalence of 39.7 % (95 % CI 27–53 %) as compared to the CHMS age-predicted prevalence of 30.5 %. When analyzed by individual age group, there were no significant differences between the observed and the CHMS predicted prevalence rates in the 40 years and older cohorts (age category 40–59, $p = 0.63$; age category 60–79, $p = 0.85$). However, hypertension rates were significantly higher than predicted in the under 40 years cohort (55.6 vs. 2.8 %, $p < 0.001$, CI 21–86 %), in which hypertensive patients with the MELAS m.3243A>G mutation were significantly clustered ($p < 0.01$). This younger MELAS cohort ($n = 4$, mean age = 24 years) with hypertension had heteroplasmy levels (mean = 68 %) that were significantly higher than the levels found in the older non-hypertensive MELAS cohort ($n = 8$, mean age = 52 years, mean = 33 %) ($p = 0.04$).

Conclusion: Relative to age, gender, and mtDNA disease subtype, young adults with high heteroplasmy levels of the MELAS m.3243A>G mutation demonstrate an increased prevalence of hypertension. Further prospective data are needed to confirm this initial finding, which has potentially important treatment implications.

Introduction

The mitochondrion is an important cellular structure responsible for energy production. Multiple causes of mitochondrial dysfunction are recognized and can be grouped into primary “inherited” (Schapira 2006; Koopman et al. 2012) or secondary causes (Koopman et al. 2012; Coskun et al. 2011; McCoy and Cookson 2011; Cairns et al. 2011; Hoppel et al. 2009; Sleight et al. 2011; Finsterer and Segal 2010; Cohen 2010). This dysfunction, regardless

of cause, disrupts cellular energy metabolism and produces reactive oxygen species (Nageswara et al. 2007) that lead to accumulation of mitochondrial DNA (mtDNA) mutations, and further impair mitochondrial function (Nageswara et al. 2007).

Despite the heterogeneity of clinical manifestations of late-onset mtDNA diseases (Koopman et al. 2012; Thorburn 2004), certain genetic mutations are associated with a predisposition to select phenotypes (Koopman et al. 2012; Thorburn 2004). The most common clinical syndrome observed in our clinic is the chronic progressive external ophthalmoplegia plus (CPEO+) syndrome, usually associated with multiple mtDNA deletions (Pfeffer et al. 2011). The most common clinical manifestations in this syndrome are bilateral ptosis and ophthalmoparesis due to myopathy affecting the extraocular muscles (Pfeffer et al. 2011). There is also a variable degree of skeletal myopathy with 62 % of patients having one or more of the following findings: objective muscle weakness, exertional myalgia, and polyneuropathy (Pfeffer et al. 2011). The Kearns-Sayre (KSS) syndrome is similar to the CPEO syndrome but includes pigmentary retinopathy and cardiac conduction abnormalities (Pfeffer et al. 2011). This syndrome is usually associated with a sporadic onset major deletion in the mtDNA (Pfeffer et al. 2011). The second most common syndrome is the mitochondrial encephalomyopathy, lactic acidosis, and stroke-like episode (MELAS) syndrome associated with the m.3243A>G mutation (Yatsuga et al. 2012). The most common clinical manifestations of the late-onset form of this syndrome are stroke-like episodes and seizures (each affecting more than 60 % of patients), diabetes mellitus (40 %), and proximal muscle weakness and general fatigue (each affecting greater than 30 % of patients) (Yatsuga et al. 2012). Another relatively common form is the myoclonic epilepsy with ragged red fiber syndrome (MERRF) associated with the m.8344A>G mutation (Silvestri et al. 1993). The most common clinical manifestations of this syndrome are central nervous system manifestations of myoclonus, seizures, and ataxia in combination with a skeletal myopathy that frequently manifests with proximal weakness and exercise intolerance (Silvestri et al. 1993). Less common forms have a variable combination of multisystemic disease manifestations. Hypertension is now associated with select subtypes of mtDNA mutations (Map of the human mitochondrial DNA 2012) including mtDNA mutations affecting mitochondrial transfer RNA coding sequences, and those affecting coding sequences for electron transport chain complex I subunit proteins.

The links between mitochondrial dysfunction, mtDNA mutation, and hypertension have not been widely appreciated prior to the past decade. In this time, mitochondrial haplogroup analysis, case reports of patients with mtDNA

diseases, and genetic studies in hypertensive pedigrees have all uncovered connections between the genetic disorder and the clinical phenotype of hypertension. Specifically, mitochondrial haplogroups represent common population-specific variants that confer relative susceptibility to common diseases such as diabetes mellitus, atherosclerosis, cancer, aging, Alzheimer's, and schizophrenia (Koopman et al. 2012; Coskun et al. 2011; McCoy and Cookson 2011; Cairns et al. 2011; Hoppel et al. 2009; Sleight et al. 2011; Finsterer and Segall 2010; Cohen 2010). These mitochondrial haplogroups are also known to influence the maternal inheritance pattern of hypertension (Schwartz et al. 2004). Moreover, several studies have shown that specific heteroplasmic mtDNA mutations, which may cause clinical symptoms in childhood or in adulthood, specifically predispose to hypertension (Schwartz et al. 2004; Borhani et al. 1969; Gerson and Fodor 1975; Bengtsson et al. 1979; Havlik et al. 1979; Higgins 1980; Hutchinson and Crawford 1981; Longini et al. 1984; Brandao et al. 1992; DeStefano et al. 2001; Sun et al. 2003; Levin et al. 1999). Finally, mtDNA sequencing in multigenerational hypertensive pedigrees reveals a high prevalence of mtDNA mutations (Schwartz et al. 2004).

Given the evolving recognition of the importance of hypertension in select cases of mtDNA diseases, we sought to determine the prevalence of hypertension in a large cohort of patients with confirmed late-onset mtDNA diseases as compared to age-matched national figures. A secondary aim was to determine whether any potential increase in the prevalence of hypertension, relative to age-matched national figures, was attributable to specific subtypes of mtDNA disease.

Methods

Study Design and Population

We undertook a retrospective chart review of 914 adult patients seen at our center between 1999 and 2012 for the investigation of questionable late-onset mtDNA diseases. Patients with definite disease (defined as the identification of either two major criteria or one major plus two minor criteria, as set by Bernier et al. (2002)) were included in the analysis. The charts were reviewed for the following variables: demographic characteristics, age at diagnosis, type of late-onset mtDNA diseases, list of medications, family history of mtDNA diseases, and hypertension. Finally, we recorded the heteroplasmy levels for each patient where available (assessed in muscle, urine epithelial cells, and/or white blood cells, using restriction fragment length polymorphism analysis with estimation of relative band intensities on ethidium bromide-stained gels). For

each group, we tabulated BP and serum TSH, glucose, ALT, and serum creatinine during the last assessment at our clinic (data not shown).

Our cohort with late-onset mtDNA diseases was further subdivided into different age categories and matched for age using the data from the Canadian Health Measures Survey (CHMS) (Wilkins et al. 2010), which is a survey on the 2007–2009 prevalence of hypertension in the 20–79 years of age cohort (total respondents = 3,514, with hypertension = 864), weighted to be representative of 23.7 million Canadian adults in this age range.

Statistical Analysis

We calculated the crude prevalence of hypertension in the entire cohort. We further divided the mtDNA diseases patients into three age categories, 20–39, 40–59, and 60–79, to determine the age-specific prevalence with 95 % confidence intervals. The prevalence within each category was compared with CHMS data (Wilkins et al. 2010) using Chi square analysis.

Results

Our chart review encompassed 914 charts of which 63 were deemed to have definite late-onset mtDNA diseases. Of the 63, 5 charts were excluded on the basis of incomplete information regarding the diagnosis of hypertension.

The demographic characteristics, mtDNA disease syndromes, comorbidities and hypertension diagnoses for the 58 patients are summarized in Table 1. The overall prevalence of hypertension in our cohort was 23/58 or 39.7 % (95 % CI 27–53 %). Based on the CHMS data (Wilkins et al. 2010); the expected prevalence based on age was 17.7 or 30.5 %. When analyzed by age groups, there was no significant difference in the prevalence of hypertension within our cohort as compared to the equivalent prevalence figure in the CHMS data (Wilkins et al. 2010) in patients 40 years of age and older. However, the observed prevalence rate was significantly higher than the equivalent CHMS data (Wilkins et al. 2010) in the younger cohort (age category 20–39), with a prevalence of 5/9 (56 %, CI 21–86 %), as compared to a CHMS rate of 2.8 % (Wilkins et al. 2010) ($n = 33/1185$) ($p < 0.001$). The increased prevalence of hypertension in this younger cohort was attributable to the high prevalence rate in the subgroup with the MELAS m.3243A>G mutation Table 2.

As the high prevalence of hypertension in the younger MELAS cohort was not observed in the 40–59 years of age MELAS cohort, we compared mtDNA disease severity between the younger and older age groups. mtDNA heteroplasmy (proportion of mtDNA that is mutated) was

selected as the marker of disease severity. Muscle and urine epithelial cell sources of mtDNA were utilized, where available (14/16 patients), as previous studies in MELAS cohorts have identified heteroplasmy levels in these specific tissue sources as reliable predictors of disease severity (McDonnell et al. 2004). Two of the 16 MELAS patients had heteroplasmy measurements performed only in white blood cells (WBC): one was a normotensive patient in his 6th decade with a WBC heteroplasmy level of 10 %, the other was a hypertensive patient in his 3rd decade who had a WBC heteroplasmy level of 80 %. The WBC heteroplasmy level from the former patient (WBC heteroplasmy level of 10 %) was not used in further calculations as WBC heteroplasmy levels are known to underestimate muscle heteroplasmy levels, with the underestimation increasing with patient age (Mehrazin et al. 2009). Therefore, subsequent analyses utilized information on tissue heteroplasmy levels from the remaining 15 of the 16 MELAS patients.

The mean mitochondrial heteroplasmy level in the 20–39 years of age MELAS patient cohort ($n = 4$, mean = 68 %, range: 45–80 %) was higher than that of the 40–59 years of age MELAS patient cohort ($n = 7$, mean = 39 %, SD = 30 %) although this difference did not reach statistical significance ($p = 0.11$). The mean heteroplasmy level in the 20–39 years of age MELAS patient cohort with hypertension ($n = 4$, mean = 68 %, range: 45–80 %) was significantly higher than the heteroplasmy level in the cohort of MELAS patients over 40 years of age who did not have hypertension ($n = 8$, mean = 33 %, SD = 28 %, $p = 0.04$).

Discussion

In view of the accumulating knowledge that variation in the mtDNA sequence accounts for a significant proportion of the heritability of hypertension, we sought to determine the prevalence of hypertension in a cohort of definite late-onset mtDNA diseases due to a wide variety of mtDNA genotypes. We sought to answer this question by specifically targeting patients with an unambiguous diagnosis of definite disease, as mitochondrial dysfunction may otherwise be associated with overlap clinical syndromes (including aging itself), (Schapira 2006; Koopman et al. 2012; Coskun et al. 2011; McCoy and Cookson 2011; Cairns et al. 2011; Hoppel et al. 2009; Sleigh et al. 2011; Finsterer and Segall 2010; Cohen 2010; Nageswara et al. 2007) which could confound any potential associations with hypertension.

We estimate the prevalence of hypertension in this cohort of mtDNA diseases to be 39.7 % ($n = 23/58$). This prevalence rate is not unexpected given the average age of our cohort, which was in the 6th decade of life. When

Table 1 Comparison of demographic, comorbid, and disease characteristics between the hypertensive and non-hypertensive mtDNA diseases cohort

Patient variable	All patients	mtDNA diseases without hypertension	mtDNA diseases with hypertension	p-value
Age group, n, years				
20–39	9	4	5	
40–59	26	20	6	
60–79	23	11	12	
Total	58	35	23	
Age, mean (SD), years				
20–39	28.7 (6)	32.5 (5)	24.8 (6)	0.07
40–59	49 (6)	58 (6)	52.5 (5)	0.11
60–79	68 (8)	65.7 (6)	71 (9)	0.16
Total	58 (15.7)	52 (12)	56 (20)	
Gender (female/age subtotal), n (%), years				
20–39	4/9 (44)	3/4 (75)	1/5 (20)	0.099
40–59	16/26 (62)	12/20 (60)	4/6 (67)	0.77
60–79	16/23 (70)	7/11 (64)	9/12 (75)	0.55
Total female, n (% of cohort)	36/58 (40)	22/35 (44)	14/23 (39)	
Ethnicity (white/age subtotal), n (%), years				
20–39	5/9 (56)	2/4 (50)	3/5 (60)	0.76
40–59	20/26 (77)	15/20 (75)	5/6 (83)	0.67
60–79	20/23 (87)	9/11 (82)	11/12 (92)	0.48
Total white, n (% of cohort)	45/58 (78)	26/35 (74)	19/23 (83)	
Inactivity (inactive/age subtotal), n (%), years				
20–39	7/9 (78)	3/4 (75)	4/5 (80)	0.86
40–59	17/26 (65)	13/20 (65)	4/6 (67)	0.94
60–79	16/23 (70)	4/11 (36)	12/12 (100)	0.0009
Total inactive, n (% of cohort)	40/58 (69)	20/35 (57)	20/23 (87)	
Diabetes (total with diabetes/age subgroup), n (%), years				
20–39	0/9 (0)	0/4 (0)	0/5 (0)	N/A
40–59	2/26 (8)	2/20 (10)	0/6 (0)	0.42
60–79	8/23 (35)	5/11 (45)	3/12 (25)	0.30
Total with diabetes, n (% of cohort)	10/58 (17)	7/35 (20)	3/23 (13)	
Smoking (total smokers/age subgroup), n (%)				
20–39 years	1/9 (11)	1/4 (25)	0/5 (0)	0.23
40–59 years	7/26 (27)	5/20 (25)	2/6 (33)	0.68
60–79 years	5/23 (22)	1/11 (9)	4/12 (33)	0.15
Total smokers, n (% of cohort)	13/58 (22)	7/35 (20)	6/23 (26)	
Heart disease (HD) (total with HD/age subgroup), n (%)				
20–39 years	1/9 (11)	0/4 (0)	1/5 (20)	0.34
40–59 years	9/26 (35)	4/20 (20)	5/6 (83)	0.004
60–79 years	11/23 (48)	6/11 (54)	5/12 (42)	0.66
Total HD, n (% of cohort)	21/58 (36)	10/35 (28)	11/23 (48)	

Table 2 Ratio of hypertensive to non-hypertensive patients in our mtDNA cohort organized by patient age and clinical syndrome subcategories

	<i>Age category, years</i>		
	20–39	40–59	60–79
<i>Clinical syndrome subcategories</i>			
CPEO+ ^a	1:2	4:9	9:8
MELAS ^a	4:0 ^b	1:7	2:2
MERRF ^a	0:0	0:3	0:1
KSS ^a	0:0	0:1	0:0
Complex I deficiency ^a	0:2	1:0	1:0

^a CPEO+, MELAS, MERRF, KSS, Complex I deficiency: mitochondrial genetic/clinical syndromes as described in the introduction

^b The ratio of total MELAS to total non-MELAS patients in the 20–39 years of age hypertensive group is significantly higher than expected ($p < 0.01$) by Chi squared analysis

analyzed by age group, in comparison to the CHMS cohorts (Wilkins et al. 2010), the 40–59 and 60–79 years of age cohorts had respective prevalence values that did not deviate significantly from the expected values. In contrast, the 20–39 years of age cohort had a surprisingly high prevalence at 56 % (CI 21–86 %). This prevalence was higher than expected based on the CHMS data (Wilkins et al. 2010) ($p < 0.001$).

There are several lines of data which suggest that the observed high prevalence rate of hypertension in the young late-onset mtDNA diseases cohort is a causal association. First, the increased prevalence rate observed in mtDNA diseases-related hypertension was primarily attributable to young patients who carry relatively high heteroplasmy levels of the common MELAS (m.3243A>G) mutation. This finding suggests that the risk of hypertension in mtDNA diseases is dependent on both the type and heteroplasmy level of the disease-causing mutation. The increased prevalence of hypertension in the younger cohort could not be solely explained by other monitored risk factors including physical inactivity (4/5), diabetes mellitus (0/5), or smoking status (0/5) as these prevalence rates did not differ significantly when compared to the older age groups (Table 1).

Second, our findings replicated data from previous studies that have shown links between mitochondrial dysfunction due to mtDNA mutations and hypertension. For instance, several studies showed evidence that novel mtDNA mutations (e.g., tRNA^{Ala} 4263A>G (Schwartz et al. 2004)) are directly associated with hypertension. One study of a hypertensive pedigree carrying a mitochondrial tRNA mutation demonstrated that the fraction of hypertension potentially due to mitochondrial dysfunction was 55 % (95 % CI 45–65 %) (DeStefano et al. 2001). Another case study identified a MELAS associated syndrome characterized by pulmonary hypertension (Sproule et al. 2008). These case studies are corroborated by studies of familial

hypertensive pedigrees, which identify high rates of mitochondrial sequence changes. In all cases, the associations between mtDNA diseases and hypertension match our findings of a link mediated by particular types of mtDNA diseases – those that involve mutations of mitochondrial tRNA (such as the common MELAS mutation) or complex I subunit coding sequences. In contrast, in our study, CPEO + status was not associated with an increased prevalence rate of hypertension. These findings reinforce the specificity of the association between mitochondrial tRNA coding region mutations and the increased prevalence of hypertension. In our findings, we also considered the possibility that the high prevalence of hypertension in the young MELAS cohort was related to particular familial nuclear genetic or environmental factors. However, the four young hypertensive MELAS patients are unrelated.

Cumulatively, these reports support the contention that the high prevalence of hypertension observed in the young late-onset mtDNA diseases cohort is in part due to a causal association. The mechanism for the putative causal association between mtDNA diseases and hypertension is that of overproduction of reactive oxygen species from dysfunctional mitochondria within endothelial cells leading to the development of vascular disease, including hypertension (Nageswara et al. 2007). However, an alternate hypothesis is that deficient endothelial cell nitric oxide production may play a role (Romero and Reckelhoff 1999).

Specific forms of mtDNA disease have been recognized as having pathology related specifically to impaired endothelial function. The MELAS syndrome, in particular, is associated with stroke-like episodes that predominate in the parieto-occipital region of the brain (Yatsuga et al. 2012). Stroke-like episodes in MELAS are atypical strokes in which the affected brain region is noted to cross regions supplied by more than one major artery (Finsterer 2009). The precise cause of the stroke-like episodes is unknown but is thought to be a combination of endothelial cell

dysfunction and neuronal susceptibility to hypoxia. The endothelial dysfunction is in turn attributed to low availability of citrulline, a product of mitochondrial metabolism that is specifically deficient in MELAS patients (Naini 2005). Citrulline is further metabolized via the urea cycle to L-arginine, a precursor of nitric oxide. (Koga et al. 2005; 2006) have shown that supplementation of L-arginine levels improves endothelial function and decreases the rate of stroke-like episodes in MELAS. The relationship of hypertension to stroke-like episodes in the MELAS syndrome is unknown. The observed endothelial dysfunction in this syndrome may represent a secondary phenomenon due to MELAS-associated hypertension. Similarly, the effect of citrulline/arginine/nitric oxide supplementation on modulation of mtDNA disease-related hypertension is unknown. However, the benefits of L-arginine on blood pressure control have been documented in other patient groups (Dong et al. 2011) and this mechanism may explain part of the benefit of this therapy in stroke-like episode prevention in MELAS patients.

Study Limitations

Our study is the first to document the prevalence of hypertension in adult patients with a wide variety of different mtDNA mutations. However, several limitations to our study exist. First, our identification of patients with hypertension was limited by the retrospective nature of the study. Moreover, the age of hypertension diagnosis in the cohort, and the age relative to the onset of mtDNA disease symptoms were difficult to determine. Second, our sample size is small with no controls drawn from the same clinic population. Given the nature of the clinic population, small cohorts of rare and distinct genetic syndromes with known or uncertain associations with hypertension, a reliable control group was not available. Possible and Probable mtDNA disease patients have an unknown prevalence of mtDNA disease and, as such, could not be used as a reliable control group. We also considered the largest group of related disorders, adult-onset carnitine palmitoyltransferase II deficiency, but there were only a total of 12 patients in the clinic. Third, multivariable logistic regression to determine if the MELAS syndrome (with high heteroplasmy levels) was an independent risk factor for hypertension, after accounting for gender, age, and other risk factors for hypertension, was not performed due to the small population size of the MELAS cohort. However, it is clear that the rate of hypertension in the young MELAS cohort is exceptionally high, and is significantly associated with MELAS patients with higher heteroplasmy levels. Therefore, our preliminary findings require confirmation by means of similar studies in other mtDNA disease centers. Specifically, the rate of hypertension in pediatric and adult patients with the MELAS m.3243A>G

mutation should be compared to age-corrected population rates as well as to that present in mtDNA disease patients without the A3243G mutation and to other metabolic disorders affecting mitochondrial metabolism such as fatty acid oxidation disorders. Should such studies specifically confirm the association of the MELAS m.3243A>G mutation with hypertension, interventional studies, such as L-arginine or L-citrulline versus standard blood pressure control, should be pursued.

Conclusion

In conclusion, the prevalence of hypertension in late-onset mtDNA diseases is high in younger adult patients with high heteroplasmy levels of the MELAS m.3243A>G mutation. This finding requires replication in a larger cohort of young MELAS patients. If verified, this relationship has potentially important therapeutic implications for the prevention of cardiovascular and cerebrovascular disease in MELAS patients.

Contribution

Each author has contributed to the conception, design, analysis, data collection, interpretation, writing, critical revision, and final approval of the article. Andre Mattman guarantees the scientific integrity of the work as a whole.

Disclosures

No financial disclosures and potential conflict of interests declared by Fady Hannah-Shmouni, Paula Waters, and Andre Mattman. Sandra Sirrs has received payment for lectures from Shire Human Genetics Therapies, Genzyme Canada, and Actelion Pharmaceuticals but these do not present any conflict with the current manuscript. Michelle Mezei has received payment for lectures from Genzyme Canada that do not present any conflict with the current manuscript.

References

- Bengtsson B, Thulin T, Schersten B (1979) Familial resemblance in casual blood pressure - A maternal effect. *Clin Sci (Lond)* 57(Suppl 5): 279S–281S
- Bernier F, Boneh A, Dennett X, Chow CW, Cleary MA, Thorburn DR (2002) Diagnostic criteria for respiratory chain disorders in adults and children. *Neurology* 59(9):1406–1411
- Borhani NO, Slansky D, Gaffey W, Borkman T (1969) Familial aggregation of blood pressure. *Am J Epidemiol* 89(5):537–546

- Brandao AP, Brandao AA, Araujo EM, Oliveira RC (1992) Familial aggregation of arterial blood pressure and possible genetic influence. *Hypertension* 19(2 Suppl):II214–II217
- Cairns RA, Harris IS, Mak TW (2011) Regulation of cancer cell metabolism. *Nat Rev Cancer* 11(2):85–95
- Cohen BH (2010) Pharmacologic effects on mitochondrial function. *Dev Disabil Res Rev* 16(2):189–199
- Coskun P, Wyrembak J, Schriener S, Chen HW, Marciniack C, Laferia F, Wallace DC (2011) A mitochondrial etiology of Alzheimer and Parkinson disease. *Biochim Biophys Acta* 1820(5):553–564
- DeStefano AL, Gavras H, Heard-Costa N, Bursztyjn M, Manolis A, Farrer LA, Baldwin CT, Gavras I, Schwartz F (2001) Maternal component in the familial aggregation of hypertension. *Clin Genet* 60(1):13–21
- Dong JY, Qin LQ, Zhang Z, Zhao Y, Wang J, Arigoni F, Zhang W (2011) Effect of oral L-arginine supplementation on blood pressure: a meta-analysis of randomized, double-blind, placebo-controlled trials. *Am Heart J* 162(6):959–965. doi: 10.1016/j.ahj.2011.09.012
- Finsterer J (2009) MELAS syndrome as a differential diagnosis of ischemic stroke. *Fortschr Neurol Psychiatr* 77(1):25–31. doi: 10.1055/s-2008-1100821
- Finsterer J, Segall L (2010) Drugs interfering with mitochondrial disorders. *Drug Chem Toxicol* 33(2):138–151
- Gerson LW, Fodor JG (1975) Family aggregation of high blood-pressure groups in two Newfoundland communities. *Can J Public Health* 66(4):294–298
- Havlik RJ, Garrison RJ, Feinleib M, Kannel WB, Castelli WP, McNamara PM (1979) Blood pressure aggregation in families. *Am J Epidemiol* 110(3):304–312
- Higgins M, Keller J, Moore F, Ostrander L, Metzner H, Stock L (1980) Studies of blood pressure in Tecumseh, Michigan. I. Blood pressure in young people and its relationship to personal and familial characteristics and complications of pregnancy in mothers. *Am J Epidemiol* 111(2):142–155
- Hoppel CL, Tandler B, Fujioka H, Riva A (2009) Dynamic organization of mitochondria in human heart and in myocardial disease. *Int J Biochem Cell Biol* 41(10):1949–1956
- Hutchinson J, Crawford MH (1981) Genetic determinants of blood pressure level among the Black Caribs of St. Vincent. *Hum Biol* 53(3):453–466
- Koga Y, Akita Y, Nishioka J, Yatsuga S, Povalko N, Tanabe Y, Fujimoto S, Matsuishi T (2005) L-Arginine improves the symptoms of stroke like episodes in MELAS. *Neurology* 64(4):710–712
- Koga Y, Akita Y, Junko N, Yatsuga S, Povalko N, Fukuyama R, Ishii M, Matsuishi T (2006) Endothelial dysfunction in MELAS improved by L-arginine supplementation. *Neurology* 66(11):1766–1769
- Koopman W, Willems P, Smeitink J (2012) Mechanisms of disease: monogenic mitochondrial disorders. *N Engl J Med* 366(12):1132–1141
- Levin BC, Cheng H, Reeder DJ (1999) A human mitochondrial DNA standard reference material for quality control in forensic identification, medical diagnosis, and mutation detection. *Genomics* 55(2):135–146
- Longini IM Jr, Higgins MW, Hinton PC, Moll PP, Keller JB (1984) Environmental and genetic sources of familial aggregation of blood pressure in Tecumseh, Michigan. *Am J Epidemiol* 120(1):131–144
- Map of the human mitochondrial DNA. Mitomap. Available: <http://www.mitomap.org/MITOMAP> (accessed 2012 June 15)
- McCoy MK, Cookson MR (2011) Mitochondrial quality control and dynamics in Parkinson's disease. *Antioxid Redox Signal* 16(9):869–882
- McDonnell MT, Schaefer AM, Blakely EL, McFarland R, Chinnery PF, Turnbull DM, Taylor RW (2004) Noninvasive diagnosis of the 3243A>G mitochondrial DNA mutation using urinary epithelial cells. *Eur J Hum Genet* 12(9):778–781
- Mehrazin M, Shanske S, Kaufmann P, Wei Y, Coku J, Engelstad K, Naini A, De Vivo DC, DiMauro S (2009) Longitudinal changes of mtDNA A3243G mutation load and level of functioning in MELAS. *Am J Med Genet A* 149A(4):584–587
- Nageswara R, Madamanchi S, Marschall S (2007) Mitochondrial dysfunction in atherosclerosis. *Circ Res* 100(4):460–473
- Naini A, Kaufmann P, Shanske S, Engelstad K, De Vivo DC, Schon EA (2005) Hypocitrullinemia in patients with MELAS: an insight into the “MELAS paradox”. *J Neurol Sci* 229-230:187–193
- Pfeffer G, Sirrs S, Wade NK, Mezei MM (2011) Multisystem disorder in late-onset chronic progressive external ophthalmoplegia. *Can J Neurol Sci* 38(1):119–123
- Romero JC, Reckelhoff JF (1999) State-of-the-Art lecture. Role of angiotensin and oxidative stress in essential hypertension. *Hypertension* 34(4 Pt 2):943–949
- Schapira AHV (2006) Mitochondrial disease. *Lancet* 368(9529):70–82
- Schwartz F, Duka A, Sun F, Cui J, Manolis A, Gavras H (2004) Mitochondrial genome. Mutations in hypertensive individuals. *Am J Hypertens* 17(7):629–635
- Silvestri G, Ciafaloni E, Santorelli FM, Shanske S, Servidei S, Graf WD, Sumi M, DiMauro S (1993) Clinical features associated with the A->G transition at nucleotide 8344 of mtDNA (“MERRF mutation”). *Neurology* 43(6):1200–1206
- Sleigh A, Raymond-Barker P, Thackray K, Porter D, Hatunic M, Vottero A, Burren C, Mitchell C, McIntyre M, Brage S, Carpenter TA, Murgatroyd PR, Brindle KM, Kemp GJ, O’Rahilly S, Semple RK, Savage DB (2011) Mitochondrial dysfunction in patients with primary congenital insulin resistance. *J Clin Invest* 121(6):2457–2461
- Sproule DM, Dyme J, Coku J, de Vinck D, Rosenzweig E, Chung WK, De Vivo DC (2008) Pulmonary artery hypertension in a child with MELAS due to a point mutation of the mitochondrial tRNA (Leu) gene (m.3243A>G). *J Inherit Metab Dis* (Epub ahead of print)
- Sun F, Cui J, Gavras H, Schwartz F (2003) A novel class of tests for the detection of mitochondrial DNA mutation involvement in diseases. *Am J Hum Genet* 72(6):1515–1526
- Thorburn DR (2004) Mitochondrial disorders: prevalence, myths and advances. *J Inherit Metab Dis* 27(3):349–362
- Wilkins K, Campbell N, Joffres M, McAlister F, Nichol M, Quach S, Johansen H, Tremblay M (2010) Blood pressure in Canadian adults. Statistics Canada, Catalogue no. 82-003-XPE • Health Reports. March 2010: Vol. 21, no. 1
- Yatsuga S, Povalko N, Nishioka J, Katayama K, Kakimoto N, Matsuishi T, Kakuma T, Koga Y (2012) MELAS: A nationwide prospective cohort study of 96 patients in Japan. *Biochim Biophys Acta* 1820(5):619–624

Niemann-Pick Disease Type C: New Aspects in a Long Published Family – Partial Manifestations in Heterozygotes

Klaus Harzer · Stefanie Beck-Wödl · Peter Bauer

Received: 27 March 2013 / Revised: 10 May 2013 / Accepted: 14 May 2013 / Published online: 3 July 2013
© SSIEM and Springer-Verlag Berlin Heidelberg 2013

Abstract Decades ago, a family with three children with a neurovisceral lysosomal storage disease was described. The patient siblings died at ages 7, 9, and 11 years, respectively, and according to the current concept had the late-infantile neurologic form of Niemann-Pick type C1 (NPC) disease, given by the present molecular study that there were severe *NPC1* gene variants: Blood samples preserved since that time from one patient sibling and his presently 55-year-old essentially healthy sister have now been studied, revealing the variants p.I1061T and p.G1162V in the *NPC1* gene, the first long known, the second newly found but predicted to be pathogenic and similar to the known G1162A. Now, with the molecular diagnosis, that initial description warrants new interest for the following reasons. The mentioned sister carries only the I1061T variant. She had storage macrophages (“Niemann-Pick cells”) in her bone marrow, but also displayed distinct splenomegaly with indurated consistency of the organ, proven in childhood and confirmed several times up to age 13, but disappeared at age 55 years. She shares the I1061T variant with her still healthy mother, and the bone marrow finding with both parents, her father having died at 66 years from a carcinoma. The present study is one of the first describing hematological and relevant clinical symptomatology, even

in heterozygotes, of molecularly diagnosed human NPC. Feline NPC is known to model such a situation. For human diagnostic and clinical NPC management, the possibility of “heterozygous disease” should be kept in mind.

Abbreviations

BMP	bis(monoacylglycero)phosphate
NPC	Niemann-Pick type C disease
NPC1 and NPC2	subtypes of NPC, and related proteins

Introduction

Niemann-Pick disease type C (NPC; OMIM 257220; OMIM 607625) is a neurovisceral lipidosis resulting from a generalized lipid trafficking defect, with lysosomal accumulation of cholesterol, sphingomyelin, glycolipids, and other lipids; defects in the *NPC1* (about 95 % of patients have NPC1 disease) or *NPC2* (5 % NPC2 disease) genes that encode the multifunctional membrane and/or transport proteins, NPC1 and NPC2, are responsible (for reviews, see Vanier 2010; Patterson et al. 2013; Stampfer et al. 2013). According to Vanier (2010), the degree of neurological involvement defines disease severity in most patients but may be preceded by cholestatic jaundice in the neonatal period, and spleno- or hepatosplenomegaly in infancy or childhood. Neurologically, single or combined signs in the following spectrum may be observed, also depending on the age of clinical onset: delay in developmental milestones, gait problems, clumsiness, cataplexy, seizures, dystonia, school problems, supranuclear gaze palsy, dysarthria, dysphagia, (cerebellar) ataxia, initial psychiatric problems, or progressive dementia. According

Communicated by: Verena Peters

Competing interests: None declared

K. Harzer (✉)

Neurometabolic Laboratory, Klinik für Kinder- und Jugendmedizin, University of Tübingen, Hoppe-Seyler-Str. 1, D-72076, Tübingen, Germany
e-mail: harzer-rottenburg@t-online.de

S. Beck-Wödl · P. Bauer

Institute of Applied Genomics and Medical Genetics, Institut für Humangenetik, University of Tübingen, Tübingen, Germany

to Patterson et al. (2013), about two-thirds of patients have infantile or juvenile onset of neurological manifestations, while one third present in adolescence or adulthood. The most frequent neurological signs, through all onset groups and in decreasing order, are ataxia, vertical supranuclear gaze palsy, dysarthria, cognitive impairment, and dysphagia. The laboratory diagnosis of NPC is usually preceded by the nonspecific, though usually helpful, screening for increased plasma chitotriosidase activity, and then made by cytochemical demonstration of lysosomally accumulated free cholesterol in skin fibroblast cultures using the staining method with filipin (Vanier 2010) and by genetic testing. However, the combined methods also leave some patients without a certain laboratory diagnosis.

In 1972, a family with “infantile-juvenile, slowly progressive lipidosis belonging to the sphingomyelinoses (Niemann-Pick – a new type?)” was described (Wiedemann et al. 1972). There were four siblings, three of whom died at ages ranging from 7 to 11 years from a severe neurodegenerative disease. Clinical signs included prolonged neonatal jaundice, early postnatal splenomegaly, foam cells in the bone marrow, and many of the above-mentioned neurological symptoms. Wiedemann et al. (1972) hesitated to classify their patients as “Crocker’s group D” or juvenile/subacute Niemann-Pick disease, but they spoke of some similarity of the patients with these groups. In fact, Crocker’s groups C and D and juvenile/subacute or dystonic Niemann-Pick disease (for review, see Frank and Lasson 1985) were defined at that time by criteria that are rather congruent, still, with a large portion of the spectrum of clinical symptoms recorded today in NPC patients diagnosed by specific laboratory methods. Wiedemann et al. (1972) could possibly have assigned their patients to those long-defined groups that are rather equivalent to NPC if they had regarded, e.g., the vertical gaze palsy which was certainly present (see below), though not described in their patients. In the early 1970s, there were already many reports describing the association of typical eye movement problems, defined as vertical gaze palsy or supranuclear ophthalmoplegia, with the long-defined NPC equivalents. These equivalents were partially substituted somewhat later for another, relatively specific NPC equivalent, termed “ophthalmoplegic neuropilidosis” (for review, see Frank and Lasson 1985).

In this study, the diagnosis of NPC was confirmed in that family (Wiedemann et al. 1972) by the demonstration of one long known and one newly recognized point mutation on either allele of the *NPC1* gene (NPC1 disease). This was made possible by the availability of blood samples frozen for 40 years from one patient and his sister, and by generous help, including an additional blood sample and clarifying information provided by family members who are still alive.

With the diagnosis known, the report by Wiedemann et al. (1972) and also that by Seng et al. (1971) deserve renewed interest for the following features: (i) This is one of the first genetically proven NPC families in which heterozygous carriers were unambiguously found to have clinical and/or hematological symptoms of the NPC spectrum. (ii) The reports have very early added to the first description of the accumulation of a key lysosomal lipid, bis(monoacylglycerol)phosphate (BMP), in a clearly diagnosed lysosomal storage disorder (Niemann-Pick disease type A) (Rouser et al. 1968), a second description of such an accumulation. Although Seng et al. (1971) and Wiedemann et al. (1972) were unsure about the disease subtype, they spoke of Niemann-Pick disease with BMP accumulation in that family and prepared the way to the present molecular definition of NPC, subgroup NPC1, for those patients. Very recently, the anionic phospholipid BMP has attracted attention for its indispensable role in lysosomal lipid homeostasis (Sandhoff and Harzer 2013) and for its marker properties in lysosomal affections including NPC disease (Scherer and Schmitz 2011). (iii) Wiedemann et al. (1972) underscored the great clinical variability in NPC disease when they described the almost directly postnatal appearance of splenomegaly versus the only juvenile manifestation of severe neurologic symptoms and the increased, instead of the usually reported reduced, growth in body length in their patients.

Case Report

The sister of the three described siblings with NPC disease (Wiedemann et al. 1972) (see pedigree in Fig. 1) is now 55 years old, essentially healthy, practicing sport and works as a hospital nurse. She was referred to as Case 1 in the original paper and is II/1 (Fig. 1) in this study. One (II/3) of the diseased siblings (II/2 to 4) was originally described as Case 3. In II/1 (sister), an enlarged spleen was noticed at the age of 8 years and was confirmed 1, 4, and 5 years later to be enlarged by 3–4 cm below the costal margin and of indurated consistency (Wiedemann et al. 1972); recently, at age 55 years, the spleen had a size of 10.7 × 5.9 cm on sonography, confirmed to be normal by the examiner. In the smear of her bone marrow studied when she was 6 years old, there were a number of foamy storage cells (Fig. 2). Patient II/3 (Fig. 1) was first remarkable by splenomegaly and slight hepatomegaly at the age of 6 weeks. When this boy was 3 months old he was found to have large numbers of foam cells in his bone marrow (Gerken and Wiedemann 1964), and with 16 months he had thrombocytopenia with lower leg subcutaneous bleedings (Wiedemann et al. 1972). It should be noted that the bone marrow foam cells were depicted at the time (Gerken and Wiedemann 1964) when

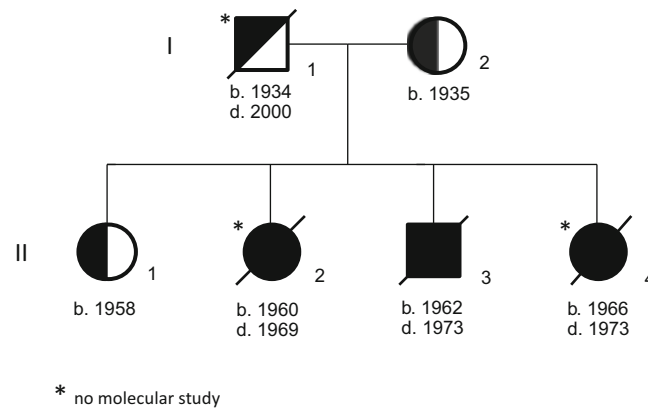


Fig. 1 Pedigree of the Niemann-Pick disease type C (NPC) family. Family members in generation I, 1 and 2, and II, 1 to 4. Squares, male; circles, female. Black/white, heterozygous; diagonal line, died;

black, NPC siblings. Letter **b.**, year of birth; **d.**, year of death. Molecular study was in I/2 (*NPC1* p.I1061T/wildtype), II/1 (same genotype) and II/3 (I1061T/G1162V)

the diagnosis in this family was erroneously suggested to be Gaucher disease, but, in fact, these storage cells resemble storage macrophages of the “Niemann-Pick type” (Fig. 2). Patient II/3 started at the age of 2 years a very insidious neurological downhill course which slowly progressed, including epileptic and cataplexic fits (for details, see Wiedemann et al. 1972), and led to a fatal end at the age of 11 years. Importantly, different caregivers who were later found and interviewed by the sister lady (II/1) clearly recalled the distinct problems the boy had when he tried to look upward and was unable to do so, but tried to compensate by extreme flexing of the head into the neck (vertical gaze palsy). The histories of patient siblings II/2 and II/4 were similar but with some variations (Wiedemann et al. 1972); II/2 died at age 9 and II/4 at 7 years (see Fig. 1). The mother, I/2, is now 78 years old and healthy. Her spleen was recently observed as being of normal size of 11.2×3.9 cm on sonography. But when she was 28 years old, a number of foam cells were found in her bone marrow (Fig. 2). The father (I/1) had similar foam cells at the age of 29 years (Fig. 2); his daughter (II/1) recently reported that he had suffered from myasthenia gravis with the inability to lift the upper eyelids, but the symptoms improved upon mestinon administration and thymectomy, and that he died from a lung carcinoma at the age of 66 years. No splenomegaly was reported for him.

Genetic Testing

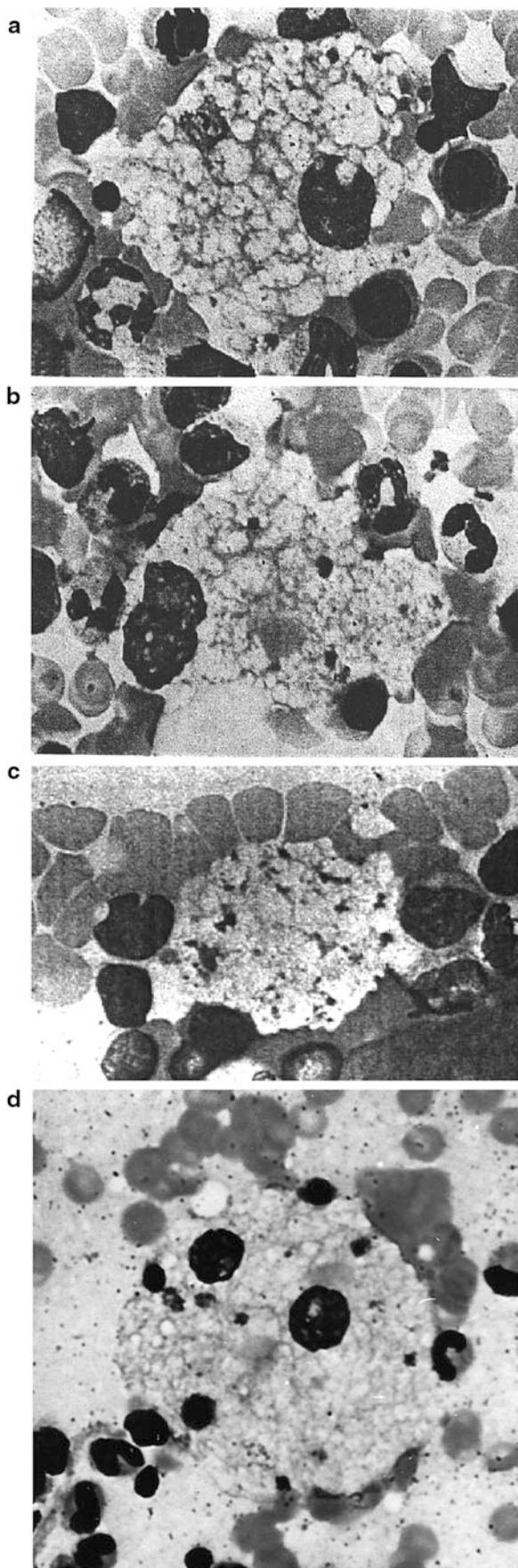
Leukocyte pellets from peripheral blood were available from II/1 and II/3 (Fig. 1), the samples of which had been frozen in the laboratory of one of the authors (K.H.) for 40 years at -20°C . A blood sample was also taken recently from the mother (I/2) with informed consent. Blood leukocytes were isolated using standard procedures. Genomic DNA was

isolated from the leukocyte pellets using the DNA isolation Kit from Roche®. Molecular genetic analysis of the 25 coding exons of *NPC1* and the flanking intronic regions was performed by Sanger sequencing. PCR conditions and primer sequences are available on request.

Results and Discussion

Forty-nine years after the first report (Gerken and Wiedemann 1964), and 41 years after the comprehensive, nosologically more adequate description (Wiedemann et al. 1972) of three siblings with a neurovisceral lysosomal storage disease, the final confirmation of the diagnosis was achieved. However, not only those careful clinical, morphological, and biochemical descriptions but also the excellent lipid chemical study on the brain of patient II/2 (Fig. 1) by Tjiong et al. (1973) have long been highly suggestive of classical NPC disease. In fact, genetic testing of patient II/3 revealed the most frequent mutation in the *NPC1* gene (Millat et al. 1999; Vanier 2010), p.I1061T (c.3182T>C), and an as yet not described mutation, p.G1162V (c.3485G>T). Both the sister (II/1 in Fig. 1) and her mother (I/2) were found to carry only I1061T and no other serious *NPC1* variants. This constellation assigned the mutations in patient II/3 to different alleles. The pathogenicity of G1162V was predicted *ex silico* and confirmed by practical experience (Heiko Runz, Heidelberg, personal communication, 2012). This mutation is similar to G1162A (c.3485G>A), known to be pathogenic (Stampfer et al. 2013).

The heterozygous NPC carriers, II/1 and I/2, and the father I/1 (Fig. 1) of II/1 and II/3, were remarkable for the findings of foamy storage cells in their bone marrow smears (Gerken and Wiedemann 1964; see Fig. 2). These bone marrow findings certainly repeat very similar, much earlier observations in heterozygotes of “ophthalmoplegic neuro-



lipidosis” (Frank and Lasson 1985); this archaic term being a very likely equivalent for NPC disease. Still, the present family is only the second in which such findings in heterozygotes can be attributed to a demonstrable pathogenic *NPC1* gene variant, i.e., I1061T in I/2 and II/1, and G1162V, presumably, in the deceased father I/1. The first report was on a family with four NPC patients in which the patients’ father had been known to have storage cells in the bone marrow (Ceuterick et al. 1986) – and also lysosomal storage inclusions in his skin biopsy – and who was studied molecularly many years later with the result of his *NPC1* heterozygous I1061T genotype (Millat et al. 1999).

Even more interesting, the present sister lady II/1 is remarkable for her distinct splenomegaly observed at age 8 and confirmed three times up to age 13 years, with an indurated consistency of the organ (Wiedemann et al. 1972), but at age 55 years no longer provable. This is one of the first observations of a relevant clinical symptom attributable to a known pathogenic *NPC1* variant (*NPC1*⁻), but in combination with a wildtype allele (*NPC1*⁺). Possible explanations remain speculative: Is there a gain of pathologic function by the mutant *NPC1*⁻ protein? Are there influences of the total genetic background or certain epigenetic constellations? Is there still a third mutant allele in this “heterozygote” and her family, given that sensitivity of *NPC1* sequencing does not reach 100%? Might an imbalance in *NPC1*⁻ and *NPC1*⁺ expression in different cells and tissues play a role? An observation of a neurological picture in an NPC heterozygote was reported by Josephs et al. (2004). They described a 75-year-old woman with continuous tremor of the head and limbs unresponsive to L-dopa/carbidopa who carried the pathogenic p.G992A (c.2974G>C) variant (Sévin et al. 2007), but her brothers with childhood onset NPC, upon examination many years before, had no tremor except when they were in stressful situations.

The present observations correlate well with a feature long known for cytochemical NPC diagnostics: In filipin-testing of skin fibroblasts cultured from NPC heterozygotes, a partial filipin positivity, i.e., NPC-typical cellular cholesterol accumulation, is not infrequently found (Vanier 2010). As to animal models, feline NPC has been described with clinical, cytological, and cytochemical disease signs in heterozygotes (Brown et al. 1994 and 1996).

Fig. 2 Foamy storage macrophages (“Niemann-Pick cells”) in bone marrow smears from heterozygotes with Niemann-Pick disease type C and a patient. Pappenheim staining; the largest diameters of the storage cells are 25 to 50 μm . (a–c) heterozygotes: (a) father, I/1, of II/1 (see Fig. 1); (b) mother, I/2; (c) II/1 (note the nucleus at the right edge of the light storage cells but beneath the dark lymphocyte); (d) a 10-year-old patient with late-infantile neurologic Niemann-Pick disease type C (independent observation). a–c are reprinted from Gerken and Wiedemann (1964), with consent of the Schweizerische Gesellschaft für Pädiatrie, and S. Karger, Basel

For the future, it should be kept in mind that even heterozygotes of NPC, at least NPC1 disease, can in some instances express not only bone marrow cytological or fibroblast-cytochemical signs typical of NPC, but can sometimes even develop relevant clinical symptoms such as splenomegaly (Wiedemann et al. 1972) and possibly tremor (Josephs et al. 2004). The generally accepted “recessive inheritance” of NPC, therefore, gains a new aspect.

The report on the NPC family by Wiedemann et al. (1972), with the genetic diagnosis in hand, also deserves renewed attention with respect to the achieved confirmation of BMP as a very essential lysosomal lipid (see [Introduction](#)).

Acknowledgment Members of the present NPC family (II/1 and I/2) are warmly thanked for their help with blood samples and disease information, which were indispensable for this study.

Synopsis

Molecularly proven human heterozygous carriers of Niemann-Pick disease type C can develop relevant clinical and/or hematological (bone marrow storage cell) symptoms.

Compliance with Ethics Guidelines

Conflict of Interest: Klaus Harzer, Stefanie Beck-Wödl, and Peter Bauer declare that they have no conflict of interest.

Informed Consent: All procedures followed were in accordance with the ethical standards of the responsible committee on human experimentation (institutional and national) and with the Helsinki Declaration of 1975, as revised in 2000 (5). Informed consent was obtained from all patients for being included in the study.

References

- Brown DE, Thrall MA, Walkley SU et al (1994) Feline Niemann-Pick disease type C. *Am J Pathol* 144:1412–1415
- Brown DE, Thrall MA, Walkley SU et al (1996) Metabolic abnormalities in feline Niemann-Pick type C heterozygotes. *J Inher Metab Dis* 19:319–330
- Ceuterick C, Martin JJ, Foulard M (1986) Niemann-Pick disease type C. Skin biopsies in parents. *Neuropediatrics* 17:111–112
- Frank U, Lasson U (1985) Ophthalmoplegic neuropilidosis – storage cells in heterozygotes. *Neuropediatrics* 16:3–5
- Gerken H, Wiedemann H-R (1964) A contribution to the genetics of Gaucher’s disease (Ein Beitrag zur Genetik des Morbus Gaucher). *Ann paediat* 203:328–341
- Josephs KA, Matsumoto JY, Lindor NM (2004) Heterozygous Niemann-Pick disease type C presenting with tremor. *Neurology* 63:2189–2190
- Millat G, Marçais C, Rafi MA et al (1999) Niemann-Pick C1 disease: the I1061T substitution is a frequent mutant allele in patients of Western European descent and correlates with a classic juvenile phenotype. *Am J Hum Genet* 65:1321–1329
- Patterson MC, Mengel E, Wijburg FA et al (2013) Disease and patient characteristics in NP-C patients: findings from an international disease registry. *Orphanet J Rare Dis* 8:12. doi:10.1186/1750-1172-8-12
- Rouser G, Kritchevsky G, Yamamoto A, Knudson AG Jr, Simon G (1968) Accumulation of a glycerolphospholipid in classical Niemann-Pick disease. *Lipids* 3:287–290
- Sandhoff K, Harzer K (2013) Gangliosides and gangliosidoses. Principles of molecular and metabolic pathogenesis. *J Neurosci* (accepted)
- Scherer M, Schmitz G (2011) Metabolism, function and mass spectrometric analysis of bis(monoacylglycerol)phosphate and cardiolipin. *Chem Phys Lipids* 164:556–562
- Seng PN, Debuch H, Witter B, Wiedemann H-R (1971) Augmentation of bis(monoacylglycerin)phosphoric acid in sphingomyelinosis (M. Niemann-Pick?). (Bis[monoacylglycerin] phosphorsäure-Vermehrung bei Sphingomyelinose [Niemann-Pick?]). *Hoppe Seylers Z physiol Chem* 352:280–288
- Sévin M, Lesca G, Baumann N et al (2007) The adult form of Niemann-Pick disease type C. *Brain* 130:120–133
- Stampfer M, Theiss S, Amraoui Y et al (2013) Niemann-Pick disease type C clinical database: cognitive and coordination deficits are early disease indicators. *Orphanet J Rare Dis* 8:35. doi:10.1186/1750-1172-8-35
- Tjong HB, Seng PN, Debuch H, Wiedemann HR (1973) Brain lipids of a case of juvenile Niemann-Pick disease. *J Neurochem* 21:1475–1485
- Vanier MT (2010) Niemann-Pick disease type C. *Orphanet J Rare Dis* 5:16. doi:10.1186/1750-1172-5-16
- Wiedemann H-R, Debuch H, Lennert K et al (1972) An infantile-juvenile, subchronically progressive lipidosis of the sphingomyelinoses (Niemann-Pick) form - a new type? Clinical, pathohistological, electron microscopic and biochemical studies (Über eine infantil-juvenile, subchronisch verlaufende, den Sphingomyelinosen [Niemann-Pick] anzureihende Form der Lipidosen – ein neuer Typ? Klinische, pathohistologische, elektronenmikroskopische und biochemische Untersuchungen). *Z Kinderheilkd* 112:187–225

Chiari 1 Malformation and Holocord Syringomyelia in Hunter Syndrome

Renzo Manara • Daniela Concolino •
Angelica Rampazzo • Alessandra Zanetti •
Rossella Tomanin • Roberto Faggini • Maurizio Scarpa

Received: 03 February 2013 / Revised: 14 May 2013 / Accepted: 15 May 2013 / Published online: 2 July 2013
© SSIEM and Springer-Verlag Berlin Heidelberg 2013

Abstract Compressive cervical myelopathy is a well-known life-threatening complication in mucopolysaccharidosis (MPS) patients. Glycosaminoglycan accumulation in the growing cartilage results in dens dysplasia, atlanto-axial instability, and subsequent periodontoid fibrocartilaginous tissue deposition with upper cervical stenosis.

Chiari malformation type 1 (CM1) is a congenital downward cerebellar tonsil ectopia determined by clivus and posterior cranial fossa underdevelopment, possibly leading to progressive spinal cord cavitation (syringomyelia) and severe neurological impairment.

We present a boy affected with Hunter syndrome (MPS II) and cerebellar tonsil ectopia who developed a holocord syringomyelia at the age of 6 years. The child underwent atlanto-occipital decompressive surgery with rapid clinical and neuroimaging improvement.

Sharing a primary mesenchymal involvement of the cervical-occipital region, the coexistence of CM1 in MPS might be not unexpected and complicate further the disease course. In these patients, strict monitoring and prompt

treatment might be of foremost importance for preventing major neurological complications.

Introduction

Hunter syndrome (Mucopolysaccharidosis type II; MPS-II; OMIM#309900) is a rare X-linked recessive lysosomal storage disorder (1/170,000 live male births) (Martin et al. 2008) caused by iduronate-2-sulphatase (IDS; EC3.1.6.13) deficiency. The resulting lysosomal accumulation of upstream metabolites affects a variety of organ systems, including visceral organs, skeleton, connective tissue, and the central nervous system. At birth, MPS-II patients appear phenotypically normal, but they gradually develop morphologic changes, recurrent respiratory infections, joint stiffness, and organomegaly (Young et al. 1982; Finn et al. 2008). About 10 % of MPS-II patients present with severe upper spinal canal stenosis causing spinal cord compression (Manara et al. 2011). Though less frequent than in other MPS forms, such as Morquio disease, severe myelopathy requiring decompressive surgery may also occur (Ballenger et al. 1980; O'Brien et al. 1997; Kaendler et al. 1990; Vinchon et al. 1995). As the clinical manifestation of spinal cord involvement might fairly overlap with signs and symptoms of concomitant multisystem involvement, myelopathy diagnosis and monitoring are mainly based on MRI evaluation of the cranio-cervical region.

Chiari malformation type 1 (CM1) is a congenital downward ectopia of cerebellar tonsils (more than 6 mm below the foramen magnum in the pediatric population). CM1 is an uncommon condition (about 1 % in the pediatric population) (Aitken et al. 2009) due to underdevelopment of mesenchymal structures forming the clivus and posterior cranial fossa bones (Milhorat et al. 2010). The abnormal position of

Communicated by: Ed Wraith

Competing interests: None declared

R. Manara (✉)
Neuroradiology, University of Salerno, via S. Allende 1,
84081 Baronissi (SA), Italy
e-mail: rmanara@unisa.it

D. Concolino
Department of Pediatrics, Magna Graecia University of Catanzaro,
Catanzaro, Italy

A. Rampazzo • A. Zanetti • R. Tomanin • M. Scarpa
Department of Pediatrics, University of Padova, Padova, Italy

R. Faggini
Neurosurgery, University Hospital of Padova, Padova, Italy

the cerebellar tonsils disrupts the normal CSF flow dynamics (Shah et al. 2011) at the cranio-cervical junction and may result in spinal cord damage. The latter presents usually with a progressive cavitation (syringomyelia) that might involve the entire length of the cord and/or the medulla oblongata. Typically, syringomyelia appears in adulthood (Masson and Colombani 2005); children might be affected and present with insidious onset and slow progression (Singhal et al. 2011). Signs and symptoms of CMI (e.g., headache, neck pain, or lower brainstem dysfunction) (Wu et al. 1999; Greenlee et al. 2002) and syringomyelia (e.g., scoliosis, motor or dissociate sensory impairment) (Isu et al. 1990; Attenello et al. 2008) also overlap or might be difficult to ascertain in MPS patients.

Here, we describe a child affected with MPS type II and CMI, who developed a holocord syringomyelia and underwent suboccipital craniectomy and laminectomy with duroplasty to decompress the foramen magnum.

Clinical Description

Second-born from unrelated parents, during the first year of life the child presented with recurrent infections of the upper respiratory tract. Concomitantly, he showed psychomotor delay and altered sleep–wake rhythm. Mild organomegaly was also noted. A metabolic storage disease was suspected and biochemical and genetic tests were performed after obtaining parents' informed consent. Analysis of urinary glycosaminoglycans (GAG) revealed a high urinary GAG/creatinine ratio of 92.2 mcg GAG/24 h (normal values 1.59–30.3). L-Iduronate-2-sulfatase activity of leukocytes was 1.2 nmol/mg/h (control: 28 nmol/mg/hr). The patient was diagnosed with MPS type II at the age of 18 months. Genetic investigation revealed a c.589-592 del CCTG of the IDS gene.

At the age of 2 years and 5 months, the patient began enzyme replacement therapy (ERT) with idursulfase (Elaprase® SHIRE HGT, Lexington, MD) at a dosage of 0.5 mg/kg per week. Therapy was well tolerated and no severe adverse events were reported. The child was monitored through routine clinical assessment, laboratory analysis, and further investigations when required. His respiratory function and endurance improved while upper respiratory tract infections were significantly reduced during the following 2 years. The sleep–wake rhythm normalized, organomegaly resolved, and joint mobility improved. Cardiac examinations demonstrated mild mitral valve insufficiency before ERT introduction and did not change during follow-up while the ophthalmologic evaluation showed exophoria with normal visual acuity, eye pressure, and fundus. The child developed moderate

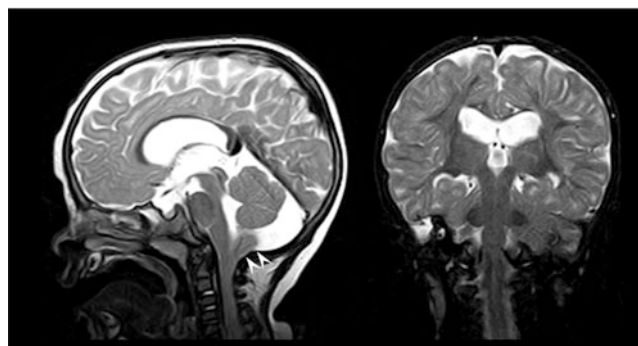


Fig. 1 Brain MRI at the age of 2 years, sagittal and coronal T2-w images showing the low position of the cerebellar tonsils (*arrowheads*) despite an enlarged cisterna magna and a posterior cranial fossa of normal size; several typical MPS features are also evident (e.g., J-shaped pituitary sella, ventricle enlargement, white matter signal abnormalities, enlarged perivascular Virchow-Robin spaces, and upper cervical stenosis due to the periodontoid cap). No signs of myelopathy were evident

mental retardation and received physical and occupational therapies both at home and at school. Sphincter control was not completely achieved. A brain MRI revealed several typical neuroradiological MPS features such as the J-shaped pituitary sella, the enlargement of perivascular (Virchow-Robin) spaces in the corpus callosum and centrum semiovale bilaterally, moderate ventricular enlargement, and enlarged cisterna magna along with ectopia of the cerebellar tonsils >6 mm below the foramen magnum, consistent with CMI. At the cranio-cervical region, the MRI showed dens hypoplasia with a periodontoid cap leading to mild stenosis of the cervical canal (score 2 according to Manara et al. 2011), while the upper cervical spinal cord was normal (Fig. 1).

A brain MRI follow-up at the age of 5 years revealed progression of cerebral atrophy while the cervical spine MRI disclosed a focal thin syringomyelia. At that time, the child complained of upper limbs numbness and no control of sphincters; no other neurological deficits were detected (Fig. 2).

A subsequent spine MRI at the age of 6 years showed a holocord syrinx, extending from the cervicomedullary junction to the conus medullaris. The neurological status was unchanged; cognitive evaluation confirmed a moderate impairment (IQ = 62 by WISH-IV and Terman-Merrill tests) (Fig. 3).

The boy underwent decompressive suboccipital craniectomy and C1 laminectomy with duroplasty. At 7-month neurological follow-up, both upper limbs numbness and bowel/bladder incontinence had disappeared. At follow-up MRI, the cerebrospinal fluid spaces at the cranio-cervical junction were well represented and the syrinx had significantly shrunken.



Fig. 2 Brain and spine MRI at the age of 6 years, midsagittal T1-w image disclosing the peg-like cerebellar tonsils (*) impinging the foramen magnum and reaching the posterior arch of C1. Holocord multiconcamerated syringomyelia is well documented also on axial T1-w and sagittal T2-w images (*arrowheads*). At this age, platyspondylia, intervertebral disk abnormalities, dens dysplasia, and cranio-cervical junction abnormalities were also evaluable

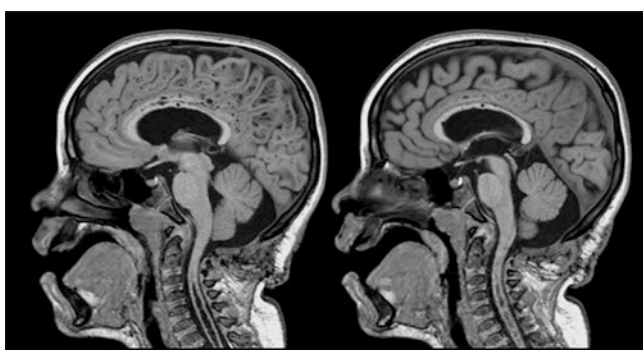


Fig. 3 Brain MRI at the age of 7 years, after decompressive surgery at the cranio-cervical junction. Sagittal T1-w images displaying cerebrospinal spaces around the upper cervical spinal cord and the cerebellar tonsils; the holocord syringomyelia has shrunken

Discussion

We reported on a boy affected with MPS-II-related spinal stenosis and Chiari malformation type 1, who developed holocord syringomyelia at the age of 6 and was successfully managed via surgical cranio-cervical decompression.

The cranio-cervical junction is known to be primarily involved in MPS patients. MRI examinations of this region are often featured by upper cervical spinal canal stenosis, which represents a major risk of myelopathy and even of sudden death after a minor fall (Northover et al. 1996). The accumulation of GAGs in the growing cartilage is thought to impair the ossification and maturation of the dens while ligamentous laxity seems to contribute to the

atlanto-axial instability. The latter likely induces the formation of reactive periodontoid fibrocartilaginous tissue that eventually cause spinal stenosis and spinal cord compression. Although the rate and the severity of spinal stenosis might vary according to the MPS form and is particularly important in MPS-I, IV, and VI, also MPS-II patients have been reported, who required decompressive surgery to prevent the progression of cervical myelopathy (Ballenger et al. 1980; O'Brien et al. 1997; Kaendler et al. 1990; Vinchon et al. 1995). From a clinical point of view, myelopathy usually results in progressive gait impairment, sensory deficits, and impaired sphincter control that might be overlooked due to concomitant brain, joint, and visceral involvement. In this context, MRI of the cranio-cervical region represents the main diagnostic tool for detecting and monitoring spinal stenosis and myelopathy and it is pivotal for planning the timing and the extension of surgical correction.

CM1 is a congenital downward impingement of cerebellar tonsils due to discrepancy between the size of the posterior cranial fossa and the volume of the cerebellar structures. The abnormal position of the cerebellar tonsils is thought to alter the CSF flow dynamic at foramen magnum level, possibly leading to spinal cord damage (Shah et al. 2011). The latter presents usually with a progressive cavitation (syringomyelia) that might involve the entire length of the cord and/or the medulla oblongata. In 90 % of cases, syringomyelia is associated with CM1 (Fernández et al. 2009). From a clinical point of view, syringomyelia typically present in children with insidious onset and slow progression (Singhal et al. 2011). Most often, scoliosis, motor or dissociate sensory impairment are noted due to sensory tract or corticospinal tract disruption and/or anterior horn cell involvement (Isu et al. 1990; Feldstein and Choudhri 1999; Attenello et al. 2008). Also, symptoms attributable to the concomitant CM1 are often observed (e.g., headache, neck pain, or lower brainstem dysfunction) (Wu et al. 1999, Greenlee et al. 2002). All these symptoms and signs might be concealed by the multiorgan involvement in MPS, often characterized by vertebral column abnormalities (scoliosis, kyphosis), joint stiffness, brain deterioration and spinal cord dysfunction.

In the general population, CM1 is due to the underdevelopment of mesenchymal structures forming the clivus and posterior cranial fossa bones (Milhorat et al. 2010). As MPS affect connective tissues with bone growth abnormalities (dysostosis multiplex), an increased rate of CM1 should not be completely unexpected. Most interestingly, as shown in our child patient, cerebellar tonsils ectopia in MPS patients might be observed despite a normal or even increased size of the posterior cranial fossa; in these cases an enlarged cisterna magna might be evident while the cerebellar tonsils are displaced downward, suggesting

or mimicking the coexistence of a retrocerebellar arachnoid cyst. A similar brain parenchyma displacement has been observed also in some closed meningoencephaloceles, a recently described skull abnormality of MPS II patients (Manara et al. 2012), where the prolapsing parenchyma is often squeezed in a marginal portion of the cavity, suggesting a more complex structure of meningocele content. The presence of sequestered arachnoid spaces and adherences to the meningeal pouch wall might be the most likely explanations, but a direct pathologic confirmation is still lacking.

Even though cerebellar tonsils are not significantly below the foramen magnum, their impingement might contribute to odontoid cap-related upper spinal canal stenosis in altering the physiological CSF dynamic at the cranio-cervical junction in MPS patients. In a previously reported case of MPS-VI associated with (holocord) syringomyelia (Hite et al. 1997), a cerebellar tonsil impingement was evident on the provided imaging, despite preserved retrocerebellar CSF spaces. Even in this case, holocord syringomyelia appeared in early childhood, but surgery was not performed due to clinical and imaging stability. In our child, the appearance and worsening of syringomyelia was documented at the age of 5 and 6. Subsequent cranio-cervical decompression determined a rapid clinical and neuroradiologic improvement, thus suggesting that surgery might be considered in MPS patients with holocord syringomyelia.

In conclusion, this case highlights that cerebellar tonsils impingement in MPS patients does not strictly depend on the size of the posterior cranial fossa and that a low position of the tonsils should be noted even in the presence of an enlarged cisterna magna. On the other hand, cerebellar tonsils impingement in MPS patients might require a more careful monitoring as clinical symptoms might be easily overlooked or misinterpreted with MPS-related myelomalacia or with the concomitant multiorgan involvement. Finally, as the MPS-related atlanto-axial instability often induces upper spinal stenosis, the spinal cord cavitation process due to cerebellar tonsils impingement and consequent disruption of CSF dynamics might have an accelerated and more severe course predisposing to early appearance of holocord syringomyelia. The role of surgery needs to be further ascertained, as the management of MPS patients affected with syringomyelia might be clinical or benefit from prompt decompression, avoiding a severe and irreversible spinal cord damage and improve the neurological impairment.

Take-Home Messages

The coexistence of Chiari I malformation in mucopolysaccharidosis patients might predispose to early myelopathy and prompts for strict clinical and MR monitoring; in these cases,

Chiari I malformation might have a different pathogenesis than posterior cranial fossa underdevelopment.

References

- Aitken LA, Lindan CE, Sidney S, Gupta N, Barkovich AJ, Sorel M, Wu YW (2009) Chiari type I malformation in a pediatric population. *Pediatr Neurol* 40(6):449–454
- Attenello FJ, McGirt MJ, Gathinji M et al (2008) Outcome of Chiari-associated syringomyelia after hindbrain decompression in children: analysis of 49 consecutive cases. *Neurosurgery* 62:1307–1313
- Ballenger CE, Swift TR, Leshner RT, El Gammal TA, McDonald TF (1980) Myelopathy in mucopolysaccharidosis type II (Hunter syndrome). *Ann Neurol* 7(4):382–385
- Feldstein NA, Choudhri TF (1999) Management of Chiari I malformations with holocord syringohydromyelia. *Pediatr Neurosurg* 31:143–149
- Fernández AA, Guerrero AI, Martínez MI et al (2009) Malformations of the craniocervical junction (Chiari type I and syringomyelia: classification, diagnosis and treatment). *BMC Musculoskelet Disord* 10(Suppl 1):S1–S11
- Finn CT, Vedolin L, Schwartz IV et al (2008) Magnetic resonance imaging findings in Hunter syndrome. *Acta Paediatr Suppl* 97(457):61–68
- Greenlee JDW, Donovan KA, Hasan DM, Menez AH (2002) Chiari I malformation in the very young child: the spectrum of presentations and experience in 31 children under age 6 yrs. *Pediatrics* 110:1212–1219
- Hite SH, Krivit W, Haines SJ, Whitley CB (1997) Syringomyelia in mucopolysaccharidosis type VI (Maroteaux-Lamy syndrome): imaging findings following bone marrow transplantation. *Pediatr Radiol* 27(9):736–738
- Isu T, Iwasaki Y, Akino M, Abe H (1990) Hydrosyringomyelia associated with a Chiari I malformation in children and adolescents. *Neurosurgery* 26:591–597
- Kaendler S, Bockenheimer S, Gräfin Vitzthum H, Galow W (1990) Cervical myelopathy in mucopolysaccharidosis type II (Hunter's syndrome). *Neuroradiologic, clinical and histopathologic findings. Dtsch Med Wochenschr* 7;115(36): 1348–1352
- Manara R, Priante E, Grimaldi M et al (2011) Brain and spine MRI features of Hunter disease: frequency, natural evolution and response to therapy. *J Inherit Metab Dis* 34(3):763–780
- Manara R, Priante E, Grimaldi M et al (2012) Closed Meningo(encephalo)cele: a new feature in Hunter syndrome. *Am J Neuroradiol* 33(5):873–877
- Martin R, Beck M, Eng C et al (2008) Recognition and diagnosis of mucopolysaccharidosis II (Hunter syndrome). *Pediatrics* 121:e377–e386
- Masson C, Colombani JM (2005) Chiari type 1 malformation and magnetic resonance imaging. *Presse Med* 34(21):1662–1667
- Milhorat TH, Nishikawa M, Kula RW, Dlugacz YD (2010) Mechanisms of cerebellar tonsil herniation in patients with Chiari malformations as guide to clinical management. *Acta Neurochir (Wien)* 152(7)
- Northover H, Cowie RA, Wraith JE (1996) Mucopolysaccharidosis type IVA (Morquio syndrome): a clinical review. *J Inherit Metab Dis* 19(3):357–365
- O'Brien DP, Cowie RA, Wraith JE (1997) Cervical decompression in mild mucopolysaccharidosis type II (Hunter syndrome). *Childs Nerv Syst* 13:87–90
- Shah S, Houghton V, del Río AM (2011) CSF flow through the upper cervical spinal canal in Chiari I malformation. *Am J Neuroradiol* 32(6):1149–1153

- Singhal A, Bowen-Roberts T, Steinbok P, Cochrane D, Byrne AT, Kerr JM (2011) Natural history of untreated syringomyelia in pediatric patients. *Neurosurg Focus* 31(6):E13
- Vinchon M, Cotten A, Clarisse J, Chiki R, Christiaens JL (1995) Cervical myelopathy secondary to Hunter syndrome in an adult. *Am J Neuroradiol* 16(7):1402–1403
- Wu YW, Chin CT, Chan KM, Barkovich AJ, Ferriero DM (1999) Pediatric Chiari I malformations: do clinical and radiologic features correlate? *Neurology* 53:1271–1276
- Young ID, Harper PS, Archer IM, Newcombe RG (1982) A clinical and genetic study of Hunter's syndrome. 1. Heterogeneity. *J Med Genet* 19(6):401–407

A Patient with Complex I Deficiency Caused by a Novel *ACAD9* Mutation Not Responding to Riboflavin Treatment

Jessica Nouws • Flemming Wibrand •
Mariël van den Brand • Hanka Venselaar •
Morten Duno • Allan M. Lund • Simon Trautner •
Leo Nijtmans • Elsebet Østergard

Received: 12 March 2013 / Revised: 14 May 2013 / Accepted: 16 May 2013 / Published online: 31 August 2013
© SSIEM and Springer-Verlag Berlin Heidelberg 2013

Abstract Here we report a patient with a new pathogenic mutation in *ACAD9*. Shortly after birth she presented with respiratory insufficiency and a high lactate level. At age 7 weeks, she was diagnosed with severe hypertrophic cardiomyopathy and she suffered from muscle weakness and hypotonia. Her condition deteriorated during intercurrent illnesses and she died at 6 months of age in cardiogenic shock. Analysis of respiratory chain activities in muscle and fibroblasts revealed an isolated complex I deficiency. A genome-wide screen for homozygosity revealed several homozygous regions. Four candidate genes were found and

sequencing revealed a homozygous missense mutation in *ACAD9*. The mutation results in an Ala220Val amino acid substitution located near the catalytic core of *ACAD9*. SDS and BN-PAGE analysis showed severely decreased *ACAD9* and complex I protein levels, and lentiviral complementation of patient fibroblasts partially rescued the complex I deficiency. Riboflavin supplementation did not ameliorate the complex I deficiency in patient fibroblasts. More than a dozen *ACAD9* patients with complex I deficiency have been identified in the last 3 years, indicating that *ACAD9* is important for complex I assembly, and that *ACAD9* mutations are a relatively frequent cause of complex I deficiency.

Communicated by: John Christodoulou

Competing interests: None declared

J. Nouws • M. van den Brand • L. Nijtmans
Nijmegen Centre for Mitochondrial Disorders at the Department of Pediatrics, Radboud University Medical Centre, 6500 HB, Nijmegen, The Netherlands

F. Wibrand • M. Duno • A.M. Lund • E. Østergard
Department of Clinical Genetics, Copenhagen University Hospital, Rigshospitalet, Copenhagen, Denmark

H. Venselaar
Centre for Molecular and Biomolecular Informatics, Radboud University Nijmegen Medical Centre, 6500 HB, Nijmegen, The Netherlands

S. Trautner
Department of Pediatrics, Roskilde University Hospital, Roskilde, Denmark

S. Trautner
Department of Neonatology, Copenhagen University Hospital, Rigshospitalet, Copenhagen, Denmark

L. Nijtmans (✉)
Nijmegen Centre for Mitochondrial Disorders at the Department of Pediatrics, Radboud University Nijmegen Medical Centre, Geert Grooteplein 10, 6525 GA, Nijmegen, The Netherlands
e-mail: l.nijtmans@cukz.umcn.nl

Introduction

Inborn errors of metabolism (IEM) is a large group of disorders, with a wide spectrum of symptoms, and this also holds true for an IEM subgroup: the oxidative phosphorylation disorders. One in every 5,000 newborns suffers from such a disorder (Skoldal et al. 2003), and 20–25% of these cases are isolated complex I deficiencies (Bugiani et al. 2004; Loeffen et al. 2000; Scaglia et al. 2004; Thorburn 2004). Complex I deficiency can be caused by mutations in genes encoding the structural components of the complex, either in mtDNA or nuclear DNA, or by mutations in genes encoding proteins aiding the assembly of the 45 subunits of the complex. Defects in assembly factors form a new class of disease (Nouws et al. 2012), which are probably responsible for 50% of the isolated complex I deficiencies. In 2010, we identified a new complex I assembly factor, *ACAD9*, and to date 14 patients in 8 families with *ACAD9* mutations have been reported (Gerards et al. 2011; Haack et al. 2010; Haack et al. 2012; Nouws et al. 2010).

The patients were identified within a period of 3 years, indicating that ACAD9 is a crucial protein in the assembly process, and that mutations in this gene are a relatively frequent cause of complex I deficiency. Most patients with ACAD9 mutations present with exercise intolerance in combination with hypertrophic cardiomyopathy, a thickening of the heart muscle with various presentations, and, when diagnosed in (pre-)adolescent children, a poor prognosis. Hypertrophic cardiomyopathy may be a consequence of mitochondrial dysfunction, caused by mutations in proteins that are involved in fatty acid oxidation, mitochondrial translation, or oxidative phosphorylation. Here we report a new pathogenic mutation in *ACAD9*, causing hypertrophic cardiomyopathy and early death. In contrast to a previous report (Gerards et al. 2011) of the beneficial effect of riboflavin in ACAD9-deficient patients, this patient did not respond to riboflavin treatment.

Materials and Methods

Clinical Data

The patient was a girl, the first child of healthy first-cousin parents of Turkish origin. The pregnancy was uncomplicated, apart from a maternal febrile urinary infection shortly before birth. The patient was born in gestation week 41+4 by cesarean section, with no clinical signs of asphyxia.

Shortly after birth, she had respiratory insufficiency requiring nasal CPAP therapy with high oxygen supplementation, and she developed a compensated metabolic acidosis with a plasma lactate up to 9 mmol/l. A chest X-ray showed bilateral dense lungs and antibiotic therapy was initiated. At the age of 23 postnatal hours, her condition deteriorated into cardiorespiratory collapse with severe pulseless bradycardia: she was given cardiac massage, intubated, and mechanically ventilated. Plasma lactate rose to a maximum of 20 mmol/l. Echocardiography demonstrated a structurally normal heart with signs of severe pulmonary hypertension. The liver was enlarged, and paralytic ileus was suspected on abdominal X-ray, but this resolved over the following week. She was extubated after 5 days, requiring nasal CPAP for another week. At 3 weeks of age, her condition had improved and she was discharged to a local hospital. Plasma lactate levels had stabilized to 2.2–3.3 mmol/l.

At age 7 weeks, she presented with tachypnea, paradoxical respiration, muscle weakness, and hypotonia. Echocardiography showed severe concentric left ventricle hypertrophy, which progressed over the next month, despite propranolol therapy. At age 3 months, treatment with 100 mg riboflavin per day was initiated. Her condition

deteriorated during intercurrent infections, and she died at age 6 months in cardiogenic failure.

Urine organic acids measured three times showed excretion of lactate, citric acid cycle metabolites and a consistent slight elevation of 3-methylglutaconic acid, in the range of 21–65 $\mu\text{mol}/\text{mmol}$ creatinine (ref < 9). Plasma amino acids showed elevated alanine (1221 $\mu\text{mol}/\text{l}$, ref 148–475) and low citrulline (7 $\mu\text{mol}/\text{l}$, ref. 8–47).

Enzyme Measurements

Respiratory chain enzyme analysis in muscle and fibroblasts was performed as described before (Cooperstein and Lazarow 1951; Janssen et al. 2007; Wibrand et al. 2010). Values are expressed relative to the mitochondrial reference enzyme citrate synthase (Srere 1969).

SNP Array Analysis and Homozygosity Mapping

DNA was extracted from peripheral blood according to standard procedures and used for a genome-wide search for homozygosity with the Affymetrix Genomewide Human SNP Array 6.0 (Affymetrix Inc., Santa Clara, CA). In brief, DNA was digested with the restriction enzymes StyI and NspI, mixed with StyI and NspI adapters and ligated with the T4 DNA ligase. The ligated DNA was PCR-amplified, pooled, and purified. The purified PCR product was fragmented with DNase I and end-labeled with biotin. The samples were hybridized to an array for 18 h in a hybridization oven. The array was washed, stained, and scanned with an Affymetrix GeneChip scanner 3000. Affymetrix software was used to analyze the data, and homozygositymapper (homozygositymapper.org) was used to identify the homozygous regions.

Mutation Analysis

PCR of genomic DNA was performed with the Promega GoTaq PCR system and the following conditions: 0.2 mM dNTPs, 1 x buffer, 1.5 mM MgCl_2 , 0.5 mM of each primer, 10 ng template and 1.5U polymerase in a total volume of 50 μl . The PCR program was: 94° C for 2 min, 35 cycles of denaturing at 94° C for 30 s, annealing at 60° C for 30 s, and extension at 72° C for 30 s, and a final extension step of 72° C for 7 min.

Sequencing was performed with the ABI Big Dye Terminator v. 1.1 Cycle Sequencing Kit (Applied Biosystems, Foster City, USA). The sequencing reactions were vacuum-purified with the Montage Seq96 Sequencing Reaction Cleanup Kit (Millipore SA, Saint-Quentin, France) and analyzed on an ABI 3130xl Gene Analyzer (Applied Biosystems). The primer sequences are available upon request.

The data were analyzed with Sequencing Analysis Software Version 5.2 from Applied Biosystems, and mutation screening was performed using Mutation Surveyor v.3.1 Software (SoftGenetics). Verified variations were evaluated through the bioinformatic tools of Alamut (interactive Biosoftware). Primer sequences and PCR conditions are available on request.

Blue Native, SDS-PAGE, and In-Gel Activity Assays

Eighty micrograms of solubilized mitochondrial protein was loaded on 5–15% blue native gradient gels or on one-dimensional 10% sodium dodecyl sulfate polyacrylamide gels (SDS-PAGE) as described previously (Calvaruso et al. 2008; Ugalde et al. 2004). After electrophoresis, the gels were processed for either complex I in-gel activity (CI-IGA) analysis or immunoblotting. For blotting, proteins were transferred to a PROTRAN nitrocellulose membrane (Schleicher & Schuell).

Antibodies and ECL Detection

Immunodetection was performed by the use of the following primary antibodies: CI-NDUFA9, CII-SDHA, CV-ATPase- α , and V5 (Invitrogen), CII-SDHB (Abcam), Porin (VWR international), ACAD9 (a gift from J. Vockley, University of Pittsburgh, USA). Secondary detection was performed using peroxidase conjugated anti-mouse or anti-rabbit IgGs (Invitrogen). The signal was generated using ECL (Pierce, Rockford, USA).

Lentiviral Complementation of Patient Fibroblasts

ACAD9WT and the Cox 8 leader sequence were cloned into pDONR201 as described before (Hoefs et al. 2008; Nouws et al. 2010). To construct the lentiviral compatible vector containing a C-terminally V5-tagged ACAD9WT or Cox 8 leader sequence, the pDONR201-ACAD9WT and pDONR201-cox8 vectors were recombined with pLenti6.2V5-DEST Gateway Vector using the Gateway LR Clonase II enzyme mix (Invitrogen). HEK293FT cells were transfected to produce lentivirus with pLP1, pLP2, pVSV/G, and one of the two expression vectors according to the manufacturer's protocol (Invitrogen). The virus was harvested after 72 h and added to the human fibroblasts overnight. The following day, the virus was removed and the medium refreshed. After 48 h, 2.5 μ g/ml blasticidin was added to the medium to select the transduced cells. Cells were selected for 14 days, in which time the mock-infected cells (without virus) died. Blasticidin-resistant cells were used for biochemical analysis within six passages after transduction.

Riboflavin Treatment of Patient Cells

Human skin fibroblasts were cultured in medium 199 (Gibco) supplemented with 10% fetal bovine serum (FBS v/v) (PAA), 1% penicillin/streptomycin (Gibco), 1mM sodium pyruvate (Sigma), and 1 μ g/ml riboflavin (Sigma) for one week, and the medium was refreshed every 2 days.

Modeling

The ACAD9 modeling was executed as described in (Nouws et al. 2010). Modeling details can be found online at http://www.cmbi.ru.nl/_hvensela/ACAD9/

Results

Enzyme Measurements and Gel Analyses

Analysis of respiratory chain enzyme activity in muscle showed a severe isolated complex I deficiency, with a CI/CS ratio of ≤ 0.01 (ref. 0.19–1.54). In fibroblasts, the CI/CS ratio was decreased to 0.16 (ref 0.24–0.37). Western blot analysis showed a severe decrease of ACAD9 protein, suggesting that the mutation leads to instability of the protein (Fig. 1a). To compare with other *ACAD9* mutations, we included fibroblasts from two previously identified patients in both the SDS and the blue native analysis. Our patient had a severe decrease of complex I in-gel activity and of the total amount of complex I by immunoblot analysis, compared both to controls and to the two other *ACAD9* patients (Fig. 1b).

Gene and Conservation Analyses

A genome-wide search for homozygosity revealed several homozygous regions, altogether comprising 298.5 Mb. No mutations were found in the structural complex I genes *NDUFA4*, *NDUFB4*, or *NDUFB9* that were located in the homozygous regions. Sequencing of *ACAD9* located in a homozygous region on chromosome 3 showed a homozygous missense mutation, c.659C>T (p.Ala220Val). The variant was absent from the dbSNP, ESP, and the 1,000 genomes databases (Altshuler et al. 2010), and in silico prediction by PolyPhen2, SIFT, and Mutation Taster all pointed to a possible pathogenic effect. Both parents were heterozygous carriers of the mutation. The affected amino acid, Ala220, is highly conserved among organisms expressing ACAD9 (Fig. 1c). In addition, this amino acid is also conserved in other ACAD family members like VLCAD (Fig. 1c) and SCAD and MCAD (not shown).

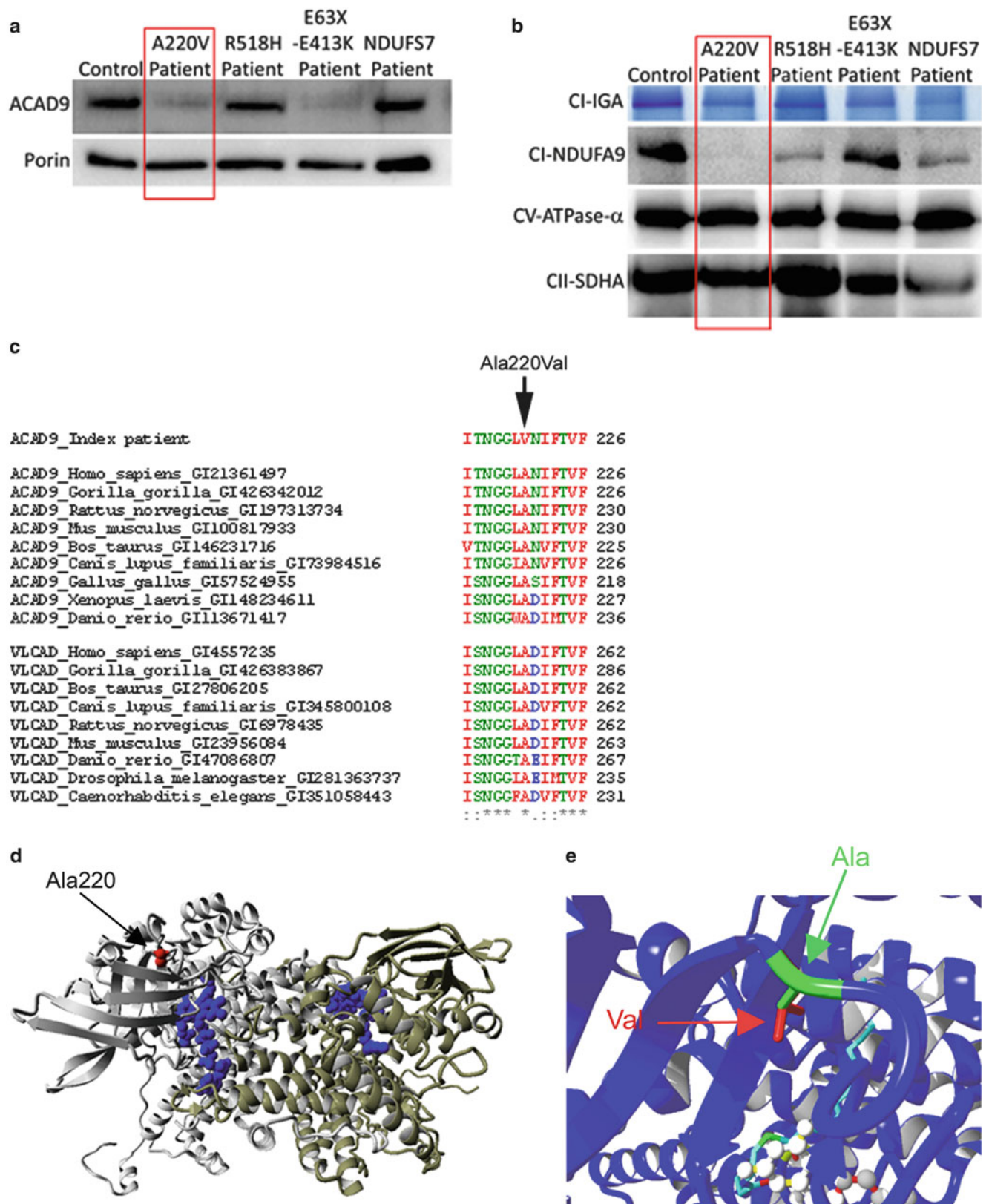


Fig. 1 The ACAD9 p.Ala220Val substitution leads to instability of the protein. (**a**, **b**) ACAD9 expression level and complex I expression level in control, *ACAD9* and *NDUFS7* patient fibroblasts. The p.Ala220Val mutation is described in this chapter, whereas the two

other ACAD9 patients (R518H and E63X-E413K) and the *NDUFS7* patient were described previously (Nouws et al. 2010; Triepels et al. 1999). (**a**) SDS-PAGE immunodetections of ACAD9 and porin, showing a decreased amount of ACAD9 in the patient. (**b**) BN-PAGE

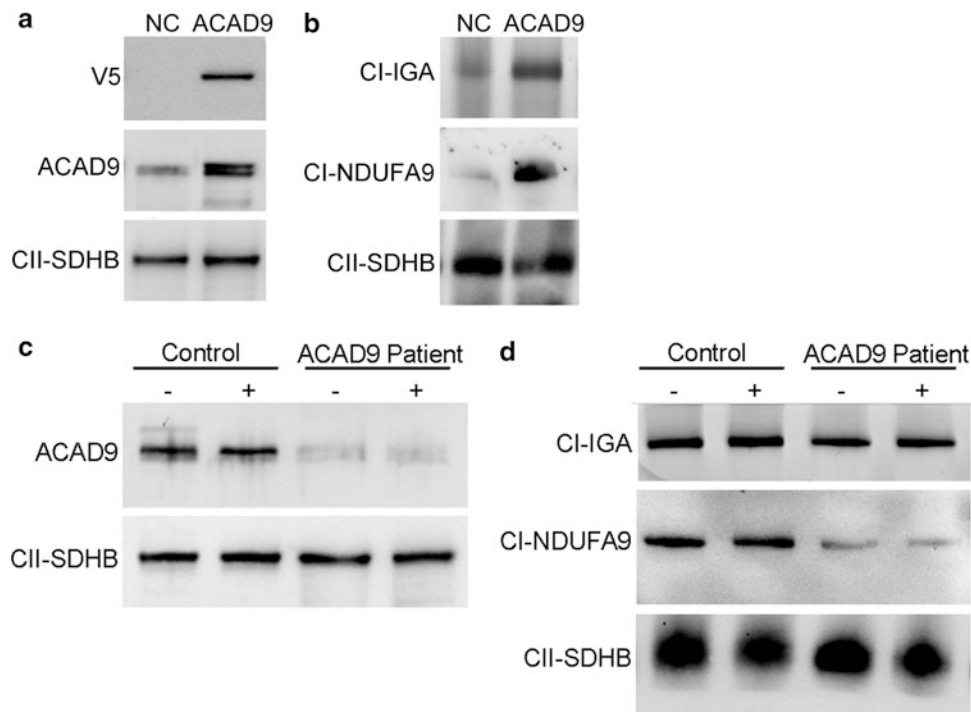


Fig. 2 Complementation and riboflavin treatment of patient fibroblasts. **(a–b)** Lentiviral complementation of patient fibroblasts with negative control V5-tagged COX8 leader sequence, indicated as NC and V5-tagged wild-type ACAD9 as ACAD9. **(a)** SDS-PAGE immunodetections of V5 and ACAD9 showing the presence of V5-tagged ACAD9. SDHB was used as a loading control. **(b)** BN-PAGE analysis of complex I in-gel activity (CI-IGA) and western blot immunodetection of the complex I subunit NDUFA9 showing an increase in complex I in-gel activity and amount by complementation with WT ACAD9. Complex II-SDHB was used as a loading control.

(c, d) Riboflavin treatment of control and patient fibroblasts. **(c)** SDS-PAGE immunodetections of ACAD9 and SDHB in control and ACAD9 patient fibroblasts, showing no differences in ACAD9 amounts between fibroblasts cultured without (–) and with (+) riboflavin supplementation. **(d)** BN-PAGE analysis of complex I in-gel activity (CI-IGA) and western blot immunodetection of complex I subunit NDUFA9 showing no differences in complex I activity or amount between fibroblasts cultured without (–) and with (+) riboflavin supplementation. Complex II-SDHB was used as a loading control.

Modeling of the p.Ala220Val Mutation

The affected alanine is located in proximity of the fatty acid and FAD (flavin adenine dinucleotide) binding sites in the core of the protein (Fig 1d–e). The mutation changes alanine to valine, which are both hydrophobic and small amino acids.

Functional Complementation

To confirm that the *ACAD9* p.Ala220Val amino acid change caused the complex I deficiency in this patient,

we complemented patient fibroblasts with C-terminally V5-tagged wild-type ACAD9. The protein was introduced in the cells by stable lentiviral transduction, and we could demonstrate the presence of V5-tagged ACAD9 on SDS western blot (Fig. 2a). Both complex I amount and activity (CI-IGA) increased, indicating that the wild-type *ACAD9* indeed rescued the complex I deficiency in the patient cells (Fig. 2b). Consistent with these results, also spectrophotometric analysis demonstrated an increase in CI/CS ratio from 0.17 to 0.23 after complementation of the patient cells, whereas this did not change in control cells.

Fig. 1 (continued) analysis of complex I in-gel activity (CI-IGA) and western blot immunodetection of the complex I subunit NDUFA9, showing a decreased activity and amount of fully assembled complex I in the patient. Complex V-CV-ATPase- α and complex II-SDHA were used as loading controls. **(c)** Conservation of the altered amino acids is shown via clustalW alignments. Asterisks (*) indicate identical amino acids, colons (:) indicate conserved substitutions, and periods (.) indicate semi-conserved substitutions. **(d)** Model of ACAD9 (PDB code 3b96)

and the p.Ala220Val mutation, showing the two ACAD9 monomers (grey and yellow), the location of the FAD cofactor (blue), and the arrow indicates the location of the mutation (red). **(e)** The mutation shown in closer detail; the replacement of alanine (in green and indicated by green arrow) by valine leads to an addition of two methylgroups (indicated in red and by a red arrow). Moreover, the mutation is in proximity to the fatty acid (light blue stretch) and FAD (white balls) binding sites in the core of the protein

Table 1 Biochemical data on patients with complex I deficiency due to *ACAD9* mutations

Publication	Amino acid substitutions	Sex	% Res CI activity in fibroblasts	% Res CI activity in muscle	Elevated blood lactate level	Elevated CSF lactate level	Elevated alanine level
Nouws et al 2010	Arg518His (I-1)	F	53%		+	+	+
	Glu63X and Glu413Lys (II-1)	F	58%	61%	+		
Haack et al 2010	Phe44Ile and Arg266Gln (I:A)	F	32%	14%	+		
	Phe44Ile and Arg266Gln (I:B)	M	38%		+		
	Arg266Gln and Arg417Cys (II)	F		13%	+		
	Ala326Pro and Arg532Trp (III)	F		26%	+	+	
Gerards et al 2011, Scholte et al 1995	Arg532Trp (VII-6)	F	38%		+		-
	Arg532Trp (VII-8)	M	40%		+		-
	Arg532Trp (VII-11)	F	50%		+		-
	Arg127Gln and Arg469Trp (CV)	F		9%	+		-
Haack et al 2012	Arg532Trp (59029)			3%	+		
	Arg532Trp (59033)				+		
	Arg532Trp (59036)				+		
This paper	Ala220Val	F	67%	≤11%	+		+

Residual CI activity in fibroblasts = complex I activity normalized for citrate synthase, percentage of lowest control value (values in bold are normalized to COX activity); grey box = percentage of control mean. Residual CI activity in muscle = complex I activity normalized for citrate synthase activity for percentage of lowest control value; grey box = percentage of control mean. + symptom present, - symptom absent, Empty box if information is not available

Riboflavin Treatment of Fibroblasts

Since riboflavin has been reported to have a beneficial effect in several cases of complex I deficiency caused by *ACAD9* mutations in patients and patient fibroblasts, we decided to test riboflavin treatment in this case as well. The patient did not show clinical improvement after riboflavin administration. We also assayed whether riboflavin had a beneficial effect on the patient fibroblasts, but treatment of the p.Ala220Val patient cell line with riboflavin did not have any effect; it did not stabilize the *ACAD9* protein nor did it increase complex I activity or amount (Fig. 2c–d).

Discussion

We report a new pathogenic mutation in the complex I assembly factor *ACAD9*. The mutation results in a p.Ala220Val substitution that affects a highly conserved amino acid. The *ACAD9* protein level was decreased, leading to a pronounced reduction of both complex I amount and activity, and functional complementation with wild-type *ACAD9* led to an increase in complex I activity and amount of fully assembled complex I. The affected

amino acid is located in the proximity of the fatty acid and FAD binding sites in the core of the protein, which may interfere with their binding. The mutation leads to the substitution of alanine with valine, and although both amino acids are hydrophobic and small, valine may fit less well in the protein structure and possibly pose a sterical hindrance for the side chains of other amino acids. Taken together, these results indicate that the mutation is disease-causing.

Including this patient, 15 patients have been reported up to date with complex I deficiency due to mutations in *ACAD9*, Tables 1 and 2 show an overview of the patients, the biochemical data, and the clinical findings. The major clinical presentation of this patient was hypertrophic cardiomyopathy, as reported in 10 out of 14 complex I-deficient patients with *ACAD9* mutations (Nouws et al. 2010; Haack et al. 2012; Gerards et al. 2011; Haack et al. 2012). Additional symptoms among these ten patients included lactic acidosis, failure to thrive, hypotonia, exercise intolerance, encephalomyopathy, cardiorespiratory depression, mild hearing loss, and short stature. We found a consistent slightly elevated excretion of 3-methylglutaconic acid, which can be an unspecific marker of a respiratory chain disorder. Excretion of 3-methylglutaconic acid was

Table 2 Clinical findings in patients with complex I deficiency due to mutations in ACAD9

Publication	Amino acid substitutions	Pregnancy duration	Age on onset	Age of death	Alive at	Riboflavin therapy	Neurological symptoms	Brain abnormalities	Seizures	Psychomotor dev. delay	Hypotonia	Hearing loss	Respiratory problems	Tachypnea	Dyspnoea	Respiratory disturbance	Other organ failure	Hypertrophic cardiomyopathy	Hepatology	Other	Failure to thrive	Exercise intolerance	Short stature	
Nouws et al. 2010	Arg518His (I-1)	Term	8 m	18 y																				
	Glu63X and Glu413Lys (II-1)	35	4 m	6 m																				
Haack et al. 2010	Phe44Ile and Arg266Gln (I:A)	39 w + 6 d	24 h	46 d																				
	Phe44Ile and Arg266Gln (I:B)	Birth	Birth	5 y																				
	Arg266Gln and Arg417Cys (II)	Birth	Birth	12 y																				
	Ala326Pro and Arg532Trp (III)	Birth	Birth	2 y																				
Gerards et al. 2011, Scholte et al. 1995	Arg532Trp (VII-6)	4 y	4 y	31 y																				
	Arg532Trp (VII-8)	4 y	4 y	38 y																				
	Arg532Trp (VII-11)	4y	4y	40 y																				
Haack et al. 2012	Arg127Gln and Arg469Trp (CV)	Early CH	Early CH	27 y																				
	Arg532Trp (59029)																							
	Arg532Trp (59033)																							
This report	Arg532Trp (59036)																							
	Ala220Val	41 w + 4 d	Birth	6 m																				

Dev. developmental, + symptom present, - symptom absent, empty box if information is not available, CH childhood, d days, w weeks, m months, y years

not reported in any of the other ACAD9 patients. The variability in the severity of the disorder was wide, with one patient dying at age 46 days, and one patient being alive at age 18 years (Nouws et al. 2010). The four remaining *ACAD9* patients presented with a primarily muscular phenotype with fatigability, exercise intolerance, and lactic acidosis in childhood, whereas cardiac function was normal (Gerards et al. 2011). Moreover, these patients had a relatively late onset of their symptoms. Three of the patients with the muscular phenotype were homozygous for a p.Arg532Trp mutation, which was also found homozygous in three patients with the cardiomyopathic phenotype (Gerards et al. 2011; Haack et al. 2010). Since the mutation is found in both groups, there does not seem to be an apparent genotype-phenotype correlation; a possible explanation for the clinical differences could be modifying variants in other genes.

In addition to the aforementioned patients, He and coworkers described two other patients with deficiency of ACAD9 who had a liver phenotype and one patient displaying cardiomyopathy. However, these patients did not have isolated complex I deficiency, and no pathogenic mutations were identified, hence the exact contribution of the ACAD9 mutations to the phenotype of these patients is unclear (He et al. 2007).

Riboflavin treatment has been reported to alleviate symptoms in a few patients with the muscular phenotype (Scholte et al. 1995). The patients reported increased endurance power and disappearance of exercise-related nausea and pain after riboflavin therapy was started. Moreover, one of the patients had had one stroke-like episode at age 13 years, and had no more episodes on riboflavin therapy. After 1–2 years of riboflavin therapy, the patients' resting lactate decreased and exercise tolerance assessed by ergometry increased.

In vitro treatment of two ACAD9-deficient fibroblast cell lines, which were compound heterozygous for the Phe44Ile and Arg266Gln substitutions resulted in 2.1- and 1.7-fold increases in complex I activity, respectively (Haack et al. 2010). We did not find any increase in ACAD9 protein level or complex I activity on riboflavin treatment of fibroblasts of our patient, in accordance with the lack of a clinical response to treatment with 100 mg riboflavin per day. None of the other patients with the cardiomyopathic phenotype were reported to receive riboflavin treatment.

Riboflavin is a precursor of flavin mononucleotide (FMN) and FAD, which are cofactors in complex I. The mode of action for riboflavin remains elusive, but it has been suggested to increase mitochondrial FAD concentration, which may support FAD binding. This binding could be necessary for the catalytic activity of ACAD9, however, also its folding or stability may improve (Henriques et al. 2010). Riboflavin might also function as an electron

acceptor, since fibroblasts from patients with deficiency of NDUFS2, a subunit without FAD or FMN binding sites, responded to riboflavin treatment (Bar-Meir et al. 2001). An explanation for the lack of response to riboflavin treatment in our patient could be the specific location of the mutation, although both Ala220Val and Arg532Trp, found in patients who apparently responded to riboflavin treatment, are located near the FAD binding site. The scarce and contrasting results of riboflavin administration suggest that further studies, both in vivo and in vitro, are needed on riboflavin treatment in patients with complex I deficiency due to *ACAD9* mutations to establish the effect of the treatment.

Take-Home Message

ACAD9 mutations are a major cause of complex I deficiency and ACAD9 patients do not always respond to riboflavin treatment.

References

- Altshuler DL, Durbin RM, Abecasis GR et al (2010) A map of human genome variation from population-scale sequencing. *Nature* 467(7319):1061–1073
- Bar-Meir M, Elpeleg ON, Saada A (2001) Effect of various agents on adenosine triphosphate synthesis in mitochondrial complex I deficiency. *J Pediatr* 139(6):868–870
- Bugiani M, Invernizzi F, Alberio S et al (2004) Clinical and molecular findings in children with complex I deficiency. *Biochim Biophys Acta* 1659(2–3):136–147
- Calvaruso MA, Smeitink J, Nijtmans L (2008) Electrophoresis techniques to investigate defects in oxidative phosphorylation. *Methods* 46(4):281–287
- Cooperstein SJ, Lazarow A (1951) A microspectrophotometric method for the determination of cytochrome oxidase. *J Biol Chem* 189(2):665–670
- Gerards M, van den Bosch BJ, Danhauser K et al (2011) Riboflavin-responsive oxidative phosphorylation complex I deficiency caused by defective ACAD9: new function for an old gene. *Brain* 134(Pt 1):210–219
- Haack TB, Danhauser K, Haberberger B et al (2010) Exome sequencing identifies ACAD9 mutations as a cause of complex I deficiency. *Nat Genet* 42(12):1131–1134
- Haack TB, Haberberger B, Frisch EM et al (2012) Molecular diagnosis in mitochondrial complex I deficiency using exome sequencing. *J Med Genet* 49(4):277–283
- He M, Rutledge SL, Kelly DR et al (2007) A new genetic disorder in mitochondrial fatty acid beta-oxidation: ACAD9 deficiency. *Am J Hum Genet* 81(1):87–103
- Henriques BJ, Olsen RK, Bross P, Gomes CM (2010) Emerging roles for riboflavin in functional rescue of mitochondrial beta-oxidation flavoenzymes. *Curr Med Chem* 17(32):3842–3854
- Hoefs SJ, Dieteren CE, Distelmaier F et al (2008) NDUFA2 complex I mutation leads to Leigh disease. *Am J Hum Genet* 82(6):1306–1315
- Janssen AJ, Trijbels FJ, Sengers RC et al (2007) Spectrophotometric assay for complex I of the respiratory chain in tissue samples and cultured fibroblasts. *Clin Chem* 53(4):729–734

- Loeffen JL, Smeitink JA, Trijbels JM et al (2000) Isolated complex I deficiency in children: clinical, biochemical and genetic aspects. *Hum Mutat* 15(2):123–134
- Nouws J, Nijtmans L, Houten SM et al (2010) Acyl-CoA dehydrogenase 9 is required for the biogenesis of oxidative phosphorylation complex I. *Cell Metab* 12(3):283–294
- Nouws J, Nijtmans LG, Smeitink JA, Vogel RO (2012) Assembly factors as a new class of disease genes for mitochondrial complex I deficiency: cause, pathology and treatment options. *Brain* 135 (Pt 1):12–22
- Scaglia F, Towbin JA, Craigen WJ et al (2004) Clinical spectrum, morbidity, and mortality in 113 pediatric patients with mitochondrial disease. *Pediatrics* 114(4):925–931
- Scholte HR, Busch HF, Bakker HD et al (1995) Riboflavin-responsive complex I deficiency. *Biochim Biophys Acta* 1271(1):75–83
- Skladal D, Halliday J, Thorburn DR (2003) Minimum birth prevalence of mitochondrial respiratory chain disorders in children. *Brain* 126:1905–1912
- Srere PA (1969) Citrate synthase : [EC 4.1.3.7. Citrate oxaloacetate-421 lyase (CoA-acetylating)]. In: John ML (ed) *Methods in enzymology. Citric acid cycle*, vol 13. Academic Press, London, pp 3–11
- Thorburn DR (2004) Mitochondrial disorders: prevalence, myths and advances. *J Inher Metab Dis* 27(3):349–362
- Triepels RH, van den Heuvel LP, Loeffen JL et al (1999) Leigh syndrome associated with a mutation in the NDUFS7 (PSST) nuclear encoded subunit of complex I. *Ann Neurol* 45(6):787–790
- Ugalde C, Vogel R, Huijbens R, van den Heuvel LP, Smeitink J, Nijtmans L (2004) Human mitochondrial complex I assembles through the combination of evolutionary conserved modules: a framework to interpret complex I deficiencies. *Hum Mol Genet* 13(20):2461–2472
- Wibrand F, Jeppesen TD, Frederiksen AL et al (2010) Limited diagnostic value of enzyme analysis in patients with mitochondrial tRNA mutations. *Muscle Nerve* 41(5):607–613

Pulmonary Manifestations in a Patient with Transaldolase Deficiency

Nada Jassim · Mohammed AlGhaihab ·
Suhail Al Saleh · Majid Alfadhel ·
Mirjam M.C. Wamelink · Wafaa Eyaid

Received: 27 March 2013 / Revised: 21 May 2013 / Accepted: 26 May 2013 / Published online: 12 July 2013
© SSIEM and Springer-Verlag Berlin Heidelberg 2013

Abstract Transaldolase deficiency is a newly recognized metabolic disorder. It is an autosomal recessive genetic disease (OMIM #606003). The effects of the defect in the TALDO gene are pleiotropic with a clinical presentation of growth retardation, dysmorphic features, cutis laxa, congenital heart disease, hepatosplenomegaly, pancytopenia, and bleeding tendencies. This is the first report of a child who was diagnosed at birth with transaldolase deficiency who subsequently developed hepatopulmonary syndrome.

Abbreviations

ASD II	Atrial septal defect secundum
AVM	Arteriovenous malformation
CEE	Contrast-enhanced echocardiography
CT	Computed tomography
HPS	Hepatopulmonary syndrome
99mTc-MAA scan	99Technetium macroaggregated albumin perfusion lung scanning
PDA	Patent ductus arteriosus
PPP	Pentose phosphate pathway
RR	Respiratory rate

SaO ₂	Oxygen saturation
TALDO	Transaldolase
US	Ultrasonography
VSD	Ventricular septal defect

Introduction

The pentose phosphate pathway (PPP) is an important metabolic pathway in which glucose-6-phosphate (G6P) is converted into ribose-5-phosphate (R5P) through a series of reactions. Some of the reactions are reversible, while others are irreversible. The irreversible part of the pathway is rate-limited by the activity of G6P dehydrogenase (G6PD), whereas the reversible component is rate-limited by the activity of transaldolase (TALDO). The PPP serves a crucial role in cellular proliferation and growth by producing R5P, which is required for the synthesis of DNA and RNA. In addition, the PPP is an important source of NADPH (Perl et al. 2011).

Two little-known disorders of PPP are deficiencies in R5P isomerase and transaldolase, both of which affect the reversible, non-oxidative branch of the pathway. R5P deficiency is an exceedingly rare disease that has only been described once: The primary phenotype was leukoencephalopathy (Valayannopoulos et al. 2006). On the other hand, several patients have been reported with transaldolase deficiency since it was first described. In these patients, while liver involvement is prominent, the phenotype appears to be more pleiotropic (refer to Table 1; Eyaid et al. 2013).

Here, we report on an infant with the transaldolase (TALDO) deficiency. The infant developed respiratory

Communicated by: Francois Feillet, Ph.D., M.D.

Competing interests: None declared

N. Jassim · M. AlGhaihab · S. Al Saleh · M. Alfadhel · W. Eyaid (✉)
Department of Pediatrics MC 1510, King Abdulaziz Medical City,
King Fahad National Guard Hospital, P.O Box 22490, Riyadh 11426,
Saudi Arabia
e-mail: eyaidw@ngha.med.sa

M. AlGhaihab · S. Al Saleh · M. Alfadhel · W. Eyaid
King Saud Bin Abdulaziz University for Health and Science, Riyadh,
Saudi Arabia

M.M.C. Wamelink
Department of Clinical Chemistry, Neuroscience Campus Amsterdam,
VU University Medical Center, Amsterdam, The Netherlands

symptoms in early infancy and was later diagnosed with hepatopulmonary syndrome (HPS). To our knowledge, this is the first such case to be reported in the literature.

Case Report

A 17-month-old boy, the fifth child born to consanguineous parents, was diagnosed with transaldolase deficiency. Two siblings were similarly affected. The diagnosis was established by autozygote analysis and biochemical evaluations of urinary sugars and polyols (Family II, Patient 3) (Eyaid et al. 2013).

The child was born at 36 weeks gestation via spontaneous natural delivery. His Apgar scores at 1 and 5 min were 7 and 8, respectively. His growth parameters were within the normal ranges. He was observed to have a heart murmur and dysmorphic features, including triangular progeroid face, low set ears, short philtrum, and wrinkled skin, as well as hepatosplenomegaly. Therefore, additional evaluations were performed. These tests included echocardiography, which showed closed patent ductus arteriosus (PDA) and atrial septal defect secundum (ASD II) with small ventricular septal defects (VSDs). An ophthalmology evaluation and abdominal and head ultrasonography (US) were all normal. He experienced one incident of decreased hemoglobin and platelets that required transfusion. Other investigations, including the liver profile, were unremarkable. He was discharged at the age of 14 days.

At the age of 3 months, he presented to the emergency department with a 1-week history of fever and cough. At presentation, he was in moderate respiratory distress and was tachypneic (RR of 50/min) and had subcostal retractions. A chest examination revealed bilateral wheezes and crackles. The oxygen saturation (SaO₂) was 84 % in room air, and he thus required supplemental oxygen of 1 L/min via a nasal cannula. He was diagnosed with bronchiolitis with negative virology. He responded slowly to the supportive management, including oxygen, fluids, and inhaled bronchodilator therapy, and was hospitalized for 40 days on the basis that his hypoxia required supplemental oxygen. After release, he continued to have frequent admissions related to respiratory symptoms and bronchospasms, some of which occurred in the pediatric intensive care unit. However, no intubations were required. He has demonstrated occasional decreases in his hemoglobin to 90 g/L. These values normalize after transfusion.

At 12 months of age, a more intensive workup was performed for the prolonged hypoxia and difficulties in weaning off oxygen (0.5 L/min). Immunodeficiency and cystic fibrosis were ruled out. An upper gastrointestinal study and modified barium swallow were performed to rule out aspiration syndrome and gastroesophageal reflux.

The results of these tests were unremarkable. A computed tomography (CT) of the chest showed bilateral diffuse ground-glass lung changes with atelectasis/consolidation in the right upper and lower and left lower lobes. The patient improved, was gradually weaned from oxygen, and was discharged to his home on room air. He was readmitted at 17 months of age in respiratory distress and was reassessed on the basis of an inability to wean him off the oxygen. He presented with pectus chest deformity, digital clubbing, and tachypnea, but with clear good bilateral breathing sounds. His SaO₂ was 66 % on room air, and he was therefore placed on 2 L/min of O₂. The arterial blood gas evaluation while on room air showed a pH of 7.365, PCO₂t of 39.00 mmHg, PO₂t of 36.1 mmHg, cHCO₃- of 21.8 mmol, and base excess ecf of -3.6 mmol. The arterial-alveolar gradient (A-a gradient) was 65, where values greater than 15 suggest the presence of a shunt. A 99Technetium macroaggregated albumin perfusion lung scanning (99mTc-MAA scan) study was performed and revealed activity within the brain and the abdomen, suggesting that systemic shunting accounted for 36 % (this parameter is normally less than 5 %). Therefore, contrast-enhanced echocardiography (CEE, bubble echo) was performed. This test showed evidence of delayed positive bubbles, indicating intrapulmonary shunting. A series of repeated liver US examinations revealed a new finding of liver cirrhosis, which was confirmed by liver biopsy. The overall conclusion was a diagnosis of hepatopulmonary syndrome.

Discussion

Transaldolase (TALDO; EC2.2.1.2) deficiency (OMIM 606003) is a recently described inborn error of the pentose phosphate pathway (PPP). The reported systemic manifestations include dysmorphic features, developmental delay, congenital heart disease, hepatosplenomegaly, hepatic fibrosis, excessive bleeding, thrombocytopenia, hemolytic anemia, and renal complications (Wamelink et al. 2008; Tylki-Szymanska et al. 2009; Balasubramaniam et al. 2011). To our knowledge, no pulmonary effects associated with TALDO deficiency have previously been reported.

In this report, we describe a child with TALDO deficiency who had recurrent respiratory symptoms in the form of bronchospasm that required frequent hospitalization since infancy. We believe these symptoms are related to the primary genetic disease.

The patient started to develop signs and symptoms of respiratory distress, possibly secondary to systemic manifestations of the transaldolase deficiency, early in life. Alternatively, these symptoms may be secondary to reflux or aspiration. The subsequent progression of symptoms and hypoxemia was considered to be associated with the

development of HPS because his clinical picture and investigations failed to meet other differential diagnoses. He had one liver US study performed at the time of birth as part of routine investigation because he appeared dysmorphic. The results of this scan were normal. A second US was performed at the age of 17 months. This US showed liver cirrhosis, which was confirmed by a US-guided liver biopsy. A review of the literature indicates that HPS can occur without liver cirrhosis, as in case of non-cirrhotic portal hypertension, and when associated with HPS, the cirrhosis may be unrelated to the severity of liver dysfunction.

The results of the bubble echo analysis were positive for the left side of the heart within the 3–4 beats during which the root of pulmonary veins were visualized in the absence of any heart defect. This result supports the possibility of intrapulmonary shunting. This result was also supported by positive ⁹⁹Tc macroaggregated albumin perfusion lung scanning.

Hepatopulmonary syndrome was first described in 1884 by Fluckiger, who noted a relationship between the liver and the lung (Kennedy and Knudson 1977). In 1997, Kennedy and Knudson described “hepatopulmonary syndrome” (Yap et al. 1999). This syndrome is defined by a classical triad of chronic liver disease or portal hypertension, hypoxemia, and intrapulmonary shunting. It is a rare complication of chronic liver disease in children (Noli et al. 2008). The prevalence of HPS in adults with cirrhosis is reported to range from 4 % to 29 % (Gupta et al. 2001; Schenk et al. 2002; Noli et al. 2008). This syndrome has been measured in children with cirrhosis or severe portal hypertension, and the prevalence in this group is similar to that in adults (Barbe et al. 1995; Sasaki et al. 2000). The diagnosis of HPS in a child with liver disease is established by the demonstration of hypoxemia or an elevated alveolar-arterial oxygen gradient on arterial blood gas analysis and the presence of intrapulmonary shunting using contrast-enhanced echocardiography (CEE) or a ^{99m}TcMAA perfusion scan (Krowka et al. 1990, 2000).

Hepatopulmonary syndrome is considered to be one of the cardiopulmonary complications of acute or chronic liver disease. It is most frequently associated with portal hypertension (with or without cirrhosis). However, severe hepatic dysfunction is not required for a diagnosis of HPS (Abrams et al. 1995).

One unanswered question is what triggered this child to develop HPS while his elder siblings did not, despite evidence that their livers were also cirrhotic. These observations suggest that the cause of the HPS is independent of the patient’s liver condition, i.e., that both conditions are secondary to the primary genetic defect in the transaldolase enzyme as described above.

Currently, the only effective treatment for HPS is liver transplantation. This option was not pursued in our patient due to the lack of outcome data in patients with transaldolase deficiency.

Conclusion

Pulmonary involvement can be a consequence of transaldolase deficiency. Our patient had recurrent reactive airway disease and was confirmed to have hepatopulmonary syndrome. After excluding common causes, we propose that the recurrent attacks of cough, difficulty of breathing, and bronchospasm are pulmonary manifestations of the disease. We recommend that patients with transaldolase deficiency, who present with recurrent respiratory distress, be further investigated for possible development of HPS.

Conflict of Interest

The authors declare no conflict of interest.

Authors’ Contributions

Nada Jassim and Wafaa Eyaid: manuscript writing

Suhail Al Saleh, Majid Alfadhel, Mirjam M.C. Wamelink, and Mohammed AlGhaihab: interpretation of results and reviewing the paper

Take-Home Message

Patients diagnosed with transaldolase deficiency need to have regular follow-up evaluations of their hepatic and pulmonary function and should have early intervention to avoid adverse sequelae associated with this condition.

References

- Abrams GA, Trauner M, Nathanson MH (1995) Nitric oxide and liver disease. *Gastroenterologist* 3(3):220–233
- Balasubramaniam S, Wamelink MM, Ngu LH et al (2011) Novel heterozygous mutations in TALDO1 gene causing transaldolase deficiency and early infantile liver failure. *J Pediatr Gastroenterol Nutr* 52(1):113–116
- Barbe T, Losay J, Grimon G et al (1995) Pulmonary arteriovenous shunting in children with liver disease. *J Pediatr* 126(4):571–579
- Eyaid W, Al Harbi T, Anazi S, et al (2013) Transaldolase deficiency: report of 12 new cases and further delineation of the phenotype. *J Inherit Metab Dis* (in press)
- Gupta D, Vijaya DR, Gupta R et al (2001) Prevalence of hepatopulmonary syndrome in cirrhosis and extrahepatic portal venous obstruction. *Am J Gastroenterol* 96(12):3395–3399
- Kennedy TC, Knudson RJ (1977) Exercise-aggravated hypoxemia and orthodeoxia in cirrhosis. *Chest* 72(3):305–309

- Krowka MJ, Tajik AJ, Dickson ER, Wiesner RH, Cortese DA (1990) Intrapulmonary vascular dilatations (IPVD) in liver transplant candidates. Screening by two-dimensional contrast-enhanced echocardiography. *Chest* 97(5):1165–1170
- Krowka MJ, Wiseman GA, Burnett OL et al (2000) Hepatopulmonary syndrome: a prospective study of relationships between severity of liver disease, PaO₂ response to 100% oxygen, and brain uptake after (99m)Tc MAA lung scanning. *Chest* 118(3):615–624
- Noli K, Solomon M, Golding F, Charron M, Ling SC (2008) Prevalence of hepatopulmonary syndrome in children. *Pediatrics* 121(3):e522–e527
- Perl A, Hanczko R, Telarico T, Oaks Z, Landas S (2011) Oxidative stress, inflammation and carcinogenesis are controlled through the pentose phosphate pathway by transaldolase. *Trends Mol Med* 17(7):395–403
- Sasaki T, Hasegawa T, Kimura T, Okada A, Mushiake S, Matsushita T (2000) Development of intrapulmonary arteriovenous shunting in postoperative biliary atresia: evaluation by contrast-enhanced echocardiography. *J Pediatr Surg* 35(11):1647–1650
- Schenk P, Fuhrmann V, Madl C et al (2002) Hepatopulmonary syndrome: prevalence and predictive value of various cut offs for arterial oxygenation and their clinical consequences. *Gut* 51(6):853–859
- Tylki-Szymanska A, Stradowska TJ, Wamelink MM et al (2009) Transaldolase deficiency in two new patients with a relative mild phenotype. *Mol Genet Metab* 97(1):15–17
- Valayannopoulos V, Verhoeven NM, Mention K et al (2006) Transaldolase deficiency: a new cause of hydrops fetalis and neonatal multi-organ disease. *J Pediatr* 149(5):713–717
- Wamelink MM, Struys EA, Salomons GS, Fowler D, Jakobs C, Clayton PT (2008) Transaldolase deficiency in a two-year-old boy with cirrhosis. *Mol Genet Metab* 94(2):255–258
- Yap FK, Aw MM, Quek SC, Quak SH (1999) Hepatopulmonary syndrome: a rare complication of chronic liver disease in children. *Ann Acad Med Singapore* 28(2):290–293

Burden of Lysosomal Storage Disorders in India: Experience of 387 Affected Children from a Single Diagnostic Facility

Jayesh Sheth • Mehul Mistri • Frenny Sheth •
Raju Shah • Ashish Bavdekar • Koumudi Godbole •
Nidhish Nanavaty • Chaitanya Datar •
Mahesh Kamate • Nrupesh Oza •
Chitra Ankleshwaria • Sanjeev Mehta • Marie Jackson

Received: 04 April 2013 / Revised: 16 May 2013 / Accepted: 26 May 2013 / Published online: 13 July 2013
© SSIEM and Springer-Verlag Berlin Heidelberg 2013

Abstract Lysosomal storage disorders (LSDs) are considered to be a rare metabolic disease for the national health forum, clinicians, and scientists. This study aimed to know

the prevalence of different LSDs, their geographical variation, and burden on the society. It included 1,110 children from January 2002 to December 2012, having coarse facial features, hepatomegaly or hepatosplenomegaly, skeletal dysplasia, neuroregression, leukodystrophy, developmental delay, cerebral-cerebellar atrophy, and abnormal ophthalmic findings. All subjects were screened for I-cell disease, glycolipid storage disorders (Niemann-Pick disease A/B, Gaucher), and mucopolysaccharide disorders followed by confirmatory lysosomal enzymes study from leucocytes and/or fibroblasts. Niemann-Pick disease-C (NPC) was confirmed by fibroblasts study using filipin stain. Various storage disorders were detected in 387 children (34.8 %) with highest prevalence of glycolipid storage disorders in 48 %, followed by mucopolysaccharide disorders in 22 % and defective sulfatide degradation in 14 % of the children. Less common defects were glycogen degradation defect and protein degradation defect in 5 % each, lysosomal trafficking protein defect in 4 %, and transport defect in 3 % of the patients. This study demonstrates higher incidence of Gaucher disease (16 %) followed by GM2 gangliosidosis that includes Tay-Sachs disease (10 %) and Sandhoff disease (7.8 %) and mucopolysaccharide disorders among all LSDs. Nearly 30 % of the affected children were born to consanguineous parents and this was higher (72 %) in children with Batten disease. Our study also demonstrates two common mutations c.1277_1278insTATC in 14.28 % (4/28) and c.964G>T (p.D322Y) in 10.7 % (3/28) for Tay-Sachs disease in addition to the earlier reported c.1385A>T (p.E462V) mutation in 21.42 % (6/28).

Communicated by: Verena Peters

Competing interests: None declared

J. Sheth (✉) • M. Mistri • F. Sheth • N. Oza • C. Ankleshwaria
Department of Biochemical and Molecular Genetics, FRIGE's
Institute of Human Genetics, FRIGE House, Satellite, Ahmedabad
380015, Gujarat, India
e-mail: jshethad1@gmail.com

R. Shah
Ankur children Hospital, Ashram road, Ahmedabad 380009,
Gujarat, India

A. Bavdekar
Department of Pediatrics, K.E.M Hospital, Pune 411011, India

K. Godbole
Department of Pediatrics, Deenanath Mangeshkar Hospital,
Erandawane, Pune 411 004, India

N. Nanavaty
Subh-nidhi children hospital, Naranpura, Ahmedabad 380013,
Gujarat, India

C. Datar
Sahyadri Medical Genetics and Tissue engineering facility
(SMGTEF), Pune 411005, India

M. Kamate
Consultant Pediatric Neurology and In-charge child development
centre, KLES Prabhakar Kore Hospital, Belgaum, Karnataka, India

S. Mehta
Ushadeep Child Neurology and Epilepsy Clinic, Naranpura,
Ahmedabad, India

M. Jackson
Biochemical Genetics Laboratory, Guys Hospital, London
SE9 1RT, UK

Introduction

Lysosomal storage disorders (LSDs) are the consequence of an abnormal storage of undigested cellular debris, proteins, fats, carbohydrates, and nucleic acids within the cell (Parkinson-Lawrence et al. 2010). They occur due to mutations in the genes that encode for lysosomal hydrolases, resulting in an attenuated enzyme activity and/or their transport to the lysosomes (Saftig and Klumperman 2009; Vellodi 2005). To date, nearly 50 such enzyme deficiencies are responsible for around 40 known storage diseases that have been identified (Vellodi 2005; Futerman and van Meer 2004).

Individually, these disorders are rare but collectively they are as common as other metabolic disorders with a reported incidence of 1:7,700 in Australia (Meikle et al. 1999). A newborn screening program in Taiwan identified a surprisingly high frequency of Taiwanese males with Fabry disease (~ 1 in 1,250). Hwu et al. (2009) identified IVS4+919G>A cryptic mutation in 86 % of the Fabry patients having a late-onset cardiac phenotype. Similarly, Gaucher disease is also one of the most common genetic disorders in Ashkenazi Jews, with a frequency of 1 in 855 live births (Staretz-Chacham et al. 2009). In the Ashkenazi Jews, 94–98 % patients with Tay-Sachs disease have three common mutations: c.1277_1278 insTATC, c.1421+1G>C, and c.805 G>A (p.G269S) (Myerowitz and Costigan 1988; Kaback et al. 1993), while a 7.6 kb deletion is the major mutation causing Tay-Sachs disease in the French Canadian population (Myerowitz and Hogikyan 1986).

A few Indian studies (Sheth et al. 2004; Verma 2000; Nalini and Christopher 2004; Verma et al. 2012) have partly addressed the incidence of LSDs in India along with mutation detection for Tay-Sachs disease (Mistri et al. 2012) and metachromatic leukodystrophy (MLD) (Shukla et al. 2011). Considering the large population and a high frequency of consanguineous marriages, the incidence of LSDs is likely to be higher in India. Hence, this study has been planned to know the burden of LSDs in high-risk group of children and identify common mutation for Tay-Sachs disease in the country, which is more commonly seen in schedule caste (SC) community of Gujarat (Mistri et al. 2012).

Material and Methods

This work is a prospective randomized study of 1,110 children referred from various Indian states and a couple of neighboring countries (Sri Lanka and Afghanistan) from January 2002 to December 2012. It comprises of 938 (84.50 %) children from western, 121 (10.9 %) from

southern, 30 (2.7 %) from northern, 1 (0.09 %) each from eastern and central parts of India, 18 (1.62 %) from Sri Lanka, and 1 (0.09 %) from Afghanistan in the age range of 1 day to 16 years. This study includes 738 male and 372 female children. The most common phenotypes for the referral were coarse facial features, hepatomegaly or hepatosplenomegaly, skeletal dysplasia, neurological involvement including developmental delay or neuroregression, spasticity, seizures, leukodystrophy, cerebral-cerebellar atrophy, and abnormal ophthalmic findings such as cherry red spot, vision loss, and corneal clouding. An institutional ethics committee approval and patient informed consent was obtained to carry out this study.

Random urine and peripheral whole blood samples were collected in all the cases and were initially processed for the screening test followed by confirmatory enzyme study. The screening study was carried out from urine samples for glycosaminoglycans (GAGs) [both quantitative and qualitative] (Dembure and Roesel 1991; Hopwood and Harrison 1982) and plasma was analyzed for chitotriosidase activity (Aerts et al. 2008; Sheth et al. 2010) and mucopolidosis II/III [ML II/III] screening (Sheth et al. 2012). Leukocytes were isolated from whole blood and were processed by standard protocol for enzyme assay using 4-MU fluorometric assay or PNCS spectrophotometric synthetic substrate as outlined by Shapria et al. (1989); Filocamo and Morrone (2011); and Sheth et al. (2004). Niemann-Pick disease-C (NPC) study was carried out on cultured skin fibroblasts in lipid-deficient medium using filipin stain (Kruth and Vaughan 1980; Sheth et al. 2008).

The mutation analysis was carried out in 28 children with enzymatically confirmed diagnosis of Tay-Sachs disease. Genomic DNA was extracted by the standard salting out method (Miller et al. 1988) and investigated for common mutations c.1277_1278 insTATC, c.1421+1 G>C, 7.6 kb deletion, the two pseudo-deficiency alleles c.739C>T (p.R247W) and c.745C>T (p.R249W) of *HEXA* gene followed by exon and intron flanking sequencing for known, rare, and private mutations in all the cases. Prediction of functional effects of non-synonymous single nucleotide substitutions (nsSNPs) was done using softwares SIFT (Sorting Intolerant From Tolerant) and Polyphen2 (Polymorphism Phenotyping v2).

Results

Out of 1,110 children, 387 (34.8 %) were found to be affected with different storage disorders (Table 1 and Fig. 1). Of these, 115 children (29.6 %) were born to consanguineous parents. Glycolipid storage disorders were the most commonly diagnosed LSDs (48 %) in this study population followed by mucopolysaccharide (MPS)

Table 1 Clinical and biochemical study of 387 children affected with different lysosomal storage disorders in India

Disease name/(enzyme name)/[substrate name]	Phenotype observed	Age at diagnosis	Number of cases investigated	Number of affected cases confirmed by enzymatic analysis	Enzyme activity detected in affected individuals (nmol/h/mg protein) Enzyme activity from leukocytes observed in normal individuals (nmol/h/mg protein)	Genotype analysis
Defects in degradation of glycolipids						
Gaucher disease (β-glucosidase) [4-MU-β-D-glucopyranoside]	Type 1 – chronic non-neuropathic: severe hepatosplenomegaly, chronic anemia, and thrombocytopenia; Gaucher cells present in bone marrow Type 3 – subacute neuropathic: degenerative of central nervous system, peripheral symptoms similar to type 1	6 M–13 Y	425	60 (15.5 %)	0.0–4.6 8.0–32.0	Not yet carried out
Tay-Sachs disease (β-hexosaminidase A) [4-methylumbelliferyl-N-acetyl-β-D-glucosamine-6-sulfate (MUGS)]	Neuroregression after 6 months of age, cherry red spot, vision loss, seizures, hypotonia, exaggerated startle response, progressive deafness, delayed mile stone, microcephaly, cerebral atrophy, partial optic atrophy	10 M–3 Y	425	02 (0.51 %)	0.0–4.0 8.0–32.0	Not yet carried out
		10 M–3 Y	465	39 (10 %)	0.0–23.4 80.4–410.0	Earlier reported mutations ^a c.340G>A (E114K) [exon 2]/c.340G>A (E114K) [exon 2] (n = 1) c.964G>A (D322N) [exon 8]/c.964G>A (D322N) [exon 8] (n = 1) c.964G>A (D322N) [exon 8]/c.1277_1278insTATC [exon 11] (n = 1) c.964 G>T (D322Y) [exon 8]/c.964G>T (D322Y) [exon 8] (n = 3) c.1178C>G (R393P) [exon 11]/c.1178 C>G (R393P) [exon 11] (n = 1) c.1385A>T (E462V) [exon 12]/c.1385 A>T (E462V) [exon 12] (n = 6) c.1432G>A (G478R) [exon 13]/c.672+30T>G [intron 6] (n = 1) c.1277_1278insTATC [exon 11]/c.1277_1278insTATC [exon 11] (n = 3) c.508C>T (R170W) [exon 5]/c.508C>T (p.R170W) [exon 5] (n = 1) c.805+1 G>C [intron 7]/c.805+1G>C [intron 7] (n = 2)

(continued)

Table 1 (continued)

Disease name/(enzyme name)/[substrate name]	Phenotype observed	Age at diagnosis	Number of cases investigated	Number of affected cases confirmed by enzymatic analysis	Enzyme activity detected in affected individuals (nmol/h/mg protein)	Enzyme activity from leukocytes observed in normal individuals (nmol/h/mg protein)	Genotype analysis
Sandhoff disease (β -hexosaminidase T) [4-MU-N-Ac- β -D-glucosaminide]	Neuroregression after 6 months of age, cherry red spot, vision loss, seizures, hypotonia, exaggerated startle response, progressive deafness, delayed mile stone, peripheral neuropathy, and organomegaly	7 M–3.5 Y	489	30 (7.75 %)	33.0–382.0 723.4–2700.0		<i>Novel mutations</i> c.788C>T (T263I)/c.788C>T (T263I) [exon 7] (<i>n</i> = 1) c.1121A>C (Q374P)/c.1121 A>C (Q374P) [exon10] (<i>n</i> = 1) c.1421G>A (W474X)/c.1420 G>A (W474X) [exon 12] (<i>n</i> = 1) c.1454G>A (W485X)/c.1454G>A (W485X) [exon 13] (<i>n</i> = 2) c.898-905delTTCATGAG/c.899-906delTTCATGAG [exon 8] (<i>n</i> = 1) Not yet carried out
Niemann-Pick disease A/B (Sphingomyelinase) [Hexadecarbonylamino-p-nitro-phenyl phosphoryl choline]	NPD A – neuropathicEarly life progressive loss of motor and intellectual capacity, hepatosplenomegaly, cherry red spot in macula, pneumonia, foamy histiocytes in bone marrow NPD B – non-neuropathicLate onset as compared to type A, hepatosplenomegaly, cherry red spot in macula, foamy histiocytes in bone marrow	5 M–2.3 Y	374	07 (1.8 %)	0.1–0.35 0.77–2.33		Not yet carried out
GM1 gangliosidosis (β -galactosidase) [4-MU- β -D-galactopyranoside]	Cherry red spot, neuroregression, mild to moderate dysostosis multiplex, coarse facies, hypotonia, delayed mile stone, hepatosplenomegaly, mongolian spot on back, MRI shows diffuse demyelination of white matter with bilaterally symmetric thalamic signal change	3–13 Y	374	17 (4.4 %)	0.25–0.46 0.77–2.33		Not yet carried out
		7 M–4 Y	1,045	30 (7.75 %)	0.0–15.3 79.6–480.0		Not yet carried out

Defects in degradation of mucopolysaccharides

Hunter syndrome (MPS I) (α -iduronidase) [4-MU- α -L-iduronide]	<i>MPS IH – Hurler syndrome</i> Progressive mental and physical disabilities, corneal clouding, coarse facies, dysostosis multiplex, stiff joints, organomegaly, hernia	7 D–2.1 Y	355	12 (3.1 %)	0.0–12 32.0–105.5	Not yet carried out
Hunter syndrome (MPS II) (α -iduronidase-sulfatase) [4-MU- α -L-iduronide-2-sulfate]	<i>MPS IHS–Hurler–Scheie syndrome</i> Progressive physical disabilities, corneal clouding, coarse facies, dysostosis multiplex, stiff joints, glaucoma, hernia	3–9 Y	355	09 (2.32 %)	2.1–12 32.0–105.5	Not yet carried out
Sanfilippo syndrome A (MPS IIIA) (Heparan sulfamidase) [4-MU- α -D-sulfoglucosaminide]	Severe mental retardation, dysostosis multiplex, coarse facies, organomegaly	6 M–7 Y	30	09 (2.32 %)	0.0–9.3 ^b 600–1616 ^b	Not yet carried out
Sanfilippo syndrome B (MPS IIIB) (N-acetyl- α glucosaminidase) [4-MU-N-Ac- α -glucosaminide]	Aggressive behavior, mental retardation, joint stiffness, hirsutism	2.5–9 Y	32	08 (2.0 %)	0.01–0.24 ^c 1.3–6.8 ^c	Not yet carried out
Morquio syndrome A (MPS IVA) (β -galactosidase-6-sulfate-sulfatase) [4-MU- β -galactose-6-sulfate]	Similar to MPS type IIIA	5–6.5 Y	128	02 (0.51 %)	0.6–4.7 ^b 300–600 ^b	Not yet carried out
Morquio syndrome B (MPS IVB) (β -galactosidase) [4-MU- β -D-galactopyranoside]	Skeletal abnormality, short stature, short neck, prominent lower ribs, odontoid anomalies, coarse facies	1.6–9 Y	54	18 (4.65 %)	4.0–5.2 14.0–32.0 ^c	Not yet carried out
Maroteaux-Lamy syndrome (MPS VI) (Arylsulfatase B) [P-nitro-catechol-sulfate]	Mild skeletal dysplasia, short stature, corneal clouding, coarse facies	6 M–10 Y	1,045	04 (1.03 %)	2.2–24.2 79.6–480.0	Not yet carried out
Sly syndrome (MPS VII) (β -glucuronidase) [4 MU- β -D-glucuronide]	Severe dysostosis multiplex, corneal clouding, coarse facies, cardiomyopathy	1 M–10 Y	389	18 (4.65 %)	0.0–0.25 0.65–8.5	Not yet carried out
	Mental retardation, coarse facies, organomegaly, corneal clouding, mild skeletal abnormality	5 M–12 Y	372	05 (1.29 %)	0.0–27.8 80–400.0	Not yet carried out

(continued)

Table 1 (continued)

Disease name/(enzyme name)/[substrate name]	Phenotype observed	Age at diagnosis	Number of cases investigated	Number of affected cases confirmed by enzymatic analysis	Enzyme activity detected in affected individuals (nmol/h/mg protein) Enzyme activity from leukocytes observed in normal individuals (nmol/h/mg protein)	Genotype analysis
Defects in degradation of sulfatides						
Metachromatic leukodystrophy (MLD) (Arylsulfatase A) [P-nitro-catechol-sulfate]	Peripheral neuropathy, absence of deep tendon reflexes, slowly progressive dementia, gait disturbance, convulsion, behavior changes. MRI shows diffuse symmetric abnormalities of periventricular myelin with hyperintensities on T ₂ -weighted images	1 M–16 Y	483	38 (9.82 %)	0.0–0.3 0.6–4.5	Not yet carried out
Krabbe disease (β-galactocerebrosidase) [6-hexadeconylamino-4-methylumbelliferyl-β-D-Galactopyranoside]	Progressive psychomotor retardation, convulsion, spasticity, absence of deep tendon reflexes, irritability, hyperthermia; progressive, diffuse, and symmetric cerebral atrophy is observed in neuroimaging	1 M–15 Y	85	17 (4.39 %)	0.0–5.50 ^c 15.2–114.9 ^c	Not yet carried out
Defects in degradation of glycoproteins						
Neuronal ceroid lipofuscinosis I (NCL I) (Palmitoyl protein thioesterase)[4-MU-6-sulfo-palmitoyl-β-D-glucoside]	Early onset psychomotor impairment, vision loss, GTC convulsion, dementia, spasticity; MRI shows variable cerebral atrophy and thalamic hypointensity in the white matter and basal ganglia	6 M–2 Y	39	05 (1.28 %)	3.0–9.3 25.5–215	Not yet carried out
Neuronal ceroid lipofuscinosis II (NCL II) (Tripeptidyl peptidase I) [Alanyl-alanyl-phenylalanyl-7-amido-4-methylcoumarin (AAF-AMC)]	Late onset psychomotor impairment, vision loss, GTC convulsion, dementia, spasticity; MRI shows progressive cerebral and cerebellar atrophy with normal basal ganglia and thalami	2–16 Y	84	13 (3.08 %)	4.3–22.5 32.8–233	Not yet carried out

Defects in degradation of glyco-

Pompe disease
(α -1-4-glucosidase)
[4-MU- α -D-glucopyranoside] Recurrent hypoglycemic seizures, cardiomegaly and hypertrophic cardiomyopathy, delayed milestone, muscle weakness, noisy breathing, respiratory distress, mild hepatosplenomegaly, gait disturbance 1 D -13 Y 384 19 (4.9 %) 0.0-0.19^d
> 0.25-0.63^d Not yet carried out

Defects in lysosomal transporters

Sialic acid storage disorder [N-acetyl-neuraminic acid (NANA)] Regression motor and physical milestone, cherry red spot, coarse facial features, hepatosplenomegaly, gum hypertrophy, inguinal hernia 1 M -9 Y 45 07 (1.80 %) Free NANA^e
7.83 (0-6 M)
4.4-17.22 (7-24 M)
4.75 (61-120 M)
Total NANA^e
8.48 (0-6 M)
3.9-20.0 (7-24 M)
5.75 (0-6 M)
Free NANA^e
0.42-1.70 (0-6 M)
0.26-1.39 (-24 M)
0.1-0.38 (61-120 M)
Total NANA^e
0.92-3.0 (0-6 M)
0.55-2.31 (7-24 M)
0.2-0.64 (61-120 M) Not yet carried out

Galactosialidosis (β -galactosidase) [4-MU- β -D-galactopyranoside] and [N-acetyl-neuraminic acid total (Total NANA)] Regression of motor milestone, seizures, coarse facies, organomegaly, mongolian spot, mild skeletal abnormality 3 M -2 Y 09 03 (0.77 %) β -galactosidase
79.6-480.0
Free NANA^e
0.6-0.7 (0-6 M)
0.51 (13-24 M)
Total NANA^e
3.5-8.25 (0-6 M)
2.8 (13-24 M)
 β -galactosidase
79.6-480.0
Free NANA^e
0.42-1.70 (0-6 M)
0.31-0.79 (13-24 M)
Total NANA^e
0.92-3.0 (0-6 M)
0.55-1.47 (13-24 M) Not yet carried out

(continued)

Table 1 (continued)

Disease name/(enzyme name)/[substrate name]	Phenotype observed	Age at diagnosis	Number of cases investigated	Number of affected cases confirmed by enzymatic analysis	Enzyme activity detected in affected individuals (nmol/h/mg protein) Enzyme activity from leukocytes observed in normal individuals (nmol/h/mg protein)	Genotype analysis
Defects in lysosomal of trafficking proteins						
Mucopolipidosis II/III	Delayed milestone, coarse features, kyphosis, mild scoliosis, hypertonia, skin pigmentations, low-set ears, mild hepatosplenomegaly, mongolian spot, thick skin	7 M–6.5 Y	179	11 (1.78 %)	Aryl sulfatase-A (416.2–2828.0) ^b β-hexosaminidase T (66560–333300) ^b β-glucuronidase (18700–40546) ^b α-fucosidase (26500–32000) ^b Aryl sulfatase-A (28–85) ^b β-hexosaminidase T (12000–30149) ^b β-glucuronidase (420–2054) ^b α-fucosidase (334–1275) ^b	Not yet carried out
Niemann-Pick disease C ^f	Psychomotor symptoms occurring in early age, neonatal jaundice, organomegaly, hypertonic limbs, facial dyskinesia	1–6 Y	11	4 (1.03 %)	Depressed cholesterol esterification and abnormal filipin staining Normal cholesterol esterification and normal filipin staining	Not yet carried out

Y Years; M Months

^a(Mistri et al. 2012)

^bEnzyme activity was carried out in plasma and activity was expressed in nmol/h/ml plasma

^cEnzyme activity was expressed in nmol/17 h/mg protein

^dEnzyme activity is expressed by calculating ratio of with acarbose and without acarbose

^eEnzyme activity was carried out in urine mmol/g creatinine

^fNPD-C was carried out in skin fibroblasts using filipin staining

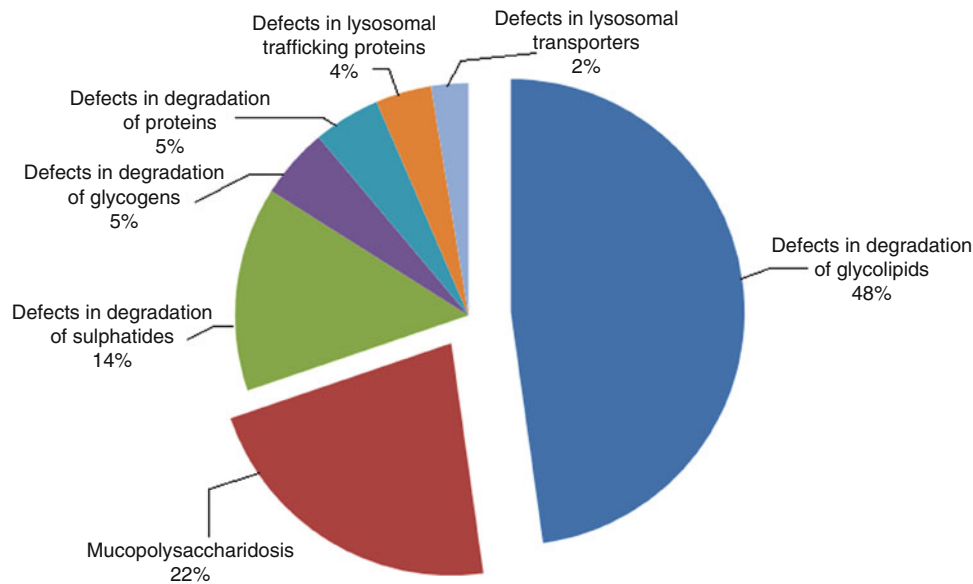


Fig. 1 Distribution of storage disorders in India

disorders (22 %) and sulfatide degradation defect (MLD and Krabbe disease) in 14 % of the patients. Glycogen storage disorder type II (Pompe disease), protein degradation defect (Batten disease), lysosomal trafficking protein defect (ML II/III and NPC), and lysosomal transporter defect (sialic acid storage disorder and galactosialidosis) were found to be comparatively less common (Fig. 1). Interestingly, all confirmed cases of Batten disease were from South India where consanguineous marriages were observed in 72 % of the cases.

Gaucher disease was one of the most common glycolipid storage disorders observed with a high frequency in Maharashtra 64.5 % (40/62) followed by GM2 gangliosidosis (Tay-Sachs disease and Sandhoff disease), which was more prevalent in Gujarat 49.7 % (34/69). Among MPS disorders, MPS I (Hurler, Hurler-Scheie, and Scheie syndrome) was the most common, followed by MPS IV (Morquio A and Morquio B), MPS VI (Maroteaux-Lamy syndrome), MPS II (Hunter syndrome), MPS III A and B (Sanfilippo syndrome A and B), and MPS VII (Sly syndrome). The remaining were sulfatide degradation defects with MLD and Krabbe disease, protein degradation defect with Batten disease (NCL I and II), lysosomal transporter defect with sialic acid storage disorder, and lysosomal trafficking protein deficiency with ML II/III and NPC (Table 1).

Mutation analysis was carried out for 28 children with confirmed diagnosis of Tay-Sachs disease. Common mutation c.1277_1278insTATC was detected in four cases and was confirmed by bidirectional sequencing. In the remaining 24 cases, exon sequence study revealed 14 different mutations, except one. This includes nine earlier reported mutations c.340G>A (p.E114K), c.1178C>G (p.R393P),

c.1432G>A (p.G478R), c.508C>T (p.R170W) in one each, c.964G>A (p.D322N) in two, c.964G>T (p.D322Y) in three, and c.1385A>T (p.E462V) in six cases. Intron 7 showed variant c.805+1 G>C in two cases and intron 6 demonstrated c.672+30 T>G in one case. Additionally, two novel deleterious missense mutations c.788C>T (p.T263I) and c.1121A>C (p.Q374P) along with one small novel deletion c.898_905delTTCATGAG was detected in one case each. Two novel nonsense mutations c.1421G>A (p.W474X) and c.1454G>A (p.W485X) were observed in one and two cases, respectively. Pathological significance of novel missense mutations was confirmed using softwares SIFT and Polyphen2. Mutation spectrum of Tay-Sachs disease detected in various states of India is shown in Table 2, which also includes one case from Iran.

Discussion

This study demonstrates glycolipid storage disorders as one of the most common LSDs in India, similar to that observed in Portugal, Australia, and Czech Republic (Pinto et al. 2004; Meikle et al. 1999; Poupetova et al. 2010) with higher frequency of Gaucher disease (Fig. 2). The high prevalence of Gaucher disease (16 %) is in accordance with previously reported study (14.4 %) from northern India (Verma et al. 2012) and Mappila Muslims from southern India encompassing Kerala (Feroze et al. 1994).

GM2 gangliosidosis accounted for 10 % of Tay-Sachs and 7.8 % of Sandhoff patients, respectively. This was in accordance to the Portugal cohort especially for Tay-Sachs disease (13.8 %), while lower prevalence was

Table. 2 Regional distribution of mutation spectrum in Tay-Sachs disease

Disease condition	Gene involved	Mutation detection	Number of cases	Region – Country
Tay-Sachs disease	<i>HEXA</i>	c.1385 A>T (p.E462V)	6	Gujarat – India
		c.1277_1278insTATC (p.Y471fsX5)	2	Gujarat – India
			2	Maharashtra – India
		c.964 G>T (p.D322Y)	2	Gujarat – India
			1	Uttar Pradesh – India
		c.964 G>A (p.D322N)	1	Gujarat – India
			1	Uttar Pradesh – India
		c.805+1G>C	1	Maharashtra – India
			1	Andhra Pradesh – India
		c.340G>A (p.E114K)	1	Maharashtra – India
		c.1432G>A (p.G478R)	1	Maharashtra – India
		c.672+30T>G	1	Maharashtra – India
		c.1178 C>G (p.R393P)	1	Tamil Nadu – India
		c.508C>T (p.R170W)	1	Iran
		c.788C>T (p.T263I)	1	Maharashtra – India
		c.1454G>A (p.W485X)	2	Maharashtra – India
		c.1121A>C (p.Q374P)	1	Maharashtra – India
		c.1421G>A (p.W474X)	1	Maharashtra – India
c.898_905delTTCATGAG	1	Maharashtra – India		

reported from Australia and Czech Republic (4.1 % and 2.5 %, respectively). High prevalence of GM2 gangliosidosis (Tay-Sachs disease and Sandhoff disease) has also been reported in children with neurological disorders from the southern region of India, where consanguinity is more common (Nalini and Christopher 2004). Higher incidence of Tay-Sachs in our study could be due to the presence of founder mutation in *HEXA* gene in the SC community of Gujarat (Mistri et al. 2012).

Mucopolysaccharidosis was the second most common LSD, which is in accordance with several other groups (Pinto et al. 2004; Meikle et al. 1999; Poupetova et al. 2010; Verma et al. 2012). Among these groups, MPS I was the most prevalent. This finding is similar to that observed by Verma et al. (2012). Although identification of MPS IV B in four cases is unique in our study, this could be either due to ethnic diversity or referral bias. A study from Czech Republic (Poupetova et al. 2010) reported only one case of MPS IV B out of 394 affected patients. Nonetheless, the prevalence of MPS IV A was found to be higher as compared to IV B which is in concordance with other reported studies (Pinto et al. 2004; Meikle et al. 1999; Poupetova et al. 2010). Occurrence of MPS III-A and III-B in this study is lower than that reported from Australia and Portugal (Pinto et al. 2004; Meikle et al. 1999) (Fig. 2). Milder clinical presentation, lack of clinical awareness, and diagnostic facility could be one of the reasons for underdiagnosis of MPS III disorders in this work.

In this study, the frequency of Pompe disease (GSD II) was higher (5 %) as compared to Czech Republic, Australia, and Portugal (Fig. 2). While Batten disease [Neuronal ceroid lipofuscinosis I and II (NCL I and II)] was observed in lower frequency (4 %) as compared to 7.5 % in Czech Republic, it was higher than that reported in Portugal (1.5 %). Interestingly, all cases of Batten disease in our study belonged to a single region of South India where higher incidence of consanguineous marriages is seen (72 %).

High carrier frequency of Fabry disease has been observed in Czech Republic and Taiwan, however, not a single case was detected in this study (Fig. 2) (Poupetova et al. 2010; Staretz-Chacham et al. 2009). This could be due to lack of awareness among clinicians involved in the cardiac and/or renal management of adults with Fabry disease. Unlike in Czech Republic, Australia, and Portugal (Meikle et al. 1999; Poupetova et al. 2010; Pinto et al. 2004), NPC was also the least observed lysosomal trafficking disorder. This could be a result of overlapping clinical phenotypes such as hepatosplenomegaly, neonatal jaundice, and psychiatric disturbances (Wenger et al. 2003) and limited investigational facilities for NPC.

In general, low prevalence of storage disorders like Fabry, NPC, and MPS III in our study is likely to be due to the lack of awareness among the clinicians and a dearth of enzyme diagnostic facilities in most parts of the country. In countries with higher incidences of aforementioned

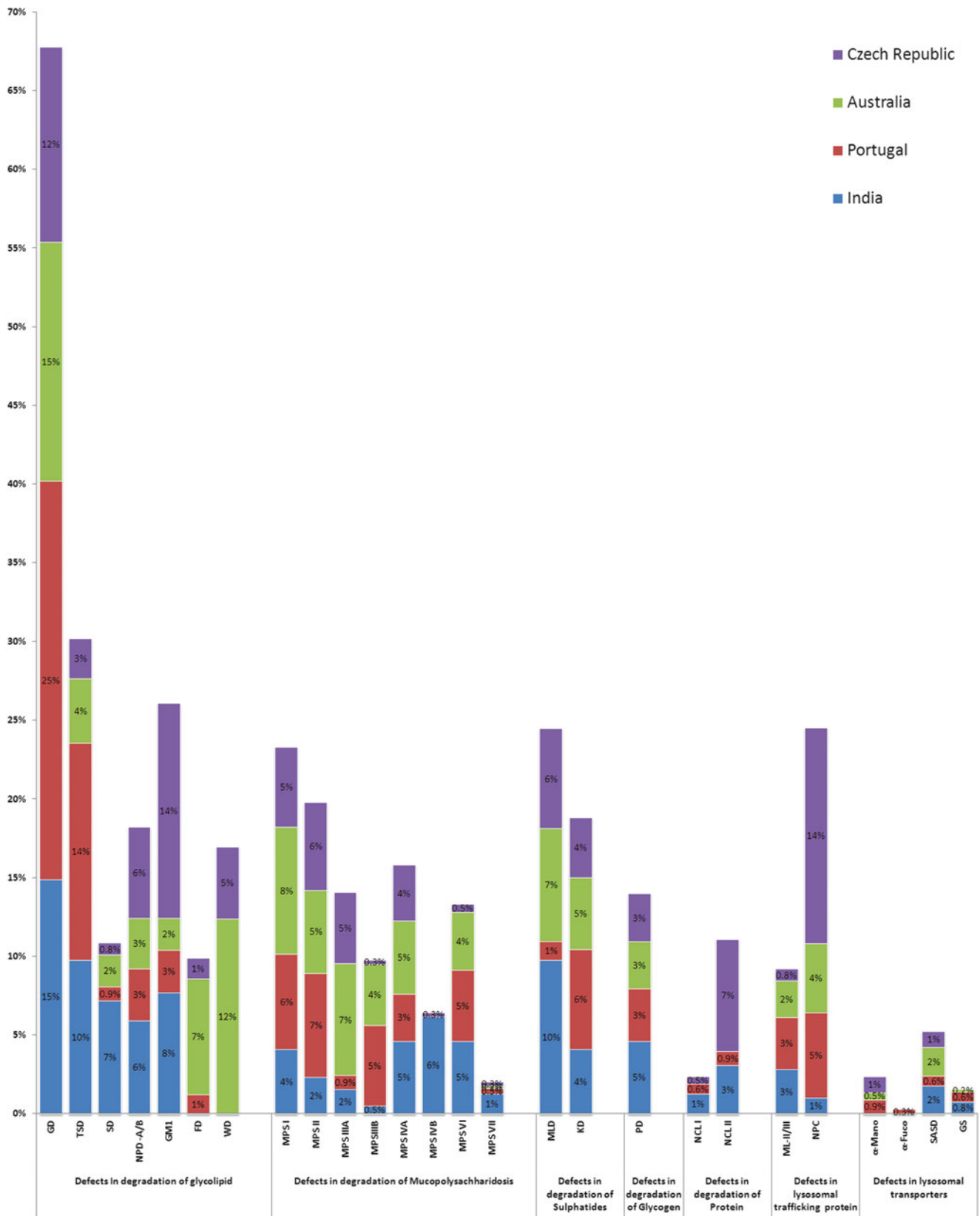


Fig. 2 Incidence of various LSDs in different countries

disorders, easy accessibility of specialized enzyme laboratory for confirming clinical diagnosis exists. Additionally, in these countries (Australia, Portugal, and Czech Republic) special working groups on LSDs increase awareness among the medical fraternity. Also patient support groups advocate the disease magnitude and support the affected families (Meikle et al. 1999; Pinto et al. 2004; Poupetova et al. 2010). In India, very recently Indian Council of Medical Research (ICMR) has set up a special task force on LSDs which will focus on the magnitude of these disorders in different parts of the country, increase awareness among the clinicians by organizing regional training program, and establish common mutation spectrum for different LSDs.

The ethnicity predilection is known to be associated with a specific lysosomal disease like Gaucher, Tay-Sachs, Niemann-Pick type A, and ML IV disease in Ashkenazi Jewish descendants (Marsden and Levy 2010); Salla disease and aspartylglucosaminuria in Finnish population; and Gaucher type III disease in people of Swedish descent (Marsden and Levy 2010). In this study, the prevalence of Gaucher disease was found to be higher in Maharashtra region, whereas GM2 gangliosidosis (Tay-Sachs) was more in Gujarat province.

Among all the LSDs, molecular analysis was carried out in 28 cases of Tay-Sachs disease by mutation identification in *HEXA* gene. Molecular study in 15 of these cases has been reported earlier with high prevalence of p.E462V mutation in a particular community (SC) of Gujarat (Mistri et al. 2012). In the remaining 13 cases, 6 aforementioned novel mutations have been observed in patients from Maharashtra region (Table 2) of the country that include two missense mutations in exon 7 and exon 10, two nonsense mutations in exon 12 and exon 13, and one small deletion (8 bp deletion) in exon 8. Deleterious effect of these mutations has been confirmed by SIFT and Polyphen2 software programs. The remaining seven patients have shown earlier reported mutations with c.1277_1278insTATC in three, p.D322Y in two, p.D322N and c.805+1G>C in one each. Thus, this study shows that p.E462V, p.D322Y, and c.1277_1278insTATC identify nearly 45 % (13/28) of the disease causing mutations in patients affected with Tay-Sachs disease from India.

Overall, the study demonstrates that glycolipid storage and MPS are the most common LSDs in India. By providing appropriate genetic counseling and offering prenatal diagnosis during subsequent pregnancies, the burden of these diseases could be reduced. Mutations p.E462V, p.D322Y, and c.1277_1278insTATC are possibly the commonest ones detected for Tay-Sachs disease in the Indian population and can be used as a part of common mutation screening program.

Acknowledgments We sincerely acknowledge the work of Meikle PJ, Pinto R, and Poupetova H and their colleagues from Australia, Portugal, and Czech Republic, respectively, whose publications were of immense help in the preparation of this manuscript. We are grateful to all the referring doctors and patients for their support without whose consent, this study could not have been possible and Indian Council of Medical Research (ICMR) for providing financial support to carry out this study.

Synopsis

This cross-sectional study provides an up-to-date description of the current scenario of different lysosomal storage disorders (LSDs) and its burden on the society and highlights the common mutation spectrum for Tay-Sachs disease in India.

Conflict of Interest

The authors declare that they have no conflict of interest.

Informed Consent

All procedures followed were in accordance with the ethical standards of the responsible committee on human experimentation (institutional and national) and with the Helsinki Declaration of 1975, as revised in 2000 (5). Informed consent was obtained from all patients for being included in the study.

Details of the Contributions of Individual Authors

JS designed the experiment and standardized the protocols. MM, NO, and CA were involved in processing of the samples. MJ provided the technical guidelines. RS, AB, KG, NN, CD, MK, and SM were involved in collection of the clinical details. MM, JS, and FS prepared the manuscript. All the authors read and approved the manuscript.

References

- Aerts JM, van Breemen MJ, Bussink AP et al (2008) Biomarkers for lysosomal storage disorders: identification and application as exemplified by chitotriosidase in Gaucher disease. *Acta Paediatr Suppl* 97(457):7–14
- Dembure PP, Roesel AR (1991) Screening for mucopolysaccharidoses by analysis of urinary glycosaminoglycans. In: Hommes FA (ed) *Techniques in diagnostic human biochemical genetics: a laboratory manual*. Wiley-Liss, New York, pp 77–86
- Feroze M, Arvindan KP, Jose L (1994) Gaucher's disease among Mappila muslims of Malabar. *Indian J Pathol Microbiol* 37(3): 307–311

- Filocamo M, Morrone A (2011) Lysosomal storage disorders: molecular basis and laboratory testing. *Hum Genomics* 5(3): 156–169
- Futerman AH, van Meer G (2004) The cell biology of lysosomal storage disorders. *Nat Rev Mol Cell Biol* 5(7):554–565
- Hopwood JJ, Harrison JR (1982) High-resolution electrophoresis of urinary glycosaminoglycans: an improved screening test for the mucopolysaccharidoses. *Anal Biochem* 119(1):120–127
- Hwu WL, Chien YH, Lee NC et al (2009) Newborn screening for Fabry disease in Taiwan reveals a high incidence of the later-onset mutation c.936 + 919G > A (IVS4 + 919G > A). *Hum Mutat* 30(10):1397–1405
- Kaback M, Lim Steele J, Dabholkar D et al (1993) Tay-Sachs disease carrier screening, prenatal diagnosis and the molecular era. An international perspective, 1970–1993. The international TSD data collection Network. *JAMA* 270:2307–2315
- Kruth HS, Vaughan M (1980) Quantification of low density lipoprotein binding and cholesterol accumulation by single human fibroblasts using fluorescence microscopy. *J Lipid Res* 21:123–130
- Marsden D, Levy H (2010) Newborn screening of lysosomal storage disorders. *Clin Chem* 56(7):1071–1079
- Meikle PJ, Hopwood JJ, Clague AE et al (1999) Prevalence of lysosomal storage disorders. *JAMA* 281(3):249–254
- Miller SA, Dykes DD, Polesky HF (1988) A simple salting out procedure for extracting DNA from human nucleated cells. *Nucleic Acids Res* 16(3):1215
- Mistri M, Tamhankar P, Sheth F et al (2012) Identification of novel mutations in HEXA gene in children affected with Tay Sachs disease from India. *PLoS One* 7(6):e39122. doi:10.1371/journal.pone.0039122
- Myerowitz R, Costigan FC (1988) The major defect in Ashkenazi Jews with Tay-Sachs disease is an insertion in the gene for alpha-chain of beta-hexosaminidase. *J Biol Chem* 263:18587–18589
- Myerowitz R, Hogikyan ND (1986) Different mutations in Ashkenazi Jewish and non-Jewish French Canadians with Tay-Sachs disease. *Science* 232(4758):1646–81986
- Nalini A, Christopher R (2004) Cerebral glycolipidoses: clinical characteristics of 41 pediatric patients. *J Child Neurol* 19(6): 447–452
- Parkinson-Lawrence EJ, Shandala T, Prodoehl M et al (2010) Lysosomal storage disease: revealing lysosomal function and physiology. *Physiology* 25(2):102–115
- Pinto R, Caseiro C, Lemos M et al (2004) Prevalence of lysosomal storage diseases in Portugal. *Eur J Hum Genet* 12(2):87–92
- Poupetova H, Ledvinova J, Berna L et al (2010) The birth prevalence of lysosomal storage disorders in the Czech Republic: comparison with data in different populations. *J Inherit Metab Dis* 33(4): 387–396
- Saftig P, Klumperman J (2009) Lysosome biogenesis and lysosomal membrane proteins: trafficking meets function. *Nat Rev Mol Cell Biol* 10(9):623–635
- Shapria E, Blitzer MG, Miller JB et al (1989) Fluorometric assays in biochemical genetics: a laboratory Manual. New York: Oxford university press, New York, pp 19–46
- Sheth J, Patel P, Sheth F et al (2004) Lysosomal storage disorders. *Indian Pediatr* 41(3):260–265
- Sheth J, Sheth F, Oza N (2008) Niemann-pick type C disease. *Indian Pediatr* 45(17):505–507
- Sheth J, Sheth F, Oza N et al (2010) Plasma chitotriosidase activity in children with lysosomal storage disorders. *Indian J Pediatr* 77(2): 203–205
- Sheth J, Mistri M, Kamate M et al (2012) Diagnostic strategy for Mucopolipidosis II/III. *Indian Pediatr* 49(12):975–977
- Shukla P, Vasisht S, Srivastava R et al (2011) Molecular and structural analysis of metachromatic leukodystrophy patients in Indian population. *J Neurol Sci* 301(1–2):38–45
- Staretz-Chacham O, Lang TC, La Marca ME et al (2009) Lysosomal storage disorders in the newborn. *Pediatrics* 123(4): 1191–1207
- Vellodi A (2005) Lysosomal storage disorders. *Br J Haematol* 128(4): 413–431
- Verma IC (2000) Burden of genetic disorders in India. *Indian J Pediatr* 67(12):893–898
- Verma PK, Rangnath P, Dalal AB et al (2012) Spectrum of lysosomal storage disorders at a Medical Genetics Center in North India. *Indian Pediatr* 49(10):799–804
- Wenger DA, Coppola S, Liu SL (2003) Insights in to the diagnosis and treatment of lysosomal storage diseases. *Arch Neurol* 60(3): 322–328

A Japanese Adult Case of Guanidinoacetate Methyltransferase Deficiency

Tomoyuki Akiyama • Hitoshi Osaka • Hiroko Shimbo •
Tomoshi Nakajiri • Katsuhiko Kobayashi • Makio Oka •
Fumika Endoh • Harumi Yoshinaga

Received: 12 April 2013 / Revised: 12 May 2013 / Accepted: 26 May 2013 / Published online: 12 July 2013
© SSIEM and Springer-Verlag Berlin Heidelberg 2013

Abstract Guanidinoacetate methyltransferase (GAMT) deficiency is a rare disorder of creatine synthesis resulting in cerebral creatine depletion. We present a 38-year-old patient, the first Japanese case of GAMT deficiency. Developmental delay started after a few months of age with a marked delay in language, which resulted in severe intellectual deficit. She showed hyperactivity and trichotillomania from childhood. Epileptic seizures appeared at 18 months and she had multiple types of seizures including epileptic spasms, brief tonic seizures, atypical absences, complex partial seizures with secondary generalization, and “drop” seizures. They have been refractory to multiple antiepileptic drugs. Although there have been no involuntary movements, magnetic resonance imaging revealed T2 hyperintense lesions in bilateral globus pallidi. Motor regression started around 30 years of age and the patient is now able to walk for only short periods. Very low serum

creatinine levels measured by enzymatic method raised a suspicion of GAMT deficiency, which was confirmed by proton magnetic resonance spectroscopy and urinary guanidinoacetate assay. *GAMT* gene analysis revealed that the patient is a compound heterozygote of c.578A>G, p.Gln193Arg and splice site mutation, c.391G>C, p.Gly131Arg, neither of which have been reported in the literature. We also identified two aberrant splice products from the patient’s cDNA analysis. The patient was recently started on supplementation of high-dose creatine and ornithine, the effects of which are currently under evaluation. Although rare, patients with developmental delay, epilepsy, behavioral problems, and movement disorders should be vigorously screened for GAMT deficiency, as it is a treatable disorder.

Communicated by: Comelis Jakobs, PhD

Competing interests: None declared

Electronic supplementary material: The online version of this chapter (doi:10.1007/8904_2013_245) contains supplementary material, which is available to authorized users.

T. Akiyama (✉) • T. Nakajiri • K. Kobayashi • M. Oka •
F. Endoh • H. Yoshinaga
Department of Child Neurology, Okayama University Hospital,
2-5-1 Shikata-cho, Kita-ku, Okayama 700-8558, Japan
e-mail: takiyama@okayama-u.ac.jp

H. Osaka • H. Shimbo
Division of Neurology, Kanagawa Children’s Medical Center,
Yokohama, Japan

H. Yoshinaga
Department of Child Neurology, Okayama University Graduate
School of Medicine, Dentistry and Pharmaceutical Sciences,
Okayama, Japan

Introduction

Guanidinoacetate methyltransferase (GAMT; OMIM 601240) deficiency is a rare autosomal recessive disorder of creatine synthesis resulting in cerebral creatine depletion (Stöckler et al. 1994, 1996b). Guanidinoacetate (GAA) accumulates in body fluids. Symptoms of GAMT deficiency usually emerge after a few months of life, such as intellectual disability, speech delay, autistic behaviors, epileptic seizures, and involuntary movements (Mercimek-Mahmutoglu et al. 2006). Making a diagnosis of GAMT deficiency is challenging; nonetheless, early diagnosis is crucial because this disorder is treatable (Stöckler et al. 1996a). Only approximately 80 cases have been reported to date, mostly from Europe and the Middle East. Here we report on the first Japanese patient with GAMT deficiency with two novel gene mutations.

Case Report

The patient, a 38-year-old female with intractable epilepsy and severe mental retardation, was born at full term with a birth weight of 3,260 g. There were no pre- or perinatal complications. She is the third of four children of Japanese non-consanguineous healthy parents. The first child, a boy, started having epileptic seizures after 1 year of age with unknown cause and died at 28 years of age at an institution for the mentally handicapped. The other two children have been healthy.

Although the patient showed a social smile by 3 months and head control by 4 months of age, her development has been delayed since then. She sat alone at 14 months, walked alone at around 20 months, and became able to take the stairs one step at a time with support around 5 years of age. She has spoken no meaningful words and gained little language comprehension. Her medical chart at 7 years of age described her as speechless, unable to follow verbal commands, but able to run and walk up the stairs one step at a time without support. She showed no involuntary movements. She was hyperactive and had trichotillomania. Neuropsychological assessment at 7 years 7 months by analytic test for development in infancy and childhood (Enjoji and Yanai 1961) demonstrated her developmental quotient was 14. Around 30 years of age, she was unable to walk for a long time but was able to take the stairs with support. At 32 years of age, she was no longer able to run. Currently, at 38 years of age, the patient has severe intellectual deficit with no speech or language comprehension. She still has trichotillomania. Her transport is mostly by wheelchair, although she is able to walk slowly for short periods. Her muscle tone is normal and there are no involuntary movements.

The onset of epilepsy was at around 18 months of age, characterized by epileptic spasms and brief tonic seizures. At 2 years of age, atypical absences appeared. Despite therapy with multiple antiepileptic drugs, the patient continued to have these seizures until 15 years of age, when her seizures were suppressed by valproic acid and clonazepam. When they recurred at 20 years of age, her seizures were characterized by consciousness impairment with head and body version to left followed by generalized tonic-clonic convulsions lasting up to 1 minute, suggesting complex partial seizures with secondary generalization. At around 23 years, brief “drop” seizures occurring in clusters started. She has continued to have these seizures since then, although she has been tried on multiple antiepileptic drugs including phenobarbital, valproic acid, clonazepam, phenytoin, clobazam, topiramate, lamotrigine, and levetiracetam.

Electroencephalograms (EEGs) at 2–12 years of age showed a slow background activity, generalized 1.5–2.5 Hz slow spike-wave bursts and some multifocal

spikes, consistent with Lennox-Gastaut syndrome. EEGs after adolescence showed multifocal spike-waves with anterior head predominance and intermittent generalized slow spike-waves. The most recent EEG at 38 years of age demonstrated background slowing and no spikes during wakefulness but intermittent focal polyspikes and polyspike-waves over bilateral anterior and left posterior head regions during sleep.

Laboratory blood tests demonstrated low levels of serum creatinine (5–7 $\mu\text{mol/L}$ by enzymatic method; normal range 40–71 $\mu\text{mol/L}$). Subsequent tests using enzymatic methods demonstrated serum creatine levels were below detection limit (normal range 23–92 $\mu\text{mol/L}$). Proton magnetic resonance spectroscopy ($^1\text{H-MRS}$) demonstrated absent creatine peak (Fig. 1a). Brain magnetic resonance imaging (MRI) demonstrated T2 high-intensity lesions in globus pallidi (Fig. 1b). Analysis of urinary creatine metabolites by weak-acid ion chromatography (Wada et al. 2012) demonstrated elevated GAA (548.53, 782.52 mmol/mol creatinine; normal 3–78 mmol/mol creatine (Almeida et al. 2004)) and creatine below detection limit. These findings suggested GAMT deficiency.

Genomic DNA analysis of the *GAMT* gene (Suppl. Table 1) showed a compound heterozygosity for two novel point mutations, an exonic splicing mutation c.391G>C located at the last nucleotide of exon 3 and a missense mutation c.578A>G, p.Gln193Arg in exon 6 (Fig. 2a). Analysis of cDNA revealed two aberrantly spliced transcription products at the allele of splicing mutation (Fig. 2b, c). One transcript had the complete exon 3 (64-bp) deletion by exon skipping and the other transcript was aberrantly spliced at exon 2 involving intron 2 insertion (44-bp) followed by exon 3 skipping, resulting in a 20-bp deletion. Both transcripts are expected to result in frame shift and premature termination of p.Val110Glyfs*30 and p.Ile111Profs*73, respectively. A novel A to G transition on exon 6 (c.578A>G) results in the replacement of arginine by glutamine at position 193 (p.Gln193Arg). This missense variation was not found in 100 control alleles. Glutamine193 is highly conserved in evolution (Fig. 2d), suggesting this mutation represents a pathogenic mutation.

This patient was recently started on supplementation of high-dose creatine and ornithine, and its effects are currently under evaluation.

Discussion

We reported on the first Japanese case of an adult patient with GAMT deficiency. Cases have been reported mostly from Europe and the Middle East (Mercimek-Mahmutoglu et al. 2006).

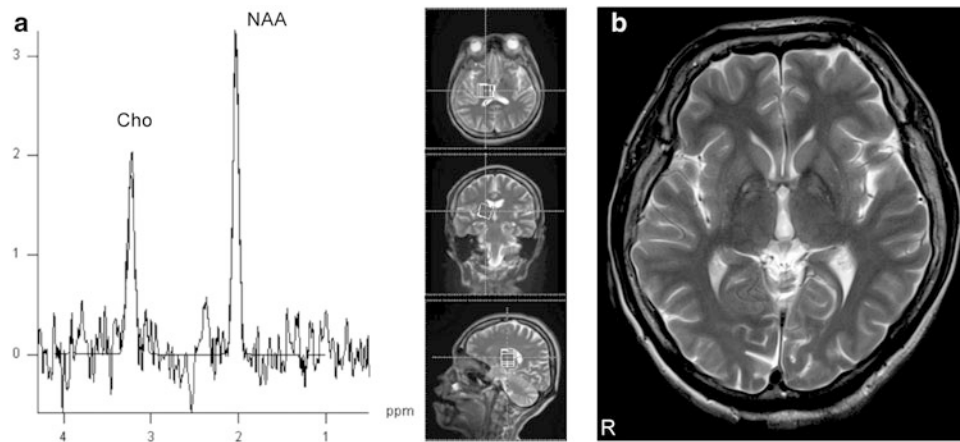


Fig. 1 MR spectroscopy and MRI from the patient with GAMT deficiency. (a) ^1H -MRS at the right basal ganglia demonstrates absence of creatine peak. (b) T2-weighted brain MRI shows high-intensity lesions in bilateral globus pallidi. *Cho* choline; *NAA* N-acetylaspartate

Compared with cases in the literature, our patient showed similar MRI findings and clinical course, with severe intellectual deficit, intractable epilepsy, behavioral problems, but she lacked involuntary movements. Although no definite progression of symptoms was seen during adolescence and young adulthood, motor regression slowly started around 30 years of age. This suggests GAMT deficiency can be slowly progressive if untreated.

Onset of symptoms in GAMT deficiency is from a few months to young childhood (Longo et al. 2011). Intellectual disability is seen in all cases and is severe (IQ < 35) in the majority, especially with profound speech disturbance (Mercimek-Mahmutoglu et al. 2006). Epilepsy is the second most frequent symptom, intractable in most cases, and partially responsive to antiepileptic drugs in two thirds (Leuzzi et al. 2013). Various types of seizures, such as generalized tonic-clonic seizures, absences, myoclonic seizures, myoclonic-astatic seizures, and partial seizures with secondary generalization, have been reported (Leuzzi et al. 2013). Involuntary movements, behavioral problems, and abnormal MRI signals in globus pallidi are seen in some cases. Adult cases that help to understand the natural history of GAMT deficiency are scarce (Schulze et al. 2003; Caldeira Araújo et al. 2005). Progression of neurological deficits, such as paraparesis, hypertonia, and rigidity, has been reported in some cases (Caldeira Araújo et al. 2005).

GAMT gene analysis revealed a compound heterozygosity of two novel mutations: c.391G>C splice donor site of exon 3 and c.578A>G, p.Gln193Arg in exon 6. The former led to two abnormal transcripts lacking exon 3, resulting in a premature stop codon. Reverse transcription polymerase chain reaction detected a higher expression level of the allele with the c.578A>G mutation, which implies the degradation of mRNA from the allele with the splice site mutation by nonsense-mediated mRNA

decay (Fig. 2b). Gln193Arg substitution by the latter mutation is presumed to destabilize the tertiary structure of GAMT (Komoto et al. 2002) by increasing the bulkiness and changing the neutral to a positively charged residue, as Gln193 is situated in the middle of α -helix and protrudes into this enzyme.

Making a diagnosis of GAMT deficiency is challenging, because of its nonspecific symptoms and limited access or capacity of ^1H -MRS. GAA assay may not be readily available. While not as specific as GAA, measurement of creatinine is helpful, as creatinine can be low in GAMT deficiency (Verhoeven et al. 2000). It should be warned that creatinine may also be low in patients with decreased muscle volume. Another caveat is that creatinine measurement by Jaffé method is not as sensitive in detecting GAMT deficiency as the enzymatic method or high-performance liquid chromatography (Verhoeven et al. 2000). Our patient showed low levels of serum creatinine as determined by enzymatic method, which directed us to the diagnosis of GAMT deficiency. The assay of creatine and creatinine is also important to detect creatine transporter 1 deficiency, another type of cerebral creatine deficiency, as the urinary creatine/creatinine ratio is elevated in this disorder (Salomons et al. 2003; Verhoeven et al. 2005). GAA is a more sensitive marker than creatine and creatinine in GAMT deficiency and arginine: glycine amidinotransferase deficiency, the other type of cerebral creatine deficiency (Verhoeven et al. 2005). Therefore, blood and urine tests of creatinine, creatine and GAA should be a part of the workup for developmental delay and/or epilepsy with unknown cause, if creatine and GAA measurements are available.

Early diagnosis is crucial to achieve a favorable outcome in GAMT deficiency. Ideally, treatment should be initiated as early as possible before the creatine pool supplied from maternal body during gestation becomes

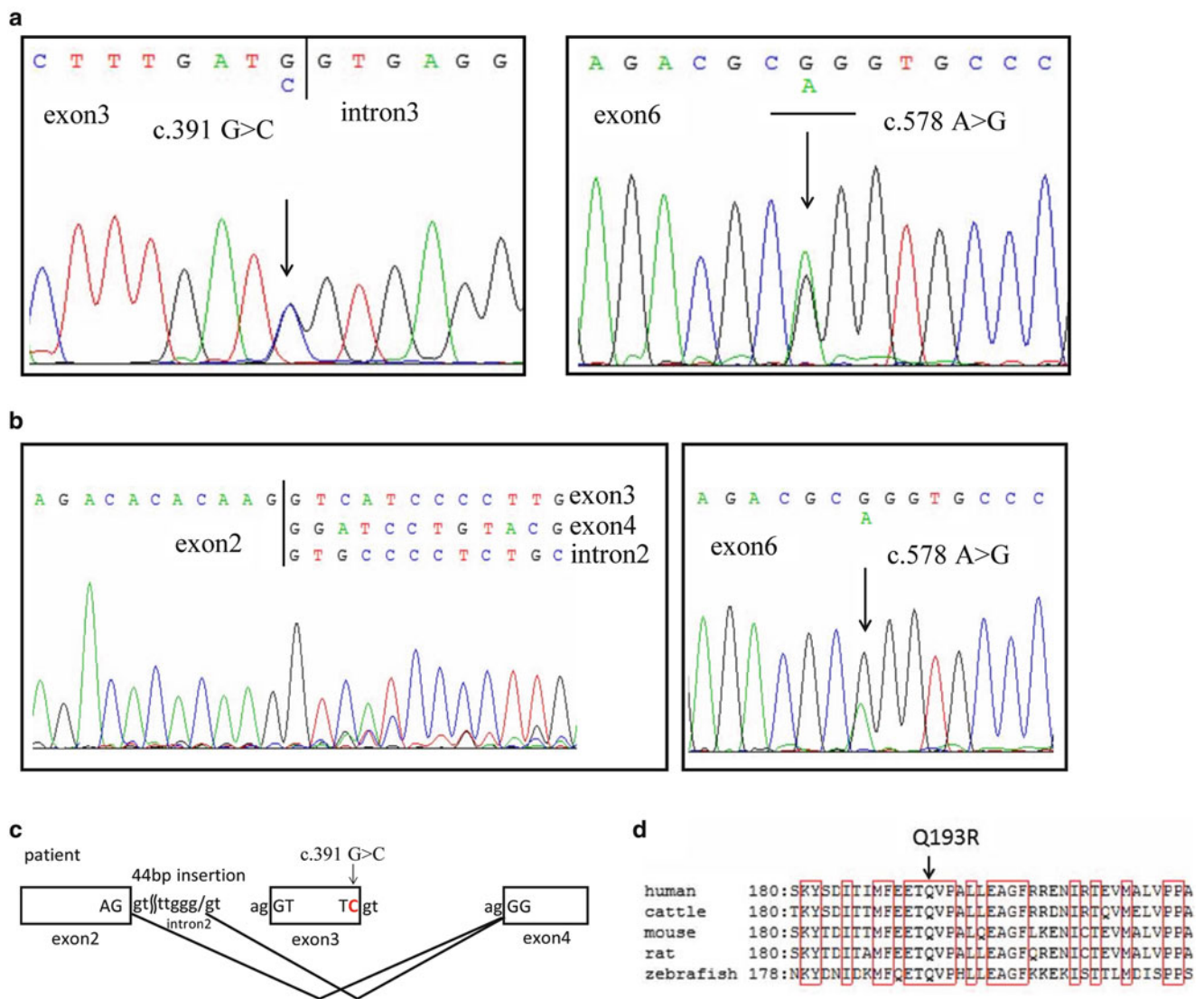


Fig. 2 Genetic analysis of the mutation in *GAMT*. **(a)** Chromatogram of genomic DNA analysis in a patient shows the heterozygote of c.391G>C (*left*) and c.578A>G (*right*). **(b)** cDNA analysis in the patient shows two aberrantly spliced transcription products (*left*) and c.578A>G (*right*). **(c)** c.391G>C mutation causes two aberrant

splicing products: one with complete exon 3 (64-bp) skipping and the other involving intron 2 insertion (44-bp) followed by exon 3 skipping. **(d)** Aligned *GAMT* amino acid sequence of the patient with several other animals, revealing Gln193 is highly conserved among species

depleted and clinical symptoms appear. Presymptomatic treatment has been shown to be successful in achieving normal development (Schulze et al. 2006; El-Gharbawy et al. 2013). Even when diagnosed later, creatine supplementation with reduction of GAA by arginine restriction and ornithine supplementation can alleviate symptoms and prevent further progression of the disease (Schulze et al. 2001). *GAMT* deficiency is a good candidate for neonatal mass screening. Elevated GAA levels in neonatal blood (Schulze et al. 2006; El-Gharbawy et al. 2013) and amniotic fluid (Cheillan et al. 2006) have been reported, and validity of these tests needs to be elucidated.

In conclusion, we presented a 38-year-old patient, the first Japanese case of *GAMT* deficiency with two novel gene mutations. We should always include this disorder on the list of differential diagnoses when seeing patients with neurological symptoms such as intellectual disability, epilepsy, behavioral problems, and involuntary movements, since *GAMT* deficiency is a treatable disorder.

Take-Home Message

A 38-year-old patient, the first Japanese case of guanidinoacetate methyltransferase deficiency with two novel gene

mutations (splice site mutation and missense mutation) was reported.

Compliance with Ethics Guidelines

Contributions of Individual Authors

Tomoyuki Akiyama, Hitoshi Osaka, Hiroko Shimbo, and Tomoshi Nakajiri: Drafting/revising the manuscript for content, analysis, and interpretation of data

Katsuhiko Kobayashi, Makio Oka, Fumika Endoh, and Harumi Yoshinaga: Drafting/revising the manuscript for content

Guarantor for the Article

Tomoyuki Akiyama

Details of Funding

None

Details of Ethics Approval

This study was approved by the ethics board at Kanagawa Children's Medical Center.

Conflict of Interest

Tomoyuki Akiyama, Hitoshi Osaka, Hiroko Shimbo, Tomoshi Nakajiri, Katsuhiko Kobayashi, Makio Oka, Fumika Endoh, and Harumi Yoshinaga declare that they have no conflict of interest.

Informed Consent

All procedures followed were in accordance with the ethical standards of the responsible committee on human experimentation (institutional and national) and with the Helsinki Declaration of 1975, as revised in 2000 (5). Informed consent was obtained from all patients for being included in the study.

References

Almeida LS, Verhoeven NM, Roos B et al (2004) Creatine and guanidinoacetate: diagnostic markers for inborn errors in creatine biosynthesis and transport. *Mol Genet Metab* 82:214–219

- Caldeira Araújo H, Smit W, Verhoeven NM et al (2005) Guanidinoacetate methyltransferase deficiency identified in adults and a child with mental retardation. *Am J Med Genet A* 133A: 122–127
- Cheillan D, Salomons GS, Acquaviva C et al (2006) Prenatal diagnosis of guanidinoacetate methyltransferase deficiency: increased guanidinoacetate concentrations in amniotic fluid. *Clin Chem* 52:775–777
- El-Gharbawy AH, Goldstein JL, Millington DS et al. (2013) Elevation of guanidinoacetate in newborn dried blood spots and impact of early treatment in GAMT deficiency. *Mol Genet Metab* (in press)
- Enjoji M, Yanai N (1961) Analytic test for development in infancy and childhood. *Pediatr Int* 4:2–6
- Komoto J, Huang Y, Takata Y et al (2002) Crystal structure of guanidinoacetate methyltransferase from rat liver: a model structure of protein arginine methyltransferase. *J Mol Biol* 320: 223–235
- Leuzzi V, Mastrangelo M, Battini R, Cioni G (2013) Inborn errors of creatine metabolism and epilepsy. *Epilepsia* 54:217–227
- Longo N, Ardon O, Vanzo R et al (2011) Disorders of creatine transport and metabolism. *Am J Med Genet C Semin Med Genet* 157:72–78
- Mercimek-Mahmutoglu S, Stoeckler-Ipsiroglu S, Adami A et al (2006) GAMT deficiency: features, treatment, and outcome in an inborn error of creatine synthesis. *Neurology* 67:480–484
- Salomons GS, van Dooren SJ, Verhoeven NM et al (2003) X-linked creatine transporter defect: an overview. *J Inher Metab Dis* 26: 309–318
- Schulze A, Ebinger F, Rating D, Mayatepek E (2001) Improving treatment of guanidinoacetate methyltransferase deficiency: reduction of guanidinoacetic acid in body fluids by arginine restriction and ornithine supplementation. *Mol Genet Metab* 74:413–419
- Schulze A, Bachert P, Schlemmer H et al (2003) Lack of creatine in muscle and brain in an adult with GAMT deficiency. *Ann Neurol* 53:248–251
- Schulze A, Hoffmann GF, Bachert P et al (2006) Presymptomatic treatment of neonatal guanidinoacetate methyltransferase deficiency. *Neurology* 67:719–721
- Stöckler S, Holzbach U, Hanefeld F et al (1994) Creatine deficiency in the brain: a new, treatable inborn error of metabolism. *Pediatr Res* 36:409–413
- Stöckler S, Hanefeld F, Frahm J (1996a) Creatine replacement therapy in guanidinoacetate methyltransferase deficiency, a novel inborn error of metabolism. *Lancet* 348:789–790
- Stöckler S, Isbrandt D, Hanefeld F, Schmidt B, von Figura K (1996b) Guanidinoacetate methyltransferase deficiency: the first inborn error of creatine metabolism in man. *Am J Hum Genet* 58: 914–922
- Verhoeven NM, Guerand WS, Struys EA, Bouman AA, van der Knaap MS, Jakobs C (2000) Plasma creatinine assessment in creatine deficiency: a diagnostic pitfall. *J Inher Metab Dis* 23: 835–840
- Verhoeven NM, Salomons GS, Jakobs C (2005) Laboratory diagnosis of defects of creatine biosynthesis and transport. *Clin Chim Acta* 361:1–9
- Wada T, Shimbo H, Osaka H (2012) A simple screening method using ion chromatography for the diagnosis of cerebral creatine deficiency syndromes. *Amino Acids* 43:993–997

Accumulation of Ordered Ceramide-Cholesterol Domains in Farber Disease Fibroblasts

Natalia Santos Ferreira · Michal Goldschmidt-Arzi ·
Helena Sabanay · Judith Storch · Thierry Levade ·
Maria Gil Ribeiro · Lia Addadi · Anthony H. Futerman

Received: 13 March 2013 / Revised: 19 May 2013 / Accepted: 30 May 2013 / Published online: 12 July 2013
© SSIEM and Springer-Verlag Berlin Heidelberg 2013

Abstract Farber disease is an inherited metabolic disorder caused by mutations in the acid ceramidase gene, which leads to ceramide accumulation in lysosomes. Farber

disease patients display a wide variety of symptoms with most patients eventually displaying signs of nervous system dysfunction. We now present a novel tool that could potentially be used to distinguish between the milder and more severe forms of the disease, namely, an antibody that recognizes a mixed monolayer or bilayer of cholesterol:C16-ceramide, but does not recognize either ceramide or cholesterol by themselves. This antibody has previously been used to detect cholesterol:C16-ceramide domains in a variety of cultured cells. We demonstrate that levels of cholesterol:C16-ceramide domains are significantly elevated in fibroblasts from types 4 and 7 Farber disease patients, and that levels of the domains can be modulated by either reducing ceramide or cholesterol levels. Moreover, these domains are located in membranes of the endomembrane system, and also in two unexpected locations, namely, the mitochondria and the plasma membrane. This study suggests that the ceramide that accumulates in severe forms of Farber disease cells is sequestered to distinct membrane subdomains, which may explain some of the cellular pathology observed in this devastating lysosomal storage disease.

Communicated by: Gregory M. Pastores, MD

Competing interests: None declared

Authors Natalia Santos Ferreira and Michal Goldschmidt-Arzi contributed equally to this study

N.S. Ferreira · M.G. Ribeiro
National Health Institute Doutor Ricardo Jorge, Genetic Department,
Centre for Medical Genetics Jacinto de Magalhães, Porto, Portugal

N.S. Ferreira
Instituto de Ciências Biomédicas Abel Salazar, Universidade do Porto,
Porto, Portugal

N.S. Ferreira · M. Goldschmidt-Arzi · A.H. Futerman (✉)
Department of Biological Chemistry, Weizmann Institute of Science,
Rehovot 76100, Israel
e-mail: tony.futerman@weizmann.ac.il

M. Goldschmidt-Arzi · L. Addadi
Department of Structural Biology, Weizmann Institute of Science,
Rehovot 76100, Israel

H. Sabanay
Department of Chemical Research Support, Weizmann Institute of
Science, Rehovot 76100, Israel

J. Storch
Department of Nutritional Sciences and Rutgers Center for Lipid
Research, Rutgers University, Rutgers, NJ 08901, USA

T. Levade
Equipe Labellisée Ligue Contre le Cancer 2013, Centre de Recherches
en Cancérologie de Toulouse (CRCT), Université de Toulouse,
Toulouse, France

T. Levade
Laboratoire de Biochimie Métabolique, Institut Fédératif de Biologie,
CHU Purpan, Toulouse, France

M.G. Ribeiro
Faculty of Health Sciences, Fernando Pessoa University, Porto,
Portugal

Abbreviations

CD	2-hydroxypropyl- β -cyclodextrin
Cer/chol	ceramide/cholesterol
LSD	lysosomal storage disease
PBS	phosphate buffered saline
TEM	transmission electron microscopy
WT	wild type

Introduction

Farber disease (Farber lipogranulomatosis: OMIM # 228000) is a lysosomal storage disease (LSD) caused by mutations in the acid ceramidase (*ASAHI*) gene, which results in intracellular ceramide accumulation (Levade et al. 2009). As with most LSDs, patients display a wide variety of symptoms, with the most severely affected displaying central nervous system involvement (Levade et al. 2009). Seven clinical subtypes of the disease are known which are associated with 17 distinct mutations in the *ASAHI* gene (Zhang et al. 2000; Bär et al. 2001; Muramatsu et al. 2002; Devi et al. 2006). The subtypes are categorized according to the age of onset, symptom severity, and the tissue where lipid accumulation appears (Levade et al. 2009). Types 1 and 5 are the most common forms, with patients displaying nervous system dysfunction and an average age of death between 2 and 3 years (Eviatar et al. 1986; Scriver 1995). Types 2 and 3 are milder forms with death occurring in the second or third decade of life (Ehlert et al. 2007). Type 4 is a very severe form, with patients displaying neurological deterioration, hepatosplenomegaly at birth, and granulomatous infiltrations in the liver, spleen, lymphoid tissue, thymus, and lungs; death typically occurs in the first years of life (Schafer et al. 1996). Type 6 disease has only been described once (Fusch et al. 1989). Type 7 Farber disease, which displays a very severe phenotype (Levade et al. 2009), is not due to mutations in the *ASAHI* gene but rather due to mutations in the gene encoding prosaposin D, which may serve as an activator for *ASAHI* (Levade et al. 2009).

Ceramide accumulation is common to all Farber disease types. Surprisingly, despite wide interest in ceramide in both intracellular signaling pathways (Hannun and Obeid 2008) and as a structural component of membrane lipid microdomains/rafts (Schenck et al. 2007; Lingwood and Simons 2010), only a few studies have used Farber cells to examine the effect of ceramide accumulation on cell function (Levade et al. 1993; Tardy et al. 2004). We now take advantage of a newly developed tool, namely, a monoclonal antibody that was raised and selected to recognize a mixed monolayer phase composed of 60:40 mol% cholesterol:C16-ceramide, at which molar ratio, the two lipids form an ordered and homogeneous phase when deposited as a monolayer at the air-water interface and as a single hydrated bilayer (Ziblat et al. 2012). This anti-C16-ceramide/cholesterol (anti-C16-Cer/Chol) antibody interacts specifically with C16-ceramide/cholesterol and does not bind to pure cholesterol or ceramide monolayers (Scheffer et al. 2006). Using this antibody, we have previously demonstrated that C16-Cer/Chol domains are found at high levels in late endosomes in a variety of cultured cells (Goldschmidt-Arzi et al. 2011). We now use this antibody to determine the levels and localization of C16-Cer/Chol

domains in Farber disease patient fibroblasts, and demonstrate that types 4 and 7 fibroblasts display high levels of the domains, which can be abrogated either by reduction of ceramide or of cholesterol levels.

Materials and Methods

Reagents

Dulbecco's Modified Eagle medium (DMEM) was from Gibco Invitrogen (Carlsbad, CA, USA). The following antibodies were used: anti-voltage-dependent anion-selective channel protein 1 (VDAC1), anti-LAMP2a, anti-calnexin, and anti-Rab7 (Abcam, Cambridge, UK); anti-Rab5 (Santa Cruz Biotechnology Inc., Santa Cruz, CA, USA); anti-Golga5 (Sigma-Aldrich, St Louis, Missouri, MO); and Cy2- and Cy3-labeled secondary antibodies (Jackson ImmunoResearch, West Grove, PA, USA). Wheat germ agglutinin (WGA), Texas Red, and 4',6-diamidino-2-phenylindole (DAPI) were from Molecular Probes (Eugene, OR, USA). An anti-mouse Fab fragment conjugated to 1.2 nm colloidal gold was from Nanoprobes (Yaphank, NY, USA). Bovine serum albumin, antibiotics for use in cell culture, fetal bovine serum, trypsin, and 2-hydroxypropyl- β -cyclodextrin (CD) were from Sigma-Aldrich (St Louis, Missouri, MO). All other reagents or solvents were of the highest grade.

Cell Culture

Farber patient cell lines were purchased from the NIGMS Human Genetic Cell Repository (see Table 1). The transformed uncorrected Farber Moh (pAS-Moh) and gene-corrected Moh (pAS-Moh-ACx5) cell lines were previously described (Medin et al. 1999). Normal human skin fibroblasts were provided by Dr. Lúcia Lacerda (National Health Institute Doutor Ricardo Jorge, Porto, Portugal). Cells were maintained in culture medium supplemented with 10% fetal bovine serum and antibiotics (100 IU/ml penicillin, 100 μ g/ml streptomycin, and 1 mg/ml fungizone) at 37°C in 5% CO₂.

Antibody Production, Screening, and Purification

The anti-C16-Cer/Chol antibody was produced as described (Scheffer et al. 2006). Briefly, antibodies were purified from ascites fluid by affinity chromatography using an ImmunoPure IgM purification kit (Thermo Scientific-Pierce, Epsom, UK). The purified antibody was extensively dialyzed against phosphate buffered saline (PBS) and stored at 4°C. Antibody concentrations were calculated using absorbance at 280 nm. The antibody was used within 7 days after purification.

Table 1 Labeling intensity of C16-Cer/Chol domains in Farber disease patient fibroblasts. The fibroblasts used in this study are shown along with information about their phenotypes. The labelingintensity with the anti-C16-Cer/Chol antibody was integrated and normalized over the cell area; data are means \pm s.e.m., $n = 50$ cells from two different cultures

NIGMS human genetic cell repository designation	Name used in this study	Age at death	Presumed Farber type	Fold-change of anti-C16-Cer/Chol labeling intensity
WT ^a	WT 1-4	20–32 years	None	1.00 \pm 0.10
GM20018	Type 1 #1	22 months	1	0.42 \pm 0.12
GM20015	Type 1 #2	24 months	1	1.19 \pm 0.08
GM02314	Type 2	6 years	2–3	0.65 \pm 0.13
GM02315	Type 3	30 years	3	1.22 \pm 0.13
GM05752	Type 4 #1	6 months	4	4.75 \pm 0.06
GM18313	Type 4 #2	11 months	4	5.08 \pm 0.08
GM20017	Type 5	3 years	5	0.35 \pm 0.12
GM20016	Type 6 ⁴	29 months	6	0.42 \pm 0.12
Prosaposin-deficient ^b	Type 7	4 months	7	2.79 \pm 0.12
GM02316	Carrier	37 years	None	0.86 \pm 0.11
pAS-Moh ^c	Type 4 #3	3 days	4	6.94 \pm 0.07
pAS-Moh-ACx5 ^c	Type 4 #3/ AC	3 days	4	0.95 \pm 0.11

^a Provided by Dr. Lúcia Lacerda (National Health Institute Doutor Ricardo Jorge, Porto, Portugal)^b See Chatelut et al. 1997; Medin et al. 1999^c In addition to mutations in the *ASAH1* gene, this patient was also reported to carry mutations in the β -hexosaminidase gene (Fusch et al. 1989; Levade et al. 1995)

Immunofluorescence Microscopy

Cells were cultured on 12–13-mm glass coverslips to a confluency of ~70%. Cells were fixed by incubating with 3% paraformaldehyde in PBS at room temperature for 45 min, rinsed three times with PBS containing 0.03% bovine serum albumin for 4 min, prior to incubation with the anti-C16-Cer/Chol antibody (10 μ g/ml) for 1 h. The anti-Rab7 antibody (which labels late endosomes) was used at a dilution of 1:50, anti-Rab5 (early endosomes) at 1:50, anti-Golga5 (Golgi apparatus) at 1:100, anti-VDAC1 (mitochondria) at 1:180, anti-calnexin (endoplasmic reticulum) at 1:250, anti-Lamp 2a (lysosomes) at 1:180, and anti-WGA (plasma membrane) at a 1:200 dilution. Cultures were rinsed three times with PBS containing 0.03% bovine serum albumin and then incubated for 30 min with the appropriate secondary antibodies. Nuclei were stained using DAPI at a dilution of 1:1,000 (5 min). Cells were mounted in Gel Mount (Molecular Probes) and observed 24 h later. Acquisition was performed using a confocal FV1000 on an Olympus IX81 microscope, using a 1.35 numerical aperture UPLSAPO 60x oil objective, and image quantification was performed using software provided with the instrument. Intensity measurements were performed by integrating the intensity values and normalizing over the cell area for a minimum of 50 cells per analysis.

Transmission Electron Microscopy

Fibroblasts grown on tissue culture plates were gently removed by washing with medium. Fixation and labeling were performed as above except that gold-conjugated (1.2 nm) secondary antibodies were used. Enhancement to a size of 10–30 nm was performed using a Gold Enhancement kit (Nanoprobes, Yaphank, NY). The pellet was left overnight in 2% glutaraldehyde. Prior to freezing, the pellets were washed by centrifugation ($290 \times g_{av}$, 4 min). The Tokuyasu method was used for immunolabeling (Tokuyasu 1973). Samples were infiltrated, cooled, and embedded in gelatin and fixed with 2% glutaraldehyde on ice, cryo-protected in sucrose, and vitrified by plunging in liquid N₂. The frozen samples were cryo-sectioned using a Leica EM FC6 cryomicrotome, and then transferred to bare 200-mesh nickel or Formvar-coated transmission electron microscopy (TEM) grids. Sucrose was removed and grids were stained with uranyl acetate and embedded in methylcellulose. Samples were viewed on a TEM, T12-Technai TEM microscope operating at 120 kV. Images were recorded on an Eagle 2 K_2 K FEI camera (Eindhoven, Netherlands).

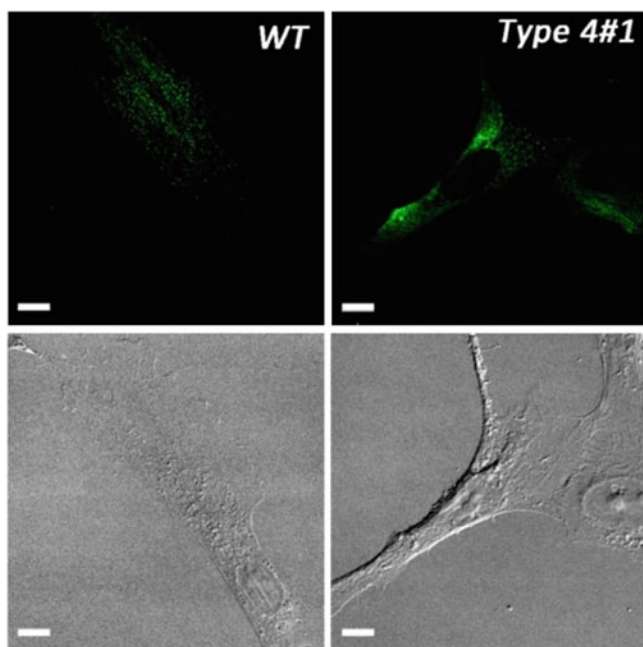


Fig. 1 Immunofluorescence using the anti-C16-Cer/Chol antibody. C16-Cer/Chol domains were labeled using the anti-C16-Cer/Chol antibody in control fibroblasts (WT-2) and in a type 4 Farber disease patient (Type 4#1). The upper panels show immunofluorescence and the lower panels are phase contrast. Scale bar = 10 μ m

Results

Upon incubating fibroblasts with the anti-C16-Cer/Chol antibody, some labeling could be detected in WT fibroblasts, with a similar distribution to that observed in a number of other cell types (Goldschmidt-Arzi et al. 2011), i.e., in a perinuclear region indicative of late endosomes and the trans-Golgi network (Fig. 1; see also Fig. 4). In contrast, substantially more intense labeling was observed in fibroblasts derived from a type 4 Farber disease patient (Type 4 #1, Table 1 and Fig. 1), suggesting that C16-Cer/Chol domains accumulate in Farber disease fibroblasts.

Levels of C16-Cer/Chol domains were subsequently quantified in fibroblasts from Farber disease patients of different severity. The most severe patients, namely, the three type 4s and one type 7, displayed the highest level of labeling (Table 1), which was ~three- to fivefold higher than in control fibroblasts. Fibroblasts derived from patients who displayed a less severe disease, or a patient who was a Farber disease carrier, did not show elevated levels of C16-Cer/Chol domains (Table 1).

We next determined whether levels of C16-Cer/Chol domains could be altered either by modifying ceramide or cholesterol levels. For the former, we used human simian virus 40 (SV40) large T-transformed skin fibroblasts derived from a patient with type 4 Farber disease (type 4 #3), which had been transduced with a recombinant

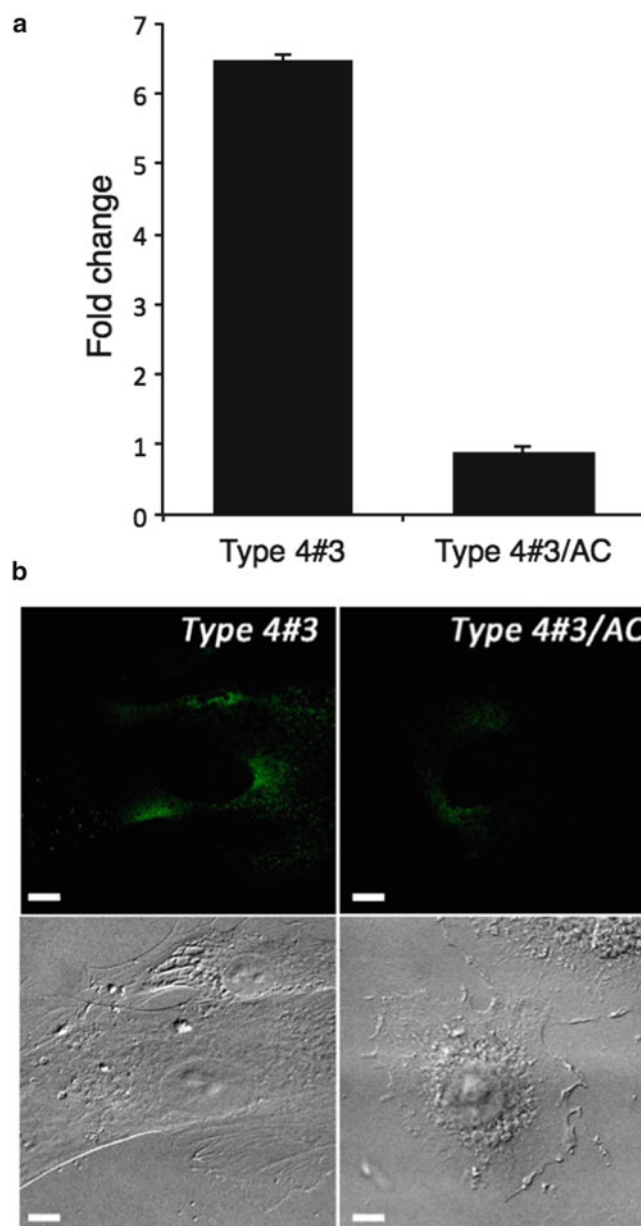


Fig. 2 C16-Cer/Chol domains in Farber disease patient fibroblasts after acid ceramidase transduction. The intensity of the C16-Cer/Chol domains was measured in fibroblasts from a type 4 Farber patient (Type 4 #3, see Table 1) that had been transduced with acid ceramidase (Type 4 #3/AC). Panel A shows the quantification (data are means \pm s.e.m, $n = 50$) and representative images are shown in panel B. The upper panels show immunofluorescence and the lower panels are phase contrast. Scale bar = 10 μ m

retroviral vector containing the *ASAHI* cDNA (type 4 #3/AC) (Medin et al. 1999). As expected, the untreated cell line showed high levels of C16-Cer/Chol domains (Fig. 2 and Table 1), whereas levels of the domains were reduced by ~sevenfold in the acid ceramidase-expressing cells (Fig. 2). Likewise, treatment of Type 4#1 Farber fibroblasts with CD, which reduces cholesterol levels in normal and

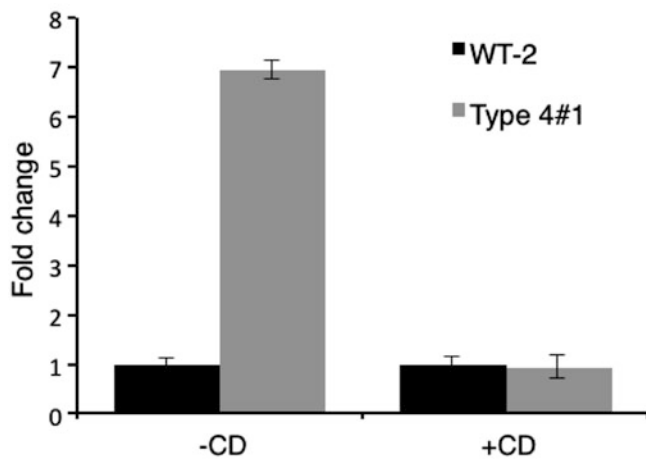


Fig. 3 Effect of CD treatment on anti-C16-Cer/Chol labeling. Domain intensity was measured in WT-2 and Type 4#1 fibroblasts after treatment with or without 100 μ M CD for 48h. Values are means \pm s.e.m., $n = 2$

a significant increase in domain labeling was also observed in both the mitochondria and in the plasma membrane of type 4 Farber disease fibroblasts (Fig. 4). This localization was confirmed by immunogold labeling and TEM, in which significant labeling was detected in the mitochondria and in the plasma membrane (Fig. 5).

Discussion

Ceramide accumulation is the defining feature of Farber disease. In this study, we demonstrate that the ceramide that accumulates in the most severe forms of Farber disease, namely, types 4 and 7, co-localizes in structured domains with cholesterol in cell membranes. Moreover, these domains are not only found in late endosomes and lysosomes as might be expected, but also accumulate in mitochondria and the plasma membrane. The latter results are consistent with the

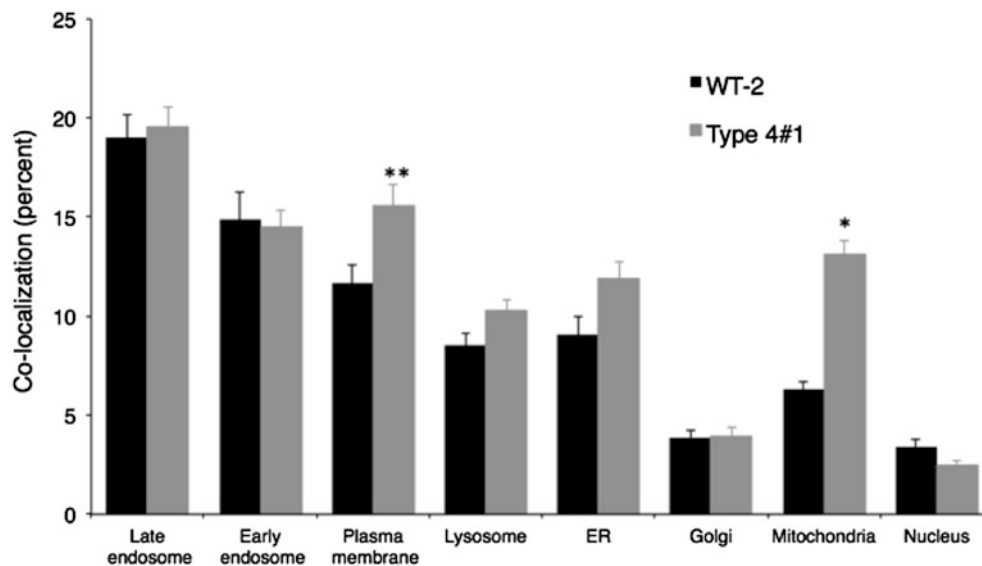


Fig. 4 Co-localization of C16-Cer/Chol domains. The extent of co-localization between the anti-C16-Cer/Chol antibody and each of the markers was determined in WT-2 and Type 4 #1 fibroblasts. Values

represent the extent of co-localization within one pair, such that the numbers are not additive. Data are means \pm s.e.m., $n = 2$ (* $p < 0.01$, ** $p < 0.0001$)

Niemann-Pick C disease cells (Kilsdonk et al. 1995; Rosenbaum et al. 2010; McCauliff et al. 2011) significantly decreased the intensity of the C16-Cer/Chol domains by ~sixfold, with no effect on levels of the domains in WT fibroblasts (Fig. 3).

The intracellular location of the C16-Cer/Chol domains was further examined by co-localization with a number of organelle markers. As observed in earlier studies (Goldschmidt-Arzi et al. 2011), significant co-localization was observed in membranes of the endocytic pathway, including early and late endosomes and lysosomes but, unexpectedly,

notion that extra-lysosomal substrates accumulate in a variety of lysosomal storage diseases (Korkotian et al. 1999; Futerman and van Meer 2004).

Ceramide and cholesterol are major components of lipid microdomains/rafts (Lingwood and Simons 2010). Each of these lipids, either together or separately, affects the biophysical properties of membrane bilayers. While ceramide is known to accumulate in Farber disease, there is no evidence that cholesterol accumulates. Our study, using an anti-C16-Cer/Chol antibody, which binds to C16-ceramide/cholesterol monolayers and not to pure

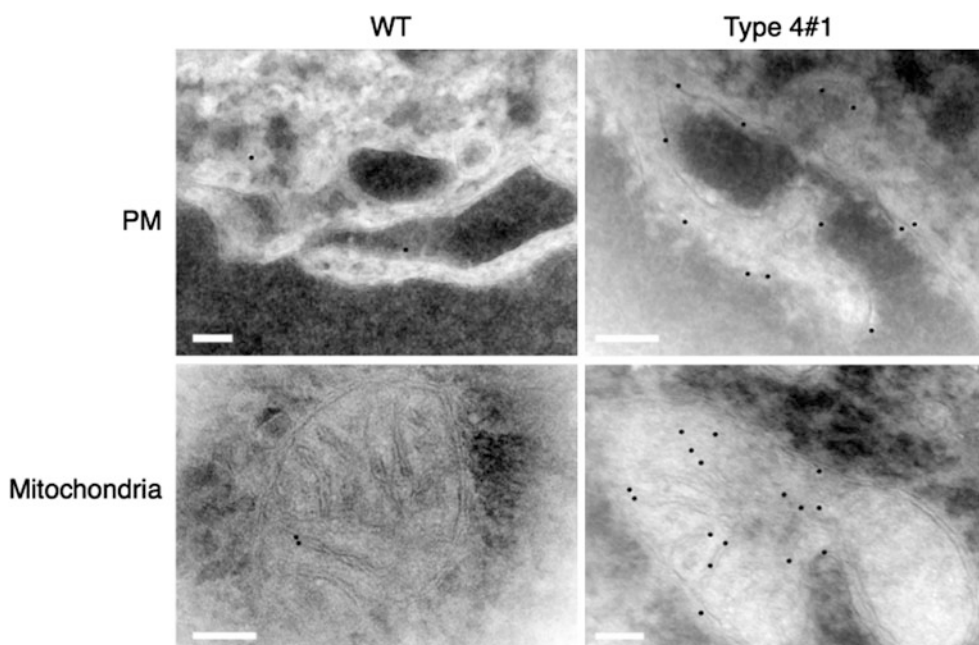


Fig. 5 Detection of C16-Cer/Chol domains by TEM. WT-2 and type 4 #1 fibroblasts were labeled using the anti-C16-Cer/Chol antibody and a gold-conjugated secondary antibody, and examined by TEM. The

images are inverted (gold particles are indicated as magnified *black dots*). The plasma membrane (PM) was identified via its invaginations, and the mitochondria via their cisternae. Scale bar = 100 nm

cholesterol or ceramide, suggests that ceramide sequesters cholesterol in microdomains upon its accumulation in Farber disease. This may be of relevance for understanding the intracellular signaling pathways that are altered in Farber disease, since many signaling pathways are modulated by the membrane lipid composition (Foster et al. 2003). This is particularly true since significant levels of C16-Cer/Chol domains were detected in the plasma membrane, which is the main interface via which cells sense their environment. Interestingly, cholesterol depletion by CD decreased levels of the domains. Whether cholesterol depletion might be a therapeutic option in Farber disease remains to be explored, it should be noted that we have not detected elevated cholesterol in Farber disease, but rather elevated sequestration of accumulated ceramide in ceramide/cholesterol domains.

The accumulation of C16-Cer/Chol domains in mitochondria was unexpected, although a significant body of data has been generated in the past few years demonstrating that mitochondria are a key hub in ceramide biology (Birbes et al. 2002). Indeed, ceramide levels in mitochondria are elevated as a response to stress (Birbes et al. 2001; Siskind et al. 2010), suggesting that Farber cells might be in a constant state of cellular stress. The accumulation of C16-Cer/Chol domains in the plasma membrane is easier to explain, since the plasma membrane is both enriched in cholesterol and part of the endomembrane system, and perhaps once lysosomes become saturated with ceramide, it could overflow into other interconnected compartments.

Interestingly, increased levels of domains were only observed in the most severe forms of the disease, suggesting that a threshold level of ceramide accumulation is required before it can sequester cholesterol and thus be detected by the anti-C16-Cer/Chol antibody.

Whether the anti-C16-Cer/Chol antibody might be used as a diagnostic tool for the most severe forms of Farber disease is open for discussion. Once a diagnosis of Farber disease has been made in the clinic (Dulaney et al. 1976) either by enzymatic or genetic analysis, the question of disease severity becomes relevant. The anti-C16-Cer/Chol antibody is able to distinguish the most severe forms of the disease in a relatively quick and inexpensive manner, but the few surviving patients with the severe forms of the disease are not conducive to widespread use of the antibody for diagnosis of severity. Moreover, the use of this antibody to demonstrate that ceramide is sequestered into domains containing cholesterol suggests that previously unexpected cellular pathways might be involved in Farber disease pathology, which could lead to novel modes of therapeutic intervention.

Acknowledgments N.S. Ferreira is a recipient of a PhD fellowship from the Fundação para a Ciência e Tecnologia (SFRH/BD/40319/2007). Electron microscopy was performed at the Irving and Cherna Moskowitz Center for Nano and Bio-Nano Imaging at the Weizmann Institute. We thank Dr. Lúcia Lacerda for providing cells and Vladimir Kiss for help with confocal microscopy. A.H. Futerman is the Joseph Meyerhoff Professor of Biochemistry and Lia Addadi is the incumbent of the Dorothy-and-Patrick-Gorman Professorial Chair of Biological Ultrastructure at the Weizmann Institute of Science.

References

- Bär J, Linke T, Ferlinz K, Neumann U, Schuchman EH, Sandhoff K (2001) Molecular analysis of acid ceramidase deficiency in patients with Farber disease. *Hum Mutat* 17:199–209
- Birbes H, El Bawab S, Hannun YA, Obeid LM (2001) Selective hydrolysis of a mitochondrial pool of sphingomyelin induces apoptosis. *FASEB J* 15:2669–2679
- Birbes H, El Bawab S, Obeid LM, Hannun YA (2002) Mitochondria and ceramide: intertwined roles in regulation of apoptosis. *Adv Enzyme Regul* 42:113–129
- Chatelut M, Harzer K, Christomanou H et al (1997) Model SV40-transformed fibroblast lines for metabolic studies of human prosaposin and acid ceramidase deficiencies. *Clinica chimica acta. Int J Clin Chem* 262:61–76
- Devi ARR, Gopikrishna M, Ratheesh R, Savithri G, Swarnalata G, Bashyam M (2006) Farber lipogranulomatosis: clinical and molecular genetic analysis reveals a novel mutation in an Indian family. *J Hum Genet* 51:811–814
- Dulaney JT, Milunsky A, Sidbury JB, Hobolth N, Moser HW (1976) Diagnosis of lipogranulomatosis (Farber disease) by use of cultured fibroblasts. *J Pediatr* 89:59–61
- Ehlert K, Frosch M, Fehse N, Zander A, Roth J, Vormoor J (2007) Farber disease: clinical presentation, pathogenesis and a new approach to treatment. *Pediatric Rheumatol Online J* 5:15
- Eviatar L, Sklower SL, Wisniewski K, Feldman RS, Gochoco A (1986) Farber lipogranulomatosis: an unusual presentation in a black child. *Pediatr Neurol* 2:371–374
- Foster LJ, De Hoog CL, Mann M (2003) Unbiased quantitative proteomics of lipid rafts reveals high specificity for signaling factors. *Proc Natl Acad Sci USA* 100:5813–5818
- Fusch C, Huenges R, Moser HW et al (1989) A case of combined Farber and Sandhoff disease. *Eur J Pediatr* 148:558–562
- Futerman AH, van Meer G (2004) The cell biology of lysosomal storage disorders. *Nat Rev Mol Cell Bio* 5:554–565
- Goldschmidt-Arzi M, Shimoni E, Sabanay H, Futerman AH, Addadi L (2011) Intracellular localization of organized lipid domains of C16-ceramide/cholesterol. *J Struct Biol* 175:21–30
- Hannun YA, Obeid LM (2008) Principles of bioactive lipid signalling: lessons from sphingolipids. *Nat Rev Mol Cell Bio* 9:139–150
- Kilsdonk EP, Yancey PG, Stoudt GW et al (1995) Cellular cholesterol efflux mediated by cyclodextrins. *J Biol Chem* 270:17250–17256
- Korkotian E, Schwarz A, Pelled D, Schwarzmans G, Segal M, Futerman AH (1999) Elevation of intracellular glucosylceramide levels results in an increase in endoplasmic reticulum density and in functional calcium stores in cultured neurons. *J Biol Chem* 274:21673–21678
- Levade T, Tempesta MC, Salvayre R (1993) The in situ degradation of ceramide, a potential lipid mediator, is not completely impaired in Farber disease. *FEBS Lett* 329:306–312
- Levade T, Enders H, Schliephacke M, Harzer K (1995) A family with combined Farber and Sandhoff, isolated Sandhoff and isolated fetal Farber disease: postnatal exclusion and prenatal diagnosis of Farber disease using lipid loading tests on intact cultured cells. *Eur J Pediatr* 154:643–648
- Levade T, Sandhoff K, Schulze H, Medin JA (2009) Acid ceramidase deficiency: Farber lipogranulomatosis. In: Valle D et al (eds) *Scriver's OMMBID (Online Metabolic and Molecular Bases of Inherited Disease)*. McGraw-Hill, New York. <http://www.ommbid.com>
- Lingwood D, Simons K (2010) Lipid rafts as a membrane-organizing principle. *Science* 327:46–50
- McCauliff LA, Xu Z, Storch J (2011) Sterol transfer between cyclodextrin and membranes: similar but not identical mechanism to NPC2-mediated cholesterol transfer. *Biochemistry* 50:7341–7349
- Medin JA, Takenaka T, Carpentier S et al (1999) Retrovirus-mediated correction of the metabolic defect in cultured Farber disease cells. *Hum Gene Ther* 10:1321–1329
- Muramatsu T, Sakai N, Yanagihara I et al (2002) Mutation analysis of the acid ceramidase gene in Japanese patients with Farber disease. *J Inher Metab Dis* 25:585–592
- Rosenbaum AI, Zhang G, Warren JD, Maxfield FR (2010) Endocytosis of beta-cyclodextrins is responsible for cholesterol reduction in Niemann-Pick type C mutant cells. *Proc Natl Acad Sci* 107:5477–5482
- Schafer A, Harzer K, Kattner E, Schafer HJ, Stoltenburg G, Lietz H (1996) Disseminated lipogranulomatosis (Farber disease) with hydrops fetalis. *Pathologie* 17:145–149
- Scheffer L, Fargion I, Addadi L (2006) Structural recognition of cholesterol-ceramide monolayers by a specific monoclonal antibody. *Chembiochem* 7:1680–1682
- Schenck M, Carpinteiro A, Grassme H, Lang F, Gulbins E (2007) Ceramide: physiological and pathophysiological aspects. *Arch Biochem Biophys* 462:171–175
- Scriver CR (1995) *The metabolic and molecular bases of inherited disease*. McGraw-Hill Health Professions Division, New York
- Siskind LJ, Mullen TD, Romero Rosales K et al (2010) The BCL-2 protein BAK is required for long-chain ceramide generation during apoptosis. *J Biol Chem* 285:11818–11826
- Tardy C, Andrieu-Abadie N, Salvayre R, Levade T (2004) Lysosomal storage diseases: is impaired apoptosis a pathogenic mechanism? *Neurochem Res* 29:871–880
- Zhang Z, Mandal AK, Mital A et al (2000) Human acid ceramidase gene: novel mutations in Farber disease. *Mol Genet Metab* 70:301–309
- Ziblat R, Fargion I, Leiserowitz L, Addadi L (2012) Spontaneous formation of two-dimensional and three-dimensional cholesterol crystals in single hydrated lipid bilayers. *Biophys J* 103:255–264

Infantile Sialic Acid Storage Disease: Two Unrelated Inuit Cases Homozygous for a Common Novel *SLC17A5* Mutation

Matthew A. Lines • C. Anthony Rupar • Jack W. Rip •
Berivan Baskin • Peter N. Ray • Robert A. Hegele •
David Grynspan • Jean Michaud • Michael T. Geraghty

Received: 12 April 2013 / Revised: 05 June 2013 / Accepted: 10 June 2013 / Published online: 31 July 2013
© SSIEM and Springer-Verlag Berlin Heidelberg 2013

Abstract Infantile sialic acid storage disease (ISSD) is a lysosomal storage disease characterized by accumulation of covalently unlinked (free) sialic acid in multiple tissues. ISSD and Salla disease (a predominantly neurological disorder) are allelic disorders caused by recessive mutations of a lysosomal anionic monosaccharide transporter, *SLC17A5*. While Salla disease is common in Finland due to a founder-effect mutation (p.Arg39Cys), ISSD is comparatively rare in all populations studied.

Here, we describe the clinical and molecular features of two unrelated Canadian Inuit neonates with a virtually identical presentation of ISSD. Both individuals presented

antenatally with fetal hydrops, dying shortly following delivery. Urinary free sialic acid excretion was markedly increased in the one case in which urine could be obtained for testing; postmortem examination showed a picture of widespread lysosomal storage in both. Both children were homozygous for a novel splice site mutation (NM_012434: c.526-2A>G) resulting in skipping of exon 4 and an ensuing frameshift. Analysis of a further 129 pan-Arctic Inuit controls demonstrated a heterozygous carrier rate of 1/129 (~0.4 %) in our sample. Interestingly, lysosomal enzyme studies showed an unexplained ninefold increase in neuraminidase activity, with lesser elevations in the activities of several other lysosomal enzymes. Our results raise the possibility of a common founder mutation presenting as hydrops in this population. Furthermore, if confirmed in subsequent cases, the marked induction of neuraminidase activity seen here may prove useful in the clinical diagnosis of ISSD.

Communicated by: Verena Peters

Competing interests: None declared

M.A. Lines • M.T. Geraghty (✉)
Division of Metabolics and Newborn Screening, University of Ottawa,
Children's Hospital of Eastern Ontario, 401 Smyth Road,
K1H 8L1, Ottawa, ON, Canada
e-mail: mgeraghty@cheo.on.ca

C.A. Rupar • J.W. Rip
Departments of Biochemistry, Paediatrics and Children's Health
Research Institute, University of Western Ontario, London,
ON, Canada

B. Baskin
Department of Immunology, Genetics and Pathology, Uppsala
University, Uppsala, Uppland, Sweden

P.N. Ray
Division of Molecular Genetics, The Hospital for Sick Children,
Toronto, ON, Canada

R.A. Hegele
Robarts Research Institute and Department of Medicine, University of
Western Ontario, London, ON, Canada

D. Grynspan • J. Michaud
Department of Pathology, University of Ottawa, Children's Hospital
of Eastern Ontario, Ottawa, ON, Canada

Introduction

Defects of the sialic acid transporter *SLC17A5* cause a lysosomal storage disease characterized by systemic accumulation of free sialic acid in a wide range of tissues (Verheijen et al. 1999). *SLC17A5*-related conditions include infantile sialic acid storage disease (ISSD; OMIM #269920, a lethal multisystem disorder), Salla disease (OMIM #604369, a slowly progressive, predominantly neurological condition), and intermediate phenotypes (Aula et al. 2000; Verheijen et al. 1999). Recently, *SLC17A5* mutations have also been identified in children and adults with cerebral palsy-like chronic encephalopathy; thus, the recognized spectrum of clinical phenotypes continues to expand (Debray et al. 2011; Mochel et al. 2009, 2010). ISSD is situated at the opposite

(severe) end of the *SLC17A5* disease spectrum; cardinal features include profound developmental delay, failure to thrive, hepatosplenomegaly, coarse facies, hypopigmentation, and (typically) death in infancy (Lemyre et al. 1999). Findings seen in a subset of cases include dysostosis multiplex, cardiomegaly, heart failure, and prematurity. A majority of ISSD cases demonstrate fetal hydrops and/or ascites; hence, this can be considered a prenatal-onset condition (Froissart et al. 2005). General genotype-phenotype correspondences have been established, and (with exceptions) most Salla disease patients have at least one copy of the common Finnish founder allele, p.Arg39Cys (NM_012434.4:c.115C>T) bearing some residual transporter activity in vitro (Aula et al. 2000; Morin et al. 2004; Verheijen et al. 1999; Wreden et al. 2005; Mochel et al. 2009). In contrast, a wide range of mutation types are seen in ISSD; those studied in vitro appear to be functionally null (Aula et al. 2000; Morin et al. 2004; Myall et al. 2007; Ruivo et al. 2008; Wreden et al. 2005).

Previous reports have described *SLC17A5* mutations in Finnish, Swedish, Danish, Italian, French, Polish, Yugoslav, Turkish, Bedouin, Japanese, and North American (including French Canadian) patients (Biancheri et al. 2002, 2005; Coker et al. 2009; Erikson et al. 2002; Landau et al. 2004; Nakano et al. 1996; Sonderby Christensen et al. 2003; Tylki-Szymanska et al. 2003; Verheijen et al. 1999). Apart from the common p.Arg39Cys allele, no other founder alleles have been described. Here, we describe the clinical features of two unrelated affected individuals of non-consanguineous Canadian Inuit descent. *SLC17A5* sequencing identified both probands to be homozygous for a novel splice site mutation, making this the first report of ISSD in the Inuit, and raising the possibility of a common ancestral mutation in this population.

Patient 1

Patient 1 was the product of a spontaneous pregnancy to healthy parents; no infectious or teratogenic risks were disclosed. Fetal hepatomegaly and ascites were first noted at 20 weeks' gestational age; karyotype was normal and maternal TORCH screen was negative. Increasing abdominal girth, cardiomegaly, and facial edema were apparent by 29 weeks. Fetal paracentesis yielded 700 cc of yellow, non-chylous fluid. Spontaneous preterm vaginal delivery of a male weighing 1,769 g (+1–+2SD) ensued at 31⁺⁴ weeks. Apgar scores were 4 at 1 min and 7 at 5 min; the child was intubated, received surfactant, and was ventilated with high-frequency oscillator in 100 % oxygen. Despite these measures, the patient was critically unstable for the first several hours of life, with a persistent mixed acidosis (pH < 6.90) and poor oxygen saturations. The clinical

picture stabilized by 12 h of age, with resolution of acidosis and improved oxygenation.

Newborn examination was significant for dysmorphic facies, massive hepatomegaly, significant peripheral edema, and bilateral talipes. CBC and Coombs' test were negative, and echocardiograph showed a structurally normal heart. The child's general condition remained poor, with marked hypotonia, absence of spontaneous movement, and complete reliance on ventilator support. The NICU course was punctuated by two abrupt episodes of decompensation, during which laboratory studies showed a nonspecific biochemical picture of hypoglycemia, hyponatremia, and mild lactic acidosis; these were attributed to suspected ventilator-associated pneumonia, and responded to empiric antibiotic treatment. Repeated red cell and platelet transfusions were required due to persistent anemia and thrombocytopenia. There was evidence of an ongoing acute-phase response, with C-reactive protein levels ranging between 44 and 222 mg/L (upper normal limit = 8 mg/L), a marked left shift, and ongoing significant bandemia ($0.41 - 8.8 \times 10^9/L$). The patient died on day 26 of life due to respiratory failure despite maximal ventilation. On autopsy, deposition of foamy, clear cytoplasmic material was seen in neural cell bodies throughout the central and peripheral nervous systems, as well as in the pituitary gland, liver, lymph nodes, and pancreatic islet cells (Fig. 1).

Biochemical investigations in this patient showed the following: Urine oligosaccharides showed increased excretion of free sialic acid, providing the major clue to diagnosis. Interestingly, repeat urine oligosaccharide on day 19 showed a normal pattern. Mucopolysaccharide screen was initially too dilute for analysis; repeat on day 19 was negative. Urine organic acids were unremarkable apart from elevated lactate and pyruvate. Plasma amino acids were normal. Lactate was high (8.5 mmol/L) immediately following birth, but normalized rapidly over the following 4 h. Ammonia and liver enzymes were normal. The most striking finding on enzymology of cultured skin fibroblasts was a nearly tenfold increase in neuraminidase activity, with less marked elevations of several other lysosomal enzyme activities (Table 1). Plasma hexosaminidases were not consistent with I-cell disease. *NPC1* and *NPC2* sequencing were normal.

Given our clinical suspicion of ISSD, *SLC17A5* sequencing was performed. This showed a homozygous change, NM_012434:c.526-2A>G, situated within the exon 4 splice acceptor site. The effect of this sequence change on splicing was examined by reverse transcriptase PCR using primers situated in exons 3 and 5 (Fig. 2a,b). While a control sample produced a band with the expected size of 420 bp, the patient's sample showed a smaller band of approximately 350 bp. Direct sequence analysis of this

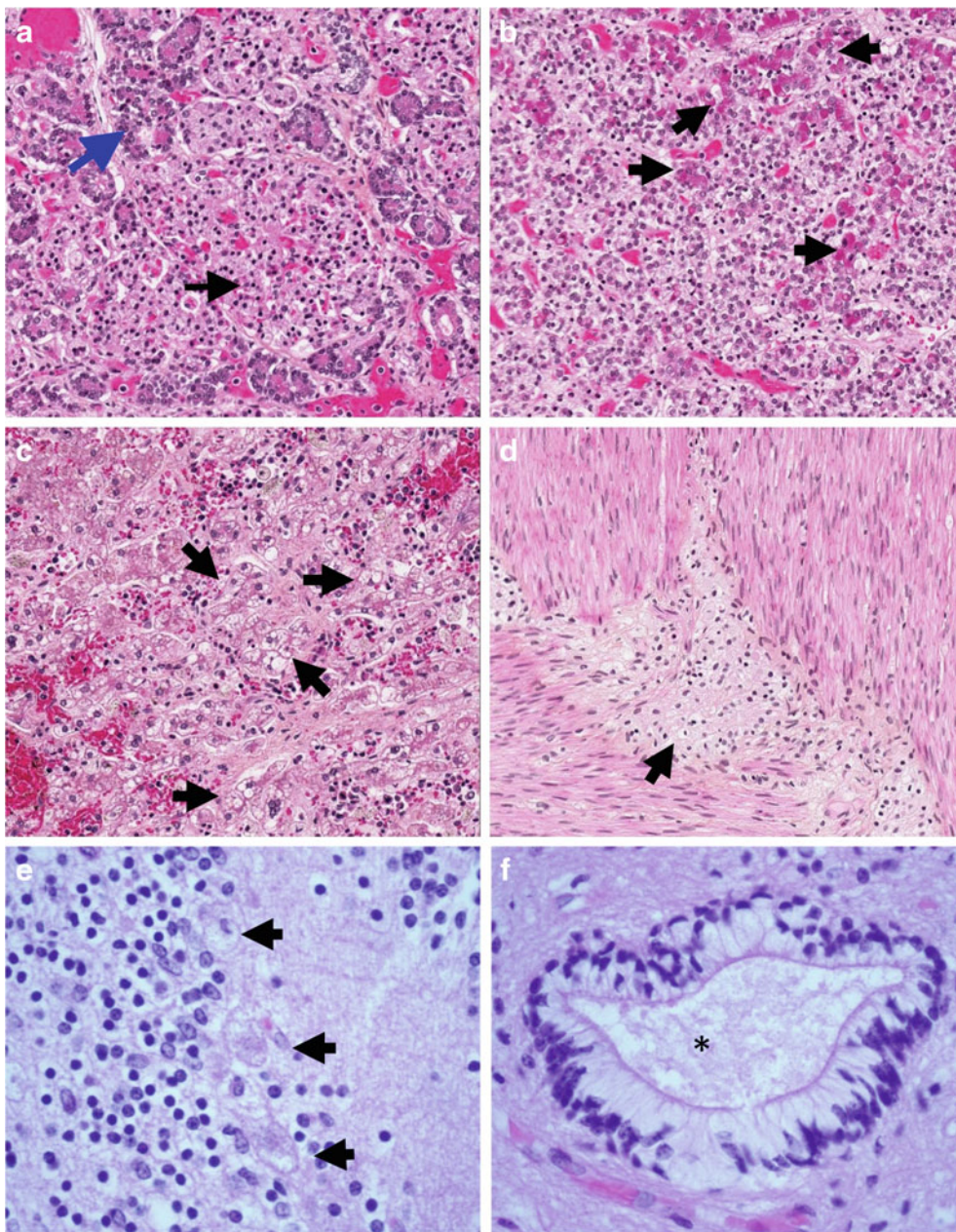


Fig. 1 Pathologic findings in Patient 1. (a) Section through pancreas showing enlarged, vacuolated islet cells (*black arrow*), with relatively normal-appearing acinar cells (*blue arrow*) at periphery (b) Pituitary gland contains a majority of pale, vacuolated cells with a foamy appearance; some acidophilic cells with a superimposed foamy quality (*arrows*) are seen (c) Sections of liver show granular, swollen, pale, foamy cells throughout (some clusters indicated by *arrows*). The stored material does not stain by Oil Red-O or periodic acid-Schiff

histochemical stains (data not shown) (d) Ganglion cells of the myenteric plexus (*arrow*) have enlarged, pale cytoplasm with a foamy quality (e) Cerebellar cortex: three Purkinje cells are swollen, with cytoplasmic accumulation of foamy storage material and loss of Nissl substance (*arrows*) (f) Ependymal canal, spinal cord: ependymal cells have a clear cytoplasm due to presence of storage material (*asterisk* indicates center of canal)

smaller fragment confirmed skipping of exon 4 (r.526_613del) (Fig. 2c). This change is predicted to result in deletion of 28 amino acid residues, a frameshift, and consequently in a prematurely truncated protein (p.Gly176_Ala204delinsfs*7). This mutation is not represented in any of the following catalogues of variation: dbSNP (<http://www.ncbi.nlm.nih.gov/projects/SNP/>),

1,000 genomes (<http://www.1000genomes.org/>), or the NHLBI Exome Variant Server (<http://evs.gs.washington.edu/EVS/>). Genotyping of 129 circumpolar Inuit samples from a variety of locales identified a single individual heterozygous for the same mutation (sample minor allele frequency: $1/258 = 0.4\%$; 95 % confidence interval = [0.01–2.2 %]).

Table 1 Lysosomal enzyme activities in ISSD

Cultured fibroblast enzyme activities (nmol/h/mg)			
Enzyme	Reference interval	Patient 1	Patient 2
Neuraminidase	11.9–20.1	181	199
β-Galactosidase	335–435	629	789
β-Glucuronidase	105–233	95 (93)	141
β-Glucocerebrosidase	71–108	237	NA
Sphingomyelinase	56–113	158	NA
Arylsulfatase A	22–50	70	78
Acid lipase	NA	801	1,108
α-Mannosidase	64–184	50	146
Total hexosaminidase	8160–11,500	18,329	20,018
Hexosaminidase A	390–750	1,925	2,155

Serum hexosaminidases (nmol/h/mL)		
Enzyme	Reference interval	Patient 1
Total serum hexosaminidase	439–1,300	572
Serum hexosaminidase A	30–45 % of total	249 (43.5 % of total)

Lysosomal enzyme activities were measured from cultured skin fibroblast extracts in the laboratory of Dr. T. Rupar according to standard methods, in triplicate with simultaneous triplicate measurement of a same-day control specimen. Skin biopsy for fibroblast culture was obtained antemortem in Patient 1, and postmortem in Patient 2. Serum hexosaminidases were tested at the Hospital for Sick Children, Toronto, Canada, according to standard methods

NA Not available

Patient 2

Patient 2 was referred to our pathology department for postmortem review and was identified retrospectively based on the strikingly similar neuropathologic findings versus those of Patient 1. Patient 2 was the product of a spontaneous singleton pregnancy to healthy non-consanguineous Inuit parents. At 25 weeks' gestation, the mother presented with threatened preterm labor, and the fetus was discovered to have severe hydrops, polyhydramnios, and mild cardiomegaly, as well as bilateral cerebral ventriculomegaly and bilateral talipes. Amniocentesis showed a normal male karyotype; TORCH screen was negative. Fetal echo was structurally normal apart from cardiomegaly. Serial ultrasounds showed a picture of progressively worsening fetal hydrops. By 27⁺ 6 weeks, the measured fetal abdominal circumference was in keeping with 41 weeks, due to hepatomegaly and massive ascites. Variable decelerations were noted, and presentation being footling breach, an emergency Caesarean section was performed. A male infant was born weighing 2,314 g (+4SD). The child died shortly after birth following an unsuccessful attempt at resuscitation.

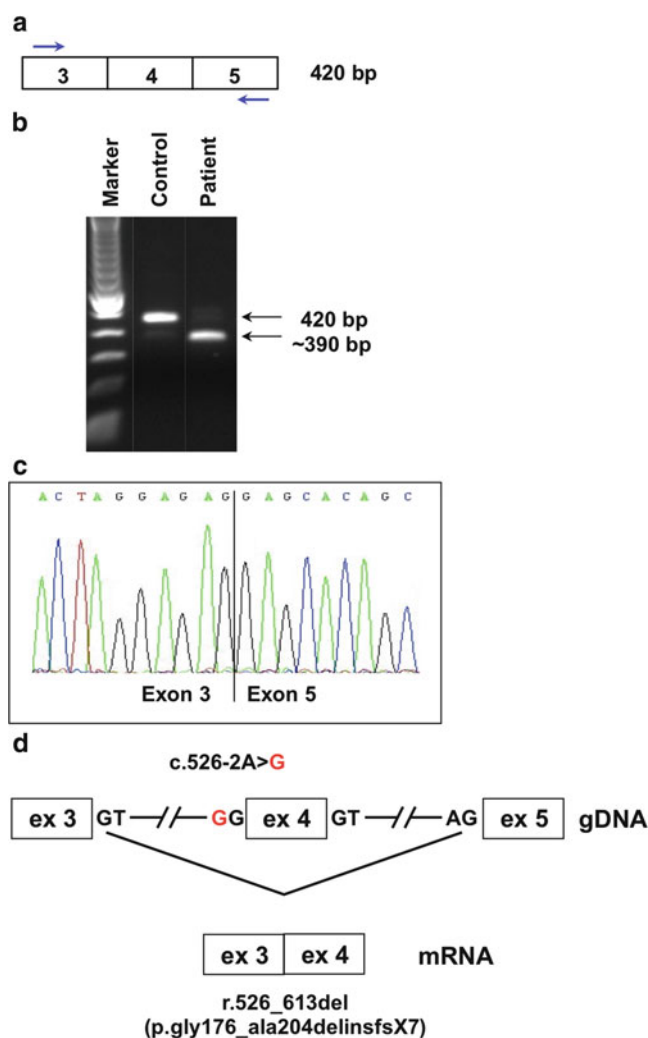


Fig. 2 Aberrant splicing due to *SLC17A5* mutation. Mutation analysis was performed on genomic DNA from whole blood by direct sequencing of all exons and exon/intron boundaries of *SLC17A5* (NM_012434.4), according to standard protocols. For *SLC17A5* mRNA studies, cDNA was prepared from cultured skin fibroblasts according to standard protocols: (a) Strategy for RT-PCR amplification of a region containing exon 4 (primer sequences and PCR protocol are available upon request). (b) The amplified product visualized on an agarose gel. The expected size of 420 bp is seen in an unaffected control, whereas in Patient 1, an additional band of approximately 350 bp was seen. (c) Direct sequence analysis of the ~350 bp fragment reveals an 88 bp deletion corresponding to exon 4. (d) A schematic overview of the gDNA with the acceptor splice site mutation c.526-2A>G. Disruption of the exon 4 splice acceptor site results in exon skipping, with exon 3 spliced directly onto exon 5 (r.526_613del). This is predicted to result in a frameshift and premature stop codon at the seventh downstream position (p.Gly176_Ala204delinsfs*7)

At autopsy, note was made of massive serous ascites, bilateral pleural effusions, and moderate diffuse subcutaneous edema. Pulmonary hypoplasia, cardiomegaly, and hepatosplenomegaly were evident. Histological findings were essentially identical to those of Patient 1, with foamy

vacuolated cells in the central nervous system, peripheral nerve ganglia, pituitary chromophobe cells, hepatocytes, renal tubular epithelium, thyroid follicular epithelium, macrophages, adrenal glands, and epithelial cells of the renal glomeruli. Placental accumulation of storage material was also seen. As for Patient 1, neuraminidase activity in cultured skin fibroblasts was shown to be markedly increased (Table 1). *SLC17A5* sequencing showed this individual to be homozygous for the same mutation previously identified in Patient 1.

Discussion

Both of the children described here followed a severe clinical course, characterized by antenatal development of fetal hydrops, multisystem involvement, and early demise despite maximal supportive treatment. This is essentially in keeping with the reported phenotype of other patients with truncating *SLC17A5* mutations, suggesting a poor prognosis in patients lacking residual transporter activity (Reviewed in Froissart et al. 2005). From a molecular standpoint, both patients were homozygous for the same *SLC17A5* mutation (c.526-2A>G). As far as we are aware, this constitutes the first report of ISSD among the Inuit; as our two patients are unrelated and from geographically remote reaches of the Arctic, the question of an ancestral founder mutation in *SLC17A5* is raised. Determining whether this is the case will require analysis of a larger ethnic cohort and/or use of SNP-based linkage disequilibrium methods, beyond the scope of this report.

The distribution of the observed storage material in our patients is similar to that reported previously (Lemyre et al. 1999), and corresponds in a general sense to the expression pattern of sialin in the mouse (Yarovaya et al. 2005).

The cause of the nearly tenfold increase in fibroblast neuraminidase activity seen in our patients is unclear. We are aware of one earlier report of two children with free sialic acid storage and increased neuraminidase activity in lymphocytes, although activity was normal in fibroblasts in these same patients (Ylitalo et al. 1986). In contrast, several authors have reported neuraminidase activity in ISSD patients as “normal” or “not decreased” (Baumkötter et al. 1985; Paschke et al. 1986; Pueschel et al. 1988; Fois et al. 1987; Nakano et al. 1996; Lemyre et al. 1999). Whether this apparent inconsistency represents true biological variation, differences in technique, or a chance observation due to the influence of other genetic modifiers is unclear at present. Neuraminidases are known to be inducible in response to various external stimuli, for instance during immune cell differentiation and activation (Stamatos et al. 2005; Wang et al. 2004), although the basal regulation of “housekeeping” neuraminidase expression is poorly understood. In general, mechanisms

that could conceivably lead to increased neuraminidase activity include (1) bulk expansion of the lysosomal compartment, (2) dysregulation of neuraminidase gene expression, and (3) allosteric effects on neuraminidase activity at the enzyme level, or some combination thereof. When present, the presence of this highly unusual finding should therefore prompt the clinician to consider testing for ISSD via conventional means, such as urine oligosaccharides analysis and/or *SLC17A5* sequencing.

Synopsis

The sequential ascertainment of two unrelated Canadian Inuit patients homozygous for the same *SLC17A5* mutation raises the possibility of a founder mutation for infantile sialic acid storage disease (ISSD) in this population.

Author Contributions

Matthew Lines: Primary authorship of manuscript

Tony Rupar and Jack Rip: Enzymatic analyses and assistance with writing

Berivan Baskin and Peter Ray: Molecular analyses

David Grynspan and Jean Michaud: Description of pathological findings and preparation of histologic images

Michael Geraghty: Corresponding author, study design, critical appraisal, assistance with writing

Guarantor

Michael Geraghty

Compliance with Ethics Guidelines

Matthew Lines, Tony Rupar, Jack Rip, Berivan Baskin, Peter Ray, Robert Hegele, David Grynspan, Jean Michaud, and Michael Geraghty each declare that they have no conflict of interest.

This manuscript is a retrospective case series containing no identifying patient information, and data were collected in the course of provisioning the routine standard of clinical care (rather than as part of a research study). All procedures followed were in accordance with the Helsinki Declaration of 1975, as revised in 2000.

References

- Aula N, Salomaki P, Timonen R, Verheijen F, Mancini G, Mansson JE, Aula P, Peltonen L (2000) The spectrum of *SLC17A5*-gene mutations resulting in free sialic acid-storage diseases indicates some genotype-phenotype correlation. *Am J Hum Genet* 67(4): 832–840

- Baumkötter J, Cantz M, Mendla K, Baumann W, Friebolin H, Gehler J, Spranger J (1985) N-Acetylneuraminic acid storage disease. *Hum Genet* 71(2):155–159
- Biancheri R, Verbeek E, Rossi A, Gaggero R, Roccatagliata L, Gatti R, van Diggelen O, Verheijen FW, Mancini GM (2002) An Italian severe Salla disease variant associated with a SLC17A5 mutation earlier described in infantile sialic acid storage disease. *Clin Genet* 61(6):443–447
- Biancheri R, Rossi A, Verbeek HA, Schot R, Corsolini F, Assereto S, Mancini GM, Verheijen FW, Minetti C, Filocamo M (2005) Homozygosity for the p.K136E mutation in the SLC17A5 gene as cause of an Italian severe Salla disease. *Neurogenetics* 6(4):195–199
- Coker M, Kalkan-Ucar S, Kitis O, Ucar H, Goksen-Simsek D, Darcan S, Gokben S (2009) Salla disease in Turkish children: severe and conventional type. *Turk J Pediatr* 51(6):605–609
- Debray FG, Lefebvre C, Colinet S, Segers K, Stevens R (2011) Free sialic acid storage disease mimicking cerebral palsy and revealed by blood smear examination. *J Pediatr* 158(1):165
- Erikson A, Aula N, Aula P, Mansson JE (2002) Free sialic acid storage (Salla) disease in Sweden. *Acta Paediatr* 91(12):1324–1327
- Fois A, Balestri P, Farnetani MA, Mancini GM, Borgogni P, Margollicci MA, Molinelli M, Alessandrini C, Gerli R (1987) Free sialic acid storage disease. A new Italian case. *Eur J Pediatr* 146(2):195–198
- Froissart R, Cheillan D, Bouvier R, Turret S, Bonnet V, Piraud M, Maire I (2005) Clinical, morphological, and molecular aspects of sialic acid storage disease manifesting in utero. *J Med Genet* 42(11):829–836
- Landau D, Cohen D, Shalev H, Pinsk V, Yerushalmi B, Zeigler M, Birk OS (2004) A novel mutation in the SLC17A5 gene causing both severe and mild phenotypes of free sialic acid storage disease in one inbred Bedouin kindred. *Mol Genet Metab* 82(2):167–172
- Lemyre E, Russo P, Melancon SB, Gagne R, Potier M, Lambert M (1999) Clinical spectrum of infantile free sialic acid storage disease. *Am J Med Genet* 82(5):385–391
- Mochel F, Yang B, Barritault J, Thompson JN, Engelke UF, McNeill NH, Benko WS, Kaneski CR, Adams DR, Tsokos M et al (2009) Free sialic acid storage disease without sialuria. *Ann Neurol* 65(6):753–757
- Mochel F, Engelke UF, Barritault J, Yang B, McNeill NH, Thompson JN, Vanderver A, Wolf NI, Willemsen MA, Verheijen FW, Seguin F, Wevers RA, Schiffmann R (2010) Elevated CSF N-acetylaspartylglutamate in patients with free sialic acid storage diseases. *Neurology* 74(4):302–305
- Morin P, Sagne C, Gasnier B (2004) Functional characterization of wild-type and mutant human sialin. *EMBO J* 23(23):4560–4570
- Myall NJ, Wreden CC, Wlizla M, Reimer RJ (2007) G328E and G409E sialin missense mutations similarly impair transport activity, but differentially affect trafficking. *Mol Genet Metab* 92(4):371–374
- Nakano C, Hirabayashi Y, Ohno K, Yano T, Mito T, Sakurai M (1996) A Japanese case of infantile sialic acid storage disease. *Brain Dev* 18(2):153–156
- Paschke E, Trinkl G, Erwa W, Pavelka M, Mutz I, Roscher A (1986) Infantile type of sialic acid storage disease with sialuria. *Clin Genet* 29(5):417–424
- Pueschel SM, O'Shea PA, Alroy J, Ambler MW, Dangond F, Daniel PF, Kolodny EH (1988) Infantile sialic acid storage disease associated with renal disease. *Pediatr Neurol* 4(4):207–212
- Ruivo R, Sharifi A, Boubekeur S, Morin P, Anne C, Debacker C, Graziano JC, Sagne C, Gasnier B (2008) Molecular pathogenesis of sialic acid storage diseases: insight gained from four missense mutations and a putative polymorphism of human sialin. *Biol Cell* 100(9):551–559
- Sonderby Christensen P, Kaad PH, Ostergaard JR (2003) Two cases of Salla disease in Danish children. *Acta Paediatr* 92(11):1357–1358
- Stamatos NM, Liang F, Nan X, Landry K, Cross AS, Wang LX, Pshezhetsky AV (2005) Differential expression of endogenous sialidases of human monocytes during cellular differentiation into macrophages. *FEBS J* 272(10):2545–2556
- Tylki-Szymanska A, Czartoryska B, Lugowska A, Verheijen FW, Mancini GM, Rokicki D, Taybert J, Chmielinska E (2003) Infantile sialic acid storage disease (ISSD): report of the first case detected in Poland. *Pediatr Int* 45(2):199–200
- Verheijen FW, Verbeek E, Aula N, Beerens CE, Havelaar AC, Joosse M, Peltonen L, Aula P, Galjaard H, van der Spek PJ, Mancini GM (1999) A new gene, encoding an anion transporter, is mutated in sialic acid storage diseases. *Nat Genet* 23(4):462–465
- Wang P, Zhang J, Bian H, Wu P, Kuvelkar R, Kung TT, Crawley Y, Egan RW, Billah MM (2004) Induction of lysosomal and plasma membrane-bound sialidases in human T-cells via T-cell receptor. *Biochem J* 380(Part 2):425–433
- Wreden CC, Wlizla M, Reimer RJ (2005) Varied mechanisms underlie the free sialic acid storage disorders. *J Biol Chem* 280(2):1408–1416
- Yarovaya N, Schot R, Fodero L, McMahon M, Mahoney A, Williams R, Verbeek E, de Bondt A, Hampson M, van der Spek P, Stubbs A, Masters CL, Verheijen FW, Mancini GM, Venter DJ (2005) Sialin, an anion transporter defective in sialic acid storage diseases, shows highly variable expression in adult mouse brain, and is developmentally regulated. *Neurobiol Dis* 19(3):351–365
- Ylitalo V, Hagberg B, Rapola J, Månsson JE, Svennerholm L, Sanner G, Tonnby B (1986) Salla disease variants. Sialoylaciduric encephalopathy with increased sialidase activity in two non-Finnish children. *Neuropediatrics* 17(1):44–47

Motor Development Skills of 1- to 4-Year-Old Iranian Children with Early Treated Phenylketonuria

Sepideh Nazi • Farzaneh Rohani • Firoozeh Sajedi •
Akbar Biglarian • Arya Setoodeh

Received: 15 March 2013 / Revised: 24 June 2013 / Accepted: 25 June 2013 / Published online: 6 August 2013
© SSIEM and Springer-Verlag Berlin Heidelberg 2013

Abstract Objective: To gauge the gross and fine motor development of early treated phenylketonuria (ETPKU) in children in the age range of 1–4 years.

Methods: A cross-sectional analytic study was conducted in PKU clinics (reference clinics for PKU follow-up), Tehran, Iran. Seventy children with ETPKU were selected as the case group for the study. ETPKU children were those with early and continuous treatment with a phenylalanine-restricted diet (the mean of blood phenylalanine level during the recent 6 months was 2–6 mg/dL or 120–360 $\mu\text{mol/L}$). Also, 100 healthy and normal children matched with the ETPKU group for age were randomly selected from 4 kindergartens in four parts of Tehran as a control group. The measurements consisted of a

demographic questionnaire, Peabody Developmental Motor Scale-2 (PDMS-2), and pediatrician assessment. Motor quotients were determined by PDMS-2 and then compared in both groups by two independent samples *t*-test.

Results: The mean ages in case and control group were 28.5 (\pm 11.6) and 29.7 (\pm 11.3) months, respectively. Comparison of the mean fine, gross, and total developmental motor quotients (DMQs) showed statistically significant differences between the two groups ($p < 0.05$). The fine and total DMQs of ETPKU children were also correlated with age. In addition, there was a negative correlation between the phenylalanine level and fine ($p < 0.001$) and total ($p = 0.001$) DMQs.

Conclusion: It seems that ETPKU Iranian children, regardless of following a phenylalanine-restricted diet or not, have lower motor development. It is recommended to plan programs for early detection and intervention of developmental delays in these children.

Communicated by: K. Michael Gibson

Competing interests: None declared

By reading this article, the reader will better understand the motor consequences of early dietary intervention in Iranian PKU children.

S. Nazi

Occupational therapy Department, Tehran University of Medical Sciences (TUMS), Tehran, Iran

F. Rohani

Endocrinologic & Metabolism Division, Aliasghar Hospital, Tehran University of Medical Sciences (TUMS), Tehran, Iran

F. Sajedi (✉)

Pediatrics, Clinical Sciences Department, University of Social Welfare & Rehabilitation Sciences (USWR), Koodakyar st. Evin., 19857138341, Tehran, Iran
e-mail: fisajedi@uswr.ac.ir; spdh.nz@gmail.com

A. Biglarian

Department of Biostatistics, University of Social Welfare and Rehabilitation Sciences, Tehran, Iran

A. Setoodeh

Endocrinologic & Metabolism Division, Children's Hospital Medical Center, Tehran University of Medical Sciences (TUMS), Tehran, Iran

Introduction

PKU is a rare metabolic autosomal recessive disease characterized by a deficiency in the phenylalanine hydroxylase enzyme that is necessary for the metabolism of the amino acid phenylalanine (Phe) (Hoeksma et al. 2009).

The incidence of PKU varies widely in different parts of the world. While the average incidence of PKU in Caucasians is approximately 1 in 10,000, it differs several-fold among different populations. The incidence of PKU in Iran can be estimated to be 1 in 3,627 (Koochmeshgi et al. 2002). This is one of the highest incidence values reported.

Untreated PKU typically results in cognitive impairment (Hoeksma et al. 2009; van Spronsen et al. 2009). With dietary treatment, intelligence is usually in the average

range, although it remains somewhat lower than that of peers and siblings without PKU (Hoeksma et al. 2009). Waisbren et al. noted that untreated PKU was associated with significant delays in developmental milestones (e.g., crawling, walking, talking), and approximately 98 % of individuals with untreated PKU fall in the range of global intellectual disability (Waisbren et al. 2007).

Although early diagnosis and dietary treatment prevent the severe impairments associated with untreated PKU, some studies have shown that individuals with early treated PKU (ETPKU) experience significant neurocognitive impairment (Christ et al. 2010). In relation to neuromotor problems, it is unusual for gross motor problems to occur when PKU is diagnosed and treated early (Yalaz et al. 2006), but impairments in fine motor control have also been reported (Moyle et al. 2007).

Screening of PKU in Iran has been ongoing for all newborns since about 2009, and, in the case of diagnosis of PKU, the newborns are placed on an early intervention with a Phe-restricted diet in the reference clinics for PKU follow-up in Tehran, Iran.

Considering the importance of follow-up, and evaluating the consequences of early intervention on developmental status of these children, we decided to prospectively investigate the development of fine and gross motor skills in ETPKU Iranian children using the Peabody Developmental Motor Scale-2 (PDMS-2).

Material and Methods

This cross-sectional analytic study was carried out between 2011 August and 2012 July in the PKU clinics of three children hospitals, Tehran, Iran. The inclusion criteria were neonatal diagnosis of PKU, early and continuous treatment with a phenylalanine-restricted diet (the mean of blood phenylalanine during the most recent 6 months, in three assessments, was 2–6 mg/dL or 120–360 μ mol/L), and 1–4 years of age. The exclusion criteria were any other degenerative, genetic, and metabolic diseases; history of other neuromotor diseases in the family; and neurological, orthopedic, and/or other acquired problems which affect motor development.

Dietary regimens for the children with ETPKU are shown in Table 1.

All children were examined by a pediatrician and if they fulfilled the above criteria were enrolled in the study. A total of 150 children with early and continuously treated PKU had been monitored in reference clinics for PKU follow-up in Tehran, Iran. Seventy children aged 1–4 years were enrolled in the study based on inclusion and exclusion criteria and defined as the case group ($n = 70$). Also, 100 healthy and normal children were matched with

Table 1 Daily amounts of phenylalanine, protein, and calories for children with PKU

Child's age	Phenylalanine (mg per day)	Protein (g per day)	Energy (kcal per day)
1–3 years	200–450	30–35	900–1,800
4–7 years	225–625	35–40	1,300–2,300

this case group for age, randomly selected from four kindergartens in four parts of the Tehran.

Informed consent form was obtained and then the questionnaire, which contains medical history and demographic information of infants, was completed. Finally, two occupational therapists blinded to the history of infants conducted PDMS-2 for each infant. Assessments were performed in the occupational therapy clinic and infants were examined individually.

The PDMS-2 is one of the most commonly used assessments for measuring motor skills of infants and toddlers from birth through age 5 years. For children with special needs, the Peabody Development Motor Scale is one of the most reliable testing instruments used by many professionals as a diagnostic tool for assessing gross and fine motor skills. It has been used in a number of follow-up studies investigating motor skills in the PKU population (Arnold et al. 1998)]. With the PDMS-2, most motor skill dysfunction will be identified. This test is composed of six subtests that assess related motor abilities that develop early in life: Reflexes, Stationary (body control and equilibrium), Locomotion, Object Manipulation, Grasping, and Visual-Motor Integration. Results from these subtests are used to generate the three composite scores: gross motor quotient, fine motor quotient, and total motor quotient, which has a mean of 100 and a standard deviation of 15 (Connolly et al. 2012).

Data Analysis

Two independent samples *t*-test was used to compare the mean fine, gross, and total developmental motor quotients. *P* values less than 0.05 were considered significant. The data were analyzed using the SPSS 16 software.

Results

Study population consisted of case group (ETPKU, $n = 70$) and normal healthy children as a control group ($n = 100$). The mean ages were 28.5 and 29.7 months in PKU and normal children, respectively. Repeated measure analysis was used to assess the stability of the three measures of phenylalanine level. The mean \pm SD of first, second, and third phenylalanine levels were 4.1 ± 1.5 , 4.2 ± 1.3 , and 4.2 ± 1.4 , respectively. The analysis showed that there

Table 2 Growth variables in normal and PKU children

Developmental variables	Normal		PKU		P value
	Mean	SD	Mean	SD	
Head circumference (cm)	49	10	46	2.4	0.049
Height (cm)	93	72	90	9.8	0.692
Weight (kg)	17	12	15	3.6	0.162
Birth head circumference (cm)	36	1	36	1.3	0.733
Birth height (cm)	51	2.6	52	3.8	0.128
Birth weight (gr)	3165	358	3173	507	0.909

Table 3 Comparison the mean fine, gross, and total motor quotients in normal and PKU children

Variable	Normal mean (SD)	PKU mean (SD)	P value
Fine DMQ	96 (11)	86 (10)	< 0.001
Gross DMQ	96 (13)	91 (8)	0.010
Total DMQ	96 (11)	88 (9)	< 0.001

was no significant difference between the mean of phenylalanine level measures at three times ($F = 0.729$, $p = 0.492$).

Table 2 shows the growth variables in PKU and normal children. There were no significant differences in indices of growth at birth between the two groups, with the exception of head circumference ($p = 0.049$).

Table 3 shows that there were significant differences between the two groups in mean fine motor ($p < 0.001$), gross motor ($p = 0.010$), and total motor quotients ($p < 0.001$).

There were significant differences between the mean fine motor quotient and total motor quotient of children less than 24 months of age in the case group in comparison with children equal or older than 24 months of age ($p = 0.014$, $p = 0.019$). Conversely, there were no significant differences between the mean fine motor quotient and gross motor quotient of children less than 24 months of age in the case group in comparison to children equal to or older than 24 months of age ($p = 0.064$) (Table 4). In addition, the correlation between the phenylalanine level and developmental motor quotients showed a negative correlation between fine ($p < 0.001$) and total ($p = 0.001$) DMQs.

Discussion

This study sets out to characterize the motor quotients and compare the fine and gross motor development of ETPKU and normal Iranian children in the age range of 1–4 years.

Table 4 Comparison of the mean fine, gross, and total motor quotients based on age in PKU children

Age	N	Mean	SD	P value	
Fine DMQ	<24 m	26	90	8.7	0.014
	≥24 m	44	84	10.3	
Gross DMQ	<24 m	26	94	8.5	0.064
	≥24 m	44	90	7.2	
Total DMQ	<24 m	26	91	8.6	0.019
	≥24 m	44	86	8.1	

Recent studies showed that although poor neurological outcomes were reported, such as abnormalities in the white matter of the brain, which may compromise brain function in untreated PKU patients (Alvord et al. 1950; Phillips et al. 2001; Anderson et al. 2004), only limited studies address real neurological issues in early and continuously treated PKU patients (Ludolph et al. 1992). Motor problems observed in ETPKU patients include brisk reflexes and tremor that may develop in poorly treated as well as well-treated PKU patients especially after adolescence (Ludolph et al. 1992). On the other hand, in poorly controlled patients, or in those who discontinued the diet in adolescence or adult life, the risk of neurocognitive, emotional, and behavioral dysfunctions and even neurologic complications such as epilepsy, ataxia, tremor, and spasticity may occur more frequently (Janzen and Nguyen 2010; Arnold et al. 1998).

One of the most consistent findings reported through studies of neurocognitive abilities of ETPKU individuals is impairment in executive function (EF) (Christ et al. 2010). Similarly, nonexecutive impairments including slowed information processing speed, motor skill problems, perception and visual–spatial difficulties, language deficits, and memory and learning impairments are found in ETPKU patients (Janzen and Nguyen 2010).

Previous studies reported that gross motor problems were rarely observed when PKU was diagnosed and treated early (Yalaz et al. 2006). Nonetheless, impairments in fine

motor control have been widely reported (Moyle et al. 2007). Some studies have shown correlations between Phe levels and fine motor scores. Arnold et al. found that children with PKU manifested significantly impaired fine motor scores on the Peabody Developmental Motor Scale (Arnold et al. 1998). Gassio et al. reported that individuals with PKU showed significantly poorer fine motor scores than controls on the Purdue test. In both of these studies, there were negative correlations between Phe levels and fine motor scores (Arnold et al. 1998; Gassio et al. 2005). Brandalize et al. mentioned that fine motor scores have also been associated with the early implementation of dietary Phe restriction in children with PKU (Brandalize and Czeresnia 2004). Weglage et al. reported poorer performance for children with ETPKU than control children on measures of arm–hand–finger precision and speed using a motor performance battery, and these deficits were significantly correlated with blood Phe levels (Weglage et al. 1995).

In our study, although both fine and gross motor development of the ETPKU cohort showed significant differences in comparison to normal children, the mean value of gross and fine DMQs showed that these differences were more prevalent in fine DMQ, with less impact on gross DMQ. Furthermore based on the Guide to interpreting PDMS-2 quotient scores in the Peabody examiner's manual, the mean of all DMQs in the ETPKU group were in the range of 80–89. This suggests that the motor development of the ETPKU group was below the average (16 %). On the other hand, the mean of all DMQs in the normal group were in the range of 90–110 which means that motor development of this group was average (50th centile). Finally, we found that the fine and total DMQs of ETPKU children correlated with age. In children less than 24 months, DMQs were significantly higher than the children older than 24 months. This may relate to poor dietary control and variation in the phenylalanine level. Several previous studies have found a relationship between Phe levels and cognitive and executive function (EF). These studies mentioned that concurrent Phe level, lifetime Phe level, and Phe level variability are the best predictors of variation in the current EF performance (Vera et al. 2008).

In conclusion, the key result of our study suggests that motor developmental delay in ETPKU children occurs regardless of following a phe-restricted diet or not. Our studies suggest that developmental screening and follow-up be conducted on all ETPKU infants, and that early intervention be undertaken in children with developmental delays.

Acknowledgment We would like to thank all children with PKU and their parents, and children and all who helped in this study.

Compliance with Ethics Guidelines

Details of the Contributions of Individual Authors

Sepideh Nazi: Conducting, data gathering, and reporting the work

Firoozeh Sajedi: Planning and reporting the work

Akbar Biglarian: Planning and data analyzing

Farzaneh Rohani: Case providing

Arya Setoodeh: Case providing

Firoozeh Sajedi serves as guarantor for this article, accepts full responsibility for the work and/or the conduct of the study, had access to the data, and controlled the decision to publish.

Conflict of Interest

Sepideh Nazi, Firoozeh Sajedi, Farzaneh Rohani, Akbar Biglarian, and Arya Setoodeh declare that they have no conflict of interest.

Details of Funding

The author(s) confirm(s) independence from the sponsors; the content of the article has not been influenced by the sponsors.

Informed Consent

All procedures followed were in accordance with the ethical standards of the responsible committee on human experimentation (institutional and national) and with the Helsinki Declaration of 1975, as revised in 2000 (5). Informed consent was obtained from all patients for being included in the study and is available upon request.

References

- Alvord E, Stevenson L, Vogel F, Engle R (1950) Neuropathological findings in phenylpyruvic oligophrenia (phenylketonuria). *J Neuropathol Exp Neurol* 9:298–310
- Anderson P, Wood S, Francis D, Coleman L, Warwick L, Casanelia S, Anderson V, Boneh A (2004) Neuropsychological functioning in children with early treated phenylketonuria: impact of white matter abnormalities. *Dev Med Child Neurol* 46:230–238
- Arnold GL, Kramer BM, Kirby RS, Plumeau PB, Blakely EM, Sanger Cregan LS, Davidson PW (1998) Factors affecting cognitive, motor, behavioral and executive functioning in children with phenylketonuria. *Acta Paediatr* 87:565–570
- Brandalize SR, Czeresnia D (2004) Evaluation of the program for prevention and health promotion in phenylketonuria patients in Brazil. *Rev Saude Publica* 38:300–306

- Christ SE, Huijbregts SCJ, de Sonnevle LMJ, White DA (2010) Executive function in early-treated phenylketonuria: profile and underlying mechanisms. *Mol Genet Metab* 99:S22–S32
- Connolly BH, McClune NO, Gatlin R (2012) Concurrent validity of Bayley-III and the Peabody Developmental Motor Scale-2. *Pediatr Phys Ther* 24(4):345–352
- Gassio R, Artuch R, Vilaseca MA, Fuste E, Boix C, Sans A, Campistol J (2005) Cognitive functions in classic phenylketonuria and mild hyperphenylalaninaemia: experience in a paediatric population. *Dev Med Child Neurol* 47:443–448
- Hoeksma M, Reijngoud DJ, Pruijm J, de Valk HW, Paans AM, van Spronsen FJ (2009) Phenylketonuria: high plasma phenylalanine decreases cerebral protein synthesis. *Mol Genet Metab* 96:177–182
- Janzen D, Nguyen M (2010) Beyond executive function: non-executive cognitive abilities in individuals with PKU. *Mol Genet Metab* 99:S47–S51
- Koochmeshgi J, Bagheri A, Hosseini-Mazinani SM (2002) Incidence of phenylketonuria in Iran estimated from consanguineous marriages. *J Inherit Metab Dis* 25:80–81
- Ludolph AC, Ullrich K, Nedjat S, Masur H, Bick U (1992) Neurological outcome in 22 treated adolescents with hyperphenylalaninemia. A clinical and electrophysiological study. *Acta Neurol Scand* 85:243–248
- Moyle JJ, Fox AM, Arthur M, Bynevelt M, Burnett JR (2007) Meta-analysis of neuropsychological symptoms of adolescents and adults with PKU. *Neuropsychol Rev* 17:91–101
- Phillips M, McGraw P, Lowe M, Mathews VP, Hainline B (2001) Diffusionweighted imaging of white matter abnormalities in patients with phenylketonuria. *Am J Neuroradiol* 22:1583–1586
- van Spronsen FJ, Hoeksma M, Reijngoud DJ (2009) Brain dysfunction in phenylketonuria: is phenylalanine toxicity the only possible cause? *J Inherit Metab Dis* 32:46–51
- Vera A, Laura K, Peter F, Susan W (2008) Stability of blood phenylalanine levels and IQ in children with phenylketonuria. *Mol Genet Metab* 95:P17–P20
- Waisbren SE, Noel K, Fahrback K, Cella C, Frame D, Dorenbaum A, Levy H (2007) Phenylalanine blood levels and clinical outcomes in phenylketonuria: a systematic literature review and meta-analysis. *Mol Genet Metab* 92:63–70
- Weglage J, Pietsch M, Funders B, Koch HG, Ullrich K (1995) Neurological findings in early treated phenylketonuria. *Acta Paediatr* 84:411–415
- Yalaz K, Vanli L, Yilmaz E, Tokatli A, Anlar B (2006) Phenylketonuria in pediatric neurology practice: a series of 146 cases. *J Child Neurol* 21:987–990

A Novel Large Deletion Encompassing the Whole of the Galactose-1-Phosphate Uridyltransferase (*GALT*) Gene and Extending into the Adjacent Interleukin 11 Receptor Alpha (*IL11RA*) Gene Causes Classic Galactosemia Associated with Additional Phenotypic Abnormalities

Rena Papachristoforou · Petros P. Petrou ·
Hilary Sawyer · Maggie Williams · Anthi Drousiotou

Received: 23 April 2013 / Revised: 10 June 2013 / Accepted: 24 June 2013 / Published online: 4 September 2013
© SSIEM and Springer-Verlag Berlin Heidelberg 2013

Abstract *Objective* The characterization of a novel large deletion in the galactose-1-phosphate uridyltransferase (*GALT*) gene accounting for the majority of disease alleles in Cypriot patients with classic galactosemia.

Methods DNA sequencing was used to identify the mutations followed by multiplex ligation-dependent probe amplification (MLPA) analysis in the cases suspected of harboring a deletion. In order to map the breakpoints of the novel deletion, a PCR walking approach was employed. A simple PCR assay was validated for diagnostic testing for the new deletion. Haplotype analysis was performed using microsatellite markers in the chromosomal region 9p. RT-PCR was used to study RNA expression in lymphoblastoid cell lines.

Results The new deletion spans a region of 8489 bp and eliminates all *GALT* exons as well as the non-translated sequences of the adjacent interleukin 11 receptor alpha (*IL11RA*) gene. In addition, the deletion is flanked by a 6 bp block of homologous sequence on either side suggesting that a single deletion event has occurred, probably mediated

by a recombination mechanism. Microsatellite marker analysis revealed the existence of a common haplotype. The RNA expression studies showed a lack of *IL11RA* transcripts in patients homozygous for the deletion.

Conclusions We have identified and characterized a novel contiguous deletion which affects both the *GALT* enzyme and the *IL11RA* protein resulting in classic galactosemia with additional phenotypic abnormalities such as craniosynostosis, a feature that has been associated with defects in the *IL11RA* gene.

Introduction

Classic galactosemia (OMIM# 230400) is the most common inherited disorder of carbohydrate metabolism resulting in the inability to metabolize galactose by the normal “Leloir” biochemical pathway (Holton et al. 2001). The incidence of classic galactosemia varies in different populations with an average incidence worldwide of 1:62,000 births (Levy and Hammersen 1978; Tyfield et al. 1999). An increased incidence has been reported in Ireland, 1:21,000 (Murphy et al. 1999), and Greece, 1 in 22,000 (Schulpis et al. 1997), and a lower incidence in Japan, 1:1,000,000 (Aoki and Wada 1988).

Classic galactosemia is caused by mutations in the *GALT* gene which encodes the enzyme galactose-1-phosphate uridyltransferase (*GALT*, EC 2.7.7.12) and is inherited in an autosomal recessive fashion (Leslie et al. 1992). The *GALT* gene is located on chromosome 9p13, is arranged into 11 exons, and spans about 4.3 kb of genomic DNA (Shih et al. 1984; Reichardt and Berg 1988; Flach et al. 1990). To date,

Communicated by: Gerard T. Berry, MD

Competing interests: None declared

Electronic supplementary material: The online version of this chapter (doi:10.1007/8904_2013_249) contains supplementary material, which is available to authorized users.

R. Papachristoforou · P.P. Petrou · A. Drousiotou (✉)
Department of Biochemical Genetics, The Cyprus Institute of
Neurology and Genetics, P.O. Box 23462, 1683 Nicosia, Cyprus
e-mail: anthidr@cing.ac.cy

H. Sawyer · M. Williams
Bristol Genetics Laboratory, Southmead Hospital, Bristol, UK

264 variants within the *GALT* gene have been identified according to the entries in the database at the ARUP Institute of Experimental Pathology (http://www.arup.utah.edu/database/GALT/GALT_welcome.php) with about 85 % being pathogenic. Most of the mutations are missense mutations (Calderon et al. 2007) with p.Gln188Arg (c.563A>G) being the most common mutation (64 %) in European populations (Tyfield et al. 1999). The p.Lys285Asn (c.855G>T) mutation is another frequent mutation in European populations with an overall frequency of about 8 %, but, as for the p.Gln188Arg mutation, there are large differences in its relative frequency in different ethnic groups. In many populations it is the second most frequent disease-causing *GALT* mutation, with a frequency in some countries of east and central Europe of 25–40 % (Greber-Platzer et al. 1997; Tyfield et al. 1999; Zekanowski et al. 1999). Together the p.Gln188Arg and p.Lys285Asn mutations account for approximately 70–80 % of classic galactosemia alleles in Caucasian populations (Tyfield et al. 1999). Although classic galactosemia occurs in numerous different countries and ethnic groups worldwide, only a few ethnicity-genotype associations have been established. For example, p.Ser135Leu, a relatively mild mutation, is almost exclusively found in individuals of black African origin (Lai et al. 1996), whereas a complex deletion of 5.5 kb in the *GALT* gene has been strongly linked to patients of Ashkenazi Jewish descent (Berry et al. 2001; Barbouth et al. 2006; Coffee et al. 2006). This large deletion in the *GALT* gene is characterized by the preservation of a segment of 117 bp that contains portions of exon 8 and intron 8 and an additional 12 bp insertion immediately downstream of the exon 8/intron 8 segment (Coffee et al. 2006).

In this study, we identified the mutations responsible for classic galactosemia in the Greek Cypriot population and characterized a novel large deletion that is present in the majority of disease alleles.

Methods

Subjects

Eight Greek Cypriot patients with classic galactosemia (Table 1) and 13 of their parents were studied (two patients were siblings). In addition, ten subjects unrelated to any of the galactosemia patients and found to be carriers were examined. Blood samples were collected after obtaining the approval of the National Bio-ethics Committee for the project and with signed consent.

GALT Enzyme Activity Measurement

Measurement of GALT activity in washed red blood cells was performed using the spectrophotometric method of Kalckar et al. (1956) which is based on UDP-glucose consumption.

PCR Amplification and DNA Sequencing

Patient DNA was isolated from whole blood using the Gentra Puregene Blood Kit (Qiagen), according to the manufacturer instructions. For bidirectional automated sequencing, *GALT* exons were amplified in eight fragments. Primers used for PCR amplification carried an M13 derived tag used for the subsequent cycle sequencing reaction. Sequences of all primers used in this study are listed in [Supplementary Table S1](#). Following PCR amplification, products were treated with ExoSAP enzyme and subjected to a cycle sequencing reaction in 96 well plates using forward and reverse M13 primers (Sigma-Proligo) (M13F: 5'-CACGACGTTGTAACACGAC-3', M13R: 5'-GGA-TAACAATTTACACAGG-3') and BigDye Terminator reagent mix (Applied Biosystems). Sequencing products were subsequently subjected to ethanol (85 %) cleanup using the Beckman Coulter Biomek NX liquid-handling robot. Final elution was in water. All samples were run on an ABI 3730 DNA analyzer (Applied Biosystems). Sequence analysis was performed using Soft Genetics "Mutation Surveyor®" DNA variant software.

Junction Fragment PCR Assay to Exclude a Previously Described Deletion

Patient samples in which none of the 11 exons could be amplified were examined by means of a junction fragment PCR assay for an already described complex deletion of 5.5 kb (Coffee et al. 2006). It is a PCR-based assay using three primers. The additional forward primer anneals to the deleted part; thus, a non-deleted allele results in a 680 bp product in contrast to the allele carrying the 5.5 kb deletion which gives a fragment of 500 bp.

MLPA Analysis

GALT exon copy number was tested using the P156 and P156-B1 SALSA MLPA (multiplex ligation-dependent probe amplification) kits from MRC Holland according to manufacturer instructions (version 11; 02-01-2007). Fragments were analyzed on a Beckman CEQ 8000 capillary analyzer and the raw data were processed using the Coffalyser software (MRC Holland).

Table 1 Clinical, biochemical, and molecular data of Greek Cypriot patients with classic galactosemia

Patient	Sex	Age at diagnosis	Age today	GALT activity ^a ($\mu\text{mol/h/g Hb}$) NR: 18–40	Clinical features at presentation	Clinical picture today	Genotype
1	M	6 months	19 years	1.1	Jaundice, diarrhea, and hypoglycemia	Severe learning difficulties and dyspraxia, behavioral problems	8.5Kb deletion/ p.Lys285Asn
2	M	5 weeks	14 years	0	Jaundice, cataracts, liver disease, ascites, FTT	Severe learning difficulties, poor vision (optic atrophy), microcephaly	Homozygous 8.5Kb deletion
3 ^b	M	7 days	13 years	0	Jaundice, feeding problems, high LFT	Normal neurological and motor development, very good at school	Homozygous p.Lys285Asn
4	F	2 weeks	9 years	4.8	Jaundice, liver disease	Normal neurological and motor development	8.5Kb deletion/ p.Lys285Asn
5	F	3 weeks	7 years	1.9	Jaundice, FTT, high LFT, diarrhea, referred from neonatal screening due to mildly elevated phenylalanine	Normal neurological and motor development	8.5Kb deletion/ p.Lys285Asn
6	F	3 days	7 years	0.05	Jaundice, FTT, high LFT	Craniosynostosis	Homozygous 8.5Kb deletion
7 ^b	M	1 day	3 years	<1.0	NIL	Normal	Homozygous p.Lys285Asn
8	F	13 days	2 years	5.9	Jaundice, FTT, vomiting, palpable liver, ascites, coagulopathy, high LFT	Craniosynostosis	Homozygous 8.5Kb deletion

M male, F female, FTT failure to thrive, LFT liver function test, NR normal range

^aSpectrophotometric method of Kalckar et al.

^bSiblings

Identification of Deletion Breakpoints

In order to map the breakpoints of the novel deletion, a PCR walking approach was employed using DNA samples from the three individuals identified as homozygous by MLPA. At first, the identification of a downstream breakpoint of the deletion was pursued. PCR primers targeting the adjacent *IL11RA* and the genes *CCL21* and *VCP*, located further downstream, were designed. A PCR product was obtained in all samples suggesting that the downstream border is located within the *IL11RA* gene (data not shown). A subsequent series of primer design/PCR steps was performed to narrow down the deleted region (Supplementary Tables S2 and S3). Finally, using the primers DEL-10 F and DEL-9R that anneal 689 bp upstream of the *GALT* ATG start codon and 186 bp downstream of the *IL11RA* ATG, respectively (flanking a region of 10,047 bp), a 1.6 kb PCR product was obtained in homozygous and heterozygous deletion carriers but not in controls. PCR bidirectional sequencing of this PCR product using primers flanking the deletion (Supplementary Table S4) was performed.

Screening for the New Deletion

A simple PCR assay was validated for diagnostic testing for the new deletion. PCR was performed using 0.5 μl AmpliTaq Gold DNA Polymerase (Applied Biosystems), with 1 μl DNA to 50 μl final volume. Three primers were added in the PCR mix: 1.2 μM forward primer DEL-10 F (5'-CCACCTAGATGGTGGCTGGAGCTT), 0.28 μM reverse primer DEL-9R (5'-ACTTACCCGGCAGTCACTCCAGG), and 0.04 μM forward primer DEL-Internal F (5'-GCGCACGCACATGCAAAGCA). The third primer was added to score the presence of the wild-type allele. PCR conditions were 94 °C for 10 min, then 40 cycles (94 °C, 20 sec; 68 °C, 30 sec; 72 °C, 1.5 min), and final extension at 72 °C for 5 min. The expected lengths of PCR amplicons for the deleted and the normal allele are 1.6 kb and 651 bp, respectively.

Haplotype Analysis

We performed haplotype analysis using the following microsatellite markers in the chromosomal region 9p: D9S1788,

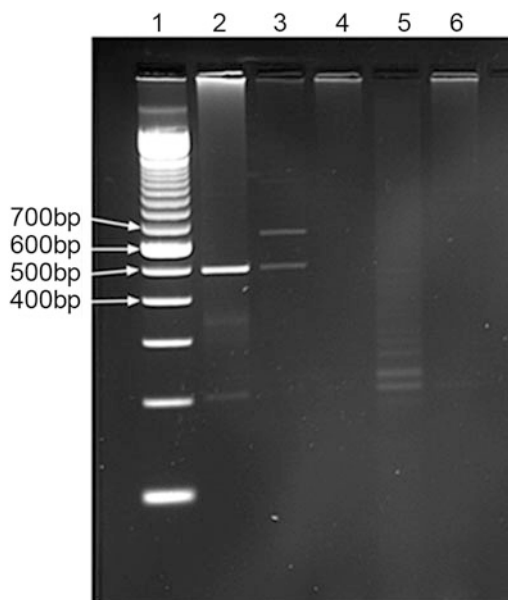


Fig. 1 Agarose gel image of the result of the junction fragment PCR assay for the 5.5Kb deletion described by Coffee et al. Lane 1: 100 bp ladder. Lane 2: homozygote control for the 5.5 kb deletion. Lane 3: heterozygote control for the 5.5 kb deletion. Lanes 4–6: Cypriot patients

D9S1845, D9S165, D9S1878, D9S1817, D9S1805, D9S1804, D9S1791, D9S1859, D9S50, D9S1874, and D9S148. The forward primer for each was labeled with either Cy3 or Cy5 at the 5' end. Primer sequences and amplification conditions for each PCR are shown in [Supplementary Table S5](#). PCR products were analyzed on a Beckman CEQ 8000 capillary analyzer. Haplotypes of individuals were constructed based on the map distance between markers estimated by means of MAP-O-MAT (Kong and Matise 2005), located at <http://compugen.rutgers.edu/mapomat>.

RT-PCR Assay

We studied RNA expression in Epstein-Barr virus (EBV)-transformed lymphoblastoid cell lines derived from two of the patients homozygous for the deletion. RNA extraction was performed using the RNeasy® Midi Kit (Qiagen, Cat. No. 75144) as per manufacturer instructions (Second edition, pages 26–31) and cDNA synthesis was achieved using the ProtoScript® M-MuLV First Strand Synthesis Kit (New England Biolabs, NEB#E6300S) following the

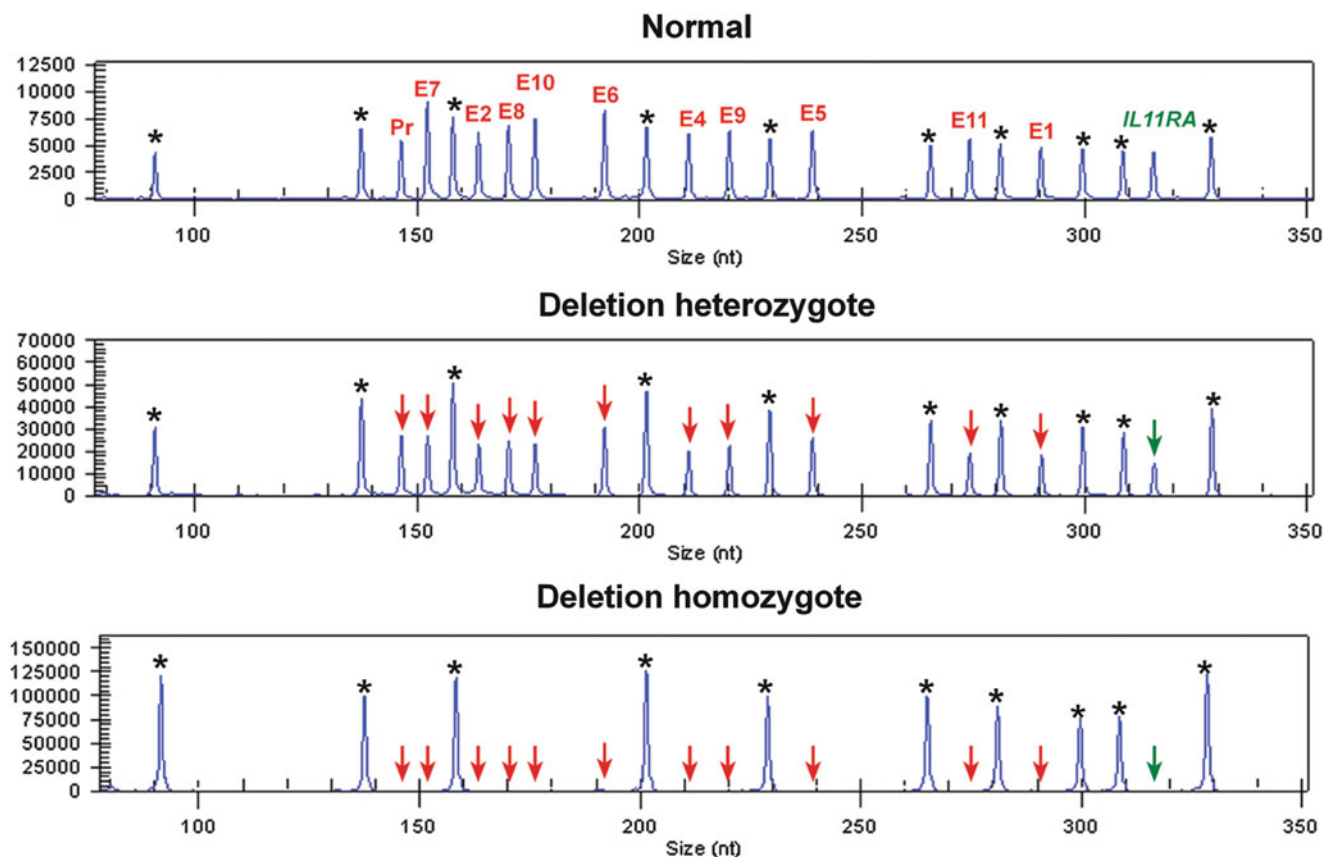


Fig. 2 Traces generated using the SALSA MLPA kit P156 GALT, for a patient homozygous for the new deletion, one of the parents and a normal control. Arrows indicate absent or reduced signal (red arrows

for GALT, green arrows for IL11RA). Exon numbers are shown at the top of the peaks (E1–E11). Reference probes are marked by an asterisk (*)

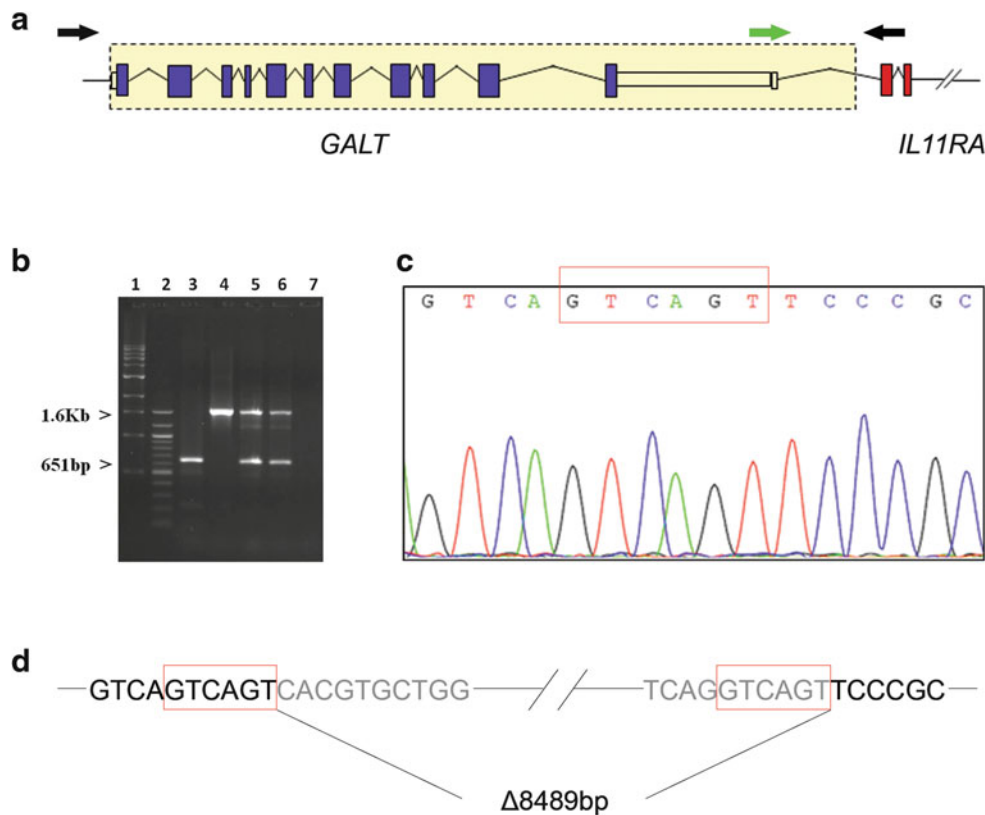


Fig. 3 (a) Schematic representation of the structure of the wild-type *GALT* gene (exons 1–11 are shown in blue) and of the first two exons of the adjacent *IL11RA* gene (red). The black arrows indicate the location of the forward and the reverse primers used for the PCR amplification, and the green arrow indicates the location of a third primer added to score the presence of the wild-type allele. The yellow boxed area includes the deleted part. (b) PCR screening test for the new deletion. 1 % agarose gel image of the PCR assay using three primers: DEL-10 F, DEL-internal F, and DEL-9R. A product of 1.6 kb was obtained for patients homozygous for the new deletion. In the

normal control, a 651 bp product was obtained. In heterozygous carriers both products were obtained. Lane 1: 1 kb ladder. Lane 2: 100 bp ladder. Lane 3: normal control. Lane 4: homozygous patient for the novel 8.5 kb deletion. Lanes 5–6: Heterozygous carriers for the 8.5 kb deletion. Lane 7: blank. (c) Bidirectional sequence analysis of the junction fragment revealed that the deletion spans a region of 8489 bp. (d) Schematic representation of the *GALT* locus indicating the deleted part and showing the presence of a homologous sequence block of six nucleotides GTCAGT (red box) flanking the deletion

manufacturer instructions (Version 1.0). We used primers specific for a region of the *IL11RA* cDNA downstream of the deletion (Supplementary Table S6). A control PCR (of the β -actin housekeeping gene) was used to evaluate sample integrity.

Results

The GALT enzyme level of the eight patients was within the expected range for patients with classic galactosemia, using the spectrophotometric method, $<6 \mu\text{mol/h/gHb}$ (Table 1). Interestingly, the most frequent mutation in Caucasian populations, p.Gln188Arg, was not found in any of the Cypriot patients with classic galactosemia. Two patients (siblings) were found to be homozygous for the p.Lys285Asn mutation and their parents were confirmed to carry the same mutation, while another three patients

appeared to be homozygous for the p.Lys285Asn mutation but only one of their parents carried this mutation. For three patients, none of the 11 exons could be amplified. All the above findings could be explained by the presence of a large deletion covering the whole gene. Patient samples in which *GALT* exons could not be amplified were analyzed for the presence of the previously reported 5.5 kb *GALT* deletion characterized by an intervening complex junction fragment (Coffee et al. 2006). All patients were apparently negative for the 5.5 kb deletion (Fig. 1) suggesting the existence of a novel large *GALT* deletion.

The MLPA results obtained for the three patient samples in which no exon could be amplified confirmed the presence of a large deletion encompassing all exons of the *GALT* gene, as no signal was produced for any of the *GALT* exons (Fig. 2). The parents of these patients were confirmed as deletion carriers. Samples from the three patients apparently homozygous for p.Lys285Asn and three of their

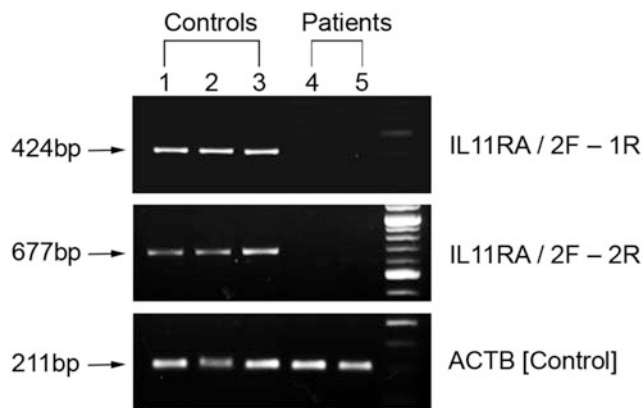


Fig. 4 1.5 % agarose gel image of the RT-PCR assay using two primer sets specific for a region of the *IL11RA* cDNA downstream of the deletion. A product of 677 bp is obtained in the controls but not in the patients. Amplification of the housekeeping gene for β -actin using primers *ACTB* F and *ACTB* R was used as a check on sample integrity. Lanes 1–3: cDNAs from normal controls. Lanes 4–5: cDNAs from two Cypriot galactosemic patients homozygous for the 8.5 kb deletion. Lane 6: 100 bp ladder

parents in whom no mutation was detected by exon sequencing were also analyzed by MLPA and found to be heterozygous carriers of the same deletion. MLPA analysis further indicated lack of amplification of the probe targeted to the 5' non-translated region of the adjacent *IL11RA* gene located 3.5 kb downstream of the *GALT* stop codon (Fig. 2). We repeated the MLPA analysis using the newer version of the MLPA kit (P156-B1), which contains a probe for exon 17 of the upstream gene *DNAIL1*, and found that this probe was amplified in individuals carrying the deletion at comparable levels to normal individuals, indicating that the upstream border of the deletion lies within the 132.5 kb region between *GALT* and exon 17 of *DNAIL1* (Supplementary Fig. S1).

Using a series of primer design/PCR steps, we narrowed down the deleted region until a fragment of 1.6 kb was obtained (Fig. 3b). Bidirectional sequencing of this PCR product using primers flanking the deletion (Supplementary Table S4) revealed that the deletion spans a region of 8,489 bp (Fig. 3c, d). Identical results were obtained for all three patients found to be homozygous for the deletion. Interestingly, the deletion borders were found to be located within a homologous sequence block of six nucleotides (GTCAGT), present on either side, and could not therefore be precisely defined (Fig. 3d). Using the simple PCR screening assay that we validated, the new deletion was found in ten more galactosemia carriers (previously diagnosed in our laboratory). Haplotype analysis of these ten carriers plus the three homozygous patients revealed a common haplotype (Supplementary Fig. S2).

We studied RNA expression in EBV-transformed lymphoblastoid cell lines derived from two of the patients

homozygous for the deletion. A PCR product was amplified in the control but not the patient samples suggesting the lack of *IL11RA* transcripts in the patients (Fig. 4). A control PCR (of the β -actin housekeeping gene) to evaluate sample integrity produced comparable results in the patient samples and the controls (Fig. 4). These findings indicate that the novel deletion simultaneously abrogates the expression of both the *GALT* gene and the adjacent *IL11RA* gene.

Discussion

In this study, eight Greek Cypriot patients with classic galactosemia were characterized at the molecular level. These patients are, to our knowledge, the only patients diagnosed with galactosemia in Cyprus in the last 20 years (approximate number of births in this period 200,000). The most frequent mutation in Caucasian populations, p.Gln188Arg, was not found in any of our patients. Two siblings were found to be homozygous for the p.Lys285Asn mutation, three of the patients were found to be homozygous for a novel large deletion and three of the patients were found to be compound heterozygous for the p.Lys285Asn mutation and the new deletion. The presence of a large deletion on one allele can make the patient appear homozygous for the mutation on the other allele, as was the case in our three patients that were compound heterozygous, and as pointed out by Barbouth et al. as a possible cause of molecular misdiagnosis in galactosemia (Barbouth et al. 2006).

The MLPA results indicated that the new deletion encompasses all *GALT* exons and extends into the adjacent *IL11RA* gene while the upstream limit lies in the 132.5 kb region between the *GALT* gene and exon 17 of the *DNAIL1* gene. We proceeded to identify the deletion breakpoints by a PCR walking approach which revealed that the new deletion spans a region of 8,489 bp and the borders lie approximately 120 bp upstream of the *GALT* ATG and 140 bp upstream of the *IL11RA* ATG start codon. The presence of a homologous sequence of 6 bp flanking the deletion borders (Fig. 3d) may imply that a recombination mediated mutational event is responsible for the occurrence of the deletion. The process of microhomology-mediated end joining (MMEJ) is a repair mechanism for DNA double-strand breaks occurring during cell division and differentiation. Repeated sequences of 5–25 bp flanking the break are recombined following annealing of the complementary strands from each repeated sequence and resulting in deletion of intervening sequences (McVey and Lee 2008).

We performed haplotype analysis on 13 individuals bearing the new deletion, three homozygous and ten heterozygous, all unrelated. A common haplotype was

found in all carriers of the deletion (Supplementary Fig. S2) suggesting a single mutational event for the occurrence of this deletion in Cyprus. Although most individuals bearing the deletion originate from the western part of the island, a more extensive study is required in order to establish whether a cluster exists.

The level of GALT activity in patients homozygous for the new deletion would be expected to be zero since the deletion abolishes the whole of the gene. This was found to be so in two of our patients (0 and 0.05 $\mu\text{mol/h/g Hb}$), but the third patient had a residual activity of 5.9 $\mu\text{mol/h/g Hb}$ (Table 1). This is probably due to the limitations of the spectrophotometric method we used to measure GALT. Use of a more specific and sensitive method like LC-MS/MS (Li et al. 2010) would probably reveal undetectable activity.

A comparison of the clinical phenotype of the galactosemic patients described in this study revealed the presence of additional clinical features in the three patients homozygous for the deletion that have so far not been described in patients with classic galactosemia (Table 1). In particular, one of the patients had microcephaly and optic atrophy and the other two displayed craniosynostosis. One of the patients with craniosynostosis was extensively studied at Great Ormond Street Hospital, London, for mutations in two genes associated with craniosynostosis (*FGFR2* and *FGFR3*), but no mutations in these genes were found. Previous reports implicate mutations in the *IL11RA* gene as being responsible for craniosynostosis (Coussens et al. 2008; Nieminen et al. 2011). Nieminen et al. have shown that IL11 signaling is essential for the normal development of craniofacial bones and teeth and that its function is to restrict suture fusion and tooth number. The same authors identified five causative mutations in the *IL11RA* gene in patients with craniosynostosis of Pakistani and European origin. Given that the downstream border of the deletion found in the Cypriot patients extends up to the non-translated region of *IL11RA*, we addressed the possibility that the identified deletion eliminates the expression of *IL11RA*. The RNA expression studies showed lack of *IL11RA* transcripts in the patients (Fig. 4). These findings strongly suggest that the new deletion simultaneously eliminates *GALT* and *IL11RA* expression (contiguous deletion). Consequently, we attribute the craniosynostosis of our galactosemia patients to a defect in the *IL11RA* gene caused by the new large deletion we have described.

In conclusion, we have described a novel large deletion responsible for classic galactosemia in Greek Cypriot patients which covers the whole of the *GALT* gene and extends into the adjacent interleukin 11 receptor alpha (*IL11RA*) gene. Patients homozygous for this deletion show additional clinical features such as microcephaly and craniosynostosis, which can be attributed to the defect in the *IL11RA* gene.

Acknowledgments We are grateful to:

Dr. Violetta Anastasiadou, Dr. Marianna Kousparou, and Dr. Andreas Hadjidemetriou, from Archbishop Makarios III Children's Hospital in Nicosia, for offering their patients to be included in this study.

Dr. Kyproula Christodoulou, Head of the Department of Neurogenetics of the Cyprus Institute of Neurology & Genetics, for her help regarding haplotype analysis.

Mr. Mark Greenslade and Ms. Sarah Burton-Jones from Bristol Genetics Laboratory, Southmead Hospital, Bristol, for excellent technical support.

We would also like to thank all the children and their parents for participating in this study and for their cooperation.

This work was funded by Telethon Cyprus and by the Cyprus Research Promotion Foundation (Project PENEK/0609/64 was cofinanced by the European Regional Development Fund and the Republic of Cyprus through the Research Promotion Foundation).

Disclosure Statement: The authors declare no conflict of interest.

Synopsis

A novel contiguous deletion eliminates all *GALT* exons as well as the non-translated sequences of the adjacent interleukin 11 receptor alpha (*IL11RA*) gene causing classic galactosemia with additional phenotypic abnormalities such as craniosynostosis.

Compliance with Ethics Guidelines

Conflict of Interest

Rena Papachristoforou, Petros Petrou, Hilary Sawyer, Maggie Williams, and Anthi Drousiotou declare that they have no conflict of interest.

Informed Consent

All procedures followed were in accordance with the ethical standards of the responsible committee on human experimentation (institutional and national) and with the Helsinki Declaration of 1975, as revised in 2000 (5). Informed consent was obtained from all patients for being included in this study.

References

- Aoki K, Wada Y (1988) Outcome of the patients detected by newborn screening in Japan. *Acta Paediatr Jpn* 30(4):429–434
- Barbouth D, Slepak T, Klapper H, Lai K, Elsas LJ (2006) Prevention of a molecular misdiagnosis in galactosemia. *Genet Med* 8(3): 178–182
- Berry GT, Leslie N, Reynolds R, Yager CT, Segal S (2001) Evidence for alternate galactose oxidation in a patient with deletion of the galactose-1-phosphate uridylyltransferase gene. *Mol Genet Metab* 72(4):316–321

- Calderon FR, Phansalkar AR, Crockett DK, Miller M, Mao R (2007) Mutation database for the galactose-1-phosphate uridylyltransferase (GALT) gene. *Hum Mutat* 28(10):939–943
- Coffee B, Hjelm LN, DeLorenzo A, Courtney EM, Yu C, Muralidharan K (2006) Characterization of an unusual deletion of the galactose-1-phosphate uridylyl transferase (GALT) gene. *Genet Med* 8(10):635–640
- Coussens AK, Hughes IP, Wilkinson CR et al (2008) Identification of genes differentially expressed by prematurely fused human sutures using a novel in vivo – in vitro approach. *Differentiation* 76(5):531–545
- Flach JE, Reichardt JK, Elsas LJ 2nd (1990) Sequence of a cDNA encoding human galactose-1-phosphate uridylyl transferase. *Mol Biol Med* 7(4):365–369
- Greber-Platzer S, Guldberg P, Scheibenreiter S et al (1997) Molecular heterogeneity of classical and Duarte galactosemia: mutation analysis by denaturing gradient gel electrophoresis. *Hum Mutat* 10(1):49–57
- Holton JB, Walter JH, Tyfield LA (2001) Galactosemia. In: Scriver CR, Beaudet AL, Sly WS, Valle D (eds) *The metabolic and molecular bases of inherited diseases*, 8th edn. McGraw-Hill, New York, pp 1553–1587
- Kalckar HM, Anderson EP, Isselbacher KJ (1956) Galactosemia, a congenital defect in a nucleotide transferase. *Biochim Biophys Acta* 20(1):262–268
- Kong X, Matisse TC (2005) MAP-O-MAT: internet-based linkage mapping. *Bioinformatics* 21(4):557–559
- Lai K, Langley SD, Singh RH, Dembure PP, Hjelm LN, Elsas LJ 2nd (1996) A prevalent mutation for galactosemia among black Americans. *J Pediatr* 128(1):89–95
- Leslie ND, Immerman EB, Flach JE, Florez M, Fridovich-Keil JL, Elsas LJ (1992) The human galactose-1-phosphate uridylyltransferase gene. *Genomics* 14(2):474–480
- Levy HL, Hammersen G (1978) Newborn screening for galactosemia and other galactose metabolic defects. *J Pediatr* 92(6):871–877
- Li Y, Ptolemy AS, Harmonay L, Kellogg M, Berry GT (2010) Quantification of galactose-1-phosphate uridylyltransferase enzyme activity by liquid chromatography-tandem mass spectrometry. *Clin Chem* 56(5):772–780
- McVey M, Lee SE (2008) MMEJ repair of double-strand breaks (director's cut): deleted sequences and alternative endings. *Trends Genet* 24(11):529–538
- Murphy M, McHugh B, Tighe O et al (1999) Genetic basis of transferase-deficient galactosaemia in Ireland and the population history of the Irish Travellers. *Eur J Hum Genet* 7(5):549–554
- Nieminen P, Morgan NV, Fenwick AL et al (2011) Inactivation of IL11 signaling causes craniosynostosis, delayed tooth eruption, and supernumerary teeth. *Am J Hum Genet* 89(1):67–81
- Reichardt JK, Berg P (1988) Cloning and characterization of a cDNA encoding human galactose-1-phosphate uridylyl transferase. *Mol Biol Med* 5(2):107–122
- Schulpis K, Papakonstantinou ED, Michelakakis H, Podskarbi T, Patsouras A, Shin Y (1997) Screening for galactosaemia in Greece. *Paediatr Perinat Epidemiol* 11(4):436–440
- Shih LY, Suslak L, Rosin I, Searle BM, Desposito F (1984) Gene dosage studies supporting localization of the structural gene for galactose-1-phosphate uridylyl transferase (GALT) to band p13 of chromosome 9. *Am J Med Genet* 19(3):539–543
- Tyfield L, Reichardt J, Fridovich-Keil J et al (1999) Classical galactosemia and mutations at the galactose-1-phosphate uridylyl transferase (GALT) gene. *Hum Mutat* 13(6):417–430
- Zekanowski C, Radomska B, Bal J (1999) Molecular characterization of Polish patients with classical galactosaemia. *J Inher Metab Dis* 22(5):679–682

Successful Desensitisation in a Patient with CRIM-Positive Infantile-Onset Pompe Disease

J. Baruteau · A. Broomfield · V. Crook
N. Finnegan · K. Harvey · D. Burke · M. Burch ·
G. Shepherd · A. Vellodi

Received: 01 May 2013 / Revised: 18 June 2013 / Accepted: 26 June 2013 / Published online: 4 September 2013
© SSIEM and Springer-Verlag Berlin Heidelberg 2013

Abstract Pompe disease (PD) is a severe life-threatening disease in which enzyme replacement therapy (ERT) with alglucosidase alfa is the only treatment available. Recently it has been shown that antibody formation may have a significant adverse effect on response to ERT. We report a cross-reactive immunologic material (CRIM)-positive PD infant who developed severe infusion-associated reactions (IARs) after 15 uneventful months of ERT. We successfully got the child to tolerate the ERT by a desensitisation protocol. We diluted the total amount of standard alglucosidase alfa infusion (20 mg/kg/dose) to 1/100 (0.2 mg/kg/dose). The original infusion rates were maintained. We doubled this dose every week. No premedication was given. In 8 weeks, we reached the standard dose without any IAR. No further reactions have been observed during 6 months of follow-up. Importantly, clinical deterioration that was observed during the period of reduced enzyme delivery has almost completely reversed. We conclude that this

protocol was effective in our patient, while being safe and easy to follow, and may be suitable in selected cases.

Introduction

Pompe disease (Glycogen storage disease type 2, OMIM 230300) is a rare neuromuscular disorder due to defective lysosomal acid alpha-glucosidase. As a result, glycogen accumulates, predominantly in skeletal muscle fibres. The disease encompasses a wide clinical spectrum. Classical infantile-onset Pompe disease (PD) develops skeletal and cardiac myopathy; untreated infants usually die without treatment within the first year of life (van den Hout et al. 2003). Juvenile and adult phenotypes are characterised by a progressive myopathy with little or no hypertrophic cardiomyopathy.

Enzyme replacement therapy (ERT) with recombinant alglucosidase alfa (Myozyme®, Genzyme Corporation, Cambridge, MA) is the only treatment available. This improves cardiomyopathy and muscular weakness, and prolongs lifespan (Nicolino et al. 2009).

The development of IgG specific for alglucosidase ('neutralising' antibody) has been shown to significantly diminish the efficacy of ERT (Banugaria et al. 2011). An important factor determining IgG production is the cross-reactive immunologic material (CRIM) status of the patient (Kishnani et al. 2010). Patients who are CRIM negative are more likely to develop antibodies. CRIM-positive patients can also develop antibodies, albeit normally a more attenuated response, which ultimately tends to be self-resolving (Kishnani et al. 2007). High-sustained antibody titres CRIM-positive patients have a similar poor outcome compared to CRIM-negative patients (Banugaria et al. 2011). Elevated IgG antibody titres are also associated with

Communicated by: Jean-Marie Saudubray

Competing interests: None declared

J. Baruteau (✉) · A. Broomfield · V. Crook · N. Finnegan ·
A. Vellodi

Metabolic Medicine Department, Great Ormond Street Hospital,
London, UK
e-mail: jbaruteau@yahoo.fr

K. Harvey · D. Burke
Metabolic Laboratory, Great Ormond Street Hospital for Children,
Great Ormond Street, WC1N 3JH, London, UK

M. Burch
Cardiology Department, Great Ormond Street Hospital, London, UK

G. Shepherd
Division of Allergy and Immunology, Weill Medical College of
Cornell University, New York, USA

Table 1 Scheme of Alglucosidase alfa desensitisation protocol. Example for a patient of 10 kg

Week	Dilution	Dose	i.e. for 10 kg
–1	1	20 mg/kg	200 mg over 2 h30
1	1/100	0.2 mg/kg	2 mg over 2 h30
2	1/50	0.4 mg/kg	4 mg over 2 h30
3	1/25	0.8 mg/kg	8 mg over 2 h30
4	2/25	1.6 mg/kg	16 mg over 2 h30
5	4/25	3.2 mg/kg	32 mg over 2 h30
6	8/25	6.4 mg/kg	64 mg over 2 h30
7	16/25	12.8 mg/kg	128 mg over 2 h30
8	1	20 mg/kg	200 mg over 2 h30

infusion-associated reactions. Overall, approximately 95 % of patients treated by alglucosidase alfa develop IgG antibodies, 52 % of patients experienced IAR (Nicolino et al. 2009), and amongst them type-I hypersensitivity reactions in 1 %, and severe allergic reactions in 14 % (Lipinski et al. 2009).

We report successful desensitisation in a patient with CRIM-positive Pompe disease who developed IARs associated with IgG antibody to alglucosidase.

Case Report

A female infant was diagnosed at the age of 5 days with Pompe disease. She was the second child of consanguineous parents, born after an uncomplicated antenatal course. The diagnosis was suspected on the basis of a previously affected sibling, and confirmed soon after birth. She was initially slow to feed and required a nasogastric tube. However, this soon resolved completely. Echocardiography showed a mild hypertrophic cardiomyopathy with normal cardiac function. The diagnosis was confirmed by demonstrating deficiency of leukocyte acid alpha-glucosidase activity. Genotyping of the affected sibling had revealed homozygosity for the pathogenic mutations c.1927G>A (pGly643Arg) of the GAA gene: This was predicted to be associated with a positive CRIM status, using a previously described method (Bali et al. 2012). Enzyme replacement therapy (ERT) with Myozyme® (alglucosidase alfa 20 mg/kg/dose) was started at 2 weeks of age, initially weekly for 12 weeks, then fortnightly.

The initial response to ERT was good, with normal growth and development at 1 year of age. Oral feeding was successfully established by 8 weeks. The cardiomyopathy improved as well.

Urinary tetraglucose level decreased rapidly after start of ERT and normalised in 3 weeks (Table 1).

At the age of 15 months, she developed a severe IAR (irritability, coughing, desaturations) until 92 % of arterial saturation of oxygen (SaO₂), florid rashes of the trunk secondary extended to face and limbs, facial swelling, tachycardia with heart rate > 150 bpm, preserved blood pressure) within minutes of commencing an infusion with a rate of 1 mg/kg/h. She continued to have similar IAR with subsequent infusions. Despite various measures such as administration at a slower rate and premedication including chlorphenamine, paracetamol and intravenous methylprednisolone, she continued to react up to a point where she was unable to receive further ERT.

All tests for IgE specific for the enzyme were negative. Plasma tryptase was normal. Complement levels showed normal C3 and initially normal C4 level at 0.17 g/L (normal 0.14–0.54) at the time of the first IAR but C4 decreased 5 months later to a minimum of 0.04 g/L suggestive of an activation of the classical complement pathway. As these levels decreased 3 months after the restart of ERT at a dose of 20 mg/kg, complement activation is unlikely related to the IAR. Her IgG titre specific for the enzyme was elevated at 1/6,400; however, the level was identical 3 months before the IAR and remained at this level after she was desensitised.

After some discussion, an empiric protocol was devised, based on an initial dilution of 1/100 (0.2 mg/kg) of her normal dose (20 mg/kg) for the first infusion administered without premedication in the same volume of fluids as usual (50 mL) and at the same rate of infusion (4 mL/h for 30 min, then 12 mL/h for 30 min, then 20 mL/h for 30 min, then 28 mL/h for the rest of the infusion). The dose was doubled every week. After 8 infusions, the normal dose of Myozyme® was administered without any further reaction (Table 1). It was given weekly for the next 10 weeks to compensate for previous lower dose infusions. The normal fortnightly protocol of 20 mg/kg/dose of alglucosidase infusion was then reinstated without incident.

The interval between the last well-tolerated infusion and return to the normal dose after desensitisation was 18 weeks. During this period, the patient initially showed progressive weakness but then started improving. Cardiac parameters remained stable. After a first increase when ERT was interrupted, urinary tetraglucose has remained mildly elevated (Fig. 1).

During 9 months of follow-up, no further IARs were experienced and home infusions were recommenced. Her motor development progressed steadily and she was able to walk independently at 19 months old. At 20 months old she developed a nystagmus, which revealed a severe myopia with a refractive error of –10 dioptres. This nystagmus improved considerably with appropriate glasses. 4 months after the end of this protocol, IgG titre anti alglucosidase alfa remained unchanged at 1/6,400.

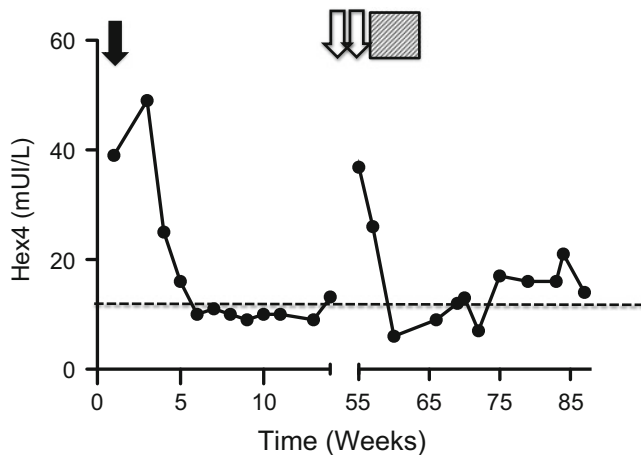


Fig. 1 Hex4 levels. Diagnosis and onset of IAR are indicated by *black* and *white* arrows respectively. Normal range is indicated below the discontinued line. Desensitisation is indicated with the hachured barr

Discussion

We present a patient whose IARs have resolved after the use of a desensitisation programme. The mechanism responsible for IARs is not understood but may be most consistent with release of cytokines. Many symptoms are not consistent with an IgE-mediated mechanism and tests for IgE are usually negative. Likewise, there is no obvious correlation with titres of IgG to the enzyme in the infantile Pompe patients (Burton and Whiteman 2011). Indeed the persistence of the same IgG antibody titres in our patient after resolution of the IARs also argues against these being IgG-mediated responses.

Three approaches to the management of potential IAR to therapeutic proteins in LSDs have been described: standard prevention and management, immunomodulation and desensitisation.

The standard prevention and management uses antihistamines and corticosteroids prophylactically. In case of any potential IAR, these drugs associated with slowing the rate of ERT's infusion, and/or antipyretics were sometimes enough to control IAR and allowed a restart of well-tolerated ERT. Immunomodulation has been successfully used in several patients. The principle of this is prevention/amelioration of the antibody response. The most widely used protocol involves suppression of B lymphocyte response using a combination of rituximab and methotrexate (Messinger et al. 2012) commencing prior to the first dose of enzyme. However this regime results in significant risk of infection secondary to hypogammaglobulinemia (from rituximab) and bone marrow suppression (from methotrexate). There are also unanswered questions about the long-term effects of such immunomodulatory agents.

Reappearance of antibodies following successful initial suppression has been reported: This has been attributed to failure to suppress long-term memory. Some initial success using either conventional immunomodulation (Messinger et al. 2012) or bortezomib has been reported (Banugaria et al. 2013).

Another potential strategy is desensitisation. Desensitisation is the induction of a state of tolerance in a patient hypersensitised to an allergen by increasing sub-therapeutic doses. Classically used for IgE-mediated reactions (hypersensitivity type I), it has been used for drugs non-IgE-mediated hypersensitivity reactions (Cernadas et al. 2010). Despite extensive experience (Castells et al. 2008), the underlying molecular and cellular basis is poorly understood but may involve depletion of allergic mediators, modification of signal transduction, generation of allergen-specific T-regulatory cells inducing of a tolerant state in peripheral T cells or 'blocking' IgG antibodies (Cernadas et al. 2010; Wachholz and Durham 2003; Akdis and Akdis 2007).

As our patient was CRIM positive, it was felt that immunomodulation, with its attendant risks, would be too aggressive. Desensitisation was therefore considered. Various approaches to desensitisation have been attempted. Transient interruption or slower rates of infusions have been successfully attempted in other patients with mucopolysaccharidosis II, VI or Fabry disease (Burton and Whiteman 2011; Bodensteiner et al. 2008; Kim et al. 2008). Desensitisation has been previously described in a child with Gaucher disease (Peroni et al. 2009) and 3 patients with infantile, juvenile and adult forms of PD, respectively (El-Gharbawy et al. 2011; Lipinski et al. 2009). These desensitisation protocols used serial microdilutions of an initial 10 mg/kg/week infusion increasing as tolerated until the every 2 weeks maintenance dose is reached of 20 mg/kg/dose in 6 and 7 weeks, respectively. This has been successfully tried in patients with either IgE positive with low IgG titres or IgE negative with high IgG titres. More than 13 patients have been reported so far. This more rapid desensitisation protocol offers the advantage to a rapid return to normal dosing. However, the protocol is complicated, potentially prone to human error, and often requires an intensive care environment.

The slower desensitisation that we describe avoids these problems. However, the patient is on lower doses of enzyme for a longer period. Our protocol seems also to be safe as our child did not experience any IAR in contrast to the 3 patients described by El-Gharbawy & Lipinski who had IARs including anaphylactic reactions requiring epinephrine injections in 2 patients. These were mixed patients: IgE negative with high IgG antibodies titres (El-Gharbawy et al. 2011) or IgE positive with low IgG antibodies titres (Lipinski et al. 2009). Not all patients may

be able to tolerate this, and so it may not be suitable in every case. Indeed during the 8 weeks of desensitisation, administered doses of enzyme remain under the recommended doses. Despite a quick decrease of Hex4 and clinical improvement of a transient muscle weakness in our patient, we advise to avoid this new protocol for patients with severe symptoms of the disease that could compromise the life prognosis in case of transient worsening.

In our experience, the IgG antibody titre is not modified by desensitisation as reported by Lipinski.

Conclusion

We report the efficacy of a new desensitisation protocol in a CRIM-positive infantile-onset Pompe patient who was previously experiencing serious infusion-associated reactions. The protocol is practical, easy to implement and well tolerated. Experience with larger cohorts is needed to confirm our observations.

References

- Akdis M, Akdis CA (2007) Mechanisms of allergen-specific immunotherapy. *J Allergy Clin Immunol* 119:780–791
- Bali DS, Goldstein JL, Banugaria S et al (2012) Predicting cross-reactive immunological material (CRIM) status in Pompe disease using GAA mutations: lessons learned from 10 years of clinical laboratory testing experience. *Am J Med Genet C Semin Med Genet* 160:40–49
- Banugaria SG, Prater SN, Ng YK et al (2011) The impact of antibodies on clinical outcomes in diseases treated with therapeutic protein: lessons learned from infantile Pompe disease. *Genet Med* 13:729–736
- Banugaria SG, Prater SN, McGann et al (2013) Bortezomib in the rapid reduction of high sustained antibody titers in disorders treated with therapeutic protein: lessons learned from Pompe disease. *Genet Med* 15:123–131
- Bodensteiner D, Scott CR, Sims KB et al (2008) Successful reinstitution of agalsidase beta therapy in Fabry disease patients with previous IgE-antibody or skin-test reactivity to the recombinant enzyme. *Genet Med* 10:353–358
- Burton BK, Whiteman DA (2011) Incidence and timing of infusion-related reactions in patients with mucopolysaccharidosis type II (Hunter syndrome) on idursulfase therapy in the real-world setting: a perspective from the Hunter Outcome Survey (HOS). *Mol Genet Metab* 103:113–120
- Castells MC, Tennant NM, Sloane DE et al (2008) Hypersensitivity reactions to chemotherapy: outcomes and safety of rapid desensitization in 413 cases. *J Allergy Clin Immunol* 122:574–580
- Cernadas JR, Brockow K, Romano A et al (2010) General considerations on rapid desensitization for drug hypersensitivity – a consensus statement. *Allergy* 65:1357–1366
- El-Gharbawy AH, Mackey J, Dearnley S (2011) An individually modified approach to desensitize infants and young children with Pompe disease, and significant reactions to alglucosidase alfa infusions. *Mol Genet Metab* 104:118–122
- Kim KH, Decker C, Burton BK (2008) Successful management of difficult infusion-associated reactions in a young patient with mucopolysaccharidosis type VI receiving recombinant human arylsulfatase B (galsulfase [Naglazyme]). *Pediatrics* 121:e714–e717
- Kishnani PS, Corzo D, Nicolino M et al (2007) Recombinant human acid [alpha]-glucosidase: major clinical benefits in infantile-onset Pompe disease. *Neurology* 68:99–109
- Kishnani PS, Goldenberg PC, Dearnley SL et al (2010) Cross-reactive immunologic material status affects treatment outcomes in Pompe disease infants. *Mol Genet Metab* 99:26–33
- Lipinski SE, Lipinski MJ, Burnette A et al (2009) Desensitization of an adult patient with Pompe disease and a history of anaphylaxis to alglucosidase alfa. *Mol Genet Metab* 98:319–321
- Messinger YH, Mendelsohn NJ, Rhead W et al (2012) Successful immune tolerance induction to enzyme replacement therapy in CRIM-negative infantile Pompe disease. *Genet Med* 14:135–142
- Nicolino M, Byrne B, Wraith JE et al (2009) Clinical outcomes after long-term treatment with alglucosidase alfa in infants and children with advanced Pompe disease. *Genet Med* 11:210–219
- Peroni DG, Pescollderung L, Piacentini GL et al (2009) Effective desensitization to imiglucerase in a patient with type I Gaucher disease. *J Pediatr* 155:940–941
- Van Den Hout HM, Hop W, Van Diggelen OP et al (2003) The natural course of infantile Pompe's disease: 20 original cases compared with 133 cases from the literature. *Pediatrics* 112:332–340
- Wachholz PA, Durham SR (2003) Induction of 'blocking' IgG antibodies during immunotherapy. *Clin Exp Allergy* 33:1171–1174

Heterozygous Mutations in the *ADCK3* Gene in Siblings with Cerebellar Atrophy and Extreme Phenotypic Variability

Lubov Blumkin · Esther Leshinsky-Silver ·
Ayelet Zerem · Keren Yosovich · Tally Lerman-Sagie ·
Dorit Lev

Received: 24 March 2013 / Revised: 29 June 2013 / Accepted: 02 July 2013 / Published online: 19 September 2013
© SSIEM and Springer-Verlag Berlin Heidelberg 2013

Abstract We describe a highly variable clinical presentation of cerebellar ataxia in two sisters. The younger sister demonstrates early onset rapidly progressive cerebellar ataxia accompanied by motor and nonmotor cerebellar features, as well as cognitive decline and psychiatric problems. Mitochondrial respiratory chain enzyme analysis in muscle showed a decrease in complex I + III. Progressive cerebellar atrophy was demonstrated on serial brain MR imaging. Coenzyme Q10 (CoQ10) supplementation, started at the age of 5 years, led to a significant improvement in motor and cognitive abilities with partial amelioration of the cerebellar signs. Discontinuation of this treatment resulted in worsening of the ataxia, cognitive decline, and severe depression.

The older sister, who is 32 years old, has nonprogressive dysarthria and clumsiness from the age of 10 years and MRI reveals cerebellar atrophy.

Exome sequencing identified compound heterozygosity for a known (p. Thr584delACC (c.1750_1752delACC)) and a novel (p.P502R) mutation in the *ADCK3* gene.

Conclusions: Patients with primary CoQ10 deficiency due to *ADCK3* mutations can demonstrate a wide spectrum of clinical presentations even in the same family. It is difficult to diagnose CoQ10 deficiency based solely on the clinical presentation.

Exome sequencing can provide the molecular diagnosis but since it is expensive and not readily available, we recommend a trial of CoQ10 treatment in patients with ataxia and cerebellar atrophy even before confirmation of the molecular diagnosis.

Introduction

The hereditary ataxias are a group of genetic disorders characterized by slowly progressive incoordination of gait and often associated with poor coordination of hands, speech, and eye movements. Cerebellar atrophy frequently occurs (Bird 2012). A recently published 10-year retrospective study on childhood onset cerebellar ataxia revealed that in the group with a known genetic diagnosis, mitochondrial disease was the most common cause of cerebellar atrophy (Al-Maawali et al. 2012). Other studies on childhood ataxias also confirm that a mitochondrial etiology may be the leading cause of the disease (Ramaekers et al. 1997; Steinlin et al. 1998; Finsterer 2009; Boddaert et al. 2010; Terracciano et al. 2012).

Primary CoQ10 deficiency is a rare, autosomal recessive, clinically heterogeneous disorder caused by defects in proteins involved in the coenzyme Q synthesis pathway (Quinzii and Hirano 2011). Five major phenotypes have been described: encephalomyopathy, cerebellar ataxia,

Communicated by: Nicole Wolf, MD PhD

Competing interests: None declared

L. Blumkin · E. Leshinsky-Silver · A. Zerem ·
T. Lerman-Sagie · D. Lev (✉)
Metabolic Neurogenetic Service, Wolfson Medical Center, Holon,
Israel
e-mail: dorlev@post.tau.ac.il

L. Blumkin · A. Zerem · T. Lerman-Sagie
Pediatric Neurology Unit, Wolfson Medical Center, Holon, Israel

E. Leshinsky-Silver · K. Yosovich
Molecular Genetics Laboratory, Wolfson Medical Center, Holon,
Israel

D. Lev
Institute of Medical Genetics, Wolfson Medical Center, Holon, Israel

E. Leshinsky-Silver · T. Lerman-Sagie · D. Lev
Sackler School of Medicine, Tel-Aviv University, Tel-Aviv, Israel

infantile multisystemic form, nephropathy, and isolated myopathy (Emmanuele et al. 2012). Cerebellar ataxia is the most common phenotype. Mutations in the *ADCK3* gene have been associated with the ataxic form of CoQ10 deficiency.

We describe two sisters with a highly variable clinical presentation: severe progressive ataxia, cognitive decline, and psychiatric abnormalities versus only mild dysarthria in whom exome sequencing revealed the same heterozygous mutations in the *ADCK3* gene.

Clinical Reports

Patient 1

The patient, now 20-year-old, presented to our metabolic-neuro-genetic clinic at the age of 19 years due to a slowly progressive cerebellar disease that had started at the age of 2 years and involved motor, cognitive, and psychiatric functions. Parents are healthy non-consanguineous Ashkenazi Jews. She has an older sister (Patient 2) and two healthy siblings. Perinatal history and early development were normal. She started walking at the age of 1 year and spoke in short sentences at the age of 20 months. At the age of 2 years, her parents noticed that her speech became slurred and her gait less stable. She did not gain any new motor skills. Between 3 and 5 years of age, her balance deteriorated and she sustained frequent falls. Neurologic examination at the age of 5 years demonstrated ataxia, dysarthria, and nystagmus. Cognitive decline and mood changes commenced at the age of 5 years. Her general IQ score deteriorated from 85 to 65 between the ages 10 and 18 years with a performance IQ well below the verbal IQ. She attended a special education school since the age of 12 years. At the age of 14 years, major depression was diagnosed and she was treated with antidepressants. She was hospitalized in a psychiatric hospital at the age of 17 years due to depression with suicidal ideation, faulty social judgment, and unbalanced mood.

Evaluation: Brain MRI at the age of 28 months demonstrated mild cerebellar atrophy that markedly progressed by the next MRI performed at 3.6 years of age. In the following MRI scans at age 4 and 8 years, the atrophy described to be stable (MRI not shown). An MRI done at the age of 18 years demonstrated marked cerebellar atrophy (Fig. 1a,b). Metabolic evaluation was unremarkable. Electroretinogram demonstrated rod and cone dysfunction. Visual-evoked potentials, echocardiography, electrocardiogram, electromyography, and nerve conduction studies were normal. A muscle biopsy revealed normal morphology by light and electron microscopy. A decrease in mitochondrial respiratory chain complexes I + III and IV

was demonstrated. Pyruvate dehydrogenase and citrate synthase activities were low. CoQ10 levels were not evaluated.

Molecular Evaluation: Mitochondrial DNA sequencing, genetic testing for SCA1, SCA 2, SCA 3, and sequencing of the *ATM*, *SURF1*, and *APTX* genes were normal.

At the age of 5 years, CoQ10 20 mg/kg/day treatment was started with partial improvement in motor skills, balance, and strength. After 6 years, she gradually stopped taking the medicine on her own and her condition deteriorated.

On examination at the age of 19 years, she was alert and communicative. She had normal weight, height, and head circumference. Her speech was dysarthric but with a good vocabulary and expressive abilities. She aggressively opposed a physical examination. She demonstrated generalized cerebellar dysfunction: horizontal nystagmus with no ophthalmoplegia or oculomotor apraxia, discontinuous pursuit, dysmetria, action tremor, past pointing, abnormal knee heel test, a wide-based ataxic gait, inability to tandem, and difficulties in imitating movements. The BARS (brief ataxia rating scale score) was 8 of 30. She could write a few words in a clear handwriting. The rest of the neurologic exam was normal.

Patient 2

The older sister came to our clinic at the age of 32 years for genetic counseling following her marriage. She described mild dysfluent speech and clumsiness since childhood with no progression. She received a Master of Arts degree and works as a manager. A brain MRI study done at the age of 30 years revealed prominent cerebellar atrophy (Fig. 2a,b). Neurologic exam revealed mild dysarthria but no cerebellar signs.

These two sisters showed a diverse clinical picture of cerebellar disorder due to progressive cerebellar atrophy, with partial response to CoQ10 supplement in the younger sister. The clinical picture was suggestive for autosomal recessive CoQ-related disorder. Although the *ADCK3* gene was the most appropriate one, there are other genes that are associated with CoQ deficiency syndromes. Thus, for cost-benefit reasons, whole exome sequencing was performed.

Methods

Exome Sequencing

Whole exome sequencing was performed on the patients' DNA. The sample was enriched with Sureselect Human All Exome v.2 kit which was targeted 50 Mb (Agilent, Santa Clara, CA, USA). Sequencing was carried out on

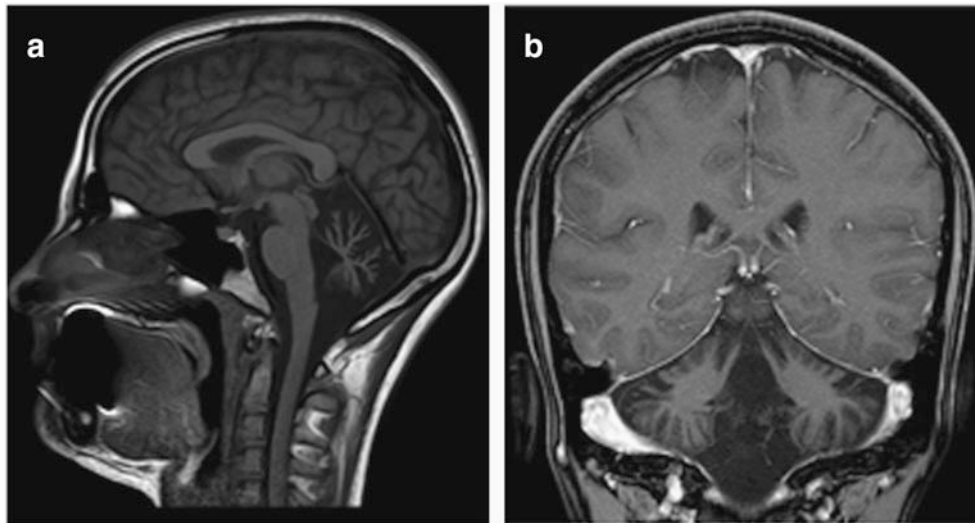


Fig. 1 (a, b) Brain MRI of patient 1 at the age of 18 years. Sagittal T1 image and coronal T1 with contrast image demonstrate prominent cerebellar atrophy most prominent in the vermis

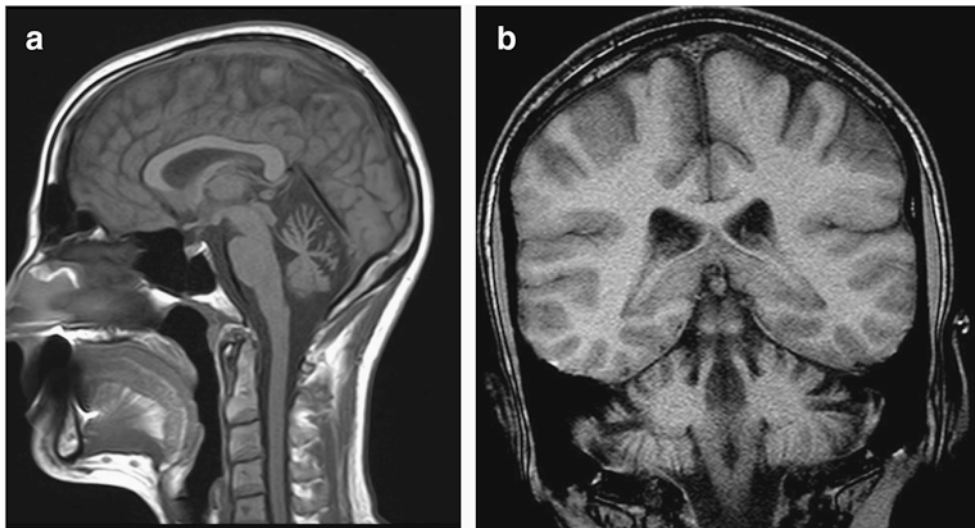


Fig. 2 (a, b) Brain MRI of patient 2 at the age of 30 years. Sagittal and coronal T1 images demonstrate prominent cerebellar atrophy

(Illumina, San Diego, CA, USA) as 100-bp paired end runs. Image analysis and base calling were performed with the Genome Analyzer Pipeline version 1.5 with default parameters. Reads were mapped to the human reference genome sequence (assembly GRCh37/hg19) using the Burrows-Wheeler Alignment Tool (BWA) version 0.5.8c, and allelic variants were detected using the Genome Analysis Toolkit (GATK). Dataset files including the annotated information were analyzed using ANNOVAR according to the dbSNP database (build 135) and the NHLBI exome variant database with the following filtering steps: autosomal recessive inheritance; variant type including missense, nonsense, and splice-site; not within segmental duplications; minor allele frequency (MAF) less

than 0.01; SIFT score < 0.05 when available; PolyPhen2 score > 0.85 when available. Primers for the *ADCK3* mutations were designed using the Primer3 software and Sanger sequencing of PCR products was used to verify the mutations in the patients and their parents.

Results

A total of 21,902 coding variants (single-nucleotide variants and small insertions and deletions) were detected in patient 1 and 21,026 in patient 2; after filtering for population frequencies less than 0.01 and synonymous-frameshift-non frameshift changes –1,458 variants were

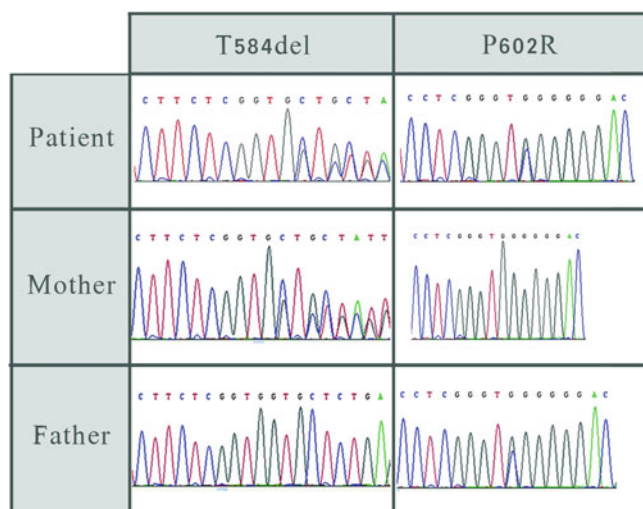


Fig. 3 Sequence electropherogram demonstrating the p. Thr584delACC (c.1750_1752delACC) and p.P502R mutations in patient and her parents

found in patient 1 and 1,500 in patient 2. Homozygous variants-200, none of these in the homozygous region and heterozygous variants-1,200, but only 19 were common in the two patients.

The only candidate gene in the double heterozygous variant list, which segregated with the disease, was *ADCK3*, previously described in association with cerebellar ataxia. The variants were the novel p.P502R substitution and the previously described p. Thr584delACC (c.1750_1752delACC). The father carries the p.P502R mutation and the mother carries the p. Thr584delACC (c.1750_1752delACC) mutation (Fig. 3). The novel p.P502R mutation is predicted to be deleterious according to Polyphen2, SIFT, and Mutation Taster softwares. The P602 is a conserved amino acid.

Discussion

We describe two sisters with an extremely variable clinical presentation who are compound heterozygotes for two mutations in the *ADCK3* gene. The Th584del has been previously described in patients with cerebellar ataxia (Lagier-Tourenne and Tazir 2008), but the P602R mutation is novel (Lagier-Tourenne and Tazir 2008; Mollet et al. 2008; Gerards et al. 2010; Horvath et al. 2012). The pathogenicity of the P602R is supported by a substitution of a neutral amino acid by a basic one, conservation of Proline602 among species and prediction as disease causing by three softwares.

Only 22 patients with *ADCK3*-associated cerebellar ataxia have been reported since the first publications in 2008 (Lagier-Tourenne and Tazir 2008; Mollet et al. 2008; Gerards et al. 2010; Horvath et al. 2012).

A progressive cerebellar ataxia is described in all reported patients. Early psychomotor development is normal in most children but some of them have been described as clumsy with frequent falls during the first 2–3 years of life. The age of onset varies from 18 to 24 months to 15 years. Adult onset has been described in a single case (Horvath et al. 2012). The first presenting symptom is usually loss of balance with later appearance of other cerebellar signs, including limb incoordination, abnormal eye movements, tremor, and dysarthria. Associated symptoms may include seizures, cognitive decline, depression, exercise intolerance, muscle weakness, dystonia, myoclonus, pyramidal signs, ptosis, migraine, swallowing difficulties, reduced vision, peripheral neuropathy, hearing impairment, and cataracts (Horvath et al. 2012).

Brain imaging demonstrates cerebellar atrophy in all patients by the time cerebellar signs are already apparent. Other findings include stroke-like lesions (Mollet et al. 2008), pontine atrophy (Gerards et al. 2010), thin corpus callosum, and ventricular enlargement (Horvath et al. 2012).

Nine families have been described with two to four affected siblings. The clinical presentation is described as similar in eight families (Horvath et al. 2012). One family with four affected siblings has been described with clinical variability: all had ataxia and cerebellar atrophy; age of onset varied from 4 to 11 years, only one had mild mental retardation and two had pyramidal signs (Lagier-Tourenne and Tazir 2008). Our patients demonstrate extreme phenotypic variability: The younger sister has early onset progressive ataxia, cognitive decline, and psychiatric involvement while the older one who is 32 years old only has dysarthria with no ataxia. Both sisters, however, demonstrate cerebellar atrophy on MRI (Figs. 1 and 2).

The pathogenesis of the disease is related to energy deficiency due to a defect in CoQ10 metabolism. CoQ10 is an essential electron carrier in the mitochondrial respiratory chain, transferring electrons from complex I and II to complex III and contributing to ATP biosynthesis. It also has a key role as a free radical scavenger, preventing the progression of lipid peroxidation in membranes or regenerating other antioxidants such as vitamin E or ascorbate in other cellular membranes (Artuch et al. 2006; Montero et al. 2007). Studies in both rats and humans have demonstrated that the lowest brain CoQ content is in the cerebellum (Montero et al. 2007), suggesting that antioxidant defenses are very limited in this brain area, and, consequently mild to moderate CoQ deficiencies might lead to cerebellar dysfunction (Montero et al. 2007).

There is no explanation for the phenotypic variations in the reported patients and no correlation has been found between the degree of mitochondrial dysfunction and the disease severity as demonstrated by serum lactate, mitochondrial morphology in muscle biopsy, or respiratory

chain activity in muscle, fibroblasts, and lymphocytes (Aure and Benoist 2004; Lagier-Tourenne and Tazir 2008; Mollet et al. 2008; Horvath et al. 2012). There must be other factors, either genetic or environmental, that influence the phenotypic expression.

Clinical improvement following CoQ10 supplementation has been documented in many patients. There is no consensus regarding the oral dose for treatment of CoQ10 deficiency, treatment protocols have not been standardized and results have not been uniform. CoQ10 supplementation has been tried in patients with *ADCK3* gene-related ataxia (Lamperti et al. 2003; Aure and Benoist 2004; Mollet et al. 2008; Pineda et al. 2010; Horvath et al. 2012; Emmanuele et al. 2012) in different regimens ranging from 5 to 30 mg/kg/day. Aure et al. reported significant improvement in exercise tolerance and decrease of vomiting episodes under CoQ10 supplementation of 6 mg/kg/day. However, this therapy did not prevent the development of cerebellar atrophy and ataxia. Emmanuele et al. recommend oral supplementation doses of up to 2,400 mg daily in adult patients and up to 30 mg/kg in pediatric patients. Pinedo et al. studied neurologic outcome in patients with CoQ10 deficiency associated cerebellar ataxia after 2 years of treatment with oral CoQ10 supplementation of 30 mg/kg/day regimen. They reported a significant improvement in all patients except in one. The best clinical response among all patients was demonstrated in a patient who showed only mild vermian atrophy (Pineda et al. 2010). All patients with CoQ10 deficiency due to mutations in *ADCK3* gene failed to improve and even worsened under treatment with the shorter chain ubiquinone analog, idebenone (Aure and Benoist 2004; Mollet et al. 2008). Our patient showed improvement in motor and academic activity under oral supplementation of 20 mg/kg daily CoQ10 started at 5 years of age but unfortunately she discontinued treatment and a further deterioration occurred including severe psychiatric involvement. Following the establishment of the molecular diagnosis, both sisters started CoQ10 treatment.

Conclusion

Cerebellar ataxia associated with CoQ deficiency due to *ADCK3* gene mutation may present with a wide spectrum of clinical phenotypes even in the same family, ranging from early onset progressive cerebellar ataxia with cognitive and psychiatric features to nonprogressive mild cerebellar signs accompanied by cerebellar atrophy. Adult onset of cerebellar symptoms may occur.

Clinical improvement under CoQ10 supplementation may be remarkable, but the dosage regimen should be appropriate and the treatment should be started early. Due to the diagnostic difficulties of CoQ deficiency-related

cerebellar ataxia, a therapeutic trial of CoQ10 should be offered to patients with cerebellar ataxia and cerebellar atrophy of unknown origin even before establishing the molecular diagnosis or enzymatic diagnosis.

References

- Al-Maawali A, Blaser S, Yoon G (2012) Diagnostic approach to childhood-onset cerebellar atrophy: a 10-year retrospective study of 300 patients. *J Child Neurol* 27:1121–1132
- Artuch R, Brea-Calvo G, Briones P, Aracil A, Galva'n A, Espinos C, Corral J, Volpini V, Ribes A, Andreu AL, Palau F, Sa'nchez-Alca'zar JA, Navas P, Pineda M (2006) Cerebellar ataxia with coenzyme Q10 deficiency: diagnosis and follow-up after coenzyme Q10 supplementation. *J Neurol Sci* 246:153–158
- Aure K, Benoist JF, Ogier de Baulny H, Romero NB, Rigal O, Lombe's A (2004) Progression despite replacement of a myopathic form of coenzyme Q10 defect. *Neurology* 63:727–729
- Bird TD (2012) Hereditary ataxia overview. In: Pagon RA, Bird TD, Dolan CR, Stephens K, Adam MP (eds) *GeneReviews™* [Internet]. University of Washington, Seattle, 28 Oct 1993–1998 [updated 2012 Nov 01]
- Boddaert N, Desguerre I, Bahi-Buisson N et al (2010) Posterior fossa imaging in 158 children with ataxia. *J Neuroradiol* 37(4):220–230
- Emmanuele V, López LC, Berardo A, Naini A, Tadesse S, Wen B, D'Agostino E, Solomon M, DiMauro S, Quinzii C, Hirano M (2012) Heterogeneity of coenzyme Q10 deficiency: patient study and literature review. *Arch Neurol* 69(8):978–983
- Finsterer J (2009) Mitochondrial ataxias. *Can J Neurol Sci* 36:543–553
- Gerards M, van den Bosch B, Calis C et al (2010) Nonsense mutations in *ADCK3* cause progressive cerebellar ataxia and atrophy. *Mitochondrion* 10:510–515
- Horvath R, Czermin B, Gulati S et al (2012) Adult-onset cerebellar ataxia due to mutations in *CABC1/ADCK3*. *J Neurol Neurosurg Psychiatry* 83:174–178
- Lagier-Tourenne C, Tazir M (2008) Lo'pez LC, et al. *ADCK3*, an ancestral kinase, is mutated in a form of recessive ataxia associated with coenzyme Q10 deficiency. *Am J Hum Genet* 82:661–672
- Lamperti C, Naini A, Hirano M et al (2003) Cerebellar ataxia and coenzyme Q10 deficiency. *Neurology* 60:1206–1208
- Mollet J, Delahodde A, Serre V et al (2008) *CABC1* gene mutations cause ubiquinone deficiency with cerebellar ataxia and seizures. *Am J Hum Genet* 82:623–630
- Montero R, Pineda M, Aracil A, Vilaseca MA, Briones P, Sa'nchez-Alca'zar JA, Navas P, Artuch R (2007) Clinical, biochemical and molecular aspects of cerebellar ataxia and Coenzyme Q10 deficiency. *Cerebellum* 6(2):118–122
- Pineda M, Montero R, Aracil A et al (2010) Coenzyme Q(10)-responsive ataxia: 2-year treatment follow-up. *Mov Disord* 25(9):1262–1268
- Quinzii CM, Hirano M (2011) Primary and secondary CoQ10 deficiencies in humans. *Biofactors* 37:361–365
- Ramaekers VT, Heimann G, Reul J et al (1997) Genetic disorders and cerebellar structural abnormalities in childhood. *Brain* 120(Pt 10):1739–1751
- Steinlin M, Blaser S, Boltshauser E (1998) Cerebellar involvement in metabolic disorders: a pattern-recognition approach. *Neuroradiology* 40(6):347–354
- Terracciano A, Renaldo F, Zanni G et al (2012) The use of muscle biopsy in the diagnosis of undefined ataxia with cerebellar atrophy in children. *Eur J Paediatr Neurol* 16(3):248–256

Clinical Presentation and Positive Outcome of Two Siblings with Holocarboxylase Synthetase Deficiency Caused by a Homozygous L216R Mutation

T.P. Slavin · S.J. Zaidi · C. Neal · B. Nishikawa · L.H. Seaver

Received: 01 May 2013 / Revised: 30 June 2013 / Accepted: 02 July 2013 / Published online: 13 September 2013
© SSIEM and Springer-Verlag Berlin Heidelberg 2013

Abstract *Purpose* The L216R mutation, seen in individuals of Polynesian descent, is considered one of the most severe mutations associated with holocarboxylase synthetase (HLCS) deficiency and is regarded as being unresponsive to biotin. This report describes the presentation and outcome in two surviving siblings, homozygous for this highly lethal mutation.

Methods and results Both cases had perinatal head imaging findings of brain hemorrhage and subependymal cysts. Both had metabolic decompensation within 24 h after birth consisting of metabolic acidosis, lactic acidosis, and thrombocytopenia. Biochemical profiles were consistent with HLCS deficiency, and genetic analysis confirmed homozygosity for the L216R mutation. After resolution of neonatal metabolic crisis, dosing of biotin was titrated on an outpatient basis to primarily control dermatitis. The eldest is currently on 1.2 g of oral biotin daily, well above any dose previously reported to treat HLCS deficiency. To date, neither patient has required hospital readmission for acute metabolic decompensation. At the age of 7, the eldest child is, to our knowledge, the oldest patient ever described in the literature who is homozygous for the L216R mutation. She has mild intellectual disability.

Conclusion This report contrasts previous reports of poor outcomes and neonatal deaths in homozygous L216R patients. We also provide data on the potential upper tolerable limit of biotin. These cases suggest that the outcome of HLCS deficiency due to a homozygous L216R mutation, when diagnosed and treated early with high-level neonatal care and biotin, may not be as severe as previously reported.

Introduction

Biotin is a water-soluble vitamin found in foods such as liver, milk, and egg yolk. Natural occurring D (+)-biotin is not synthesized by mammals and must be acquired by exogenous sources (Suormala et al. 1998). The adequate intake for adults is 30 µg/day. To date, sufficient data has not been collected to establish a tolerable upper intake level (Institute of Medicine (US) Standing Committee on the Scientific Evaluation of Dietary Reference Intakes and its Panel on Folate, Other B Vitamins, and Choline 1998). Biotin acts as a cofactor for five human carboxylase enzymes: acetyl-CoA carboxylase 1 and 2, pyruvate carboxylase, propionyl-CoA carboxylase, and 3-methylcrotonyl-CoA carboxylase (Bailey et al. 2008). If biotin metabolism is disturbed, these enzymes are affected leading to a disruption of normal cellular function (Mayende et al. 2012). The enzyme holocarboxylase synthetase (HLCS) is important for binding biotin to these enzymes.

Mutations in *HLCS* are responsible for HLCS deficiency (HLCS deficiency; OMIM #253270), a rare heritable disease transmitted in an autosomal recessive pattern. Many patients with HLCS deficiency present in the neonatal period with poor feeding, respiratory distress, lethargy, vomiting, hypotonia, seizures, and coma (Morrone et al.

Communicated by: Gregory Enns

Competing interests: None declared

T.P. Slavin · S.J. Zaidi · C. Neal · B. Nishikawa · L.H. Seaver
Department of Pediatrics, University of Hawai'i John A. Burns School of Medicine, Honolulu, HI, USA

T.P. Slavin · C. Neal · B. Nishikawa · L.H. Seaver
Kapi'olani Medical Specialists, Kapi'olani Medical Center for Women and Children, Honolulu, HI, USA

T.P. Slavin (✉)
Hawaii Community Genetics, 1441 Kapi'olani Blvd., STE 1800,
Honolulu 96814, HI, USA

2002). Skin findings can be particularly severe and include facial and full body erythrodermic dermatitis, hyperkeratosis, and diffuse non-scarring alopecia (Esparza et al. 2011). Laboratory abnormalities may include metabolic and/or lactic acidosis, organic acidemia, mild hyperammonemia, and variable hypoglycemia (Morrone et al. 2002). HLCS deficiency can lead to repeated bouts of metabolic decomposition, developmental delay, and is a potentially fatal condition if left untreated (Morrone et al. 2002, Dupuis et al. 1999).

With oral daily biotin supplementation (10–20 mg), most cases of HLCS deficiency can be successfully treated (Bailey et al. 2008; Dupuis et al. 1999). Untreated cases or patients who display an incomplete response to biotin supplementation, however, have a poor long-term prognosis (Bailey et al. 2008; Dupuis et al. 1999). Of the many discrete gene mutations, errors between amino acids 159 and 314 in the N terminal extension outside of the biotin-binding domain of HLCS are believed to be the most severe mutations and are considered biotin unresponsive (Mayende et al. 2012). The L216R mutation is seen in individuals of Polynesian ancestry. It causes one of the most severe forms of HLCS deficiency. Individuals homozygous for this mutation are considered biotin unresponsive, and the homozygous mutation is associated with high infant mortality (Bailey et al. 2008; Morrone et al. 2002; Wilson et al. 2005). In the first case report of a homozygous L216R patient, it was unclear if there was any clinical response on 100 mg/day of biotin (Morrone et al. 2002). At the age of 2, the patient had severe full body eczema with global developmental delay and deafness. This child was reported to have died at age 3 years in a later report (Wilson et al. 2005). Wilson et al. also describe another six homozygous L216R patients from a family of seven affected children. Four of these children died between the ages of 3 days and 3 years, one had a good recovery after birth, but had recurrent infections and metabolic acidosis at 18 months on 40–80 mg of biotin daily, and one was lost to follow-up at age 18 months (Wilson et al. 2005). Bailey et al. (2008) studied fibroblasts from two of the above patients. The fibroblast K_m in their study could not be differentiated from negative controls and the mutant HLCS enzyme was found to have a faster turnover rate than that of the wild-type enzyme (Bailey et al. 2008). Other studies have also demonstrated that the L216R mutant has a biotin ligase activity near zero (Esaki et al. 2012).

In contrast to these patients with biotin unresponsiveness, patients heterozygous for a biotin-unresponsive allele and a biotin-responsive allele show good clinical response to biotin therapy between 20 and 40 mg/day (Dupuis et al. 1999). The favorable outcome is attributed to the presence of the biotin-responsive allele.

The purpose of this report is to present the clinical course of two siblings homozygous for the L216R mutation, a 7-year-old female and a 5-month-old male. The eldest is the longest surviving case for this severe mutation reported in the literature. Both are doing well on very large doses of biotin, much larger than any previously reported.

Subjects, Methods, and Results

Case 1

A female was born to an 18-year-old Samoan/Tongan primigravida and her 19-year-old Samoan/German partner. The pregnancy was complicated by maternal thrombocytopenia. The mother received a diagnosis of idiopathic thrombocytopenic purpura (ITP) at the age of 12 years and had been treated intermittently with corticosteroids, including during the pregnancy. The mother presented in labor at 34–6/7 weeks' gestation after premature rupture of membranes. She had an uncomplicated spontaneous vaginal delivery. The birth weight was 2,262 g, the length was 44.5 cm, and the occipitofrontal circumference (OFC) was 36 cm. Apgar scores were 5 and 7, at 1 and 5 min, respectively. The infant had poor respiratory effort and tone. In the newborn intensive care unit (NICU), the infant's initial course was complicated by a large subgaleal hematoma, thrombocytopenia, and coagulopathy with an initial platelet count of $36,000 \times 10^9/L$ with elevated prothrombin time, partial thromboplastin time, and fibrin degradation products, and a low fibrinogen. Computed tomography (CT) of the head on day 1 of life revealed moderate bilateral intraventricular hemorrhages, left cerebellar hemorrhage, acute subdural hemorrhage of the posterior cerebellum and left occipital lobe, diffuse hypodensity in the cerebral white matter, and bilateral subgaleal hemorrhage. Brain magnetic resonance imaging (MRI) on day 3 confirmed the CT scan findings. A diffusion scan showed small cortical infarctions in the occipital, left temporal, and inferior right frontal lobes. Periventricular cysts were noted. She was treated with intravenous immunoglobulin (IVIG) for the first 4 days of life and required multiple platelet, fresh frozen plasma, and cryoprecipitate transfusions.

Persistent metabolic acidosis was noted. The serum lactic acid was 11.4 mmol/L on day of life (DOL) 10. Initial qualitative urine organic acids showed a complex pattern considered to be consistent with HLCS deficiency. Biotinidase activity could not be reported on the newborn screening due to the transfusions, but was eventually normal. Total and free carnitines were low (2.2 and 12.7 $\mu\text{mol/L}$, respectively), with an elevated acyl/free ratio



Fig. 1 Images of neonatal dermatitis. (a) The dermatitis in Case 1 in early infancy, showing the significant skin denudation and erythematous rash. (b) The dermatitis in Case 2 in early infancy after neonatal discharge from the hospital

of 4.8. An acylcarnitine profile revealed an abnormal elevation of propionylcarnitine and 3-hydroxyisovalerylcarnitine, supporting the diagnosis of HLCS deficiency. Plasma amino acids on DOL 10 revealed numerous elevations including leucine (973 nmol/mL), isoleucine (413 nmol/mL), valine (980 nmol/mL), and the presence of alloisoleucine (24 nmol/mL), thought to be secondary derangements. Holocarboxylase synthetase activity was performed on lymphocytes and showed an elevated K_m of 30.6 nmol/L (reference range 1.0–7.8), with maximum velocity (V_{max}) of 187 fmol/mg/h compared to simultaneous control K_m of 7.28 nmol/L and V_{max} of 222 fmol/mg/h. HLCS gene sequencing documented homozygosity for a c.647T>G (L216R) mutation.

Biotin, at a dose of 10 mg/day, and carnitine were started on DOL 10. She developed a significant erythematous rash in the diaper area (Fig. 1a) that progressed over time to involve her intertriginous regions. Neutropenia was noted at 3 weeks of age with an absolute neutrophil count of 328, which gradually improved. Cholestasis was also noted at 3 weeks of age, associated with hepatomegaly and a liver palpable 4 cm below the right costal margin. Direct hyperbilirubinemia improved, but at 7–8 weeks of age, she had elevated liver transaminases and acholic stools. She was treated with ursodiol and vitamins A, D, E, and K without improvement. A liver biopsy was consistent with giant cell hepatitis with bile duct hyperplasia. A hepatobiliary iminodiacetic acid (HIDA) scan showed no excretion. The intraoperative cholangiogram, however, was normal, and her cholestasis gradually resolved. The postoperative course was complicated by possible seizures. She had no further recurrence of seizure-like activity and phenobarbital therapy was weaned over time and discontinued.

The biotin dose was gradually increased to control dermatitis. Her most recent daily maximum dose was 1.2 g/day (25 mg/kg/day) of a biotin powder compounded with carboxymethyl cellulose powder, simple syrup, and sterile water to make a 5 mg/mL oral solution; no specific solubility was sought by the pharmacy. She has had improvement in her rash on this higher dose of biotin, with only minimal chronic rash remaining around her eyes (Fig. 2). Carnitine at 50–100 mg/kg/day has been continued. No dietary restrictions were recommended, except avoidance of prolonged fasting. Propionylcarnitine (6.5–10 umole/L, reference range 0.08–1.77) and 3-hydroxyisovalerylcarnitine (0.36–0.82 umole/L, reference range 0.01–0.11), when checked at ages 6 and 7 years, remained elevated above clinical baseline. There was no persistence of elevated branch chain amino acids. Serious metabolic decompensation did not recur. She received early intervention services due to her high-risk status, although her early motor and language milestones were within normal limits. Speech delay was noted at age 5 years. She repeated kindergarten and qualified for special education services upon entering grade 1, however, neurodevelopmental testing results are unavailable. Formal audiology testing at age 5 revealed only conductive hearing loss, secondary to cerumen impaction. When last seen at 7½ years of age, her height was at the 75th centile for age, with a weight of 44.5 kg (>97th centile for age), and an OFC of 55 cm (>97th centile).

Case 2

The prenatal course was complicated by abnormal ultrasound findings including fetal ventriculomegaly and possible brain hemorrhage first noted at 27 weeks.



Fig. 2 Case 1 at age 2 years. Note the persistent rash at the outer canthi bilaterally

Subependymal cysts were additionally noted on follow-up fetal MRI. During this pregnancy, the mother had normal platelet counts and no evidence of ITP. Prenatal diagnosis by molecular testing for the L216R mutation was declined. Due to the risk of recurrent HCLS deficiency, and based on the limited available information on biotin use for at-risk pregnancies (Suormala et al. 1998; Thuy et al. 1999), it was recommended that the mother take 10 mg/day of biotin, although she only took it during the last week prior to delivery. A male infant was born at 40 weeks gestation by normal vaginal delivery. The infant initially had poor respiratory effort but responded well to continuous positive airway pressure. Apgar scores were 7 and 9.

In the first few hours of life, the infant began having respiratory distress and petechiae were noted on the face, torso, and limbs. Complete blood count was obtained revealing a platelet count of $26,000 \times 10^9/L$. The infant was transferred to the NICU, where initial blood pH was

7.1. Initial lactate level was 18 mmol/L, which slowly decreased over the first week of life. Given the family history of HCLS, oral biotin was started on DOL 1 at 25 mg/kg/day divided three times daily. A carnitine profile collected on DOL 2 showed an elevated propionylcarnitine level of 20.56 $\mu\text{mol/L}$ (reference range 0.07–14.85) as well as an elevated 3-hydroxyisovalerylcarnitine of 1.23 $\mu\text{mol/L}$ (reference range 0.01–0.07). Free carnitine was depleted with an elevation in acyl/free ratio. Oral levocarnitine was started at 50 mg/kg/day.

A mild intertriginous rash, without skin breakdown, was noted throughout the NICU stay. The thrombocytopenia persisted and IVIG was given two times requiring multiple platelet transfusions (5 total). Platelet counts and biochemical status improved and the infant was discharged on DOL 34 on biotin 40 mg/kg of compounded (as above) 5 mg/ml oral solution divided twice daily, and levocarnitine 50 mg/kg/day. Molecular analysis confirmed L216R homozygosity. Enzyme assay was not performed.

As an outpatient, biotin was increased to 60 mg/kg/day divided twice daily to control dermatitis (Fig. 1b), he also remained on carnitine. No dietary restrictions were recommended except avoidance of prolonged fasting. At 5 months, no major developmental delays were noted.

Discussion

These siblings, affected with a severe form of HCLS deficiency due to a homozygous L216R mutation, presented within hours of birth with thrombocytopenia and metabolic acidosis. Both cases had perinatal CNS findings and brain hemorrhage. Ventriculomegaly and subependymal cysts have been reported previously in cases homozygous for the L216R mutation (Wilson et al. 2005). Hemorrhage may have been a result of fetal thrombocytopenia. The generalized acidosis and accumulation of organic acids during episodes of severe metabolic imbalance have been postulated to account for the neonatal thrombocytopenia sometimes seen in HCLS (Roth et al. 1980; Briones et al. 1989). However, the thrombocytopenia in this family is also complicated by the maternal history of ITP and possible bleeding disorder that has never been fully evaluated. Although, there was no maternal thrombocytopenia or significant bleeding disorder noted during the second pregnancy, this could have been a confounding factor in both cases, especially since the IVIG seemed to stabilize the platelet counts.

These siblings have required very large doses of biotin but are doing well with normal growth and only mild cognitive delays in the oldest girl. The dose of 25 mg/kg/day (1.2 g/day) of biotin in the eldest child, to control

dermatitis, is sixfold above the daily reported maximum dosing of up to 200 mg/day previously reported in the literature to treat biotin deficiency due to any underlying cause (Institute of Medicine (US) Standing Committee on the Scientific Evaluation of Dietary Reference Intakes and its Panel on Folate, Other B Vitamins, and Choline 1998; Bailey et al. 2008; Morrone et al. 2002; Wilson et al. 2005). The risk of human toxicity from the usual dietary intake of biotin or from supplements appears to be low and no tolerable upper intake level has been determined (Institute of Medicine (US) Standing Committee on the Scientific Evaluation of Dietary Reference Intakes and its Panel on Folate, Other B Vitamins, and Choline 1998). In our experience, high-dose biotin titration clearly improves the dermatitis. Anecdotally, when the eldest sibling goes days without biotin, her periocular rash significantly worsens. Although no pharmacokinetic data was collected on the siblings, it was postulated that at least four times per day dosing would be desirable based on the rapid clearance studies and estimated 1 h and 50 min half-life of biotin (Bitsch et al. 1989). However, two times daily dosing was chosen to improve compliance.

This report provides documentation about the natural history and the potential positive outcomes in patients with HLCS deficiency due a homozygous L216R mutation when treated with high-dose oral biotin, avoidance of fasting, and carnitine supplementation. More research will need to be completed on HLCS deficiency with special attention to prenatal diagnosis and biotin therapy. Pregnancies at risk for severe HLCS deficiency can be monitored by prenatal ultrasound with close attention given to CNS findings. Prenatal diagnosis and maternal biotin therapy can be considered. Evaluation of the affected or at-risk neonate may need to include special attention to the platelet count, cranial imaging studies, and prompt treatment of any metabolic derangements. The dose of biotin should be minimally optimized to prevent metabolic decompensation and control dermatitis, but ideally should try to maximize the long-term developmental outcome.

Acknowledgments We would like to thank the family and all of the laboratory and medical personnel involved in the care of these children. We would like to particularly thank Dr. Wade Kyono, the hematologist involved in their care.

Synopsis

This report provides documentation about the natural history and potential positive outcomes in two patients with HLCS deficiency due a homozygous L216R mutation when treated with high-dose oral biotin.

Compliance with Ethics Guidelines

Conflict of Interest

Thomas Slavin, Syed Zaidi, Charles Neal, Brenda Nishikawa, and Laurie Seaver declare that they have no conflict of interest.

Contributions by Authors

Thomas Slavin and Laurie Seaver were the metabolic clinicians involved in the care of the siblings and primary writers of the report. Charles Neal provided neonatal care and assisted with report editing and the discussion of IVIG therapy. Syed Zaidi helped care for Case 2 as a neonate and assisted with the background research. Brenda Nishikawa was the children's pediatrician and helped edit this report for overall accuracy.

Informed Consent

Patients described in this case report were treated with standard medical care. Proper consent was obtained for inclusion of the patients in this case report. This report was reviewed by Hawai'i Pacific Health and was found to meet the definition of a case report and is in compliance with applicable research and patient privacy regulations. Additional informed consent was obtained for all patients for whom identifying information is included in this report.

References

- Bailey LM, Ivanov RA, Jitrapakdee S, Wilson CJ, Wallace JC, Polyak SW (2008) Reduced half-life of holocarboxylase synthetase from patients with severe multiple carboxylase deficiency. *Hum Mutat* 29:E47–57
- Bitsch R, Salz I, Hotzel D (1989) Studies on bioavailability of oral biotin doses for humans. *Int J Vitam Nutr Res* 59:65–71
- Briones P, Ribes A, Vilaseca MA, Rodriguez-Valcarcel G, Thuy LP, Sweetman L (1989) A new case of holocarboxylase synthetase deficiency. *J Inher Metab Dis* 12:329–330
- Dupuis L, Campeau E, Leclerc D, Gravel RA (1999) Mechanism of biotin responsiveness in biotin-responsive multiple carboxylase deficiency. *Mol Genet Metab* 66:80–90
- Esaki S, Malkaram SA, Zemleni J (2012) Effects of single-nucleotide polymorphisms in the human holocarboxylase synthetase gene on enzyme catalysis. *Eur J Hum Genet* 20:428–433
- Esparza EM, Golden AS, Hahn SH, Patterson K, Brandling-Bennett HA (2011) What syndrome is this? Infantile periorificial and intertriginous dermatitis preceding sepsis-like respiratory failure. *Pediatr Dermatol* 28:333–334
- Institute of Medicine (US) Standing Committee on the Scientific Evaluation of Dietary Reference Intakes and its Panel on Folate,

- Other B Vitamins, and Choline (1998) Dietary reference intakes for Thiamin, Riboflavin, Niacin, Vitamin B6, Folate, Vitamin B12, Pantothenic Acid, Biotin, and Choline. National Academies Press (US), Washington (DC)
- Mayende L, Swift RD, Bailey LM, Soares da Costa TP, Wallace JC, Booker GW, Polyak SW (2012) A novel molecular mechanism to explain biotin-unresponsive holocarboxylase synthetase deficiency. *J Mol Med (Berl)* 90:81–88
- Morrone A, Malvagia S, Donati MA et al (2002) Clinical findings and biochemical and molecular analysis of four patients with holocarboxylase synthetase deficiency. *Am J Med Genet* 111:10–18
- Roth KS, Yang W, Foremann JW, Rothman R, Segal S (1980) Holocarboxylase synthetase deficiency: a biotin-responsive organic acidemia. *J Pediatr* 96:845–849
- Suormala T, Fowler B, Jakobs C et al (1998) Late-onset holocarboxylase synthetase-deficiency: pre- and post-natal diagnosis and evaluation of effectiveness of antenatal biotin therapy. *Eur J Pediatr* 157:570–575
- Thuy LP, Belmont J, Nyhan WL (1999) Prenatal diagnosis and treatment of holocarboxylase synthetase deficiency. *Prenat Diagn* 19:108–112
- Wilson CJ, Myer M, Darlow BA et al (2005) Severe holocarboxylase synthetase deficiency with incomplete biotin responsiveness resulting in antenatal insult in samoan neonates. *J Pediatr* 147:115–118

No Mutation in the *SLC2A3* Gene in Cohorts of GLUT1 Deficiency Syndrome–Like Patients Negative for *SLC2A1* and in Patients with AHC Negative for *ATP1A3*

C. Le Bizec · S. Nicole · E. Panagiotakaki · N. Seta · S. Vuillaumier-Barrot

Received: 11 June 2013 / Revised: 4 July 2013 / Accepted: 5 July 2013 / Published online: 4 September 2013
© SSIEM and Springer-Verlag Berlin Heidelberg 2013

Abstract The facilitative glucose transporter-1 (GLUT1) deficiency or de Vivo syndrome is a rare neuropediatric disorder characterized by drug-resistant epilepsy, acquired microcephaly, delayed psychomotor development, intermittent ataxia, and other paroxysmal neurological disorders due to the presence of dominant mutations in the *SLC2A1* gene. Alternating hemiplegia of childhood (AHC) is another rare neuropediatric disorder characterized by episodes of hemiplegia developing during the first 1.5 years of life. Before the recent finding of the gene *ATP1A3*

as the major cause of AHC, a heterozygous missense mutation in the *SLC2A1* gene encoding GLUT1 was described in one child with atypical AHC, suggesting some clinical overlap between AHC and GLUT1 deficiency syndrome (GLUT1DS1). Half of patients with symptoms evocative of GLUT1DS1 with hypoglycorrachia and up to 25 % of patients with AHC remain molecularly undiagnosed. We investigated whether mutations in *SLC2A3* encoding GLUT3, another glucose transporter predominant in the neuronal cell, may account the case of a cohort of 75 *SLC2A1* negative GLUT1DS1-like patients and seven patients with AHC who were negative for *ATP1A3* and *SLC2A1* mutations. Automated Sanger sequencing and qPCR analyses failed to detect any mutation of *SLC2A3* in the patients analyzed, excluding this gene as frequently mutated in patients with GLUT1DS1 like or AHC.

Communicated by: Daniela Karall

Competing interests: None declared

C. Le Bizec · N. Seta · S. Vuillaumier-Barrot
Assistance Publique-Hôpitaux de Paris, Hôpital Bichat-Claude Bernard, Biochimie, Paris, France
e-mail: CLebizec@aol.com; nathalie.seta@bch.aphp.fr

S. Nicole
Centre de Recherche de l'Institut du Cerveau et de la Moelle épinière, Université Pierre et Marie Curie-Paris 6, UMR-S975, Paris, France
e-mail: sophie.nicole@upmc.fr

S. Nicole
INSERM, U975, Paris, France

S. Nicole
CNRS, UMR 7225, Paris, France

E. Panagiotakaki
Service Epilepsie, Sommeil, Explorations Fonctionnelles Neurologiques Pédiatriques, Hôpital Femme Mère Enfant, University Hospitals of Lyon (HCL), Lyon, France
e-mail: eleni.panagiotakaki@chu-lyon.fr

N. Seta
Université Paris Descartes, Paris, France
e-mail: nathalie.seta@bch.aphp.fr

S. Vuillaumier-Barrot (✉)
INSERM, U773, CRB3, Paris, France
e-mail: sandrine.vuillaumier@bch.aphp.fr

Abbreviations

AHC	Alternating hemiplegia of childhood
CSF	Cerebrospinal fluid
ENRAH	European Network for Research on Alternating Hemiplegia
GLUT1	Glucose transporter-1
GLUT1DS1	GLUT1 deficiency syndrome-1
GLUT1DS2	GLUT1 deficiency syndrome-2
PED	Paroxysmal exercise-induced dyskinesia

Introduction

Glucose transporter protein 1 (GLUT1) deficiency or de Vivo syndrome (GLUT1DS1 OMIM#606777) is a rare severe neurological disease with hypoglycorrachia due to impaired

glucose transport across the blood–brain barrier of capillary endothelial cells (Leen et al. 2010). This syndrome classically presents with encephalopathy with drug-resistant epilepsy, acquired microcephaly, delayed psychomotor development, intermittent ataxia, and other paroxysmal neurological disorders. Abnormal movements, such as chorea of the extremities or paroxysmal dyskinesia induced by exercise, are sometimes observed in isolation without epilepsy (PED) (GLUT1DS2: OMIM#612126). Dominant mutations in *SLC2A1* encoding GLUT1 are found in only 20 % of patients with symptoms evocative of GLUT1 deficiency, suggesting the implication of other genes (Klepper and Leidencker 2007).

Alternating hemiplegia of childhood (AHC, OMIM#104290) is another rare neurodevelopmental disorder. Six clinical criteria are to be considered for the diagnosis of AHC and include: (1) onset of paroxysmal events before 18 months of age; (2) repeated attacks of hemiplegia lasting from a few minutes to several days and involving either side of the body; (3) episodes of bilateral hemiplegia or quadriplegia; (4) other paroxysmal disturbances occurring during hemiplegic bouts or in isolation; (5) immediate disappearance of symptoms upon sleep; and (6) developmental delay and nonparoxysmal neurologic abnormalities such as dystonia, ataxia, cognitive impairments, and epileptic events in up to 50 % of patients (Panagiotakaki et al. 2010).

Dominant mutations in *ATPIA3*, encoding the Na⁺/K⁺-ATPase α 3 subunit, recently emerged as the major cause for AHC since they account for more than 74 % of AHC cases according to studies (Heinzen et al. 2012; Rosewich et al. 2012). Moreover, dominant mutations in the *SLC1A3*, *CACNA1A*, and *ATPIA2* genes, respectively, encoding the glutamate transporter EAAT1, the α 1 pore-forming subunit of the calcium channel Cav2.1, and the α 2 subunit of the Na⁺/K⁺ ATPase pump, were first found as causing atypical cases of AHC (Jen et al. 2005; de Vries et al. 2008; Bassi et al. 2004). Interestingly, a *SLC2A1* mutation was found in one child fulfilling all criteria for AHC diagnosis except delayed age at onset of symptoms, hypoglycorrhachia, and deceleration of head growth not usually found in AHC but clinical criteria for GLUT1 deficiency (Rotstein et al. 2009). This case suggests some clinical overlap between AHC and GLUT1 deficiency syndrome. However, *SLC2A1* mutations were later excluded in a large cohort fulfilling all the criteria for AHC diagnosis, including seven patients studied here without mutations later found in *ATPIA3* (Vuillaumier-Barrot et al. 2011).

GLUT3 (encoded by the *SLC2A3* gene) is the predominant glucose transporter expressed by neuronal cells and has not yet been associated with disease in humans. *SLC2A3* and *SLC2A1* are not equally distributed in brain: *SLC2A1* is

expressed in glial cells and *SLC2A3* in neuronal cells. Homozygous GLUT3-null mice are embryonic lethal, whereas heterozygous (GLUT3 +/-) mice display epilepsy and autistic behavior with stereotypies (Zhao et al. 2010). These observations suggest that GLUT3 may be associated with a dominant neurological disease in humans. In this report, we questioned the occurrence of *SLC2A3* mutations in *SLC2A1* negative GLUTDS1-like patients with epilepsy and mental retardation with or without hypoglycorrhachia, and in patients with typical AHC without mutation in *ATPIA3* or *SLC2A1*.

Methods

Patients

Eighty-two patients with a neurodevelopmental disorder molecularly undiagnosed were studied: 75 GLUTDS1-like patients with epilepsy who were negative for *SLC2A1* and seven patients with typical AHC and no mutations in the *ATPIA3* and *SLC2A1* genes. AHC patients, all previously described (Vuillaumier-Barrot et al. 2011), were included in the European Network for Research on Alternating Hemiplegia Registry (ENRAH) from which clinical data were extracted (Panagiotakaki et al. 2010). Collections were undertaken with the informed consent of patients and their legal representative in accordance with the relevant bioethics legislation.

Table 1 summarizes the clinical data of the 75 GLUT1DS1-like patients. All the patients presented with epilepsy (pharmacoresistant in 16 patients, and early onset epilepsy before 4 years for at least 44 patients), associated with abnormal movements in 15 patients and behavioral autism-like symptoms in seven patients. Four familial cases (dominant inheritance) were studied. The average age at the request of GLUT1DS1 molecular diagnosis was 7 years (1 month to 29 years). The ratio of cerebrospinal fluid (CSF)/plasma glucose concentrations was documented for 36 patients and was reported to be <0.5 for 16 patients (44 %) and >0.5 for 20 patients (56 %). A positive ketogenic diet response was observed for four patients.

The seven AHC patients tested were clinically representative of the French cohort of AHC and fulfilled all the criteria for AHC diagnosis (Vuillaumier-Barrot et al. 2011). All had a paroxysmal event before the age of 18 months. Two suffered from at least one epileptic seizure (Table 2).

Molecular Study

Genomic DNA was isolated from blood samples using standard phenol-chloroform procedures or Qiacube kit (Qiagen, Valencia, CA). *SLC2A3* was analyzed by automated

Table 1 Clinical description of the 75 GLUT1DS1-like patients

Clinical and biological data	Number of patients
Sporadic/familial	71/4
H/F	41/32
Age	1 month to 29 years (mean 7 years)
Microcephaly	5 (7 %)
Epilepsy (absences or myoclonies)	75 (100 %)
Pharmacoresistance	16 (21 %)
Early onset epilepsy (before 4 years)	44 (59 %)
Ketogenic diet positive response	4 (5 %)
Ataxia	6 (8 %)
Paroxysmic dyskinesia	11 (15 %)
Autistic behavior	7 (9 %)
CSF/blood glucose <0.5 (n = 36)	16 (44 %)
CSF/blood glucose >0.5 (n = 36)	20 (56 %)

Table 2 Clinical description of the seven patients with AHC

Clinical and biological data at last examination	Number of patients
H/F	3/4
Age at last examination in years (mean)	7.5–52 (19.4)
Age at first paroxysmic events in months (mean)	1–14 (4.2)
Age at first plelegic attack in months (mean)	3–36 (9.8)
Repeated bouts of hemiplegia	7 (100 %)
Episodes of bilateral hemiplegia	5/5 (100 %, 2 unknown)
Abnormal eye movements	7 (100 %)
Disappearance upon sleep	6/6 (100 %)
Dystonia	6 (86 %)
Ataxia	7 (100 %)
Dysarthria	6 (86 %)
Seizures	0 (0 %)
Developmental delay	7 (100 %)
Autonomic dysfunction	7 (100 %)
CSF/blood glucose	Normal in 4 cases (not tested in other cases)

Sanger sequencing using the BigDye v3.1 reaction mix and the ABI 3130 capillary sequencer after polymerase chain reaction (PCR) amplification of the 10 *SCL2A3* exons and intron–exon boundaries using AmpliTaq Gold (Applied Biosystems, Carlsbad, California). Large deletions were searched in 35 patients without heterozygous SNPs using qPCR on two exons (exon 2 and 9). The GenBank

[NM_006931] sequence was used as the reference. SNP data were obtained from dbSNP (<http://www.ncbi.nlm.nih.gov/projects/SNP/>) and frequency from Caucasian population-based databases (HapMap CEU population/CEPH). All primer sequences and PCR conditions are available upon request. Pathogenicity of unknown missense variant was assessed using five prediction software programs: Polyphen (<http://genetics.bwh.harvard.edu/pph/>), Panther (<http://www.pantherdb.org/tools/csnpscoreForm.jsp>), SIFT2 (<http://blocks.fhrc.org/sift/SIFT.html>), SNPs3D (<http://www.snps3d.org/>), and Align GVGD (http://agvgd.iarc.fr/agvgd_input.php).

Results

Sequencing the 10 exons of *SLC2A3* in the 82 patients revealed five variants known as polymorphisms and two unknown variants in the heterozygous state: c.163T>A (p.Ser55Thr) in exon 3 in one GLUT1DS1-like patient and c.966 +100T>C in intron 7 in one patient with AHC (Table 3). This intronic variant was found to be inherited by the unaffected mother, which excluded its pathogenicity. The Ser55 residue is not conserved between species. The p.Ser55Thr variant is predicted as nonpathogenic by four prediction softwares (Polyphen, SIFTV2, Panther, and SNPs3D) out of the five used. Align GVGD was the only one to predict that this variant could most likely interfere with function (class C55). Unfortunately, parent samples were not available to determine whether this variant was inherited.

Fifty-six patients were heterozygous for known SNPs. Twenty-six patients had no heterozygous SNPs and therefore might have a gene deletion in the heterozygous state resulting in haploinsufficiency. We therefore performed qPCR on two exons of the gene (exon 2 and 9) to determine whether their homozygous status was due to large-scale deletion. None of the 26 samples were found to harbor any copy number variation.

Discussion

Clinical and metabolic arguments led us to search mutations in GLUT3 in patients with epilepsy, mental retardation, or AHC. The analysis of 82 patients excluded *SLC2A3*, encoding GLUT3, as a major mutated gene in GLUT1DS1 and AHC.

The classical presentation of GLUT1DS1 includes intractable epilepsy developing in infancy with delayed development, ataxia, dystonia, and low CSF but normal serum glucose (hypoglycorrachia). All types of *SLC2A1* mutations have been reported in GLUT1DS1, including hemizygoty due to

Table 3 Variants identified in the 82 patients (75 GLUT1DS1-like patients and 7 AHC) screened for *SLC2A3* mutation

Gene location	Sequence change	Protein change	SNP ID (dbSNP)	Number of heterozygous alleles/164	Number of homozygous alleles/164	Number of total alleles/164	Observed frequency of minor allele	Known frequency of HapMap CEU population
Exon 3	c.163T>A	p.Ser55Thr	Unknown	1	0	1	0.6 %	Unreported
Intron 3	c.269+36A>G	?	rs2541279	27	3	33	20.1 %	27 %
Exon 6	c.774A>G	p.Leu258=	rs17847967	18	5	28	17.1 %	15.8 %
Intron 7	c.966+100T>C	?	Unknown	1	0	1	0.6 %	Unreported
Intron 8	c.1069-65T>C	?	rs741361	39	7	53	32.3 %	36 %
Intron 9	c.1273+131G>A	?	rs9668489	21	60	141	17.1 %	10.4 %
Exon 10	c.1308C>T	p.Thr436=	rs25684	38	20	78	47.5 %	40 %

large-scale genomic deletions (Leen et al. 2010). In our laboratory, the molecular screening of *SLC2A1*, including sequencing all coding exons and intron–exon junction, and searching for large deletion by MLPA identified a mutation in only 22 % of patients with GLUT1DS1-like presentation. Moreover, half of the GLUT1DS1-like patients with documented hypoglycorrhachia from our series had *SLC2A1* mutation, a result similar to Leen et al. who found *SLC2A1* mutations in 41 % of their 132 requests for *SLC2A1* analysis (Leen et al. 2010). These negative *SLC2A1* cases could be due to another presently unknown genetic defect, reversible transient glucose transport defect (Klepper et al. 2003), or even other nonidentified causes such as infectious, traumatic, some antiepileptic drugs (phenobarbital, valproate sodium). Elevated blood glucose level due to stress hyperglycemia, tested after lumbar puncture, may also result in lowered CSF/blood glucose ratio and so, to misdiagnosis. Alternatively, some *SLC2A1* mutated patients have been described with normoglycorrhachia, rendering this criteria not absolute for GLUT1-DS diagnosis (Mullen et al. 2010; Suls et al. 2008). One case of atypical AHC has been associated with a missense mutation in *SLC2A1*, which suggests clinical overlaps between the two pathologies (Vuillaumier-Barrot et al. 2011). The seven AHC patients included in our analysis were typical ones, fulfilling all criteria for typical AHC diagnosis but did not display *ATPIA3* mutation, the major cause of typical AHC. We hypothesized that *SLC2A3* could be a candidate in some of these AHC patients as for GLUT1DS1-like patients with or without hypoglycorrhachia. The commonly accepted “astrocyte–neuron shuttle hypothesis” (Pellerin and Magistretti 2011) that describes energy metabolism at the cellular level in the brain would predict that patients with *SLC2A3* mutations may suffer from normal to high CSF glucose levels rather than hypoglycorrhachia as for *SLC2A1* mutated patients. Autistic features are not a characteristic of GLUT1DS or AHC, which shows on the contrary a happy outgoing behavior, but it was suspected to be a feature of human GLUT3 deficiency as heterozygous GLUT3-null mice (GLUT3 +/-) display epilepsy and autistic behavior with stereotypies. In our GLUT1DS1-like cohort, seven patients on 75 had behavioral autism-like disorders.

Therefore, we studied *SLC2A3* and sequencing the 10 exons of *SLC2A3* did not reveal any obvious changes except five variants known as polymorphisms and two unknown benign variants in the heterozygous state. The observed frequency of known polymorphisms was close to that observed in the Caucasian population-based databases (HapMap CEU population/CEPH). One unknown missense variation (p.Ser55Thr) was observed in the heterozygous state in one patient with GLUT1DS1-like phenotype. Serine 55 is neither conserved between species nor among the class I GLUT transporters (GLUT1 to GLUT4), and p.Ser55Thr

was predicted as nonpathogenic by four prediction softwares, which arguments for its benign status. Heterozygous large gene deletion was also excluded, either by observation of heterozygosity or quantitative PCR.

Taken together, our results indicate that *SLC2A3* is not a major gene accounting for GLUT1DS1-like phenotype without *SLC2A1* mutations or typical AHC negative for *ATP1A3* and *SLC2A1*. The absence of known human pathology associated with GLUT3 could be related to the presence of GLUT6 and GLUT8 glucose transporters in neurons (that may supplement GLUT3). This is also consistent with the fact that GLUT3 haploinsufficiency in mice do not display any decrease in brain glucose utilization as determined by fluorodeoxyglucose micro-PET (Stuart et al. 2011). Furthermore, it is commonly reported that glucose utilization is more important in astrocytes than in neurons (Bouzier-Sore et al. 2006). An in vivo study has even shown that the brain prefers lactate over glucose as an energy substrate when both substrates are available (Wyss et al. 2011).

Candidate genes involved in other parts of cerebral energetic metabolism could be considered at least for GLUT1DS1-like, such as genes encoding molecules that modulate the expression of GLUT1: transcription factors, genes involved in posttranslational modifications like glycosylation or phosphorylation and other energy substrate transporters. An actual promising way to find new mutated genes is the high throughput sequencing approach, either exome or whole genome sequencing. Both AHC and GLUT1 deficiency syndromes occur de novo, which will facilitate the search for new genes in our cohorts by performing trio analyses, that is, comparing the sequence of the index case to the sequence of the two parents.

Acknowledgments We thank all the participating families and physicians. We thank the ENRAH for SMEs consortium supported by grant (LSSM-CT-2005-516513 ENRAH for SMEs) of the European Commission Research Programme FP6, especially its validation committee, for the clinical validation on the patients with AHC. This work was funded by “*La fondation Jerome Lejeune*”, *l’association française contre les myopathies* (AFM), and “*l’association française de l’hémiplégie alternante de l’enfant*” (AFHA).

Competing Interest

None declared

Synopsis

No mutation found in the *SLC2A3* gene in cohorts of 75 GLUT1 deficiency syndrome-like patients negative for

SLC2A1 and in seven patients with AHC negative for *ATP1A3* and *SLC2A1*.

Conflict of Interest

C Le Bizec, S Nicole, E Panagiotakaki, N Seta, and S Vuillaumier-Barrot declare that they have no conflict of interest.

Informed Consent

All procedures followed were in accordance with the ethical standards of the responsible committee on human experimentation (institutional and national) and with the Helsinki declaration of 1975, as revised in 2000.

Informed consent was obtained from all patients for being included in the study.

Details of the Contributions of Individual Authors

C Le Bizec did the work (technical results). S Nicole, E Panagiotakaki, N Seta, and S Vuillaumier-Barrot planned, conducted, and reported the work.

References

- Bassi MT, Bresolin N, Tonelli A et al (2004) A novel mutation in the ATP1A2 gene causes alternating hemiplegia of childhood. *J Med Genet* 41(8):621–628
- Bouzier-Sore AK, Voisin P, Bouchaud V, Bezancon E, Franconi JM, Pellerin L (2006) Competition between glucose and lactate as oxidative energy substrates in both neurons and astrocytes: a comparative NMR study. *Eur J Neurosci* 24(6):1687–1694
- de Vries B, Stam AH, Beker F et al (2008) CACNA1A mutation linking hemiplegic migraine and alternating hemiplegia of childhood. *Cephalalgia* 28(8):887–891
- Heinzen EL, Swoboda KJ, Hitomi Y et al (2012) De novo mutations in ATP1A3 cause alternating hemiplegia of childhood. *Nat Genet* 44(9):1030–1034
- Jen JC, Wan J, Palos TP, Howard BD, Baloh RW (2005) Mutation in the glutamate transporter EAAT1 causes episodic ataxia, hemiplegia, and seizures. *Neurology* 65(4):529–534
- Klepper J, Leiendecker B (2007) GLUT1 deficiency syndrome—2007 update. *Dev Med Child Neurol* 49(9):707–716
- Klepper J, De Vivo DC, Webb DW, Klinge L, Voit T (2003) Reversible infantile hypoglycorrhachia: possible transient disturbance in glucose transport? *Pediatr Neurol* 29(4):321–325
- Leen WG, Klepper J, Verbeek MM et al (2010) Glucose transporter-1 deficiency syndrome: the expanding clinical and genetic spectrum of a treatable disorder. *Brain* 133(Pt 3): 655–670
- Mullen SA, Suls A, De Jonghe P, Berkovic SF, Scheffer IE (2010) Absence epilepsies with widely variable onset are a key feature of familial GLUT1 deficiency. *Neurology* 75(5):432–440
- Panagiotakaki E, Gobbi G, Neville B et al (2010) Evidence of a non-progressive course of alternating hemiplegia of childhood:

- study of a large cohort of children and adults. *Brain* 133(Pt 12): 3598–3610
- Pellerin L, Magistretti PJ (2011) Sweet sixteen for ANLS. *J Cereb Blood Flow Metab* 32(7):1152–1166
- Rosewich H, Thiele H, Ohlenbusch A et al (2012) Heterozygous de-novo mutations in ATP1A3 in patients with alternating hemiplegia of childhood: a whole-exome sequencing gene-identification study. *Lancet Neurol* 11(9):764–773
- Rotstein M, Doran J, Yang H, Ullner PM, Engelstad K, De Vivo DC (2009) Glut1 deficiency and alternating hemiplegia of childhood. *Neurology* 73(23):2042–2044
- Stuart CA, Ross IR, Howell ME et al (2011) Brain glucose transporter (Glut3) haploinsufficiency does not impair mouse brain glucose uptake. *Brain Res* 1384:15–22
- Suls A, Dedeken P, Goffin K et al (2008) Paroxysmal exercise-induced dyskinesia and epilepsy is due to mutations in SLC2A1, encoding the glucose transporter GLUT1. *Brain* 131(Pt 7):1831–1844
- Vuillaumier-Barrot S, Panagiotakaki E, Le Bizec C, El baba C, The ENRAH for SME consortium, Fontaine B, Arzimanoglou A, Seta N, Nicole S (2011) Absence of mutation in SLC2A21 gene in a cohort of patients with alternating hemiplegia of childhood (AHC). *Neuropediatrics* 42:1–3
- Wyss MT, Jolivet R, Buck A, Magistretti PJ, Weber B (2011) In vivo evidence for lactate as a neuronal energy source. *J Neurosci* 31(20): 7477–7485
- Zhao Y, Fung C, Shin D et al (2010) Neuronal glucose transporter isoform 3 deficient mice demonstrate features of autism spectrum disorders. *Mol Psychiatry* 15:286–299

Novel Association of Early Onset Hepatocellular Carcinoma with Transaldolase Deficiency

Charles A. LeDuc · Elizabeth E. Crouch ·
Ashley Wilson · Jay Lefkowitz ·
Mirjam M.C. Wamelink · Cornelis Jakobs ·
Gajja S. Salomons · Xiaoyun Sun · Yufeng Shen ·
Wendy K. Chung

Received: 10 June 2013 / Revised: 15 July 2013 / Accepted: 22 July 2013 / Published online: 6 October 2013
© SSIEM and Springer-Verlag Berlin Heidelberg 2013

Abstract We evaluated a family with a 16-month-old boy with cirrhosis and hepatocellular carcinoma and his 30-month-old brother with cirrhosis. After failing to identify a diagnosis after routine metabolic evaluation, we utilized a combination of RNA-Seq and whole exome sequencing to identify a novel homozygous p.Ser171Phe Transaldolase (TALDO1) variant in the proband, his brother with cirrhosis,

as well as a clinically asymptomatic older 8-year-old brother. Metabolite analysis and enzymatic testing of *TALDO1* demonstrated elevated ribitol, sedoheptitol, and sedoheptulose-7P, and lack of activity of TALDO1 in the three children homozygous for the p.Ser171Phe mutation. Our findings expand the phenotype of transaldolase deficiency to include early onset hepatocellular carcinoma in humans and demonstrate that, even within the same family, individuals with the same homozygous mutation demonstrate a wide range of phenotypes.

Communicated by: K. Michael Gibson

Competing interests: None declared

C.A. LeDuc · A. Wilson · W.K. Chung
Department of Pediatrics, Columbia University, New York, NY, USA

E.E. Crouch
Department of Neuroscience, Columbia University, New York, NY, USA

J. Lefkowitz
Department of Pathology, Columbia University, New York, NY, USA

M.M.C. Wamelink · C. Jakobs · G.S. Salomons
Metabolic Unit, Department of Clinical Chemistry, VU University Medical Center Amsterdam, Amsterdam, The Netherlands

X. Sun · Y. Shen
JP Sulzberger Columbia Genome Center, Columbia University, New York, NY, USA

Y. Shen
Initiative in Systems Biology, Columbia University, New York, NY, USA

Y. Shen
Department of Biomedical Informatics, Columbia University, New York, NY, USA

W.K. Chung
Department of Medicine, Columbia University, New York, NY, USA

W.K. Chung (✉)
■, Room 620 RBP, 1150 St Nicholas Ave, New York, NY 10032, USA
e-mail: Wkc15@columbia.edu

Introduction

With the advent of next-generation sequencing (NGS), we now have the tools to identify the etiology of even the rarest of familial diseases in a less biased manner (Chung et al. 2009). As we identify the etiology of these diseases by this method, we often redefine the spectrum of the phenotype of rare diseases. For diseases associated with cancer, identifying an underlying hereditary cause has significant implications for treatment, long-term cancer surveillance, and risk stratification for other family members.

We describe a 16-month-old male with hepatocellular carcinoma and a history of hepatomegaly and liver dysfunction with a family history significant for a brother with cirrhosis. The use of genomic analysis of the hepatocellular carcinoma identified a transaldolase (taldo) deficiency, a rare inborn error of metabolism in the pentose phosphate pathway (PPP). Taldo is a reversible enzyme of the non-oxidative branch of the PPP, catalyzing the transfer of a three-carbon keto unit, corresponding to dihydroxyacetone (DHA), from sedoheptulose-7-phosphate (S7P) to glyceraldehyde-3-phosphate (G3P) generating erythrose-4-phosphate (E4P) and

fructose-6-phosphate (F6P). The first transaldolase-deficient patient was described by Verhoeven with liver cirrhosis, hepatosplenomegaly, thrombocytopenia, and dysmorphic features (Verhoeven et al. 2001). Since then, 22 additional cases have been described in the literature, but the condition continues to be rare (Verhoeven et al. 2005; Valayannopoulos et al. 2006; Fung et al. 2007; Wamelink et al. 2008b; Tylki-Szymanska et al. 2009; Balasubramaniam et al. 2011; Eyaid et al. 2013). The transaldolase knockout mouse is associated with a significant risk of hepatocellular carcinoma observed in 46% of the mice (Hanczko et al. 2009).

Methods

All individuals provided informed consent, and all studies were approved by the Columbia University Institutional Review Board. Blood and urine specimens were collected. Liver tissue from the proband (II.4) was collected at the time of liver resection and immediately flash frozen and stored at -80°C .

Homozygosity mapping was performed by genotyping the four children and both parents using an Affymetrix 500k NspI genotyping array according to the manufacturer's instructions (Affymetrix, Santa Clara, CA) and homozygosity mapper (<http://www.homozygositymapper.org/>) to identify regions of homozygosity in the 30-month-old brother of the proband (II.3) and the proband (II.4).

RNA was extracted from normal liver by homogenizing tissue and adding to Qiazol (Qiagen) (Chomczynski and Sacchi 1987). Total RNA was purified using RNeasy kit with DNase treatment (Qiagen) and mRNA isolation using a poly-A pulldown (Wang et al. 2009) and reverse transcription to generate cDNA. The cDNA was sequenced using 14 million (normal liver) and 21 million (tumor) 100 bp single-end sequencing reads on a HiSeq2000 according to manufacturer's recommendations (Illumina; San Diego, CA). The pass filter (PF) reads were mapped to human reference genome hg19 using TopHat (version 2.0.4) (Trapnell et al. 2009). For each read, we allowed up to three mismatches during the mapping. For variant calling, we used SAMTools (Li et al. 2009) combined with additional false-positive filters to call single nucleotide variants (SNVs) and short indels. For each candidate variant site, we allowed the maximal read depth = 1,000,000, minimum mapping quality = 5, minimum base quality = 17. We removed the variant calls in which the fraction of reads carrying the non-reference allele was less than a 10 % threshold. For exome sequencing, genomic DNA was extracted from blood, fragmented and captured with the Agilent SureSelect XT Human All Exon v.2 44Mb capture kit. Libraries were

sequenced on an Illumina HiSeq2000 with 100bp paired end reads at average on-target depth of coverage of $60\times$.

Urine polyols, heptuloses, and sugar-phosphates (sugar-P) were measured using liquid chromatography-tandem mass spectrometry (LC-MS/MS) and gas chromatography with flame ionization detection (Jansen et al. 1986, Wamelink et al. 2005a, 2007).

Transaldolase enzyme activity in lymphoblasts was measured by incubating the cells for 2 h with ribose-5P and measuring the sugar-P formed by LC-MS/MS (Wamelink et al. 2005b).

Results

Clinical Description

The proband (II.4 in Fig. 1) presented at 7 months of age with tachypnea and was found on physical examination to have hepatomegaly, which was confirmed on ultrasound. He was also found to have liver dysfunction with elevated aspartate aminotransferase (AST) of 228 (normal 12–36 U/L), alanine aminotransferase (ALT) of 104 (normal 7–41 U/L), and alpha-fetoprotein (AFP) of 2,108 (a marker for hepatocellular carcinoma, normal 0–9 ng/mL). Serum acylcarnitines, amino acids, very long chain fatty acids, copper, ceruloplasmin, iron, urine organic acids, and alpha 1 antitrypsin genotype were all normal. He was the product of a full-term pregnancy without prenatal or neonatal complications and had a normal New York State newborn screen. His growth and development were normal. His family history was significant for a 30-month-old brother (II.3) who had a history of hepatomegaly and elevated AST and ALT that progressed to cirrhosis. Both of his parents are from the Gambia, and there is no known history of consanguinity. All three pregnancies were uncomplicated by intercurrent illness, diabetes, or hypertension. The mother used no prescription or recreational drugs, alcohol or tobacco during any pregnancy. Routine prenatal testing was unremarkable. Birth weights were unremarkable, ranging from 5 lbs to 6 lbs 4 oz (Table 1). Each was discharged within 3 days of birth without complications. The proband had an abdominal MRI at 13 months of age that showed a $1.7\text{ cm} \times 1.6\text{ cm} \times 2.1\text{ cm}$ mass in segment 5 and another $1.3\text{ cm} \times 1 \times 1.4\text{ cm}$ mass in segment 6. The masses were biopsied, and both cores demonstrated well-differentiated hepatocellular carcinoma (Fig. 2) within a background of cirrhosis with mild inflammation. There was no evidence of storage material. The proband received a cadaveric liver transplant at 16 months of age at which time liver specimens were obtained for genomic analysis. The proband had normal cardiac structure and function with an

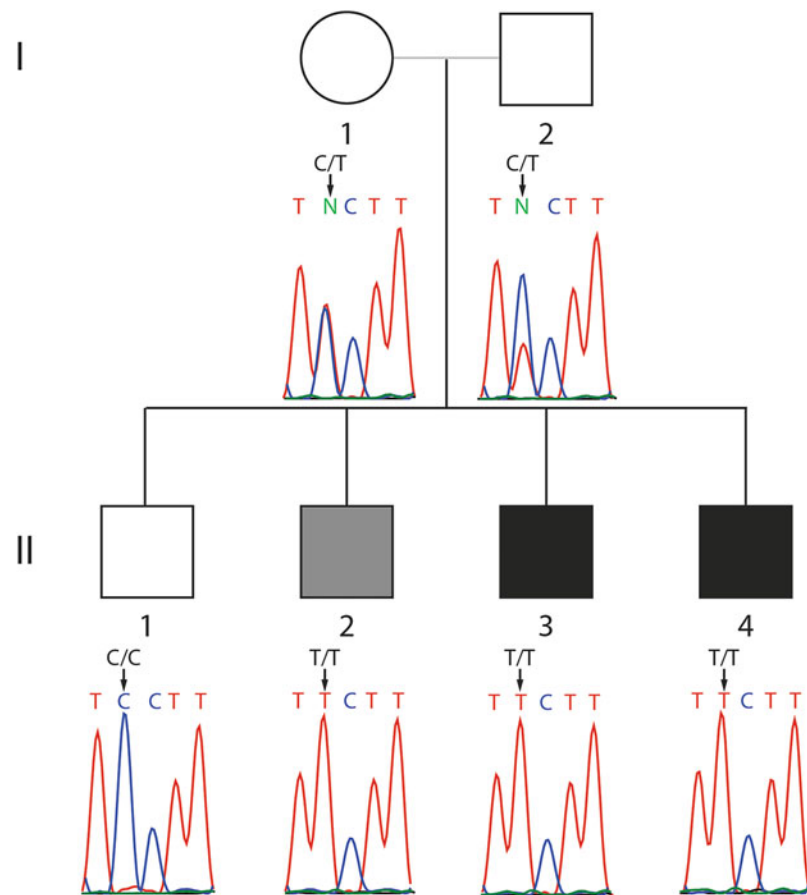


Fig. 1 Pedigree with clinically affected individuals indicated in *black* and biochemically affected but asymptomatic individual indicated in *gray*

ejection fraction of 68% and normal cardiac dimensions, normal renal function with blood urea nitrogen (BUN) of 8–19 mg/dL (7–20 mg/dL), creatinine of 0.2 mg/dL (0.6–1.2 mg/dL), and normal platelet counts ranging from 281 to 402 (165–415). There was no succinylacetone in the urine of the proband to suggest tyrosinemia.

The affected child has three older brothers (Fig. 1). One brother (II.3), as mentioned above, had a history of hepatomegaly and cirrhosis associated with increased AST and ALT diagnosed at 1 year of age. Acylcarnitines, urine organic acids, and serum amino acids were normal. A liver biopsy demonstrated cirrhosis. II.3 has normal platelet counts ranging from 171 to 325 (165–415) and normal renal function with BUN of 7–18 mg/dL (7–20 mg/dL), creatinine of 0.3 mg/dL (0.6–1.2 mg/dL).

The oldest two brothers, ages 12 and 8 years old (II.1 and II.2), have normal liver size and liver function studies. II.2 has normal platelet counts ranging from 273 to 275 (165–415) and normal renal function with BUN of 14 mg/dL (7–20 mg/dL), creatinine of 0.47 mg/dl (0.6–1.2 mg/dL).

Both parents are clinically asymptomatic but have not undergone clinical investigation.

Genomic Analysis

Based upon the family history, we assumed either an autosomal-recessive or X-linked mode of inheritance. There were no stretches of homozygosity > 1 Mb shared by II.3 and II.4.

We identified 1,901 homozygous rare/novel variants in the RNA-Seq data from the liver of the proband. Of these variants, 121 were either novel or appeared in the HGMD database of known mutations. Of these, 21 were either in the HGMD database or called damaging by SIFT. These variants were filtered to remove variants in the EVS database (<http://evs.gs.washington.edu/EVS/>) to eliminate those variants with an allele frequency in African Americans of greater than 5 %, leaving only five variants. One of these five variants (rs59947000) was a common indel. Another variant is in a repeat region that presumably is an alignment error. Two variants were not confirmed by Sanger sequencing. The remaining variant (aligned to 22 alternate and no reference alleles), confirmed to be homozygous in the proband, was c.512C>T (p.Ser171Phe) at *TALDO1* (chr11: 763394 in hg19).

Table 1 Metabolic and genetic results of four siblings. Urinary excretion of polyols, heptuloses, and sugar-phosphates in mmol/mol creatinine. Urine of II.4 collected after liver transplant

Phenotype	II.4	II.3	II.2	II.1	Control values
Age at time of sample collection	1 year	3 years	9 years	13 years	Control values
Clinical status	Proband with hepatocellular carcinoma and cirrhosis	Cirrhosis	Asymptomatic	Unaffected	
Birth weight	6 lbs 4 oz	5 lbs	5 lbs 4 oz		
Genetic status at TALDO1	Homozygous Phe171	Homozygous Phe171	Homozygous Phe171	Homozygous Ser171	
ALT	228	57	16	19	7–41 U/L
AST	104	70	20	23	12–36 U/L
GGT	70	20	21	15	9–58 U/L
AFP	2,108	15.2	4.6	0.8	0–9 ng/mL
Platelet count	281–402	171–325	273–275		165–415
BUN	8–19	7–18	14		7–20 mg/dL
Creatine	0.2	0.3	0.47		0.6–1.2 mg/dL
Erythritol ^a	203	117	103	22	1–2 years: 76–192 2–6 years: 55–105 6–18 years: 35–179
Ribitol ^a	54	60	54	5	1–2 years: 9–24 2–6 years: 8–11 6–18 years: 4–11
Arabitol ^a	152	124	77	17	<89 ^c
Sedoheptitol ^b	2	2	1.1	<1	<1
Perseitol ^b	<1	2	3	<1	<1
Sedoheptulose ^b	600	300	270	2.7	<9
Mannoheptulose ^b	Disturbed ^d	Disturbed ^d	Disturbed ^d	2.8	<3
Sedoheptulose-7P ^b	0.93	0.96	1.7	n.d.	<0.07 ^c
Ribose-5P ^b	0.76	0.23	0.26	n.d.	<0.13 ^c
Ribulose-5P + xylulose-5P ^b	0.84	0.53	0.46	0.09	<0.44 ^c
Transaldolase activity	Undetectable	Undetectable	Undetectable	Normal	

n.d. Not detectable, bold values which are elevated

^a Gas chromatography-flame ionization detection (Jansen et al. 1986)

^b LC-MS/MS (Wamelink et al. 2005a, 2007)

^c Control ranges are age dependent, this value is the upper limit of the age ranges together

^d Disturbed due to high sedoheptulose

We identified 24,967 variants in the coding regions by whole exome sequencing in blood from the proband. As expected, many more variants were identified by exome sequencing compared to RNA-Seq. Of these variants, 8,584 were homozygous, and 233 were novel and homozygous; 146 were non-synonymous; 26 were predicted to be damaging by SIFT. After filtering out common SNPs found in the EVS dataset for African Americans (allele frequency >5%), 11 variants remained. Of these 11 variants, 5 were confirmed by Sanger sequencing as homozygous in the proband. However, only the p.Ser171Phe *TALDO1* variant was also homozygous in the other affected brother, II.3.

Genotyping of all the family members for c.512C>T *TALDO1* identified that both parents were carriers, the two clinically affected children (II.3 and II.4) were homozygous mutant (T/T), and unaffected brother (II.1) was homozygous wild type (C/C), and, surprisingly, a clinically asymptomatic brother (II.2) was homozygous for the mutation (T/T).

To functionally evaluate the transaldolase activity, urine samples of the four siblings (collected after liver transplant in II.4) were analyzed for polyols, heptuloses, and sugar-P (Table 1). All three boys that were homozygous 171Phe *TALDO1* had elevated excretion of ribitol, sedoheptitol, perseitol, sedoheptulose, and sedoheptulose-7P (Table 1)

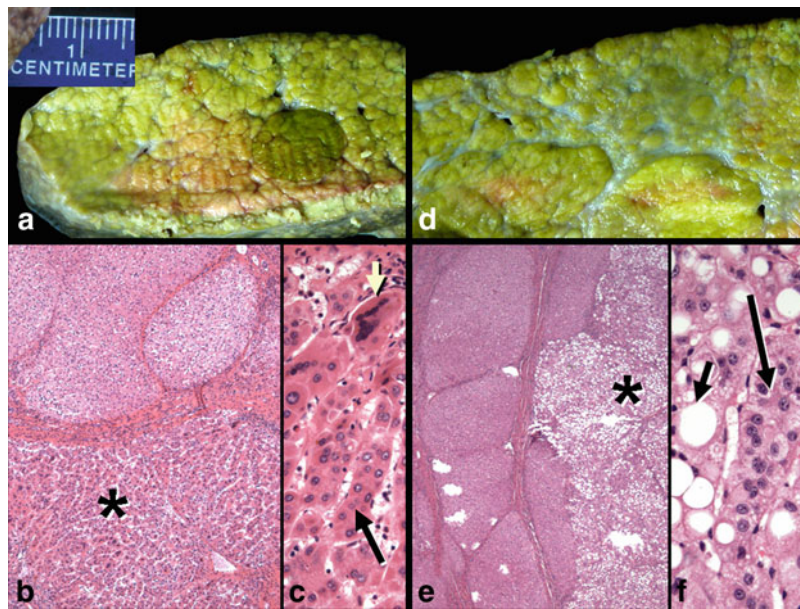


Fig. 2 Explanted liver specimen from II.4 showing mixed micro-macronodular cirrhosis and several well-differentiated hepatocellular carcinomas. **(a)** A well-circumscribed carcinoma (*dark green nodule*) is present. **(b)** Microscopic section of the lesion seen in panel A shows an inactive cirrhosis at top and the hepatocellular carcinoma (*) below. **(c)** High magnification of the tumor in panel B shows partial microtrabecular pattern (*long arrow*) and many giant, multinucleated

tumor cells (*short yellow arrow*). **(d)** Another nodule is grossly pale and is a steatotic hepatocellular carcinoma. **(e)** The underlying inactive cirrhosis (*left*) contrasts to the multilobulated fatty carcinoma at right (*). **(f)** The steatotic carcinoma shows many neoplastic hepatocytes with large fat vacuoles (*short arrow*) as well as focal microtrabecular growth (*long arrow*). (Hematoxylin and eosin stains; b: x 40; c: x 200; e: x 40; f: x 200)

consistent with transaldolase deficiency. Erythritol and arabitol were only mildly elevated in the two youngest children (II.3 and II.4) and normal in II.2. Mannoheptulose could not be separately measured due to co-elution with sedoheptulose. The sugar-P ribose-5-P and xylulose-5P + ribulose-5P were also highly elevated in urine of II.3 and II.4 and mildly elevated in II.2. II.1 had a normal metabolite profile consistent with his normal genotype.

We directly tested the transaldolase activity in lymphoblasts. After incubating lymphoblasts with ribose-5P, there was normal formation of glucose-6P + fructose-6P in the controls and II.1 while there was no formation of glucose-6P + fructose-6P in II.2, II.3, and II.4, confirming Taldo deficiency (Table 1).

Discussion

We have identified a family with three children with a novel homozygous p.Ser171Phe mutation in *TALDO1* associated with complete enzymatic deficiency of TALDO1 and a clinical course of hepatomegaly progressing to cirrhosis and hepatocellular carcinoma by 16 months of age. Intriguingly, within the same family, another sibling has cirrhosis but no hepatocellular carcinoma by age 30 months, and one 8-year-old child is clinically asymptomatic with normal liver size, function, and histology. None of the affected children have

evidence of renal impairment, thrombocytopenia, or cardiac disease. It is unclear what is responsible for the clinical variability between individuals with the same *TALDO1* genotype and whether there might have previously been a phenotype in the oldest affected brother. In two other families, a deletion of Ser171 was found in the *TALDO1* gene as the cause of TALDO deficiency (10–11). This amino acid is part of a highly conserved region (Thorell et al. 2000). These data, the fact that serine 171 is highly conserved, and that this variant was not detected in a cohort of 13,005 alleles (EVS), indicate that this variant is pathogenic. Taldo deficiency in humans has been associated with a range of phenotypes from intrauterine lethality associated with fetal multimalformation syndrome and hydrops fetalis to the more common presentation of cirrhosis, liver failure, hepatosplenomegaly, anemia, thrombocytopenia, dysmorphism, congenital heart defects, and tubulopathy (Verhoeven et al. 2001, 2005; Valayannopoulos et al. 2006; Fung et al. 2007; Wamelink et al. 2008b; Tylki-Szymanska et al. 2009; Balasubramaniam et al. 2011; Eyaid et al. 2013). Our family fits into the range of phenotypes most commonly observed; however, only the liver is affected and without extrahepatic involvement. This is the first association of transaldolase deficiency with hepatocellular carcinoma and an asymptomatic presentation to our knowledge.

Lower concentrations of the polyols erythritol and arabitol could be relevant for the asymptomatic phenotype

in II.2, but could also be related to the older age, since in other patients the polyol concentrations tend to be highest in the neonatal period and accumulate less when they are older (Wamelink et al. 2008a).

Taldo1^{+/-} and *Taldo1*^{-/-} mice are 27- and 79-fold more likely to spontaneously develop liver cirrhosis and nodular dysplasia, respectively, than their wild-type *Taldo1*^{+/+} littermates (Hanczko et al. 2009). Seventeen percent of *Taldo1*^{+/-} and 46% of *Taldo1*^{-/-} mice spontaneously developed hepatocellular carcinoma, and there was evidence of significant oxidative stress in the animal model with accumulation of sedoheptulose-7P, failure to recycle ribose 5-phosphate, depleted NADPH and glutathione, and increased production of lipid hydroperoxides. When *Taldo1*^{-/-} mice were administered the antioxidant N-acetylcysteine, there was a marked reduction in the incidence of hepatocellular carcinoma (Hanczko et al. 2009), supporting the hypothesis that oxidative stress is responsible for tumorigenesis and possibly suggesting a strategy to prevent hepatocellular carcinoma in these patients. Because of the effectiveness of the antioxidant strategy in the mice, we are treating the three children with antioxidants.

Taldo deficiency is particularly challenging to diagnose with routine clinical tests. Routine metabolic tests including acylcarnitines, urine organic acids, serum amino acids, very long chain fatty acids, copper, ceruloplasmin, iron, alpha 1 antitrypsin genotype were all normal in this patient, and there was no identifiable storage material in hepatocytes or unique pathology. Lack of routine measurement of urinary polyols may account for the small number of recognized cases. In this case, homozygosity mapping did not identify genomic regions upon which to focus. Only with the advent of NGS were we able to make a diagnosis because transaldolase deficiency had not previously been associated with hepatocellular carcinoma in humans and was therefore not considered in the original differential diagnosis.

Notably, II.4 continues to have an abnormal metabolic profile in the urine, characteristic of transaldolase deficiency even after a liver transplant, suggesting that other tissues also contribute significantly to pentose phosphate metabolism. Having a definitive diagnosis for the proband and his siblings will now allow for surveillance of liver and kidney functions and hepatocellular carcinoma in the future.

We identified the disease mutation using both RNA-Seq and exome sequencing. However, the reduced cost of the experiment and the significantly smaller number of variants (~5x less) generated from the RNA-Seq data suggest that this can offer a significant advantage to genomic analysis when the appropriate tissue for analysis is available since the analysis will focus only on genes expressed within the

tissue of interest. Mutations that lead to nonsense-mediated decay would, however, be expected to pose a challenge if only the sequence itself were analyzed, and RNA expression levels should also be included in the analysis. The availability of RNA-seq data from many primary tissues (such as GTEx projects) in healthy individuals will provide a background model for such analysis.

Transaldolase can now be added to the list of other inborn errors associated with increased risk of hepatocellular carcinomas including tyrosinemia and glycogen storage disease IV. It would be interesting to compare our RNA-Seq results with those of other inborn errors of metabolism to better understand if there are common drivers of carcinogenesis in inborn errors of metabolism and better define the mechanism of carcinogenesis.

Acknowledgments Birthe Roos and Erwin Jansen are kindly acknowledged for their analytical contributions.

One-Sentence Summary

We utilized a combination of RNA-Seq and whole exome sequencing to identify a novel homozygous p.Ser171Phe Transaldolase (*TALDO1*) mutation in a 16-month-old child to develop cirrhosis and hepatocellular carcinoma and biochemically confirmed that three affected siblings demonstrate a wide range of phenotypes from being asymptomatic to cirrhosis to hepatocellular carcinoma.

Conflict of Interest

Charles A. LeDuc, Elizabeth E. Crouch, Ashley Wilson, Jay Lefkowitz, Mirjam M.C. Wamelink, Cornelis Jakobs, Gajja S Salomons, Xiaoyun Sun, Yufeng Shen, and Wendy K. Chung declare that they have no conflict of interest.

Informed Consent

All procedures followed were in accordance with the ethical standards of the responsible committee on human experimentation (institutional and national) and with the Helsinki Declaration of 1975, as revised in 2000 (5). Informed consent was obtained from all patients for being included in the study.

Details of the Contributions of Individual Authors

CAL and WKC wrote the manuscript with assistance from EEC, YS, MW, CJ, and GS. JL did the histological analysis. MW, CJ, and GS did the metabolic analysis. YS and XS did the alignment and variant calling. CAL and EEC tested and

analyzed the variants. AW and WKC did the clinical workup on the patient. The study was designed by WKC.

References

- Balasubramaniam S, Wamelink MM, Ngu LH et al (2011) Novel heterozygous mutations in TALDO1 gene causing transaldolase deficiency and early infantile liver failure. *J Pediatr Gastroenterol Nutr* 52(1):113–116
- Chomczynski P, Sacchi N (1987) Single-step method of RNA isolation by acid guanidinium thiocyanate-phenol-chloroform extraction. *Anal Biochem* 162(1):156–159
- Chung WK, Shin M, Jaramillo TC et al (2009) Absence epilepsy in apathetic, a spontaneous mutant mouse lacking the h channel subunit, HCN2. *Neurobiol Dis* 33(3):499–508
- Eyaid W, Al Harbi T, Anazi S et al (Jan 12 2013) Transaldolase deficiency: report of 12 new cases and further delineation of the phenotype. *J Inherit Metab Dis* (Epub ahead of print)
- Fung CW, Siu S, Mak C, Poon G et al (2007) A rare cause of hepatosplenomegaly-Transaldolase deficiency. *J Inherit Metab Dis* 30(Suppl 1):62
- Hanczko R, Fernandez DR, Doherty E et al (2009) Prevention of hepatocarcinogenesis and increased susceptibility to acetaminophen-induced liver failure in transaldolase-deficient mice by N-acetylcysteine. *J Clin Invest* 119(6):1546–1557
- Jansen G, Muskiet FA, Schierbeek H, Berger R, van der Slik W (1986) Capillary gas chromatographic profiling of urinary, plasma and erythrocyte sugars and polyols as their trimethylsilyl derivatives, preceded by a simple and rapid prepurification method. *Clin Chim Acta* 157(3):277–293
- Li H, Handsaker B, Wysoker A et al (2009) The sequence alignment/Map format and SAMtools. *Bioinformatics* 25(16):2078–2079
- Thorell S, Gergely P Jr, Banki K, Perl A, Schneider G (2000) The three-dimensional structure of human transaldolase. *FEBS Lett* 475(3):205–208
- Trapnell C, Pachter L, Salzberg SL (2009) TopHat: discovering splice junctions with RNA-Seq. *Bioinformatics* 25(9):1105–1111
- Tylki-Szymanska A, Stradowska TJ, Wamelink MM et al (2009) Transaldolase deficiency in two new patients with a relative mild phenotype. *Mol Genet Metab* 97(1):15–17
- Valayannopoulos V, Verhoeven NM, Mention K et al (2006) Transaldolase deficiency: a new cause of hydrops fetalis and neonatal multi-organ disease. *J Pediatr* 149(5):713–717
- Verhoeven NM, Huck JH, Roos B et al (2001) Transaldolase deficiency: liver cirrhosis associated with a new inborn error in the pentose phosphate pathway. *Am J Hum Genet* 68(5):1086–1092
- Verhoeven NM, Wallot M, Huck JH et al (2005) A newborn with severe liver failure, cardiomyopathy and transaldolase deficiency. *J Inherit Metab Dis* 28(2):169–179
- Wamelink MM, Smith DE, Jakobs C, Verhoeven NM (2005a) Analysis of polyols in urine by liquid chromatography-tandem mass spectrometry: a useful tool for recognition of inborn errors affecting polyol metabolism. *J Inherit Metab Dis* 28(6):951–963
- Wamelink MM, Struys EA, Huck JH et al (2005b) Quantification of sugar phosphate intermediates of the pentose phosphate pathway by LC-MS/MS: application to two new inherited defects of metabolism. *J Chromatogr B Analyt Technol Biomed Life Sci* 823(1):18–25
- Wamelink MM, Smith DE, Jansen EE, Verhoeven NM, Struys EA, Jakobs C (2007) Detection of transaldolase deficiency by quantification of novel seven-carbon chain carbohydrate biomarkers in urine. *J Inherit Metab Dis* 30(5):735–742
- Wamelink MM, Struys EA, Jakobs C (2008a) The biochemistry, metabolism and inherited defects of the pentose phosphate pathway: a review. *J Inherit Metab Dis* 31(6):703–717
- Wamelink MM, Struys EA, Salomons GS, Fowler D, Jakobs C, Clayton PT (2008b) Transaldolase deficiency in a two-year-old boy with cirrhosis. *Mol Genet Metab* 94(2):255–258
- Wang Z, Gerstein M, Snyder M (2009) RNA-Seq: a revolutionary tool for transcriptomics. *Nat Rev Genet* 10(1):57–63

Lathosterolosis: A Disorder of Cholesterol Biosynthesis Resembling Smith-Lemli-Opitz Syndrome

A.C.C. Ho · C.W. Fung · T.S. Siu · O.C.K. Ma ·
C.W. Lam · S. Tam · V.C.N. Wong

Received: 01 November 2012 / Revised: 29 July 2013 / Accepted: 30 July 2013 / Published online: 20 October 2013
© SSIEM and Springer-Verlag Berlin Heidelberg 2013

Abstract Lathosterolosis is an inborn error of cholesterol biosynthesis due to deficiency of the enzyme 3-beta-hydroxysteroid-delta-5-desaturase (or sterol-C5-desaturase or SC5D). This leads to a block in conversion of lathosterol into 7-dehydrocholesterol. Only three patients with lathosterolosis have been reported in literature, of which one survived. We report a patient with dysmorphism, multiple congenital anomalies, and developmental delay, initially suspected to have Smith-Lemli-Opitz syndrome, who was later found to have elevated levels of lathosterol in both plasma and fibroblasts. Genetic study confirmed a compound heterozygous mutation in the sterol-C5-desaturase-like (*SC5DL*) gene on chromosome 11q23. Simvastatin was started as a treatment therapy and it resulted in normalization of blood lathosterol level and improvement in the neurodevelopmental profile. However, additional patients are needed for better delineation of the clinical spectrum, genotype-phenotype correlation, and potential efficacy of simvastatin treatment in this rare disorder. If the presence of distinctive facial features and limb anomalies raise the suspicion of a

cholesterol biosynthesis defect, testing of full sterol profile is warranted as normal cholesterol or 7-dehydrocholesterol levels cannot rule out the diagnosis of cholesterol synthesis defect like lathosterolosis.

Introduction

Lathosterolosis (OMIM 607330) is an inborn error of cholesterol biosynthesis due to deficiency of the enzyme 3-beta-hydroxysteroid-delta-5-desaturase (or sterol-C5-desaturase or SC5D). This results in a defect in conversion of lathosterol into 7-dehydrocholesterol. Lathosterolosis was first reported by Brunetti-Pierri et al. in 2002 (Brunetti-Pierri et al. 2002). There were three reported cases in literature so far, of which only one patient survived. From the reported cases, patients with lathosterolosis were characterized by multiple congenital anomalies, learning disability, and liver involvement. We report a child with lathosterolosis confirmed both biochemically and genetically. Simvastatin was started as treatment with clinical response and normalization of blood lathosterol level.

Case History

The proband is the first child of a non-consanguineous Caucasian couple. His parents were healthy and family history was unremarkable for any neurodevelopmental or neurometabolic disorder. The antenatal period was uneventful. He was born at 39 weeks of gestation by vaginal delivery with a birth weight of 3.3 kg and normal Apgar scores. He was noted to have dysmorphic features (bitemporal narrowing, broad nasal tip without anteverted nostrils, and micrognathia) after birth. Physical examination

Communicated by: Verena Peters

Competing interests: None declared

A.C.C. Ho · C.W. Fung · V.C.N. Wong (✉)
Department of Paediatrics and Adolescent Medicine, Queen Mary Hospital, Li Ka Shing Faculty of Medicine, The University of Hong Kong, Hong Kong Special Administrative Region, China
e-mail: vcnwong@hkucc.hku.hk

T.S. Siu · O.C.K. Ma · S. Tam
Division of Clinical Biochemistry, Queen Mary Hospital, Hong Kong Special Administrative Region, China

C.W. Lam
Department of Pathology, Queen Mary Hospital, Li Ka Shing Faculty of Medicine, The University of Hong Kong, Hong Kong Special Administrative Region, China

also revealed microcephaly (his head circumference dropped from third percentile at birth to 2 cm below third percentile at the age of 18 months and grew along this centile line afterwards), central hypotonia, single umbilical artery, bilateral postaxial hexadactyly of feet, and bilateral soft tissue syndactyly between the second and third toes, for which he subsequently received a corrective operation at 20 months. He did not have any ptosis, cleft palate, or abnormal genitalia. He was noted to have developmental delay without regression since early childhood. Assessment using Griffiths Mental Developmental Scales performed at 20 months of age demonstrated global developmental delay with an overall mental age of 11 months and a developmental quotient of 55 adjusted for chronological age. The mental age of motor, speech, and performance domains were 11.5 months, 10 months, and 7.5 months, respectively. Practical reasoning could not be assessed due to the young age of the patient. Magnetic resonance imaging (MRI) brain performed at 18 months was normal.

The proband was suspected to have Smith-Lemli-Opitz syndrome in view of the dysmorphism, limb anomalies, and developmental delay. Plasma sterol profile was checked at the age of 22 months. Instead of an increased 7-dehydrocholesterol level as typically found in Smith-Lemli-Opitz syndrome, the analysis showed marked elevation of lathosterol [81.6 $\mu\text{mol/L}$ (normal level <18 $\mu\text{mol/L}$)]. The levels of both 7-dehydrocholesterol [0.21 $\mu\text{mol/L}$ (normal level <0.65 $\mu\text{mol/L}$)] and cholesterol (4.1 mmol/L) were normal. This profile was biochemically compatible with the diagnosis of lathosterolosis. Moreover, the patient's skin fibroblasts were sent to the Metabolic Centre of the University Children's Hospital in Heidelberg, Germany, for analysis before commencement of simvastatin. Concentration of lathosterol was elevated (1.48% of total sterol), which was in accordance with the diagnosis of lathosterolosis. Genetic study demonstrated a novel compound heterozygous mutation of sterol-C5-desaturase-like (*SC5DL*) gene.

Liver cirrhosis and liver failure had previously been reported in a patient with lathosterolosis. We have performed regular ultrasound monitoring of the liver for our patient from three months of starting simvastatin onwards. Serial ultrasound scans showed mild, nonprogressive increase in liver heterogeneity, signifying liver parenchymal disease. Two MRI scans performed 2 years apart demonstrated a normal sized liver with nonprogressive mild T2 hyperintensities along the subcapsular region of the right anterior lobe, which could represent early changes of fibrosis. However, the liver function was normal all along. Over a period of more than 3 years, the level of aspartate aminotransferase (AST) ranged from 43 to 57 U/L (normal level <60 U/L), while that of alanine aminotransferase (ALT) ranged from 10 to 38 U/L (normal level <53

U/L). The highest level of bilirubin and ammonia was 11 $\mu\text{mol/L}$ and 19 $\mu\text{mol/L}$, respectively. The level of bile acid was 1.7 $\mu\text{mol/L}$ (normal level: 1–10 $\mu\text{mol/L}$). Regular ophthalmological evaluation was performed after the diagnosis was confirmed. The initial examination was unremarkable. However, subsequent examination at the age of 4 years showed small dot opacity of each lens with no visual significance. Patient's father was also found to have bilateral small dot lens opacity, which did not affect his vision.

At the age of 23 months, we prescribed simvastatin [3-hydroxy-3-methylglutaryl coenzyme A (HMG-CoA) reductase inhibitor] as a therapeutic intervention, with the aim of normalizing the lathosterol level. It was started at a dose of 0.2 mg/kg/day and was gradually stepped up to 1 mg/kg/day. The level of lathosterol normalized 4 weeks after starting the treatment. The highest lathosterol level after starting simvastatin was 18.3 $\mu\text{mol/L}$, which decreased to 7.2 $\mu\text{mol/L}$ after optimizing the dose. Liver function and creatine kinase were all along normal. The level of creatine kinase ranged from 115 U/L to 215 U/L after starting simvastatin treatment (Normal <365 U/L). Developmental assessment using Griffiths Mental Developmental Scales was repeated at the chronological age of 45 months with an overall mental age of 29 months. The mental age of motor, speech, performance, and practical reasoning domains were 25 months, 36 months, 22.7 months, and 36.5 months respectively. The finding was still compatible with global developmental delay, but the overall developmental quotient increased from 55 in the first assessment to 64. It is worth noting that the practical reasoning domain, which was an indicator of patient's cognitive performance, had a standard quotient of 9 and a z score of -1.341 , which fell into the low normal range.

Method

Cholesterol was measured with automated enzymatic method in Roche-Hitachi system. The analysis of sterols was performed by the clinical biochemist. 200 μL of plasma was mixed with 20 μL of 200 $\mu\text{g/mL}$ 5 α -cholestane (internal standard) and was saponified in 1 mL of 4% (w/v) KOH in 90% ethanol at 80°C for 60 min. After saponification, the samples were mixed with 1 mL of water and were extracted two times with 2 mL of hexane. The pooled hexane extracts were dried under nitrogen. The trimethylsilyl ethers of sterols were obtained by derivatizing the residues with 100 μL DMF Sil-Prep™ (Grace, IL, USA) at 60°C for 30 min. Two microliters of derivative mixture was injected at a split ratio of 1:10 into an Agilent 6890/5973 Gas Chromatograph-Mass Selective Detector system installed with a Supelco SAC-5 capillary column (30 m \times 0.25 mm I.D., film thickness 0.25 μm). The carrier gas was helium at a

Table 1 In silico analysis of effect of mutations by PolyPhen-2^a and SIFT^b softwares

Mutations ^c	PolyPhen-2 (prediction score)	SIFT	Reference
c.442A>G; p.K148E	<i>Possibly damaging</i> (0.764)	Affect protein function	Novel
c.630C>A; p.D210E	Probably damaging (0.995)	Affect protein function	Novel
c.86G>A; p.R29Q	Probably damaging (0.996)	Affect protein function	1
c.137A>C; p.Y46S	Probably damaging (0.999)	Affect protein function	5
c.632G>A; p.G211D	Probably damaging (1.000)	Affect protein function	1

^a <http://genetics.bwh.harvard.edu/pph2/index.shtml>

^b <http://sift.jcvi.org>

^c Mutation numbering is based on NCBI reference sequence NM_006918.4 & NP_008849.2

linear rate of 1 mL/min. The oven temperature was 60°C at the beginning and was raised at a rate of 50°C/min up to 280°C and was held for 20 min. The injector temperature and detector temperature were 300°C. Measurements were done in the electron impact mode at 70 eV with an ion source temperature of 230°C. The quadrupole temperature was 150°C. Mass spectrometric acquisition was performed in the SIM (single ion monitoring) mode at $m/z = 357$ for 5 α -cholestane, $m/z = 325$ for 7-dehydrocholesterol, and $m/z = 458$ for lathosterol. The quantification of sterol levels was linear at least up to 50 $\mu\text{mol/L}$. The proband's result was confirmed by twofold dilution. The Mayo Clinic reference range was adopted in this case as the proband is a non-Chinese. Our established normal range for local Chinese is <6 $\mu\text{mol/L}$.

Genomic DNA was extracted from peripheral blood samples according to the manufacturer's standard procedure using the QIAamp DNA Blood Mini Kit (Qiagen). All four coding exons of SC5DL gene and their flanking intronic sequences were amplified from the genomic DNA by polymerase chain reaction (PCR) as previously described (Krakowiak et al. 2003). The PCR product was purified using ExoSAP-IT (GE Healthcare) and direct sequencing was performed on both strands with the PCR primers and the Big Dye terminator 3.1 cycle sequencing kit (Applied Biosystems) using an ABI-3730XL genetic analyzer.

Correlation between the position of missense mutation, level of residual enzyme activity (if any), and severity of the clinical phenotype is always difficult to predict, whereas the pathogenicity of nonsense or frameshift mutation is much easier to conclude as truncated protein is usually produced. Testing the effect of the variants in a functional assay of the protein should confirm the pathogenicity of the missense mutation, which is not available in this patient.

Results

Genetic study demonstrated a novel compound heterozygous mutation of sterol-C5-desaturase-like (*SC5DL*) gene. Two novel missense mutations were found in the proband's DNA, p.K148E, and p.D210E. Each parent was heterozygous for one of the two mutations (K148E in mother and D210E in father). Bioinformatics softwares were used for in silico prediction of effect of mutations on the structure and function of protein and the data were summarized in Table 1. These two variants were not listed in the NCBI dbSNP database and were also absent in 150 normal controls.

The patient's skin fibroblasts were sent to the Metabolic Centre of the University Children's Hospital in Heidelberg, Germany, for analysis before commencement of simvastatin. Fibroblasts were cultivated on lipid-depleted medium for 10 days in order to stimulate cholesterol biosynthesis. Sterols were then quantified by gas chromatography/mass spectroscopy (GC/MS). Concentration of lathosterol was elevated (1.48% of total sterols) and was in accordance with the diagnosis of lathosterolosis. Concentration of 8,9-cholestenol was elevated as well (17.53% of total sterols). This was mentioned in the case reported by Brunetti-Pierri et al. (2002), though the level of lathosterol was higher than that of 8,9-cholestenol in Brunetti-Pierri's case. Plant sterols were not increased when compared with controls. Beta-sitosterol and stigmastanol were both 0.01%. The sterol profile is presented in Table 2. The patient's sterol profile in skin fibroblasts after simvastatin treatment is not available. Filipin staining performed in the Institute of Human Genetics, Heidelberg, Germany, showed a "variant" cholesterol storage pattern. Perinuclear cholesterol content was moderately elevated when compared to reference fibroblasts. This finding was also described by

Table 2 Quantification of sterols in fibroblasts

Cholesterol	97%
Lathosterol	1.48%
7-Dehydrocholesterol	0.11%
8-Dehydrocholesterol	0.18%
Desmosterol	0.02%
Lanosterol	0.05%
8,9-Cholestenol	17.53%
Beta-sitosterol	0.01%
Stigmastanol	0.01%

Each sterol is given in percent of total sterols

Krakowiak and colleagues (2003) and supported the diagnosis of lathosterolosis. Electronic microscopic study of the fibroblasts was not performed.

Discussion

Cholesterol is an essential lipid which has multiple crucial functions in the human body. Apart from being a structural lipid in membranes and myelin, cholesterol also acts as the precursor for bile acid, steroid hormone, neuroactive steroid, and oxysterol synthesis. In addition, cholesterol is also necessary for maturation and function of the hedgehog morphogens during embryonic development (Porter 2003). Defects in cholesterol synthesis result in various human malformation syndromes. Smith-Lemli-Opitz syndrome (OMIM 270400) is the most common one and is caused by mutation of the 7-dehydrocholesterol reductase (*DHCR7*) gene. 7-dehydrocholesterol reductase catalyzes the reduction of 7-dehydrocholesterol to cholesterol in the final step of the Kandutsch-Russel cholesterol synthetic pathway. On the other hand, lathosterolosis (OMIM 607330) is a recently recognized defect of cholesterol synthesis, which is due to mutations of the sterol-C5-desaturase-like (*SC5DL*) gene on chromosome 11q23. This leads to deficiency of the enzyme 3-beta-hydroxysteroid-delta-5-desaturase (or sterol-C5-desaturase), which catalyzes the conversion of lathosterol to 7-dehydrocholesterol. Inheritance of both Smith-Lemli-Opitz syndrome and lathosterolosis is autosomal recessive.

Lathosterolosis is a very rare disease. It was first reported by Brunetti-Pierri in 2002 (Brunetti-Pierri et al. 2002). The second case was reported initially as apparent Smith-Lemli-Opitz syndrome by Parnes in 1990 (Parnes et al. 1990), but was subsequently diagnosed to have lathosterolosis by postmortem examination by Krakowiak et al. in 2003 (Krakowiak et al. 2003). The third case was reported by Rossi in 2007 who followed up on the first case reported by Brunetti-Pierri and described her affected

sibling who was a stillborn (Rossi et al. 2007). Our patient contributed to the fourth reported case of lathosterolosis in the literature. Features of our patient were compared with those of the other three cases (Table 3).

Lathosterolosis appears to have features overlapping with those of Smith-Lemli-Opitz syndrome. However, there may be ascertainment bias as all cases of lathosterolosis were diagnosed after excluding Smith-Lemli-Opitz syndrome. Therefore, additional patients are needed to delineate the definite clinical features of this rare disorder and to know if there is a true phenotypic overlap between two cholesterol synthesis disorders. Smith-Lemli-Opitz syndrome is characterized by distinctive facial appearance (microcephaly, ptosis, small upturned nose, and micrognathia), limb anomalies (polydactyly, 2–3 toe syndactyly), cleft palate, hypospadias, and variable degrees of learning disabilities (Porter 2003). Apart from the fetus who was aborted at 21 weeks of gestation, all three reported cases of lathosterolosis had microcephaly, dysmorphic features, developmental delay/learning disabilities, and appendicular anomalies, namely, postaxial polydactyly and toe syndactyly. However, cleft palate was not detected in all four reported cases of lathosterolosis. The similar phenotypic findings in both Smith-Lemli-Opitz syndrome and lathosterolosis could be due to decreased cholesterol/functional sterol and/or toxic effects of increased sterol precursors. This may in turn have an effect on the different hedgehog functions. The appendicular anomalies may be explained by the impaired Sonic hedgehog function in cholesterol synthesis defect, which plays a role in limb development (Porter 2003). Both Smith-Lemli-Opitz syndrome and lathosterolosis serve as good illustrations that inborn errors of metabolism can merely present with dysmorphic features and developmental delay/learning disability, without any acute or progressive clinical deterioration as in other neurometabolic diseases. If the presence of distinctive facial features and limb anomalies raises the suspicion of cholesterol synthesis defect, testing of full sterol profile is of utmost importance as normal cholesterol or 7-dehydrocholesterol levels cannot rule out the diagnosis of cholesterol synthesis defect, as in our patient with lathosterolosis.

Treatment of Smith-Lemli-Opitz syndrome includes cholesterol supplementation and reduction of the sterol precursor, 7-dehydrocholesterol (Porter 2003). HMG-CoA reductase catalyzes the conversion of HMG-CoA into mevalonic acid in the cholesterol synthesis pathway. Simvastatin, a HMG-CoA reductase inhibitor, is therefore theoretically useful in decreasing the level of sterol precursors in patients with cholesterol synthesis defect. To our knowledge, our patient is the first lathosterolosis patient receiving a therapeutic trial of simvastatin. This drug was started at a low dose (0.2 mg/kg/day) and was

Table 3 Comparison of clinical features of reported lathosterolosis cases

	Case 1 (Fetus) (Rossi et al. 2007)	Case 2 (Brunetti-Pierrri et al. 2002) (Rossi et al. 2007)	Case 3 (Krakowiak et al. 2003) (Parnes et al. 1990)	Case 4 Our patient
Gender	Female	Female	Male	Male
Ethnic origin	Not available	Not available	French Canadian	Caucasian
Age at diagnosis	N/A	7 years	N/A	22 months
Dysmorphism	N/A	Neonatal period: ptosis, prominent nose with bulbous nasal tip, and micrognathia with protruding upper lip At 7 years old: bitemporal narrowing, epicanthic folds, ptosis, small nose with anteverted nares, small chin, puffy cheeks, and a long philtrum	Ptosis, short nose, micrognathia, prominent alveolar ridges	Bitemporal narrowing, broad nasal tip without anteverted nostrils, micrognathia
Microcephaly	Yes	Yes	Yes	Yes
Limb anomalies	Postaxial hexadactyly of upper and lower limbs Bilateral club feet	Postaxial hexadactyly of left foot Bilateral syndactyly between the 2nd and 4th toes Syndactyly between the 5th toe and the extra digit of the left foot	Bilateral postaxial hexadactyly of feet Bilateral syndactyly between the 2nd and 3rd toes	Bilateral postaxial hexadactyly of feet Bilateral syndactyly between the 2nd and 3rd toes
CNS abnormalities	Type II Arnold-Chiari malformation Lumbosacral meningocele	No	Refractory myoclonic jerks	No
Developmental delay/learning disability	N/A	Yes (unknown severity)	Yes (unknown severity)	Yes (moderate severity)
Liver dysfunction	N/A	Progressive intrahepatic cholestasis resulting in liver failure at 7 years old	Progressive hepatosplenomegaly	USG and MRI showed mild nonprogressive liver parenchymal disease. Normal liver function
Other anomalies	No	Horseshoe kidneys Right cataract Conductive hearing loss Cleft of 8th thoracic vertebra	Bilateral cataract Ambiguous genitalia	Bilateral small dot cataract
Outcome	Aborted at 21 weeks due to multiple malformations	Alive	Died at 18 weeks	Alive
Mutation	<i>SC5DL</i> gene [p.R29Q and p.G211D]	<i>SC5DL</i> gene [p.R29Q and p.G211D]	<i>SC5DL</i> gene [homozygous for p.Y46S]	<i>SC5DL</i> gene [p.K148E and p.D210E]
Parental genetic analysis	Heterozygote carriers	Heterozygote carriers	Heterozygote carriers	Heterozygote carriers

gradually stepped up to 1 mg/kg/day. The level of lathosterol successfully decreased from 81.6 $\mu\text{mol/L}$ to 15.1 $\mu\text{mol/L}$ within 4 weeks time (normal level: $<18 \mu\text{mol/L}$) and remained at a relatively low level afterwards. The highest lathosterol level after starting treatment was 18.3 $\mu\text{mol/L}$, which normalized after optimizing the dose of simvastatin. As rhabdomyolysis is a known adverse effect of statin treatment, creatine kinase level had been monitored regularly and was normal. Since serum cholesterol level was consistently normal in our patient, cholesterol supplementation was not given.

The patient's condition was stable during the follow-up period. He was noted to have developmental progress from a mental age of 11 months to 29 months within a period of 24 months, that is, a gain of 9 points in the overall developmental quotient. The mild, nonprogressive liver parenchymal disease shown by serial ultrasound and MRI scans could be hepatic involvement of the disease. It might already be present before commencement of treatment. Liver diseases were also reported in the other two lathosterolosis patients (Brunetti-Pierri et al. 2002; Rossi et al. 2005, 2007; Krakowiak et al. 2003). Although there are some adult studies suggesting cataract as an adverse effect of statin (Hippisley-Cox and Coupland 2010), the causal relationship between cataract and statin use has not been fully established. The bilateral small dot cataract with no visual significance could also be a manifestation of the disease. Except the stillborn, the other two lathosterolosis patients also had either unilateral or bilateral cataract (Rossi et al. 2007; Krakowiak et al. 2003). Furthermore, hereditary factor could not be completely ruled out as the patient's father also had bilateral small dot opacity without any visual significance. We are still monitoring the long-term outcome to document the efficacy and adverse effects of this therapeutic trial. Apparently, our patient might have a milder phenotype as compared to the other three patients with lathosterolosis. The relative attribution of this milder phenotype to the different underlying genetic mutations or simvastatin treatment is not known. We postulated that the severity of phenotype might be related to the level of lathosterol. The patient reported by Krakowiak had the most severe phenotype. Lathosterol accounted for 35% of total sterols in fibroblasts after 6 days in culture (Krakowiak et al. 2003). On the other hand, the patient reported by Brunetti-Pier had an intermediate phenotype among the three cases. The level of lathosterol in fibroblasts

was 12.5% of total sterols after 15 days in culture (Brunetti-Pierri et al. 2002). While in our case, the level of lathosterol in fibroblasts was 1.48% of total sterols after 10 days in culture. Additional patients are required to delineate the genotype-phenotype correlation.

Conclusion

Lathosterolosis is a recently recognized autosomal recessive cholesterol synthesis defect which shares certain phenotypic features with Smith-Lemli-Opitz syndrome. Simvastatin was started as treatment in our patient and normalization of lathosterol level had been clearly demonstrated. Additional patients are required for better delineation of the clinical spectrum of this disorder and the effect of statin treatment.

Acknowledgment We would like to acknowledge Dr. P Tse, private pediatrician, for referring the patient to our centre; Dr. Dorothea Haas, Division of Inborn Metabolic Diseases, University Children's Hospital, Heidelberg, Germany, for giving us support on managing the patient, and Dr. Heiko Runz, Institute of Human Genetics, Heidelberg, Germany for performing the filipin staining and granting us permission to publish the result in this report.

References

- Brunetti-Pierri N, Corso G, Rossi M et al (2002) Lathosterolosis, a novel multiple-malformation / mental retardation syndrome due to deficiency of 3-beta-hydroxysteroid-delta-5-desaturase. *Am J Hum Genet* 71:952–958
- Hippisley-Cox J, Coupland C (2010) Unintended effects of statins in men and women in England and Wales: population based cohort study using the QResearch database. *BMJ* 340:c2197
- Krakowiak PA, Wassif CA, Kratz L et al (2003) Lathosterolosis: an inborn error of human and murine cholesterol synthesis due to lathosterol 5-desaturase deficiency. *Hum Molec Genet* 12:1631–1641
- Parnes S, Hunter AG, Jimenez C, Carpenter BF, MacDonald I (1990) Apparent Smith-Lemli-Opitz syndrome in a child with a previously undescribed form of mucopolidiosis not involving the neurons. *Am J Med Genet* 35(3):397–405
- Porter FD (2003) Human malformation syndromes due to inborn errors of cholesterol synthesis. *Curr Opin Pediatr* 15:607–613
- Rossi M, Vajro P, Iorio R et al (2005) Characterization of liver involvement in defects of cholesterol biosynthesis: long term follow-up and review. *Am J Med Genet Part A* 132A:144–151
- Rossi M, D'Armiento M, Parisi I et al (2007) Clinical phenotype of lathosterolosis. *Am J Med Genet* 143A:2371–2381